Department of Mechanical Engineering

Utopia or Opportunity?

Predicted Performance of 21st Century Technology Steam Locomotives

Iiro Hirvensalo

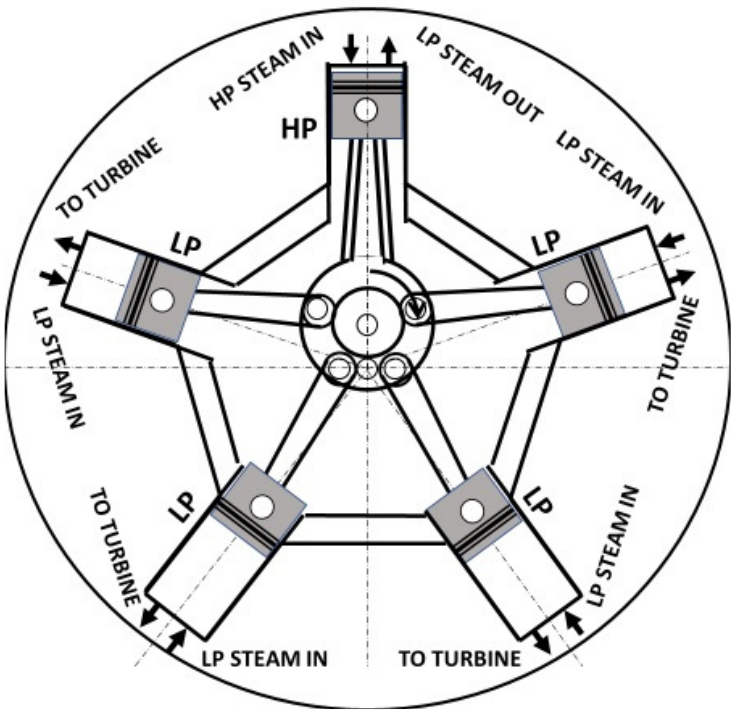

Aalto University

DOCTORAL DISSERTATIONS

Aalto University publication series
DOCTORAL DISSERTATIONS 165/2021

Utopia or Opportunity?

Predicted Performance of 21st Century Technology Steam Locomotives

Iiro Hirvensalo

A doctoral dissertation completed for the degree of Doctor of Science (Technology) to be defended, with the permission of the Aalto University School of Engineering, at a public examination held at the lecture hall K216 of the school on 10 December 2021 at 12.

Aalto University
School of Engineering
Department of Mechanical Engineering

Supervising professor
Professor Martti Larmi, Aalto University, Finland

Thesis advisor
D.Sc. Tuomas Paloposki, Aalto University, Finland

Preliminary examiners
Professor Lucien Koopmans, Chalmers University of Technology, Sweden
Assistant Professor Tatiana Minav, Tampere University, Finland

Opponents
Professor Esa Vakkilainen, Lappeenranta University, Finland
Assistant Professor Tatiana Minav, Tampere University, Finland

Aalto University publication series
DOCTORAL DISSERTATIONS 165/2021

ISBN 978-952-64-0606-0 (printed)
ISBN 978-952-64-0607-7 (pdf)
ISSN 1799-4934 (printed)
ISSN 1799-4942 (pdf)
http://urn.fi/URN:ISBN:978-952-64-0607-7

Images: Iiro Hirvensalo

Unigrafia Oy
Helsinki 2021

Finland

Publication orders (printed book):
hirvensaloiiro@gmail.com

NORDIC SWAN ECOLABEL
Printed matter
4041-0619

Aalto University

Abstract

Aalto University, P.O. Box 11000, FI-00076 Aalto www.aalto.fi

Author
Iiro Hirvensalo

Name of the doctoral dissertation
Utopia or Opportunity?

Publisher School of Engineering

Unit Department of Mechanical Engineering

Series Aalto University publication series DOCTORAL DISSERTATIONS 165/2021

Field of research Energy Technology

Manuscript submitted 3 August 2021 **Date of the defence** 10 December 2021

Permission for public defence granted (date) 1 November 2021 **Language** English

☒ **Monograph** ☐ **Article dissertation** ☐ **Essay dissertation**

Abstract

The objective of this study is to predict the performance of liquid fuel burning steam locomotives based on the technology available today. Diesel engine tribology, electronic valve control, and substantially higher steam parameters than those of classic steam locomotives have been applied. Such locomotives have not been built yet but appear to offer promising possibilities. A hypothetic pattern locomotive called Hs1 has been configured, to predict the performance of such locomotives. Several methods have been used for virtual creating and testing of the Hs1. Firstly, the evolution of classic steam locomotives has been discussed in terms of their strengths and weaknesses, with resulting pre-requisites from potential customers for any steam power. Secondly, classic, and recent literature has been studied in search for advances in steam- and other applicable technologies, materials, and practices. Thirdly, innovative experimental locomotive designs have been discussed. Fourthly, properties and adaptability of bio-oil vs. fossil oil as fuels have been discussed. Finally, enginemen's know-how has been exploited, to include practical and operational views in the design of the Hs1. Conclusions of the findings within the discussions constitute the basic specifications of the Hs1. A radial reciprocating steam engine is opted for the prime mover, with a turbine to recover the energy of the exhaust steam of the radial engine, and with an electrical transmission to power the driving wheels. The power chain downstream of the prime mover is thus identical with that of diesel-electric locomotives. Diesel components have been exploited to unify the operational and maintenance characteristics of the Hs1 with those of diesel-electric locomotives. Electric transmission enables recovery of energy generated by the traction motors in dynamic braking by storing it into accumulators or by feeding resistors that heat the feedwater. A simulation program has been created for assessing the performance of the Hs1, and for comparing the figures with those of a reference diesel-electric locomotive as well as of a classic steam locomotive. Road test simulations predict a drawbar efficiency of 21-27 % for the Hs1, depending on whether and in which way the braking energy is recovered, and 33 % for the reference diesel-electric locomotive. The simulated classic steam locomotive attains 6,5-7 % at the maximum in the same assignment, the round-the-year figures being 3-4 %. Yard work involves a lot of braking and thus potential for recovery of braking energy, resulting in predicted drawbar efficiency of 29-36 % for the Hs1 vs. 33% of the diesel electric locomotive. In light passenger trains with frequent stops, the Hs1 is predicted to attain an efficiency of 18-29% vs. 33 % of the diesel-electric locomotive. Bio-oil combustion enhances the sustainability of the Hs1 as motive power when compared with engines dependent on fossil fuel. External combustion enables exploiting lower grade pyrolysis oil that would require further refining to make it fit for internal combustion engines. The CO_2 emissions of diesel engines originate from fossil fuel unless 100 % bio-oil is used whereas the fuel of Hs1 is made of forest residue releasing its CO_2 content even if left in the woods.

Keywords locomotive, piston steam engine, biofuels, efficiency, electric transmission

ISBN (printed) 978-952-64-0606-0 **ISBN (pdf)** 978-952-64-0607-7

ISSN (printed) 1799-4934 **ISSN (pdf)** 1799-4942

Location of publisher Helsinki **Location of printing** Helsinki **Year** 2021

Pages 186 **urn** http://urn.fi/URN:ISBN:978-952-64-0607-7

Tekijä
Iiro Hirvensalo

Väitöskirjan nimi
Utopia vai mahdollisuus? Nykytekniikalla toteutetun höyryveturin ennakoitu suorituskyky

Julkaisija Insinööritieteiden korkeakoulu

Yksikkö Konetekniikan laitos

Sarja Aalto University publication series DOCTORAL DISSERTATIONS 165/2021

Tutkimusala Energiatekniikka

Käsikirjoituksen pvm 03.08.2021 **Väitöspäivä** 10.12.2021

Väittelyluvan myöntämispäivä 01.11.2021 **Kieli** Englanti

☒ **Monografia** ☐ **Artikkeliväitöskirja** ☐ **Esseeväitöskirja**

Tiivistelmä

Tutkimuksen tarkoitus on arvioida nykytekniikalla toteutetun, nestemäistä polttoainetta käyttävän höyryveturin suoritusarvoja. Veturissa on hyödynnetty dieseltoleransseja ja -tribologiaa, sähköistä venttiiliohjausta ja huomattavasti perinteisiä korkeampia höyryarvoja. Tällaisia vetureita ei vielä ole rakennettu, mutta ennakoidut ominaisuudet näyttävät lupaavilta. Ennakointia varten on hahmoteltu hypoteettinen esimerkkiveturi, jolla on tutkimuksessa työnimi Hs1, ja jonka suunnittelu ja virtuaalitestaus perustuvat useisiin eri menetelmiin. Ensinnäkin klassisen höyryveturin vahvuudet ja heikkoudet on käyty läpi kehityshistorian ja käyttökokemusten valossa, jotta voitaisiin arvioida, mitä potentiaalinen käyttäjä odottaisi uuden sukupolven höyryveturilta. Toiseksi on tutkittu klassisen ja tuoreimman kirjallisuuden avulla edistysaskeleita, jotka höyrytekniikan kehitys, uudet materiaalit ja menettelytavat ovat mahdollistaneet. Kolmanneksi on analysoitu innovatiivisia ratkaisuja soveltavien prototyyppiveturien koeajotuloksia. Neljänneksi on vertailtu eräitä bio- ja fossiilisten polttoöljyjen käyttö- ja soveltuvuusominaisuuksia vetureissa. Lopuksi on hyödynnetty veturimiesten käytännön osaamista, jotta Hs1 olisi mahdollisimman realistinen ja luonteva työkaluna. Hs1:n pääspesifikaatiot perustuvat kuvattujen menetelmien johtopäätöksiin. Päävoimanlähteeksi on valittu radiaali- eli tähtityyppinen mäntähöyrykone, jota on täydennetty höyryturbiinilla mäntäkoneen poistohöyryn loppupaisunnan saavuttamiseksi. Voima on välitetty vetopyöriin sähkögeneraattorin ja ratamoottorien avulla, joten voimansiirto on pääkoneesta eteenpäin täysin sama kuin dieselsähkövetureissa. Dieselkomponentteja on käytetty soveltuvin osin, jotta Hs1:n käyttö- ja huoltorutiinit poikkeaisivat mahdollisimman vähän dieselvetureista. Sähköinen voimansiirto mahdollistaa ratamoottorien käytön generaattoreina jarrutuksessa, jolloin jarrutusenergiaa voidaan hyödyntää joko akuissa tai kattilan syöttövettä lämmittävissä vastuksissa. Hs1:n ja vertailuveturien suorituskyvyn arvioimiseksi on rakennettu simulointiohjelma, jota on sovellettu sekä linja- että ratapiha-ajossa. Linjalla Hs1:n arvioitu hyötysuhde on vaihdellut välillä 21–27 % riippuen siitä, onko jarrutusenergia otettu talteen. Dieselsähköveturin simuloitu hyötysuhde on 33 %. Vertailuveturina käytetyn klassisen höyryveturin tulos on 6,5–7 % matkaa kohti (vuositasolla vain 3–4 %). Ratapihatyöskentelyn runsaat jarrutukset tarjoavat potentiaalia jarrutusenergian talteenottoon nostaen Hs1:n simuloidun hyötysuhteen välille 29-36% dieselsähköveturin pysyessä tasolla 33 %. Usein pysähtyvissä keveissä taajamajunissa Hs1:n simuloitu hyötysuhde on 18-29 % ja dieselsähköveturin 33 %. Biopoltto on ympäristön kannalta tulkittavissa Hs1:n eduksi verrattuna dieselvetureihin, jos näiden polttoaineena käytetään fossiilista öljyä. Hs1:ssä käytetty pyrolyysiöljy ei myöskään ilman huomattavaa jatkojalostusta sovellu käytettäväksi polttomoottoreissa. Veturien CO2-päästöt ovat jälkimmäisissä fossiilista alkuperää, ellei polttoaineena käytetä bioöljyä, kun taas pyrolyysiöljy on tehty hakkuujätteestä, jonka hiilidioksidi joutuu ilmakehään joka tapauksessa.

Avainsanat veturi, mäntähöyrykone, biopolttoaineet, hyötysuhde, sähköinen voimansiirto

ISBN (painettu) 978-952-64-0606-0 **ISBN (pdf)** 978-952-64-0607-7

ISSN (painettu) 1799-4934 **ISSN (pdf)** 1799-4942

Julkaisupaikka Helsinki **Painopaikka** Helsinki **Vuosi** 2021

Sivumäärä 186 **urn** http://urn.fi/URN:ISBN:978-952-64-0607-7

Acknowledgements

I owe the realization of my thesis to the expertise and support of countless people, many of whom did not survive to see the work finished. I wish to honour the memory of those people with my deepest gratitude. Mr Arno Saraste, my close relative, planted the first seed of this thesis already in my boyhood. He tried to cool down my passion for steam engines by pointing out their miserably poor efficiency. After losing my father quite early, Arno took his place and always remained my idol in engineering. As early as in 1982 he initiated my membership in SKIY, the Association of Finnish Manufacturing Engineers, the organization that became my most important professional advisor and the only one to financially support my thesis project. Arno did not live to see the SKIY appointing me the "Steam locomotive Counsellor" in 2000, but many of his colleagues did. This playful title became an enormously serious kick for me to get finished with my project! Like Arno himself, many of the SKIY members greatly contributed to the rise and prosper of Finnish metal industry and logistics, a considerable amount of which had to do with locomotives. The late Mr Heimo Rumpunen was *primus inter pares* in this field, having started his railway career from the challenging job of wartime fireman on steam locomotives and having retained his interest in these to the very end. Having been among the first to understand the pathbreaking innovations of L.D. Porta he was technically my most knowledgeable advisor until his death. My late boss and close friend Veikko Tervonen hired me in 1997 in Eastern Finland to assist in networking of regional industries and technical universities. Such an assignment incidentally made it occur to me that all the know-how and capacity needed for creating a 21st century technology steam locomotive was in fact available in domestic hands. Our mutual friend, the late Prof. Ilkka Lapinleimu shared Veikko's enthusiasm when I told them about my dream of a thesis on the subject. Veikko only saw a sketch of it whereas Ilkka who lived long enough to support me with all his accumulated industrial and academic know-how, only left us when the thesis was in its pre-examination stages. The most recent departure of my late supporters occurred only weeks ago that Mr Louis M. Newton of the former Norfolk & Western Railroad (later Norfolk & Southern) passed away. He was one of the key engineers to have worked for the last effort of his employer to keep on steam power with a steam turbine electric locomotive in 1954-1957. I got the privilege of meeting Mr Newton personally in 2004, to discuss the *pro's* and *con's* of this remarkable engine.

Still going strong, my most faithful supporter Prof. Pier A. Abetti turned 100 in February 2021. He is the only person I know to have performed two magnificent careers in row, at first the 33 industrial years in General Electric Co. both in the USA and in Europe, then the most fruitful 34 academic years as a Professor of Rensselaer Polytechnic Institute, NY. Since the days of 2001 when I told him about my thesis dream, his insight and support have endured the slow progress of my project. In the spirit of his ancient idol *Seneca*, Pier never failed to encourage his student who now reaches the destination at last. Himself a railroad fan, he opened his magnificent library on the subject to my disposal. A keen interest in Finland took him and his late wife Betty Burr to our country every year from 1994 to 2014 and secured his online touch with my project.

My leaving East-Finland in 2006 did not cut my contacts with the local companies – on the contrary. Mr Harri Kivelä, my long-time workmate during the said assignment, and Mr Ari Isopoussu who accepted me as a partner in putting up a machining shop together with Componenta Suomi-valimo, frequently invited me to re-visit the region. The metamorphosis of my imaginary locomotive then got started within discussions of water-tube boilers with Mr Taisto Sepponen (Warkaus Works Oy and KPA Unicon Oy), of biofuels and grates with Mr Juha Huotari (Sermet Oy and Wärtsilä Biopower Oy), of steam turbines with Mr Jukka Huttunen (Savonia Power Oy and Savonia Polytechnic), and of harvesting of forest residue with Mr Juho Nummela (Ponsse Oy). The earliest stages of the resulting visions even got a literal shape as Ms Raisa Leinonen of Kuopio Design Academy made her student Ms Taina Bergqvist prepare a 3D-study of the locomotive by 'clothing' my sketches. The present revisions of my work, having destroyed Taina's beautiful creations, would dearly call for her industrial designer's skills! Starting the actual post-graduate studies in 2010 was a challenge after my 40-year absence from academic life, resulting in dropping off everything related with working life. I was lucky, though, as Prof. Martti Larmi of Aalto University immediately showed his interest in my subject and sent me to Mr Tuomas Paloposki, the courses of whom were voted by international students as the best of that academic year. Being both an expert in power plant engineering and a pragmatic researcher, Tuomas became my instructor and the best possible person to guide me through the practical problems of thermodynamics. Those two teachers of mine, together with Prof. Abetti whom I had the privilege of introducing to them both in 2014, always extended their full support to my project, patiently trusting to see the results now at hand. Tuomas invited my musician friend Mr Kari Saari of Aalto university to join in as an active member of our team. Kari exploited his wide expertise of heat exchangers within the complex twin-phase calculations of the condenser which I never could have accomplished by myself. Mr. Ralf Wikstén, now retired from Aalto University, was my indispensable help in heat exchanger calculations.

Ms Mari Tuomaala conducted a most rewarding course in energy efficiency and added a serious note to my project by reminding that all combustion is a concern of climate change, be the fuel whatever. Mari thus convinced me about the need for further studies of the environmental impacts of locomotives involving either external or internal combustion process although not included in the scope of the thesis. Attending the bi-annual International Flame Days brought me the invaluable contact with Mr Matti Kytö of Metso Oy and Valmet Oy. Matti had also worked for Oilon Oy, thus being an expert both in boilers and burners, a combination that resulted in his participating in the joint research project of Fortum Oy, Valmet Oy, and the Finnish Institute for Technical Research (VTT) on production and research of fast pyrolysis oil. In this context Matti made me acquainted with Ms Anja Oasmaa, Mr Yrjö Solantausta and Mr Jani Lehto of the VTT. Without the input of all the four people my thesis would still be in its wavering initial stages.

Mr Vesa Kumpulainen, my long-time friend and boss of Kumera Corporation, reached his helping hand by letting Vesa Tarula, one of his key engineers, work out my sketchy ideas for a novel type of poppet valve into handsome 3D illustrations and put in a lot of know-how related with gears, generators and electrotechnics.

Mr Davidson Ward of the Coalition for Sustainable Rail in Minnesota kept me well informed about the proceedings of their bio-coal research project and provided me with valuable notes of the work of the late Argentinean steam celebrity, Mr L.D. Porta. My former student mate Kai Vehmersalo kindly donated one of my most excellent reference books concerning British steam loccomotives.

Mr Hannu Lehikoinen of FenniaRail Oy opened-up the technicalities and extensive test reports of the diesel-electric locomotive Dr18, thus enabling its use as a reference locomotive in the simulations. My former colleague and expert of generating sets Mr. Olavi Miinalainen was my helping hand in laying out the electric circuit of my locomotive proposal.

Mr Dmitrij Khimenkov helped me in acquiring lots of technical data concerning the Russian ТЭМ18В class diesel-electric locomotives equipped with Finnish Wärtsilä 6L20 series diesel engines, this data having been useful when assessing the fuel consumption of state-of-the-art diesel engines. Mr. Sakari K Salo provided me with excellent photographs of locomotives relevant for the study.

Engine drivers Tarmo Reunanen, Seppo Kähönen and Kai Rosenberg have provided me with their experienced views about today's locomotives as a working environment and thus brought in crucial shop floor knowhow to improve the operability of the proposed locomotive.

The chalk lines of the thesis were at hand when Prof. Mauri Haataja, a contact of my friend Ari Isopoussu, contributed to the thesis by telling me about a supercapacitor project in the University of Oulu concerning a heavy-haul truck, thus bringing about an extremely relevant subject for further studies.

Now that the work was in its final stages the practical formalities would have been beyond my capacities without the helping hand of Ms Laura Mure who made miracles in clothing my manuscript. Not only did she tackle with the endless tables and sketches but simply made the frames look better than the painting. Ms Ritva Viero and Ms Reetta Mannola whom I seldom met personally, worked as indispensable 'liaison officers' as regards the Doctoral Programme Committee, always making me feel the work was proceeding regardless of my slow speed.

As for my newly born academic life my classmates Kate Suominen and Mickey Whitzer made me feel like a member of the group despite the vast gap between our ages. It was a pleasure to study together in the international classes.

It is only too common that the family of the science-maker carries the heaviest load. My case is no exception. Inkeri must have sensed the limits of her tolerance during the past ten years of literal steaming at our home. Thanks to her doctor's degree she is one of 'those who know'. During many past years the visits of our daughters and their families as well as of my sister and my brother have been filled with trains from my side -nothing much else. Love and hugs to my great, blessed family!

None of the people who know me have escaped hearing endless stories about locomotives. It is impossible to list all the names but everyone having listened to me has contributed to the project and filled it with fun. Thank you all for sharing this excursion of my fantasy!

Järvenpää 2021-10-25
Iiro Hirvensalo

Contents

Author's contribution

The author initiated the present study by compiling and discussing the late- and post-steam age efforts and proposals to improve the viability of steam locomotives as alternative motive power.

The study is an effort to bring the 'nuts and bolts' of steam engine technology, including the most recent advances in the development, into the knowledge of the science community, to further support the academic research of the subject.

Efficiency has been considered as the key issue of the study and discussed in each case within the scope of available data, including methods of assessing it.

The author has configured a steam-electric locomotive exploiting a hybrid concept for recovery and re-use of the braking energy for traction after electrically accumulating it. Such a concept appears as a novelty in steam locomotive practice.

The steam process exploits the *monotube flow-through* concept of an industrial *Mitchell*-type vertical boiler rather than the traditional horizontal firetube design of steam locomotive boilers.

Combustion of liquid bio-oil is a novelty of the boiler, with the aim of corrosion-free exhausting of the flue gas at a lower than traditional temperature by virtue of sulphurless bio-oil.

The consequent potential of preheating the combustion air up to temperatures exceeding 500 K is a novelty in steam locomotives.

The prime mover is a novel-type combination of *radial compound* steam engine and a steam turbine resulting in triple expansion of steam to atmospheric pressure.

The 4-fold expansion of the compound engine is attained within a set of 5-cylinder radial engines by exploiting one high-pressure cylinder and four low-pressure cylinders in each engine, all the cylinders having identical dimensions in contrast to the conventional compound engine solutions with different-size cylinders.

The cylinders are unlubricated as in the German *Zero Emission Engine* concept introduced in 2001.

The steam distribution exploits a novel-type concentric and electronically controlled poppet valve design, the valves themselves being the author's modification of widely used *Caprotti*-valves whereas the actuators rely on techniques developed within commercial automotive solutions.

A scientific novelty of the work is the calculational evaluation of the proposed locomotive concept and its comparison with other types of motive power in various assignments by means of a simulation program designed and tailored by the author.

The viability of the simulation results has been assessed by comparing them with actual data collected from the reference diesel-electric locomotive during official and publicly reported tests executed by its owner's staff.

Additional comparison material has been acquired by simulating the performance of a heavy classic steam locomotive, known to the author from footplate working.

Glossary of terms

adhesive weight	weight resting on the driving wheels of a locomotive
articulated	divided frame; driving wheels are mounted in frames, pivoted with each other, opposite to *rigid frame*
bio-oils	oils processed from biomass
blind axle	wheelless axle connected with driving wheels
blast pipe	exhaust steam pipe under the smokestack
carryover	coal particles unburnt due to seizure by draught
clearance volume	space between cylinder head and piston in its top or bottom dead center
CME	Chief Mechanical Engineer
coasting	running idle due to downhill or kinetic energy
compound engine	double expansion engine, opposite to *simple*
crankshaft (single- vs. multi-throw)	shaft type necessary for locomotives having one or more cylinders inside the frames; 'throw' refers to the number of cranks on one shaft
crown sheet	roof plate of firebox, most critical for boiler safety
dead centre	extreme position of piston stroke with *zero* torque
direct drive	mechanical transmission of power from prime mover directly to driving wheels
displacement	cylinder volume between extreme positions of piston
drag	influence of air resistance to the train
drawbar	coupler transmitting the pulling force of engine to train
drawbar tractive effort	pulling force transmitted from wheel rims to drawbar
drawbar thermal efficiency	ratio *drawbar work* to *thermal energy consumed*
dry saturated line	the line in *Mollier h, s* graph to separate the saturated vs. superheated areas of water vapour
dynamic brake	braking by traction motors that work as generators when power is cut off; opposite to friction brake, the dynamic one does not involve any mechanical contact and enables substantial recovery of braking energy
ECE	external combustion engine (e.g., steam engine); combustion takes place outside of engine
emissions	gaseous, liquid, or solid residues, noise or odours caused by working or idling of locomotive
efficiency	ratio *work performed* to *energy consumed*
expander	in the engine the section in which the expansion takes place; a turbine, or pistons engines are the relevant alternatives
fast pyrolysis oil	oil extracted from biomass in a *pyrolyzer, ie*. heated chamber with controlled residence time of particles
feedstock	biomass used for material of bio-oil
fire-tube boiler	boiler type consisting of a water- and steam space through which the combustion gases are conducted via tubes; opposite to *water-tube* boiler
flue gas	mixture of gases formed from combusting the fuel
forced draught	draught built by overpressure, *e.g*., by means of fans, opposite to *induced* draught caused by vacuum
forest-to-tank	delivery chain of biofuel from harvesting of feedstock, to filling fuel tank of locomotive

forest-to-wheels	delivery chain of biofuel from harvesting of feedstock, to generating *wheelrim* tractive force
forest residue	primary *feedstock* of pyrolysis process
friction or mechanical brake	braking by pressing brake blocks against wheel rims, or wheel- or axle-mounted discs; opposite to dynamic brake
GTM/h	gross ton miles/hour; unit of performance capability
	geared drive transmission by means of gears or gearbox
ICE	internal combustion engine (*e.g.*, diesel); combustion takes place inside of cylinders
idle wheel or axle	non-driving wheel or axle
induced draught	draught caused by vacuum; opposite to *forced* draught
loading gauge	the cross-section outside of which no part of the rolling stock or load is allowed to protrude
LFO	light fuel oil
monotube boiler	steam generator made of spiral tubes
pattern locomotive	author's proposal for an advanced technology steam locomotive
piston thrust	cylinder pressure multiplied by piston area
piston valve	device controlling the inlet steam flow from steam chest to cylinders, and flow of exhaust steam from cylinders to receiver, to condenser, or to blast pipe
pivot	a flexible coupling between sections of frames
poppet valve	ICE type valve, adapted to steam engine[1]
prime mover	primary source of power of locomotive, e.g., steam engine in a steam locomotive, or diesel engine in a diesel-electric locomotive
PYR	pyrolysis oil
pyrolysis	thermal process by means of which the bio-oil content of biomass is extracted in the absence of oxygen
Rankine cycle	steam cycle consisting of stages: 1. isentropic raising of the pressure of feedwater to boiler pressure; 2. evaporation and eventual superheating of steam; isentropic expansion; 4. condensing or exhausting the steam
receiver	steam vessel between high- and low-pressure cylinders
rigid frame	all driving axles are mounted in a common frame, opposite to *articulated frames* with a pivot between the frames
rolling stock	any equipment moving on the rails
specific emission	emission per unit of energy or power produced
specific consumption	consumption per unit of generated energy or power
simple	single expansion engine, opposite to multi-expansion, usually *compound*
steam chest	the space from which valves admit steam to cylinders
steam jacket	cast-iron or welded construction around the cylinders, filled with steam to prevent cooling of cylinder walls
stoker	mechanical firing device, or coal feeding system
state-of-the-art technology	construction, standardization, materials, components, and production methods to match with contemporary diesel or electric locomotives, enabling the use of components and modules common to both types
state-of-the-art operability	operation with multiple units by a single crew like in diesel or electric locomotives or remote control, and serviceability in facilities designed for diesels
state-of-the-art energy efficiency	minimized losses at every stage of a given process,
super-power	term used to describe some of the most powerful steam locomotive designs in USA since 1926
SWOT	assessing method considering *Strengths, Weaknesses, Opportunities,* and *Threats* of the object
T.E.	a frequently used abbreviation for *tractive effort*
thermic syphon	heat exchanger element in the combustion chamber
traction coefficient	the ratio *drawbar tractive effort* to *adhesive weight*
traction motor	motor coupled on a driving axle
tractive effort	the force transmitted from prime mover to the reference point, usually to *drawbar*

transitory	momentary, or short-term, as opposed to *continuous*
transmission	power chain between the *prime mover* and driving wheels
tribology	science and engineering of interacting surfaces in relative motion
truck	one or more axles attached to a frame pivoted into the main frame of the locomotive; may be *idle* or powered
water hammer	shock caused by water condensed in the cylinder and trapped between the piston and the cylinder head
waterleg, or water-jacket	double-wall space filled with water around the firebox
watertube boiler	walls of the boiler are water-filled tubes
waterwall	wall of a watertube boiler
well-to-tank	stages from fossil fuel mining through refinery to delivery to the locomotive
wheelrim	circumference of driving wheels
wheelrim tractive effort	pulling force on wheelrims
wiredrawing	harmful throttling of steam within its flow path

Symbols, indexes, and subscripts

Latin symbols

A	[m^2]	area
a	[m/s^2]	acceleration
b	[m]	width
c	[J/kg K]	specific heat capacity
$\dot{C}$	[W/K]	heat capacity flow
D	[m]	inside diameter
d	[m]	outside diameter
E	[J]	energy
F	[N]	force
f	[1/s]	1. frequency
	[]	2. reduction coefficient in formula of mean indicated pressure
G	[W/K]	conductance
g	[m]	fin thickness in condenser plate heat exchanger
h	[J/kg]	specific enthalpy
k	[]	isentropic index
L	[m]	depth of fins of heat exchanger
LHV	[J/kg_F]	lower heat value per kg of fuel
l	[m]	length
l	[J/kg]	specific heat of evaporation of water
M	[kg/mol]	molar mass
m	[kg]	mass
$\dot{m}$	[kg/s]	mass flow
N	[]	number
n	[r/s]	rotational speed in revolutions per second
P	[kW]	power
p	[Pa = N/m^2]	pressure
Q	[J]	heat
R	[]	ratio of heat capacity flows $\dot{C}_{min}/\dot{C}_{max}$
r	[m]	crank radius
s	[m]	1. distance
	[m]	2. stroke
	[J/kg K]	3. specific entropy
T	[K]	absolute temperature
t	[s]	time

u	[m]	height
V	[m^3]	volume
v	[m/s]	speed
$\dot{V}$	[m^3/s]	volumetric flow
W	[J]	work
w	[m/s]	flow velocity
X	[%]	power setting
x	[m]	horizontal distance
y	[m]	vertical distance
Z	[]	dimensionless conductance

Greek symbols

α	[W/m^2K]	1. convective heat transfer coefficient
	[rad]	2. angle between connecting rod and cylinder axis
β	[]	gradient factor of track profile
Δ	[m]	difference
δ	[m]	1. width of flow path in heat exchanger
	[m]	2. distance between fins in heat exchanger
ε	[]	1. ratio admission-volume-to-displacement
	[]	2. recuperation rate of heat exchanger
ζ	[]	1. resistance factor
	[]	2. absorption factor of firebox calculations
η	[]	efficiency
θ	[K]	temperature range within heat exchanger
κ	[]	isentropic index
λ	[W/m K]	1. thermal conductivity
	[]	2. excess air factor
$\bar{\lambda}$	[W/m K]	average thermal conductivity
μ	[kg/s m]	1. dynamic viscosity
[]		2. friction coefficient
$\bar{\mu}$	[kg/s m]	average dynamic viscosity
ν	[m^2/s]	1. kinematic viscosity
	[m^3/kg]	2. specific volume
ξ	[rad]	angle between crank and line perpendicular to conn. rod
ρ	[kg/m^3]	density
$\bar{\rho}$	[kg/m^3]	average density
Σ	[]	sum, or total
τ	[Nm]	torque
ω	[1/s]	angular velocity
ϕ	[kW]	thermal power
φ	[rad]	crank angle

Universal constants

$\bar{R}$	[J/mol K]	gas consta

Dimensionless numbers

Nu	[]	Nusselt number
Pr	[]	Prandtl number
Re	[]	Reynolds number

Other coefficients

ψ	0,46 [$kcal^{0,5}h^{-0,5}m^{-1}$]	coefficient of *Hudson-Orrok* formula

Subscripts if abbreviated; in case not abbreviated, the subscripts are regarded as self-explanatory.

a	acceleration
ab	absorbed
abs	absolute
acc	accumulated
act	actual
adh	adhesion, adhesive
adm	admission
air	air
aux	auxiliary
av	average
B	boiler
b	brake
C	Carnot
cl	clearance
burn	burner
calc	calculated
comp	compound
cond	condensing, condenser
conv	convective
cyl	cylinder(s)
da	dry air
db	drawbar
disp	displacement
E	energy
eng	engine(s)
exc	excess
exh	exhaust
exp	exploited
ev	evaporation
evap	evaporator
F	fuel
fb	firebox
fg	fluegas
fw	feedwater
fin	fin of a plate-type heat exchanger
gen	generator
g	gradient
HP	high pressure
i	mean indicated
ind	indicated
inl	inlet
ins	insulation
LP	low-pressure
loc	locomotive
m	mass

ma	moist air
max	maximum
mech	mechanical
mom	momentary
min	minimum
mt	mixing tank preheater
n	variable from 1 to n
p	constant pressure
pn	piston
oc	own consumption
preh	preheater coil
prop	proportional
prov	provided
rec	recovered
rej	rejected
res	resultant
r	rolling
ru	re-used
s	isentropic
sat	saturated steam
set	preset or selected
st	steam
stc	steam cycle
stoich	stoichiometric
stor	stored
sup	superheated steam, superheater
sw	piston-swept
T	train
tab	tabulated
TB	turbine
tot	total
tr	traction
trans	transmission
trm	traction motor(s)
v	constant volume
W	work
w	water
wv	water vapour

1. Introduction

1.1 Background and motivation of the study

The author's life-long interest in steam locomotives is the principal trigger of the present study, the objectives of which are discussing the vast gap between efficiencies of classic steam versus diesel locomotives and searching for an up-to-date configuration with potential of alleviating the said gap.

Regardless of the fast-growing share of renewable energy in power generation, coal or gas fired steam power plants generated 63 % of global electric power in 2016.[2] At the same time the worldwide round-the-year average ratio between electric output and energy input of coal-fired steam power plants was 0,34 while the average figure of the most advanced countries was 0,38, with an estimated technical potential of attaining 0,44.[3] The mainstream construction of classic steam locomotives with single expansion 2-cylinder engines hardy attained figures like 0,06 – 0,09 for the maximum ratio between drawbar work and energy input on a transitory basis, i.e., as measured during tests with given conditions of constant nature, neglecting non-productive fuel consumption during idling or standby, not to mention the typical carryover of unburnt coal when working at maximum capacity of the boiler.[4] Actual round-the-year figures thus remained as low as 0,03 – 0,04 e.g., on South African Railways where the fleet of steam locomotives was relatively modern and well-maintained.[5] At the same time, the round-the-year efficiency of contemporary GM diesel-electric locomotives was 0,23.[6] Such records imply that the round-the-year efficiency of steam power plants was up to 10 times that of steam locomotives as shown by the above figures. Late- and post-steam age specialists worked hard to improve the efficiency of steam locomotives, but applications of the results, many of them substantial as discussed within appropriate chapters, remained minuscule in proportion of the demand due to the rapid demise of steam traction on railways.

Steam power dominated on railways until after World War II when the large-scale takeover by diesel and electric power started to phase steam out. After 200 years of the birth of steam locomotive, heritage or scenic railways practically remain its only users.

Besides the low thermal efficiency, the labour-intensive operation initially started to pave the road for the competitors of steam power. Even if the overall cost analysis, in certain cases, turned the scale in favour of steam, operational aspects such as versatility, and multiple-unit drive by one crew, made diesel and electric locomotives more flexible as working tools.[7] The ergonomically challenging work in steam engines ceased to tempt competent crews.[8] Physically stressing, dirty, and draughty work was replaced by clean and comfortable job in electric and diesel engines.[9] Environmental aspects started to become a serious concern towards the end of the steam age even in terms of passenger complaints while emissions to the environment also constitute a burden for diesel power.[10] [11]

Several notable advocates of steam power who were involved with steam operations until the end of steam age, maintain that the above drawbacks were generally treated as unavoidable issues inherent in steam locomotives, and they also maintain that detail design relied on rules of thumb, or trial-and-error

basis, rather than on theoretical analysis.[12] The engines thus became impressive in size, power, and speed, but not in efficiency.[13]

Steam locomotives were challenged for the first time in the end of the 19th century after *Werner Siemens* had introduced the first electric locomotive. Its use was initially limited to areas with abundant hydropower, but its efficiency, cleanliness and traction properties soon proved superior over those of steam power, prompting experiments with electric transmission even in steam locomotives as early as in 1894-97.[14]

The first useful long-haul diesel-electric locomotive started in 1924 on the Soviet Railways (SŽD), remained in service until 1954, and became the pattern of many later Soviet designs.[15]

Challenger's position made diesel manufacturers respond quickly to initial faults whereas the steam designers were slow to apply the improvement potential envisaged by scarce even if capable innovators, as further discussed in the evolution review.[16]

Diesel locomotive design was early to adopt a versatile concept that made it equally suitable for hauling long-distance trains, and for shunting work at track yards. Such a concept became possible due to the independent power trucks that enabled the locomotive to negotiate sharp curves at high speed, regardless of the weight or length of the locomotive.[17] This feature, together with multiple-unit drive, speeded up the demise of steam power that never reached a similar degree of versatility, as the direct drive of steam locomotives resulted in compromising between tractive power and speed, due to the limited speed range of piston steam engines that made locomotives task-specific.[18]

Steam was ultimately gone in the USA by the early 1960's while lasting some 15 more years in the rest of the industrialized world, or until the end of the Millennium in a few developing countries.[19]

Steam advocates never vanished but remained individuals that had to compromise between proven vs. innovative solutions, while diesels appeared to many as a proven, if not the only viable option.[20]

A new interest in steam technology was prompted by energy crises of the 1970's, but remained short-lived at the time, due to repeated fall of oil prices.[21] Rapidly increasing environmental concern of recent times has revived interest in the advancing steam technology that may potentially benefit of various bio-fuel sources like bio-oils or bio-coal, both being current objects of serious academic research.[22]

The popularity of heritage steam trains is growing rather than fading, regardless of the paradox that the demise of steam in commercial service was catalyzed by its primary sources of touristic attraction:

- smoke – a token of incomplete combustion,
- visible steam – indication of waste of heat energy,
- reciprocating rod mechanisms – cause of lateral, longitudinal, and vertical oscillations of uncomfortable if not harmful magnitudes, and spilling of lubricants to the environment.

All the factors mentioned above constitute the basis for the author's motivation to study the efficiency gap, together with alternative configurations for a 21st century steam locomotive. The topics have been approached, based on following assumptions, more or less evident to any observer:

1. Environmental concern reinforces the railways' position as a 'green' transport modality, as literally witnessed in print in tickets or shipping documents for customers in many countries.
2. Motive power is the principal factor of energy efficiency and emissions of railways, as moving freight or people involves all the energy the locomotives require.
3. Electrification will not be globally applied to all railway networks in near future due to reasons varying from techno-economical, like the expensive infrastructure, to political ones. In 2018 the share of electrified railways worldwide was 26 % of the total 1,3 Mkm route length, the

corresponding figure of e.g., the USA having been 1 % by the same time.[23] The vulnerability of the infrastructure is a relevant argument as e.g., a falling tree may stop an entire section of railway due to cut-off of electricity. Different electrification systems in neighbour countries belong to drawbacks of electrification even if the connection lines were electrified like e.g., in Russia and Finland.

4. Recent and ongoing research of steam technology indicates advances in green fuel production further discussed in Chapter 2, as well as in efficiency and tribology discussed in Chapter 3.
5. Rapid advance of accumulators makes recovery of braking energy an attractive potential in all kinds of vehicles equipped with electrical transmission as shown i.a. by the fast-growing popularity of battery-powered buses, trams, cars and even light vehicles.
6. Heritage railways grow in popularity, involving thousands of restored steam locomotives worldwide, such an activity being extensive enough to stress the relevance of efficiency and emission issues even within leisure and attraction businesses.

1.2 Hypothesis concerning the efficiency of steam locomotives vs. steam power plants

1.2.1 The basic assumption

The *dilemma* of choice of motive power exists if electrification of railways is not completely carried out, some potential reasons having been listed in Paragraph 1.1.3 above. By 2021, Switzerland was the only country in the world to have electrified all its railway lines.[24]

1.2.2 The hypothesis:

The roughly 10-fold difference between round-the-year efficiencies of steam powered electricity-producing power plants and steam locomotives is wasteful both in terms of economics and of energy conservation but can be substantially alleviated.

1.2.3 Aspects of the hypothesis

A. Theoretical aspect
A steam locomotive is a mobile rather than a stationary power plant, this fact being the principal difference of the two. The theory of thermodynamics thus applies to both, the viability of ranges of pressures and temperatures constituting the main limitation of the locomotive. Steam parameters 5,2 MPa and 810 K opted for the proposed locomotive concept of the present study yield a theoretical cycle efficiency of 0,31 with exhaust to condenser at atmospheric pressure and feedwater preheating to 373 K as later discussed in Paragraph 4.3. Such an efficiency would be 79 % of the predicted global average efficiency of modernized steam power plants.[25] The gap between the latter and the actual efficiency of the proposed locomotive is thus dependent on all the individual factors of efficiency further analyzed in Chapter 3.

B. Operational aspect
Since the advent of steam engines, efforts have been made to increase the efficiency even if only rare cases appear to have been based on the message of *Carnot's* theorem. By the time of the greatest advances in efficiency during the late 1920's the steam power was challenged by both electric and diesel traction seriously enough for the operators to neglect or overlook the said advances, to result in a stagnation of large-scale development of steam power. The

demonstrated *doubling* of efficiency of a steam locomotive considered to represent the state-of-the-art standard during late steam age and further discussed in Paragraph 3.5 was too late to attract more than marginal attention while other than efficiency-related aspects speeded up the demise of steam power as discussed in Chapter 2.

C. Statistical aspect
Many of the cited sources of the study discuss the issue of efficiency, suggesting a drawbar thermal efficiency between 0,06-0,09 for late steam age locomotives as discussed in Chapter 3. However, the given figures refer to test results rather than to round-the-year statistics, the latter thus inevitably yielding worse than the recorded results as proved by e.g., the case of South African Railways.[26] As for the power plants, the reported efficiency figures refer to operation on a continuous basis due to the nature of the production of electricity only involving stopping of turbines for maintenance. The statistics thus support the view of a vast gap between the efficiencies of classic steam locomotives and steam power plants. The cited report gives an efficiency range of 0,25 – 0,38 between the lowest and the highest current average power plants when comparing top 20 countries, and 0,30 – 0,44 for the same in case the suggested modernizing potential has been exploited.[27]

D. Concluding remarks
Some railways benefitted of plentiful and cheap coal reserves, the last North American big steam railroad having been 100 % steam powered until 1955 while e.g., South African Railways used steam locomotives until the 1990's and China as late as 2020. Today's global concern of conservation of energy renders the waste of energy intolerable and thus enhances the importance of efficiency. Other than efficiency aspects have aroused to emphasize the significance of proper configuration in making a locomotive a viable working tool.

1.3 Research questions

Diesel and electric traction obviously phased out steam traction primarily due to the low efficiency of the latter, even if there were cases like South Africa and East Africa where the actual operation costs of late steam age locomotives were lower than those of diesels when all the capital, interest and maintenance costs were taken in account.[28] [29] However, numerous other technical, operational, and even attitudinal aspects catalyzed the demise of steam. Characterizations like "steam *cannot* be as flexible, ergonomic or efficient as diesel" belong to the latter group.[30] Such a setting tends to render the key issue of efficiency rather academic on the *technical* level unless the revival of interest in steam locomotives is at first aroused by proving their viability as working tools. On the other hand, the fast-growing *global* concern of energy preservation indisputably adds to the significance of energy efficiency at all levels. The above said, the research thus culminates in two basic questions, in the below order:

1.3.1 What would be the optimum mechanical configuration of a 21st century steam locomotives, taking in account its tractive effort, operational flexibility and ergonomy?

1.3.2 What would be the efficiency of such locomotives, both in absolute figures and in relation to the efficiency of a state-of-the-art steam electric power plant?

Consequent sub-questions deal with:

- Selection of the prime mover and its operation characteristics
- Steam distribution system of the prime mover
- Recovery of the enthalpy of exhaust steam of the prime mover
- Recovery of kinetic energy of the train in downhill, or when braking.

1.4 Methodology

1.4.1 Assessing of characteristics and performance of locomotives analysed in the study follows the below systematics:

1. The evolution of classical steam locomotives, with an emphasis on analysing their configuration and efficiency, has been discussed within a desk study based on literature.
2. Assessing of the efficiency has been based on published data acquired during tests with dynamometer car, or at stationary testing plants, both methods being widely used for testing performance of different locomotives even today.
3. Pre-requisites from potential customers for eventual new type of steam power have been deducted from literature or reports of decision makers involved in motive power issues.
4. Advances in steam technologies, materials, and practices also covering automotive applications, have been considered within the desk study.
5. Innovative departures from the *Stephensonian* tradition have been discussed.

1.4.2 Predicting and comparing the performance of the pattern locomotive vs. diesel power relies on the acquired data, and on the selections and calculations following the below pattern:

1. Configuration and specifications of the pattern locomotive have been opted on the basis of conclusions of the desk study, and of the recognised pre-requisites of potential customers.
2. Detailed calculations have been executed, to determine the dimensions and adequate capabilities of functional elements of the pattern locomotive.
3. A simulation program has been created for virtual testing of locomotives in both yard work on level track and runs over a simulated actual line consisting of gradients, aptly taking in account all relevant resistances caused by bearings, friction, gradients, and air within appropriate speed ranges.
4. Simulations have been conducted within three different assignments for the pattern locomotive and a comparable diesel-electric locomotive with equivalent power settings, for obtaining and comparing results regarding energy consumptions.
5. The validity of the simulation program has been verified, by comparing results of the reference diesel-electric locomotive within actual tests conducted by its owner, with the results obtained from simulations.
6. Additional support for assessing of the simulation program has been acquired by simulating freight train runs with a classical steam locomotive, the performance of which is rather well known to the author from footplate working.
7. Properties and adaptability of bio-oil vs. fossil oil have been discussed referring to combustion tests made and jointly reported by equipment manufacturers and a research institute.

8. Locomotive crews have been consulted during various design stages of the pattern locomotive, to include the users' view of operability and ergonomy in the construction.

2. Evolution of the steam locomotive configurations

2.1 Pioneering locomotives

Richard Trevithick built the first usable steam locomotive in 1804. Like many of its early successors, it was too heavy for the contemporary trackwork and did not gain any wide popularity until the time of *George* and *Robert Stephenson* (father and son) who built their *'Rocket'* in 1829. This locomotive soon became - and remained - the basic pattern for almost all steam locomotives. Only rare experiments like turbine-driven and condensing locomotives partially departed from the functional principles of the *'Rocket'*. [31] Fig. 2.1 is a schematic view of the locomotive, the main characteristics of which are listed under the figure.

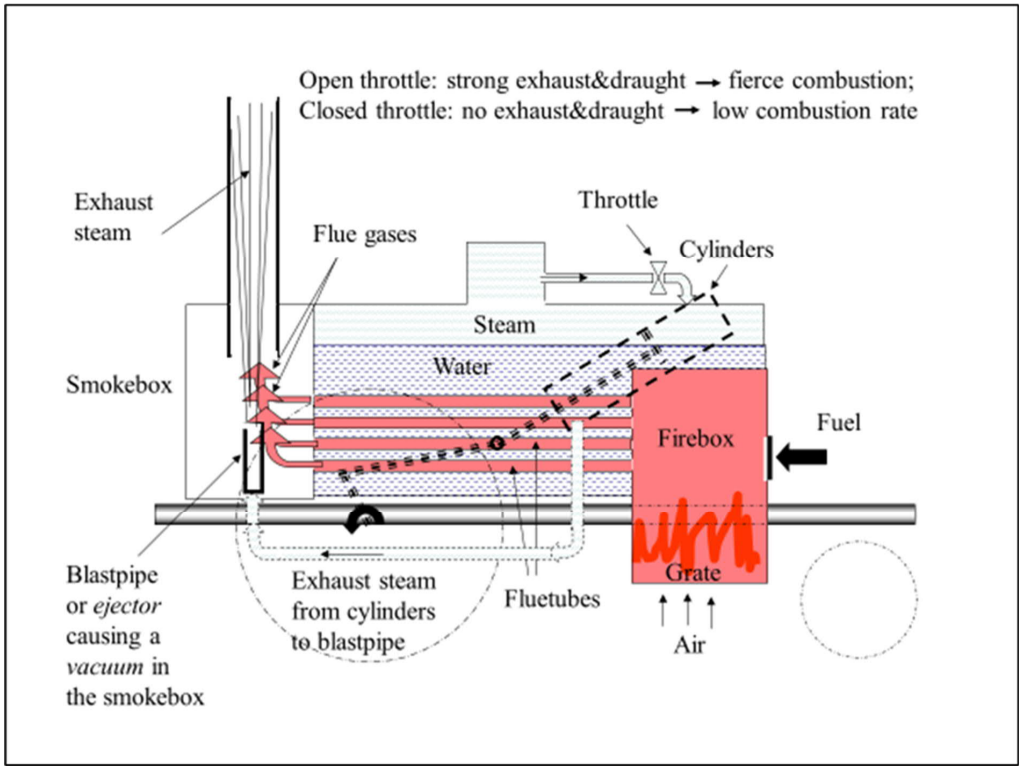

Figure 2.1: Functional sketch of the 'Rocket'.

The *'Rocket'* was the first one of the pioneering engines to demonstrate all the below features in a single locomotive:

- firebox surrounded by a water jacket increasing the direct evaporating surface,
- horizontal boiler with flue tubes that further increased the evaporating surface, [32]
- draught of the vacuum in the smoke box, caused by the exhaust steam nozzles or *blast pipe* ejecting the steam into the stack, thus linking the steam consumption and evaporation as it automatically regulates the rate of combustion, [33]
- two cylinders directly connected to the driving wheels, the cranks of which were staged by 90 degrees to secure adequate torque over the inevitable dead centres of cranks on both sides.

2.2 Working principle of a double-acting steam engine

The working cycle of elementary steam engines consisted of two stages:

- the *admission* stage let full pressure steam push the piston down to the bottom dead center,
- the *release* or *exhaust* stage made the piston push the steam out of the cylinder by returning the piston to top dead center.

Fig. 2.2 illustrates the principle of such an engine already employing *James Watt's* inventions like automatic steam distribution, *double-acting* cycle, and *expansion stage* described below. [34]

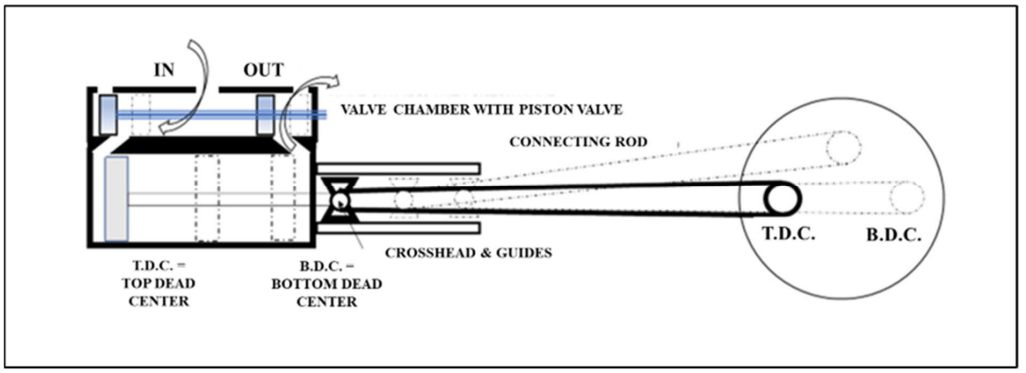

Figure 2.2: Principle of a steam engine with crosshead and piston valve.

In a double-acting engine, the events simultaneously take place on the opposite side of the piston, in reverse order. As stated above, *Watt* had discovered the expanding property of steam, consequently adding expansion stage to the working cycle as a third stage by *cutting off* the admission stage soon after it had started, rather than letting it fill the entire cylinder volume. [35] The steam trapped in the cylinder now expanded for the rest of the piston stroke, resulting in substantially lower steam consumption per stroke. Such an improvement still left two drawbacks in a three-stage engine:

- throttling of steam in valve passages during start of admission and release stages, and
- abrupt change of direction of reciprocating masses at both dead centres.

Three more stages were accordingly added, to mitigate the drawbacks. The resulting operation cycle thus consisted of six stages:

1. *lead*, or *advance admission*, to let the admission port open slightly before the top dead center, ensuring the full opening of valve by the time the actual admission started,
2. admission,
3. expansion,
4. *exhaust lead*, or *advance release*, to let the exhaust port open before the end of the bottom dead center, ensuring the full opening of valve by the time the actual release started,
5. exhaust, and
6. *compression* by closing the exhaust valve before the end of the release stage, to trap some steam in the cylinder to make up a cushion to smoothen the change of direction of the reciprocating components and consequently their bearings.

All the stages remained focal points of experimenting and research until the end of steam age and are shown in the *indication diagram* of Fig. 2.3 depicting pressure changes at one side of the piston.[36]

Admission pressure, *i.e.,* the boiler pressure *minus* pressure losses, at first prevails in the cylinder, this pressure then decreasing after *cut-off* point towards the end of expansion. Consequently, the shorter the admission stage, the lower the *mean indicated pressure.* The admission stage is characterized by admission ratio $\boldsymbol{\varepsilon} = V_{adm}/V_{disp}$, or the ratio between admission volume and the *displacement*, *i.e.,* the cylinder volume corresponding to full piston stroke. The *clearance space,* resulting in a corresponding *clearance volume* V_c, is necessary to prevent the piston from hitting the cylinder heads. The exhaust pressure p_{exh} is the higher the longer the admission stage, *i.e.,* the later the cut-off takes place. The incompleteness of expansion is thus directly proportional to the admission ratio ε. The significance of $\boldsymbol{\varepsilon}$ in steam engines lies in the crucial impact of expansion on the performance and efficiency of the engine, as the steam consumption is directly proportional to $\boldsymbol{\varepsilon}$. Typical minimum admission ratio of a piston engine is $\boldsymbol{\varepsilon}$ = 15 – 20 % (0,15 – 0,20), and the resulting expansion thus 85-80 % of the displacement.[37] All the parameters are taken in account within calculations of the *prime mover* of the pattern locomotive in Chapter 4.

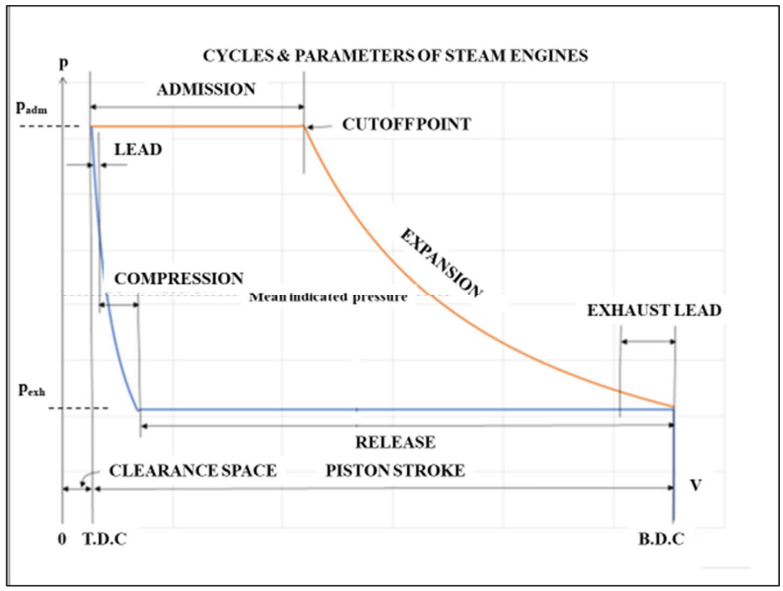

Figure 2.3: Indication diagram of the working cycle of a steam engine.

Plane-shaped *slide valves* constituted the mainstream system of steam distribution during the first century of locomotives, whereafter *piston valves* became prevalent, enabling a substantial widening of steam ports with consequent reduction of pressure drops.[38] Fig. 2.4 illustrates cross-sections of both slide and piston valves, the elevation of the latter having already been shown in Fig. 2.2. Other systems of steam distribution existed and are discussed in Chapter 3.

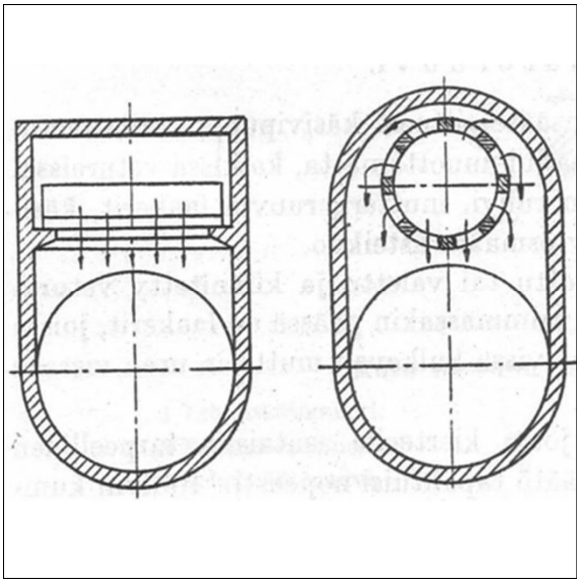

Figure 2.4: Steam flow to cylinder through slide valve on the left, and piston valve on the right.[39]

2.3 Variations of the *Stephensonian* concept of steam locomotives

The vast majority *steam age* locomotives were functionally direct heirs of the *Rocket* and hence often called *Stephensonian* locomotives, the universal characterics of which are listed in Table 2.1.

1. FIRETUBE BOILER TYPICALLY BURNING SOLID FUEL WHILE OIL-BURNERS WERE NO RARITIES
2. SUPERHEATED STEAM OF 623 K - 673 K (IN RARE CASES UP TO 723 K) AND 1,3 - 2,1 MPa (abs)
3. MAINSTREAM OF SINGLE EXPANSION STEAM CYCLE WITH OUTSIDE CYLINDERS
4. MINORITY OF COMPOUND CONFIGURATION OF EITHER RIGID-FRAME OR *MALLET* APPLICATION
5. NON-CONDENSING STEAM CYCLE, i.e. EXHAUST INTO THE ATMOSPHERE
6. FEEDWATER PREHEATING SYSTEMS WERE WIDELY USED
7. A CREW OF 2 ENGINEMEN WAS A MUST DUE TO PHYSICALLY STRESSING JOB OF FIREMEN, AND TO THE RESTRICTED VISIBILITY FROM THE MAINSTREAM CAB LOCATION
8. POOR VISIBILITY FROM TENDER LOCOMOTIVES RESTRICTED RUNNING AT THE REVERSE; TURN-AROUND FACILITIES WERE NEEDED AT TERMINUS STATIONS
9. MECHANICAL STOKERS WERE A MUST IN ENGINES WITH A GRATE > 6 m2
10. WATER AND FUEL REPLENISHMENT, LUBRICATION, AND ASH REMOVAL PRACTICALLY DICTATED THE FREQUENCY AND DURATION OF INTERMEDIATE STOPS OF TRAINS

Table 2.1: Typical characteristics of *Stephensonian* steam locomotives.

Rigid frame was the basis of pioneering locomotives and prevailed as the mainstream configuration until the end of steam age.[40] The frame with the boiler rested on two or more wheelsets, one or more of which were connected via rod mechanism to cylinders fixed in the frame. Fuel and water were carried in a separate wagon called *tender* and being fixed into the locomotive by a *pivot*. The size of driving wheels was increased, to add speed, while more driving axles were needed for hauling heavier trains.

The rigid frames set a limit to such a development, so after reaching a maximum diameter of 2,44 m in locomotives with a single pair of driving wheels during the mid-19th century, the diameters came down to 1,7 m in the all-time biggest rigid-frame locomotives built in 1926-30 with 6 pairs of driving wheels.[41] [42] Both types had additional supporting axles or trucks as shown in Fig. 2.5. The notation codes 4-2-2 and 4-12-2 refer to the *Whyte* system counting wheels rather than axles. Cross-section of the boiler of a steam locomotive is illustrated in Fig. 2.6. The cab and tender are not shown.

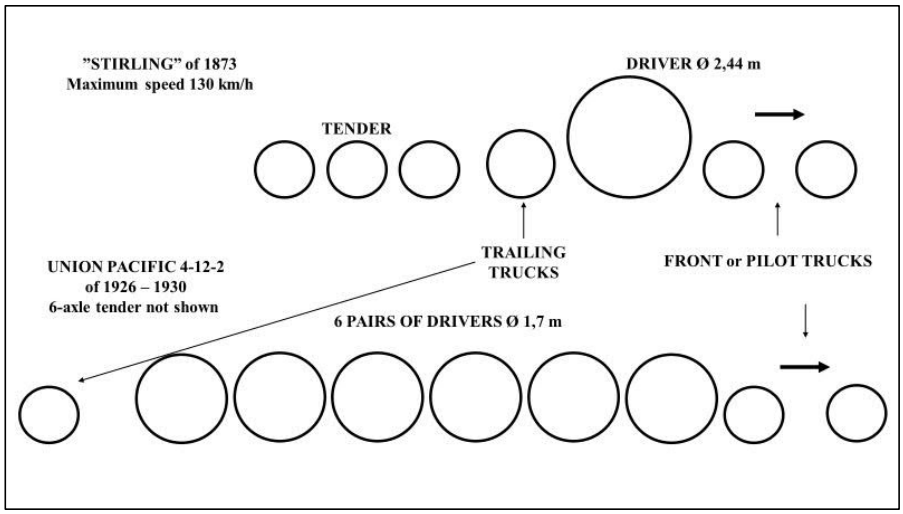

Figure 2.5: Wheel systems of British *"Stirling"* 4-2-2 and North American Union Pacific 4-12-2.

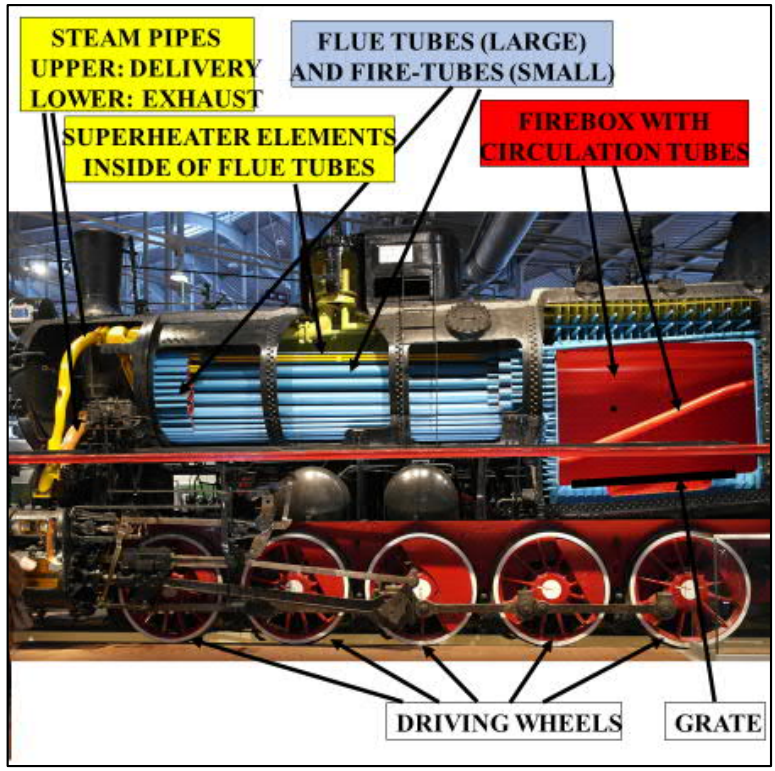

Figure 2.6: Cross-section of the boiler of a Russian Class Э locomotive. *Photo by the author.*

Imbalance of mass forces made truckless locomotives like the 'Э' suffer from drawbacks inherent of all 2-cylinder engines as described in Fig. 2.7, especially "nosing" being emphasized in the 'Э'.

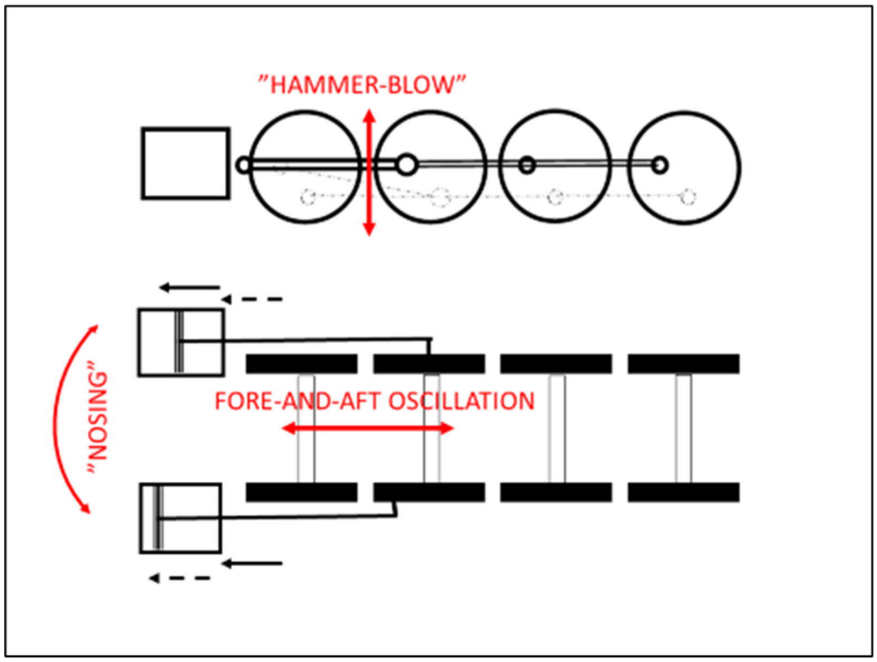

Figure 2.7: The imbalance caused by reciprocating masses of a 2-cylinder engine.

The *Whyte* system classifies the locomotive of Fig. 2.6 as a 0-10-0. The digits '0' indicate missing of both pilot and trailing trucks. The rigid frame restricted the speed of such engines to *ca.* 65 km/h, particularly due to reciprocating masses, *i.e.,* the 90-degree phase-shift between their movements on opposite sides of the locomotive. A pilot truck would substantially mitigate the imbalance, regardless of which more than 10 000 'Э's were built, making it the most numerous steam locomotive ever built.[43] The class was mainly used for freight traffic and heavy shunting work. The relatively light rod mechanism and slow speed of the 'Э' kept its mass forces at a tolerable level whereas the fore-and-aft oscillations of big 2-cylinder express train engines may be sensed by any attentive passenger even today on a heritage railway if seated in a coach close to the locomotive. The reciprocating masses of a '7MT', or the last British serial production fast train locomotive, were 383 kg *per* cylinder, these masses moving *ca.* 0,7 m back and forth once *per* revolution of driving wheels, *e.g.,* 5 times a second at a speed of 106 km/h. [44] Counterweights were used for balancing 40 % of the resulting fore-and-aft forces, the penalty being a 6,6-ton 'hammer blow' at the said speed.[45] In other words, the static load of *ca.* 60 tons on drivers was increased to 66 tons and decreased to 54 tons, 5 times *per* second, these having been substantially *lower* than average figures. The masses were up to 700 kg in the USA.[46]

Oscillating torque and tractive force made all 2-cylinder engines prone to slipping at start, or when climbing a gradient with a heavy train. Fig. 2.8 depicts the torque and resulting tractive force within a full revolution of driving wheels of a Finnish *Tr1* class locomotive working at 40 % admission ratio. The conspicuous difference in wave form and size is due to the geometry of the rod mechanism: if the ratio between connection rod and crank were infinite, the waves would be identical, but since the said ratio rarely exceeds 10:1, there is a substantial difference between the torque diagrams of outwards *vs.* inwards strokes of the piston, this difference being further emphasized by the 90-degree phase-shift of the opposite engines. It is the more notable, the higher the admission ratio.

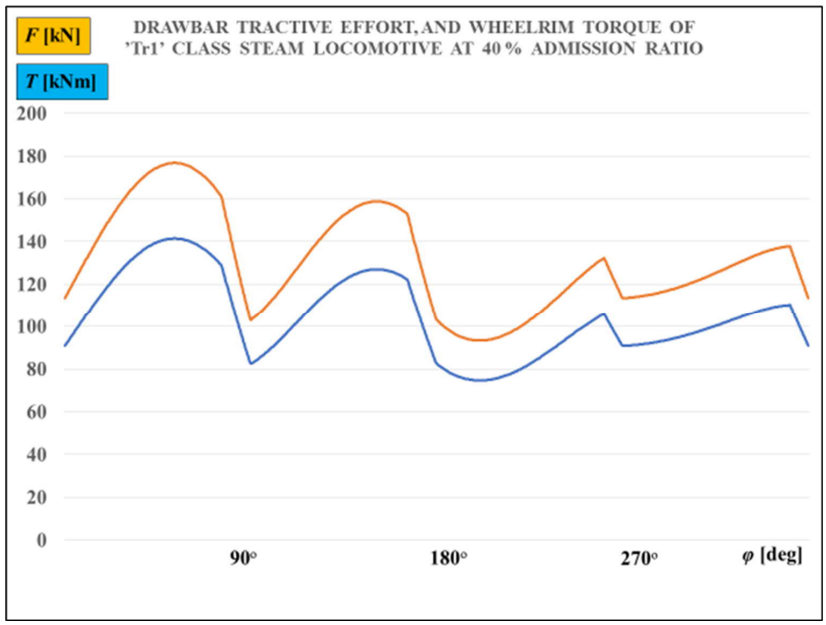

Figure 2.8: Torque and tractive force of a *Tr1* class locomotive within one revolution of drivers.

Tank locomotives, carrying the fuel bunker and water tanks on the engine frame itself, constituted an important subgroup of rigid-frame locomotives, Fig. 2.9 showing a popular *2-8-2 T* configuration.[47]

Figure 2.9: *Pr1* class 2-8-2T suburban traffic locomotive of Finnish State Railways. *Photo by the author*

Tank locomotives particularly excelled in suburban traffic, short line freight trains, and shunting work in which their bi-directional operability was a must. The wheel arrangement 2-8-2T ('T' for *tank*) of the

illustrated locomotive was re-known as a practical compromise between tractive effort and speed, making both the tank and tender versions popular as all-round engines in Europe.[48]

Double expansion or compound engines originated from efforts to improve the efficiency of steam engines, as further discussed in Chapter 3. On the other hand, compounding also introduced additional cylinders which substantially alleviated the drawbacks discussed above. *Anatole Mallet* pioneered in applying *compounding* in a locomotive in 1876.[49] His original concept consisted of a high-pressure (HP) and a low-pressure (LP) cylinder mounted on opposite sides of the locomotive, the arrangement being called a *cross compound* and shown in the left-most case of Fig. 2.10. The most common number of cylinders of later rigid-frame compounds was four, while the latest applications had three.

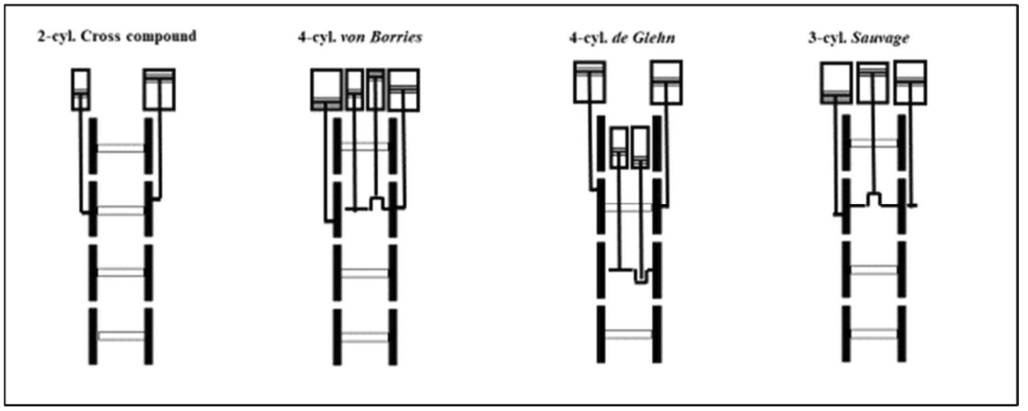

Figure 2.10: Compound configurations labelled by established terms.

The additional cylinders substantially improved the balance of reciprocating masses. Application of *August v. Borries* placed all the cylinders in-line, making them drive a common axle, whereas *Alfred de Glehn* divided the drive between two axles, thus reducing the mechanical stress of the crankshaft.[50] He aimed at minimizing thermal losses by placing the low-pressure cylinders inside of engine frame, but the inverse layout was a must in case the available space only accommodated the high-pressure cylinders.[51] The 3-cylinder layout by *Edouard Sauvage* is of special interest, as the single high-pressure cylinder in the middle exhausts the steam in two low-pressure cylinders, all the three cylinders having roughly the same dimensions and thus easy-to-balance reciprocating masses.[52] The inside cylinder necessitated a crankshaft and rod mechanism with restricted space and access between the frames and were thus regarded as burdens for efficient maintenance.[53]

Articulated locomotives had two or more *pivoted* frames, *i.e.,* the frames were connected by a flexible joint or *pivot*. The idea was a brainchild of *Mallet* who continued his developing of compound engine, by adding two cylinders and placing them in a frame separate from the one carrying the two original cylinders. Fig. 2.11 shows the last American *'Mallet'* side-by-side with Stephenson's *Rocket*.

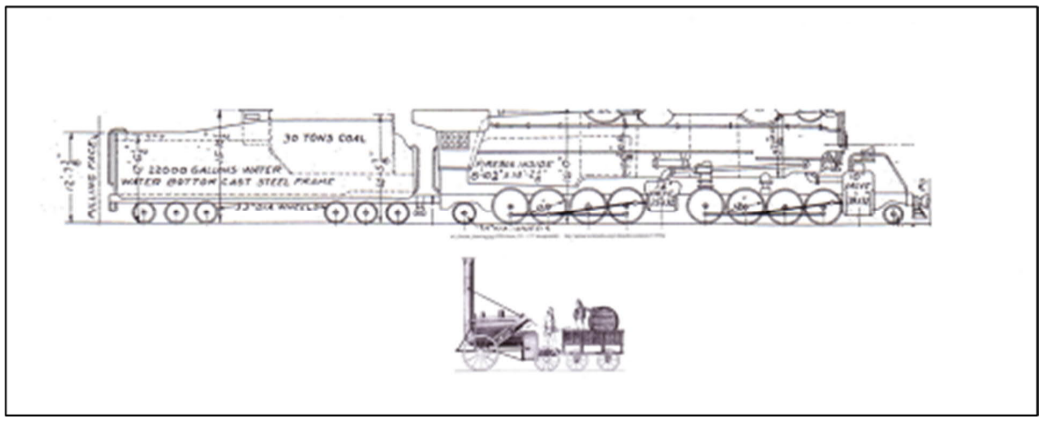

Figure 2.11: N&W's '*Y6b*' of 1952 was a true *compound* while most US *Mallet's* were *simples*.

Mallet's original concept comprised of 2 high-pressure cylinders attached to the rear frame with the boiler, and 2 low-pressure cylinders in the swiveling front frame, thus also contributing to easy negotiation of curves. Curiously enough, the configuration itself never found too many applications in Europe regardless of many European railways being re-known of tight curves and severe gradients. In contrast, it was quickly adopted in the USA where the configuration ultimately gave rise to the most powerful steam locomotives ever built, albeit being *simples* rather than *compounds*. *Mallet's* name was used in the USA to label the articulation concept irrespective of the expansion system.[54] The '*Y6b'* of Fig. 2.11 was a rare but successful exception of the American practice of favouring simple expansion over compound engines.[55]

The ***Cab-ahead*** configuration in Fig. 2.12, the reverse layout of which oil-firing made possible, would have theoretically enabled oneman operation due to the excellent visibility together with the combustion system. Smoke abatement in long tunnels promoted the success of the most numerous (256 units) application of this unusual concept on the Southern Pacific Railroad since 1908.

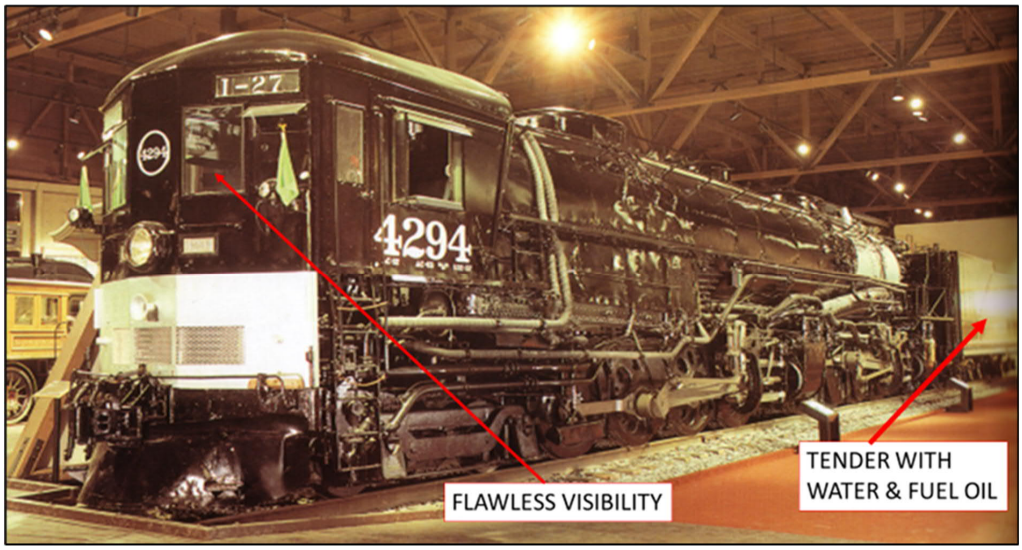

Figure 2.12: Southern Pacific (SP) *articulated cab-forward* locomotive at Sacramento, California.[56]

Beyer-Garratt type invented by *Herbert W. Garratt* in 1908 and patented by *Beyer & Peacock Co.,* has been regarded as the ultimate articulated configuration of classical steam, as most of its weight rested on driving wheels and the layout was better adapted to bi-directional operation than the poor-visibility *Mallet's*. [57] Fig. 2.13 shows a late-steam age example of *Beyer-Garratt's* of South African Railways (SAR). Many narrow-gauge railway systems world-wide benefitted of the *Garratt's* low center of gravity, as well as of its ability to negotiate both sharp curves and steep gradients. [58]

A *Beyer-Garratt* locomotive essentially consisted of two power trucks pivoted in a girder carrying the boiler. Both power trucks carried water tanks while the rear tank also included a fuel bunker. The underside of the boiler, without driving wheels, accommodated a deep firebox in contrast to a *Mallet* necessitating a trailing truck below its large firebox, in case the latter could not be fitted over drivers. The girder frame of the *Beyer-Garratt* was rigid enough, to carry the weight of the entire boiler.

A drawback, common to both *Mallet* and *Garratt* concepts, was their long steam pipes with flexible joints necessitated by swiveling frames, thus constituting potential sources of heat losses or leaks.

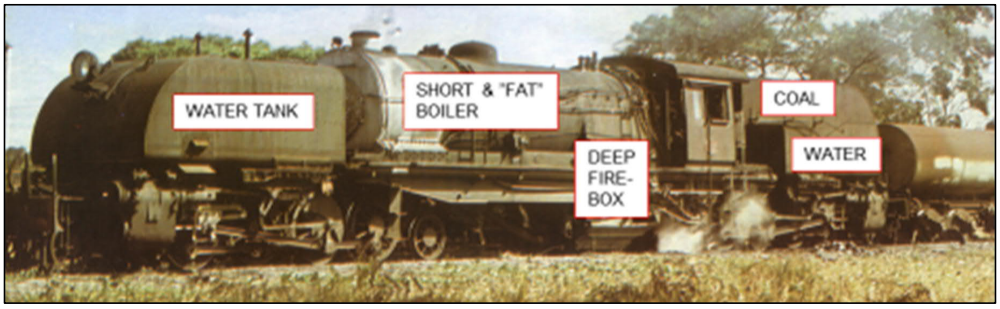

Figure 2.13: A South African *Beyer-Garratt* locomotive; no big wheels under the boiler.[59]

Geared drive version of articulation concept was practically the only one capable of traversing on poorly laid tracks of logging lines with extremely steep grades and sharp curves. Fig. 2.14 shows the construction patented by *Ephraim Shay* in 1881 and built until 1945, the engine shown being the last.

Figure 2.14: All the 162-ton weight of this *Shay*, including the invisible tender, is adhesive. *Photo by the author.*

All the 3 trucks (one below the tender not visible) are powered by the vertical 3-cylinder engine rotating a flexible line shaft at the bottom of the photo. Bevel gears transmit the power to each axle, making the engine capable of climbing 8 % grades and negotiating extremely sharp curves.[60]

Figure 2.15: An Italian version of *Franco-Crosti* boiler without the conventional chimney.[61]

Franco-Crosti boilers received their name from the two Italian inventors of the concept of exploiting heat of flue gasses to preheat the boiler feedwater. Fig. 2.15 shows the appearance of such a boiler.

The flue gasses are not exhausted through a conventional chimney in the front end of the boiler but turned around by 180 degrees to pass through a heat exchanger under the boiler after which they exhaust to the atmosphere *via* a side-mounted pipe. The photo shows the lid of the heat exchanger, the steam above the boiler indicating the location of the side-mounted exhaust pipe. Oddly enough, the first testing of the concept did not take place in its native country but in Belgium in 1932 while the Italians seriously started the research in 1939 and continued until the 1950's, the last one of roughly 200 engines being built in 1954. The concept was also adopted and developed in Germany, a prototype of class 42^{90} shown in Fig. 2.16 and featuring a single smoke box door that enabled an easy access to both the boiler and the preheater. Ultimately 33 engines were converted in Germany.[62]

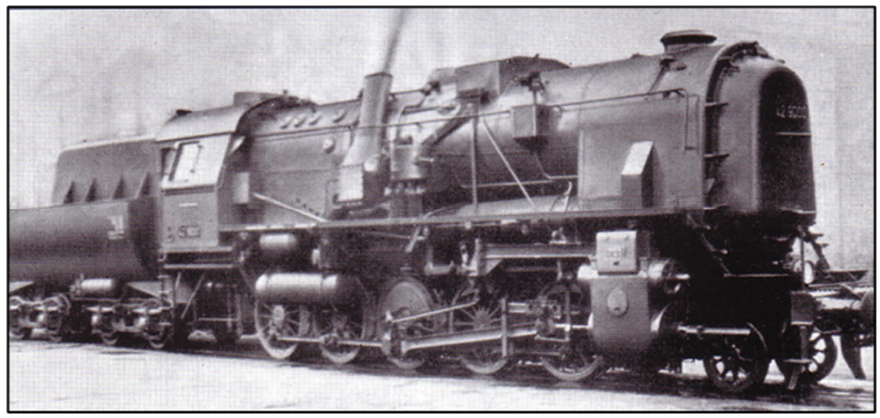

Figure 2.16: A German *Franco-Crosti* version, the 'normal' chimney being used for light-up.[63]

The preheater was to raise the temperature of water close to, and the pressure exactly to those of the boiler, potentially resulting in boiler efficiency of up to 0,91 or more as discussed in Chapter 3.[64] Thermodynamical assets did not everywhere justify the increased maintenance bills from corrosion problems, to the extent that British experiments with 10 *Franco-Crosti* conversions were regarded as unsuccessful resulting in blanking-off of the preheaters.[65] Condensing of moisture in the flue gasses containing fuel-based sulphur appears to have been the root-case of the problems.[66] Regardless of such drawbacks the savings brought by *Franco-Crosti* boilers proved sufficient to make the German engines survive until 1967, and the Italians well into the 1970's, or to the end of Italian steam age.[67]

2.4 Proven departures from the *Stephensonian* concept

Condensing locomotives deviated from the Stephensonian ones by their draughting system as the exhaust steam was not available for inducing the draught in the firebox so special draughting turbines were necessary. Condensers were introduced in small scale in the 1890's.[68] Latest applications of the 1950's had a condensing tender as big as the locomotive itself as shown by the sketch in Fig. 2.17.

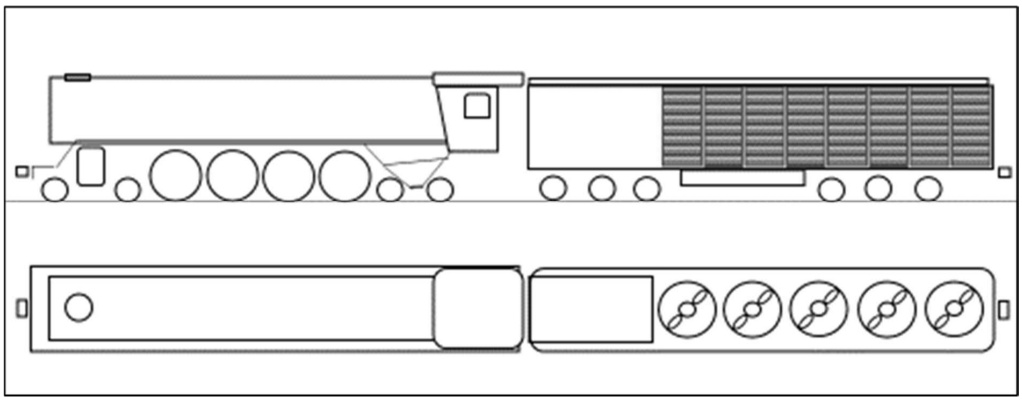

Figure 2.17: Sketch of the South African Railways (SAR) Class 25C condensing locomotive. *Sketch by the author.*

Condensing of exhaust steam has been motivated by both thermodynamical and environmental assets as it recovers part of the heat otherwise lost within the exhaust steam but also saves the correspondent amount of water.[69] The clumsy construction of condensers together with their labour-intensive maintenance hampered benefitting of their thermodynamical assets, resulting in their principal role as water-savers.[70] The tender of the SAR 25C represented about half of the 240-t total weight of the locomotive while only 78 tons of this total rested on driving wheels.[71] The configuration with side-mounted condensers could not exploit any natural cooling air flow, all of which had to be created by means of turbine-powered fans. Condensers ruled out the use of natural draught through the blast pipe that had to be replaced by a draughting turbine, the blades of which seem to have been the key problem of the condensing 25C locomotives, as abrasive coal particles in the flue gas quickly destroyed the blades.[72] Lubricating oil remnants in exhaust steam were inherent in reciprocating steam engines and had to be prevented from contaminating the boiler surfaces. This problem was known since the advent of condensing applications, but advance steps in lubrication and filtration systems ultimately brought the oil remnants to a tolerable level of 1-3 ppm.[73] The SAR accepted the maintenance costs of the 25C's only as a part of the water shortage problem, so the condensers were quickly removed after diesels took over at the dry areas.[74]

Steam turbines were tested for the first time in a locomotive in 1908 by *Ansaldo*, Italy, when an 1876-built conventional shunting locomotive was retrofitted with four turbines, each one individually geared to the four wheels of the locomotive that remained in service until 1920.[75] Turbines remained a marginal group as prime movers throughout the steam age as their drawbacks partially countered their evident assets. Table 2.2 shows a *pro-contra* assessment.

ASSETS OF TURBINES
1. HIGH POWER-TO-WEIGHT RATIO
2. PERFECT BALANCE THANKS TO LACK OF RECIPROCATING PARTS
3. ALMOST COMPLETE EXPANSION OF STEAM
4. NO MECHANICAL CONTACT BETWEEN ROTOR AND STATOR
5. OIL-FREE EXHAUST STEAM
DISADVANTAGES OF TURBINES
1. HIGH ROTATIONAL VELOCITY RULES OUT A DIRECT TRANSMISSION
2. EFFICIENCY DEPENDS HEAVILY ON THE SIZE OF THE TURBINE; BIG IS BETTER
3. EFFICIENCY DECLINES FAST ALONG DECREASE OF LOAD
4. ON-BOARD CONDITIONS ARE HOSTILE FOR PRECISION PARTS LIKE TURBINES

Table 2.2: Assets and disadvantages of turbines as prime movers of steam locomotives.[76]

Regardless of the above drawbacks some geared turbine locomotives were successful enough to prompt further constructions and survive to the end of the steam age. Applications of turbines by the Swedish *Fredrik Ljungström* in steam locomotives proved a success and became duplicated in Great Britain in a locomotive called *Turbomotive*.[77] The first *Ljungström* turbine locomotive had a condenser and was delivered to dry regions of Argentina where it initially performed well, but harsh conditions and inadequate maintenance ultimately brought it to a state beyond repair. It was later replaced by reciprocating locomotives.[78] The turbine had proved itself, though, and after extensive tests the Swedish State Railways (SJ) ordered and received one in 1927. The private Swedish Grängesberg&Oxelösund Järnväg (TGOJ) noted the success of SJ and eventually acquired 3 non-condensing versions based on a reciprocating class of their own. These ultimately proved to be the longest-living turbines anywhere in the world. [79] Their reliability has been addressed to three factors:

1. the design of the turbine itself was successful,
2. the overall construction was based on a conventional locomotive of proven design,
3. the *pro/contra*- analysis of condensing systems resulted in omitting the condenser.

In comparison with the same-size conventional TGOJ steam locomotives the turbines saved 7,5 % of coal while hauling trains with 1800 tons of weight instead of the previous 1400 tons, resulting in *ca.* 40 % increase in productivity per locomotive.[80] Fig. 2.18 shows one of the engines, all three of which still exist today, one of them being operational for special events.[81] The class was only used for freight traffic whereas the British *Turbomotive,* built in 1935, was dedicated to fast passenger train workings, resulting in its 4-6-2 wheel arrangement.[82] Preliminary results were positive, as heavy loads were hauled faster with lower consumption figures, the crews also having appreciated the smooth running of the engine, but World War II eventually ended the positive development due to maintenance problems that ultimately resulted in dropping the repair plans of the *Turbomotive* after the war.[83]

Figure 2.18: A non-condensing Swedish NOHAB-built geared steam turbine locomotive.[84]

The *Krupp*-built German condensing turbine locomotive of 1926 shown in Fig. 2.19 became a victim of World War II with its *Maffei*-built twin. Until their destruction, both the two operated with reported savings of up to 30 % in steam and fuel consumption at full power when compared with the same-size classical engines.[85]

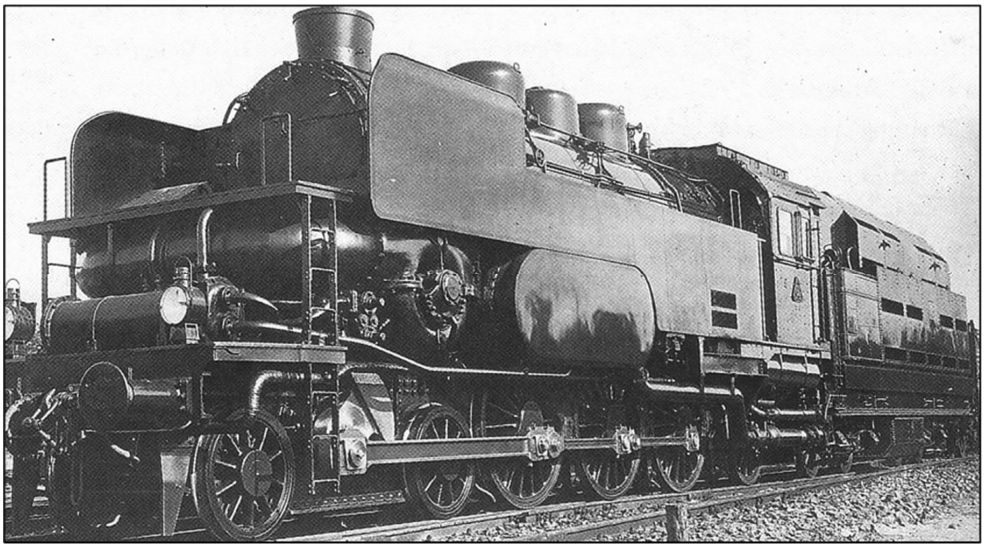

Figure 2.19: A German KRUPP-built condensing steam turbine locomotive.[86]

In both the Swedish and German versions, a transversal gearbox was mounted in front of the boiler. A *blind shaft*, *ie.* shaft without wheels, protruded from gearbox and transmitted the power to the side rods and thence to the driving wheels while the *Turbomotive* was driven by a gearbox directly mounted on a driving axle.[87] A similar system was applied in the last and by far the biggest experiment with geared turbine drive of the Pennsylvania Railroad *'S2'* built in 1944, weighing 450 tons and exerting 5070 kW power on the output shaft of the turbine, resulting in drawbar pull and top speed (160 km/h) to surpass even those of contemporary diesel-electric locomotives.[88] On the other hand, the specific steam and fuel consumptions at partial loads were regarded as inordinate, so after serving fast passenger traffic until 1947 the engine was scrapped as diesels took over.[89] A drawback common to all geared turbine locomotives was their need to have a separate turbine for reverse running as turbines only rotate in one direction.[90]

2.5 Experimental departures from mainstream constructions

Attempts to increase the efficiency of steam locomotives prompted innovative departures from the classical construction. All remained experimentals or non-materialized proposals while some of them included ideas worth exploitation within configurating the pattern locomotive in Chapter 4.

Ultra-high-pressure boiler with 12 MPa boiler pressure and 773 K steam temperature was tested in 1929-31 in a locomotive of the *Deutsche Reichsbahn*. The engine was a 3-cylinder compound, the two small-diameter high-pressure cylinders exhausting to a single low-pressure cylinder working at 1,3-1,4 MPa and 573 K. The boiler was equipped with a watertube firebox and forced circulation. Both the pressure and the superheat temperature were the highest ever used in steam locomotives while the complexity and maintenance costs of the boiler outweighed the reported 20 % coal savings over conventional locomotives.[91] The contemporary technology could not secure the tightness of piston rods of the HP cylinders.[92]

Yarrow type watertube boiler re-known for its marine applications was adopted by *The London and North-Eastern Railway* (L.N.E.R) in 1929, to be tested in an experimental high-pressure locomotive '10 000'. Working pressure was 3,16 MPa. The cross-section of the boiler in Fig. 2.20 shows its triangular overall shape with four water drums at the bottom and a single steam drum at the top. The slightly arched tube banks connected the drums. The cylinder layout with two inside high-pressure and two outside low-pressure cylinders was conventional whereas even the original volume ratio 1:2,8 which was later augmented to 1:4, deviated from the common practice of 1:2.[93] The change proved to be necessary since the original volume ratio resulted in an uneven distribution of power between HP and LP cylinders. Reducing the diameter of HP cylinders resulted in the latter volume ratio and was reported to rectify the problem.[94] Other innovations included a combustion air preheater which exploited the air space between boiler lagging and superheater tube bank, and a water preheater system to raise the feedwater temperature to *ca.* 480 K.[95] The benefits attained by the innovative design of the locomotive did not counter its maintenance costs resulting in eventual scrapping of the engine in 1938.[96] ***NB*:** The 1:4 volume ratio has been opted for the pattern locomotive in Chapter 4.

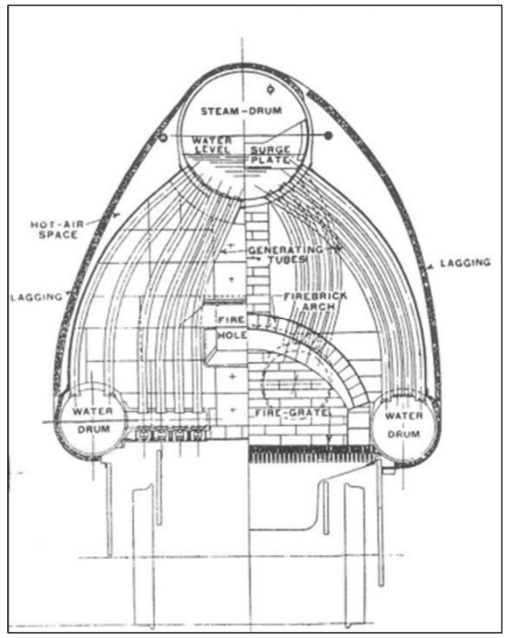

Figure 2.20: Cross-section of *Yarrow*-boiler of the British experimental locomotive '10 000'.[97]

Diesel steam locomotive was a Russian effort to combine the *Rankine* and *Diesel* cycles in search for benefitting of the unique ability of the steam engine to develop its full torque at zero speed without any gearbox, and further to exploit the efficiency of diesel cycle after attaining the required speed. [98]

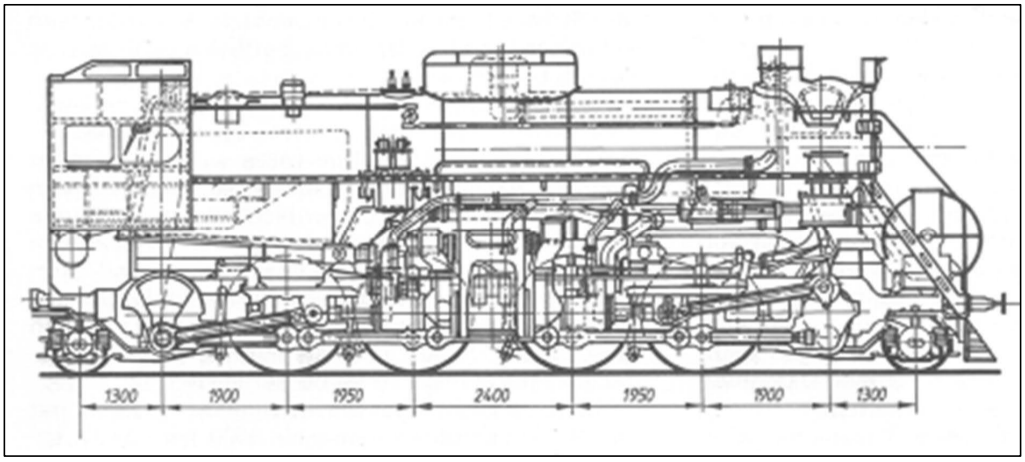

Figure 2.21: Prototype of a Russian diesel steam locomotive built in 1939. [99]

The pioneering efforts date back to the mid-1920's when *Ansaldo* in Italy and *Kitson* in England independently worked towards a similar aim, using compressed air (*Ansaldo*) or steam (*Kitson* with a *Still* boiler) to accelerate the engine enough for the diesel cycle to start. [100] Both the trials were marred by either pre-ignition or insufficient air or steam during the start-up, but the *Kitson-Still* concept was picked up by the Russians in 1935 with the aim of creating a locomotive that would employ both the cycles at a continuous basis. [101] The small *Still* boiler was replaced by an ample size conventional boiler with a capacity to enable the locomotive to exert maximum outputs simultaneously from both cycles and recover some of the waste heat from the diesel cycle to heat the feedwater. [102] Except for the similarity with *Ansaldo's* opposed-piston *Junkers* motor drive the resulting engine differed from both the experiments mentioned above, with a centrally mounted pair of opposed-piston cylinders driving blind shafts, these in turn driving the coupling rods. From mechanical point of view the concept was advanced, with the reciprocating masses practically balancing the fore-and-aft forces of each other, as the pistons on each side were in opposing motion by virtue of the return cranks on the blind shafts as seen seen in Fig. 2.21. During the start, boiler steam was admitted to the cylinders, and at a speed of *ca.* 15-25 km/h the space between the opposing pistons was started as a 2-stroke diesel by means of a turbocharger for combustion air, and of a high-pressure diesel fuel injection pump. [103] Even if the war interrupted the project and the maximum output could not be tested due to weight-related speed restrictions as the axle-weight exceeded 25 tons, the locomotive was tested in revenue traffic over the years and remained in service until 1948 after which it was withdrawn but preserved. [104] Table 2.3 is a brief summary of the reported test results. [105]

+	-
RANKINE & DIESEL CYCLES IN A SINGLE ENGINE	**COMPLEX CONSTRUCTION**
BALANCE OF RECIPROCATING MASSES	**CHALLENGING MATERIALS TECHNOLOGY**
VIABILITY OF RETURN CRANKS IN TRANSMISSION	**NARROW FEASIBLE SPEED RANGE**
	LOW POWER-TO-WEIGHT RATIO

Table 2.3: Summary of reported findings during runs of the diesel steam locomotive of Fig. 2.21.

Chain drive in steam locomotives was a brainchild of Sir *Oliver Bulleid,* the CME of Southern Railway, England, re-known for several uncommon designs. His aim was to introduce the best practices of ICE technology to steam traction by oil tight casing around the chain drive and thus prevent the transmission from getting dirty or spill lubrication oil to the environment.[106] Other pathbreaking innovations of the engine sketched in Fig. 2.22 included a welded boiler without staybolts in firebox, driver's cabs at both ends, and offsetting the boiler from centre line to accomodate a corridor to fireman's cab in the middle.

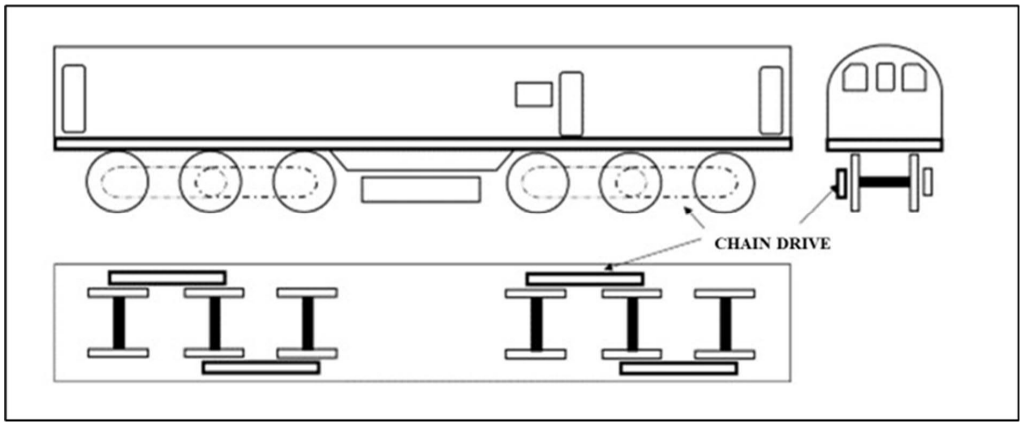

Figure 2.22: A sketch of *Bulleid's 'Leader'* with chain drive and cabs in both ends. *Sketch by the author*

Both trucks were powered by 3-cylinder steam engines driving the centre axles of the trucks, the drive to the other axles being transmitted by enclosed outside chains. Four thermic syphons compensated the missing waterlegs of the firebox, to secure a sufficient evaporative surface. Sleeve-type valves, practically unknown in locomotive use, distributed steam to the single expansion steam engines.[107] The sleeve valves proved to be one of the key sources of problems resulting in cancellation of the *'Leader project'* when Bulleid left the company, all the 5 engines in various manufacturing stages having been scrapped in 1951.[108] Many details of the '*Leader'* such as chain drive and truck-mounted compact steam engines were adopted into the construction of the *'Turf Burner'* of Irish Railways (CIE) tested in 1957-58, the most evident visual difference - regarded as a shame - being the centrally located single cab of the *'Turf Burner'*.[109] Table 2.4 is a combined review of the two chain drive prototype locomotives.

+	-
NO STAYBOLTED WATERLEGS	**SLEEVE VALVE SEIZURES IN *'LEADER'***
CHAIN DRIVE PROVED ITS VIABILITY	**OIL LEAKS OF CHAIN DRIVE**
ALL THE WEIGHT WAS ADHESIVE	**FIELD FIRE HAZARD OF *'TURF BURNER'***

Table 2.4: Summary of reported views of characteristics of *Bulleid's* chain drive locomotives.

Independent axle drive without coupling rods had been tested in France both in piston engine and turbine applications albeit with little success before the German *Henschel & Sohn* completed their experimental locomotive in 1941.[110] Technical solutions of both diesel and electric locomotives were applied. War conditions pained the time of the debut and operation of the engine which nevertheless turned out to be a considerable success.[111] The piston engines were fully enclosed, and the *Pawelka* couplings between motors and driving axles were adaptations from electric locomotives of *Siemens*.[112] In addition to its oil-tightness, the construction brought the reciprocating forces to a low level not experienced before in reciprocating steam locomotives.[113] Fig. 2.23 shows the locomotive.

Figure 2.23: The German 19.1001 class locomotive with four V-type steam motors.[114]

The slipping tendency of driving axles was a penalty of lacking coupling rods, resulting in pressure drops at the other motors in case one of them slipped, but the locomotive was known to have coped with up to 650-t express trains, and to have attained a speed of 186 km/h during braking tests.[115] The regulator was scheduled for modification, to resolve the slipping problem, but disastrous bomb attacks changed the course of events, bringing the career of the sole engine to an abrupt end in October 1944.[116]

+	-
DIESEL TECHNOLOGY STEAM MOTORS	**SINGLE *pro* DOUBLE EXPANSION**
MODULAR CONSTRUCTION	**LIMITATIONS OF FIRETUBE BOILER**
SMOOTH RIDING QUALITIES	**LIMITATIONS OF TRADITIONAL LAYOUT**

Table 2.5: Review of reported characteristics of the German 19.1001.

Electric transmission to the driving wheels of a locomotive with a non-electric prime mover was tested for the first time by the French *J. Jaques Heilmann,* whose first patent was issued in 1890.[117] His first version employed a saturated-steam firetube boiler with 1,26 MPa pressure, and an opposed-piston compound engine propelling a DC-generator while the boiler of the second version worked at 1,4 MPa and powered a 6-cylinder in-line compound engine, Fig. 2.24 showing this 2nd version.

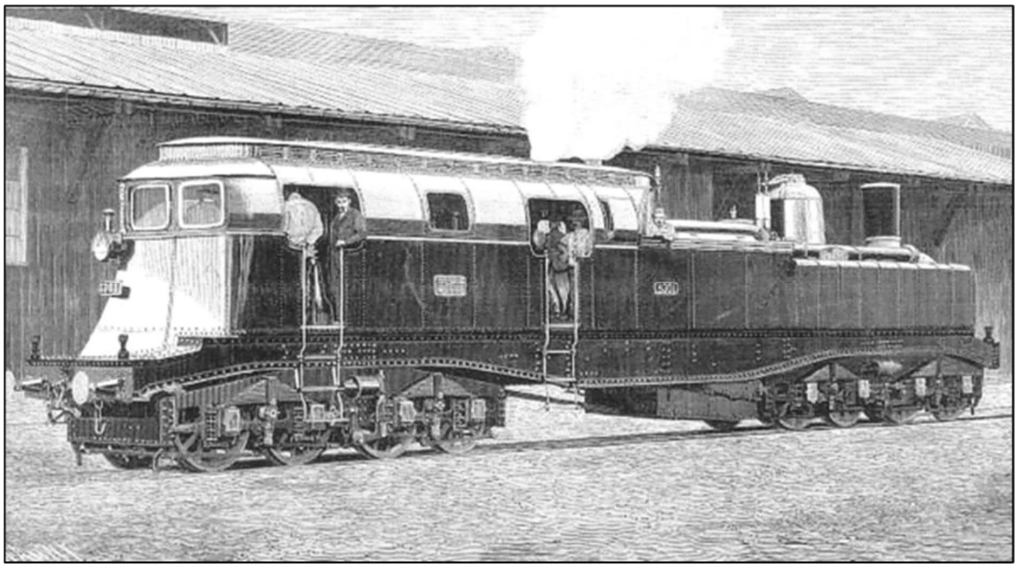

Figure 2.24: The second version of *Heilmann* steam-electric locomotives of 1897.[118]

Heilmann aimed at avoiding the handicaps earlier discussed in Fig's 2.7 and 2.8. All the 8 axles of the 2 trucks were powered by individual direct-current traction motors. The construction has been regarded as the forerunner of diesel-electric locomotive, since it was the first electric locomotive powered by its own carry-on power plant.[119] Acceleration, drawbar power and riding qualities of the locomotive throughout its speed range aroused positive comments in contemporary journals whereas its complexity, low power-to-weight ratio, and high personnel costs were criticized, as the crew consisted of a driver, a fireman, and an electrician.[120]

+	-
FORERUNNER OF CAB-AHEAD LAYOUT	SATURATED STEAM & LOW PRESSURE
FORERUNNER OF ELECTRIC TRANSMISSION	LIMITATIONS OF CONTEMPORARY DC-TECHNICS
FORERUNNER OF POWER TRUCK CONFIGURATION	LOW POWER-TO-WEIGHT RATIO
	ENGINE CREW OF 3 PEOPLE

Table 2.6: Review of reported operation features of *Heilmann* locomotives.

The General Electric steam turbine electric locomotives initiated from collaboration of the builder with the railroad company *Union Pacific* in 1938. The two locomotives were equipped with 10 MPa water-tube boilers, automatic oil firing, condensers, and dynamic brakes, at least in theory enabling operation by one-man crew.[121] Fig. 2.25 shows one of the locomotives, the boiler being marked with item number 16 in the drawings and appearing compact in relation to all other equipment. Practical information regarding the technical specifications, construction and performance of the locomotives is scattered, as both the main builder *GE* and the boiler manufacturer *Babcock&Wilcox Co.* appear to have erased the project from their files.[122] A neutral overall picture of the locomotive thus remains obscure, a compact summary being cited from *M. Klein's UNION PACIFIC*: "Despite some snags, the radical new engine lived up to its billing".[123] On the other hand, criticism regarding the complex construction, unreliability, and the ultimate returning of the engines to their builder, supports the conclusion that the teething problems were too challenging for the contemporary technology.[124] The two identical units were usually coupled as a twin and therefore generally referred as one locomotive. The 200 km/h design speed made the locomotives fit for passenger trains, but by the time of their introduction, diesels had just started to overtake in passenger services while the Union Pacific's decision to operate freight by conventional steam locomotives rendered a sole experimental couple of turbine locomotives useless, particularly in war conditions, as easy and standardized maintenance duties were a must.[125]

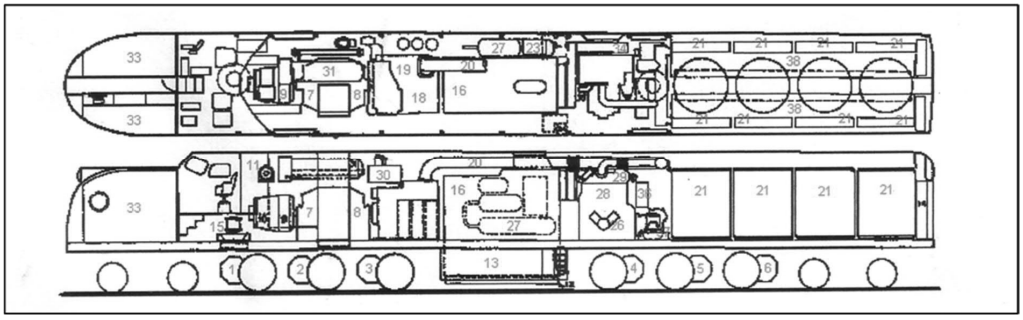

Figure 2.25: Unit of the GE/UP twin-unit steam turbine electric locomotive.[126]

The main characteristics of each unit of the twin are compiled in Table 2.7.[127]

THE GE/UP STEAM TURBINE ELECTRIC LOCOMOTIVE		
BOILER CONFIGURATION	WATER-TUBE	
COMBUSTION SYSTEM	OIL BURNER	
EXHAUST SYSTEM	CONDENSING	
GENERATOR TYPE	TWIN ARMATURE DC	
BRAKES	DYNAMIC AND AIR	
BRAKE COOLING SYSTEM	REGENERATIVE WATER COOLING	
DRAWBAR THERMAL EFFICIENCY	2 x CONVENTIONAL STEAM*)	
WORKING PRESSURE	10	[MPa]
STEAM TEMPERATURE	766	[K]
TURBINE SPEED	208	[r/s]
TURBINE-TO-GENERATOR GEAR RATIO	10:1	[]
MOTOR-TO-DRIVING-WHEEL-AXLE GEAR RATIO	65:31	[]
DRAWBAR POWER	1900	[kW]
STARTING DRAWBAR TRACTIVE EFFORT	385	[kN]
CONTINUOUS DRAWBAR TRACTIVE EFFORT	140-180	[kN]
RATED MAXIMUM SPEED	200	[km/h]
WEIGHT IN WORKING ORDER	249	[t]
*) AS SPECIFIED BY GENERAL ELECTRIC CO.		

Table 2.7: Main characteristics of the General Electric/Union Pacific steam turbine locomotive.

The locomotives were known to have undergone tests with dynamometer, but the author has not encountered any documents of such tests. The inaccurate efficiency statement is assumed to refer to a typical estimated efficiency of 0,07-0,08 of a classical steam locomotive. The unexact claim of the efficiency would thus yield 0,15. Remarks exist about combustion problems at high altitudes, and of retarded reacting of condensers.[128] The wavering reliability in war-time conditions contributed to the early withdrawal of the non-standard locomotives, after they had relieved a serious motive power shortage of *Great Northern Railroad* during 1943.[129] Table 2.8 is a summary of reported findings.

+	-
ADVANCED CLOSED-CYCLE DESIGN	SENSITIVITY OF CONTEMPORARY AUTOMATION
CHARACTERISTICS OF DIESEL ELECTRIC LEVEL	COMBUSTION PROBLEMS AT HIGH ALTITUDES
DYNAMIC BRAKES WITH ENERGY RECOVERY	INSUFFICIENT CONDENSING CAPACITY

Table 2.8: Summary of reported performance of the GE/UP steam turbine locomotive.

Norfolk & Western Railroad (N&W) steam turbine locomotive TE-1, called *'Jawn Henry'* and shown in Fig. 2.26, was the last materialized effort up to the present (2021), to create a standard gauge coal burning steam turbine electric locomotive. The N&W was the last big North American railroad to operate with steam power, having remained 100 % steam powered as late as until October 1955.[130]

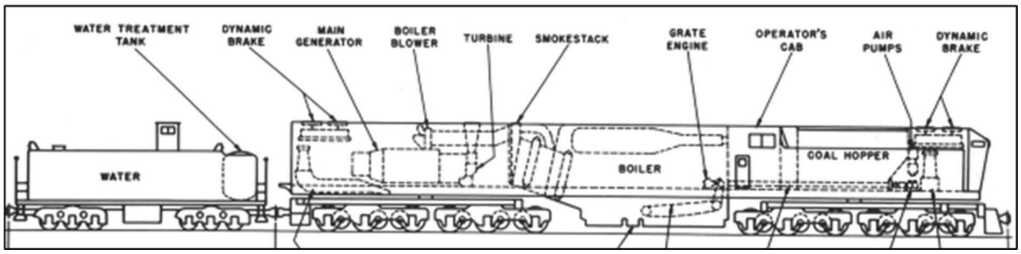

Figure 2.26: The N&W TE-1, with all the axles of the engine unit powered.[131]

The company was well informed of the success of diesel electric traction elsewhere and hence considered the viability of a steam turbine instead of a diesel prime mover to drive the electric generator.[132] The configuration and thus also the characteristics downstream of the prime mover are identical in diesel and steam powered alternatives. Fig. 2.27 shows a qualitative comparison between performances of diesel-electric and classical steam locomotives, the power range roughly conforming to Finnish rather than North American circumstances.

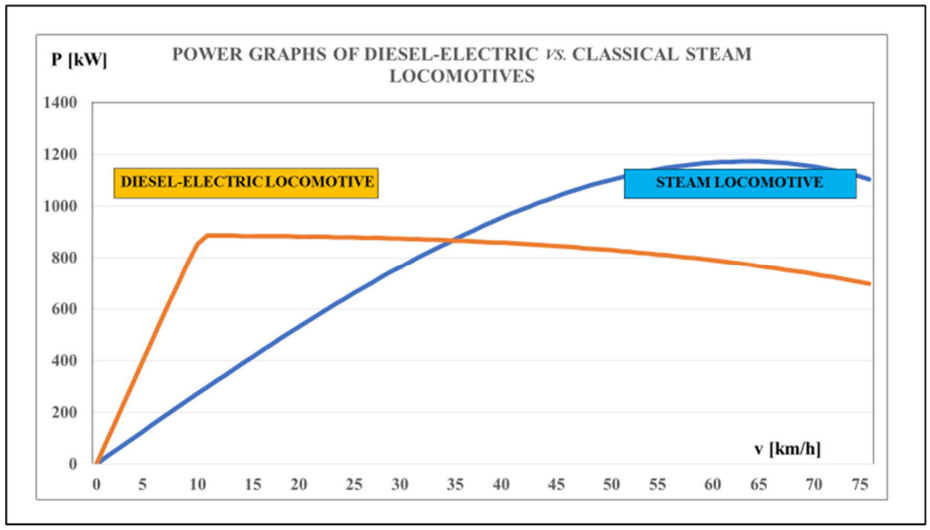

Figure 2.27: Power/speed relation of typical diesel-electric and steam locomotives.

The message of Fig. 2.27 is in the difference between the power curves of diesel *vs.* steam engines, as the former exerts power straight out from the start whereas the latter is a torque engine and only develops its maximum power at a higher speed, the ultimate power limit being set by the steaming capacity of the boiler. Even the classical steam power of the N&W was considered competitive in operation cost (price of drawbar horsepower) and therefore the predicted 50 % coal saving of an up-to-date version of modern steam locomotive appeared as a chance to keep on steam.[133] The Chesapeake & Ohio Co., at that time the biggest coal carrier of the world, made a turbine experiment by building three units without a prototype, albeit relying on traditional fire-tube boiler and having several idle axles in their engines.[134] In contrast, the N&W used all but the tender weight for adhesion. The specifications in Table 2.9 are given in rounded-up SI unit figures instead of the original ones.[135]

THE N&W 'TE-1' STEAM TURBINE ELECTRIC LOCOMOTIVE		
WHEEL ARRANGEMENT	4 x 3-axle trucks	
RATED POWER AT TURBINE SHAFT	3310	[kW]
STARTING TRACTIVE EFFORT	810	[kN]
RATED CONTINUOUS TRACTIVE EFFORT	665	[kN]
RATED MAXIMUM SPEED	95	[km/h]
TOTAL LENGHT INCL. TENDER	49	[m]
TOTAL WEIGHT IN WORKING ORDER	531	[t]
ADHESIVE WEIGHT	340	[t]
DRAWBAR THERMAL EFFICIENCY AT FULL POWER	0,08	[]
MAXIMUM RECORDED DRAWBAR THERMAL EFFICIENCY	0,12	[]

Table 2.9: Main characteristics of the N&W steam turbine locomotive 'TE-1'.

A summary of the runs has been compiled by the author, based on *L.M. Newton's* book about the locomotive covering both the construction stages and the test runs within the first year of operation, all the recorded events having been used for a database behind Fig's 2.28 and 2.29.[136] The graphs indicate that pumps of the feedwater system were the most frequent reasons for troubles, while the flashing of the generator caused the longest downtime. On the other hand, the boiler never failed on the road, although having been the principal topic of scepticism at the outset.[137] Condensers were omitted, due to the anticipated complexity of the system, but it remains an open question whether the numerous pumps and filters together with carry-on feedwater treatment system were less complex.[138]

The *'TE-1'* bet conventional steam locomotives in climbing hills, and in starting heavy trains, but fell behind at speed on level track. Its optimum use appears to have been helping heavy freight trains over the severest grades of the Norfolk & Western routes over the *Appalachian Mountains.*[139]

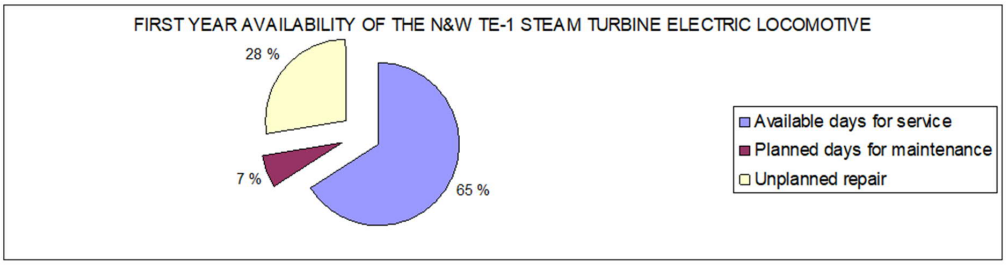

Figure 2.28: Availability of the N&W TE-1 locomotive 1st June '54 to 31st May '55.

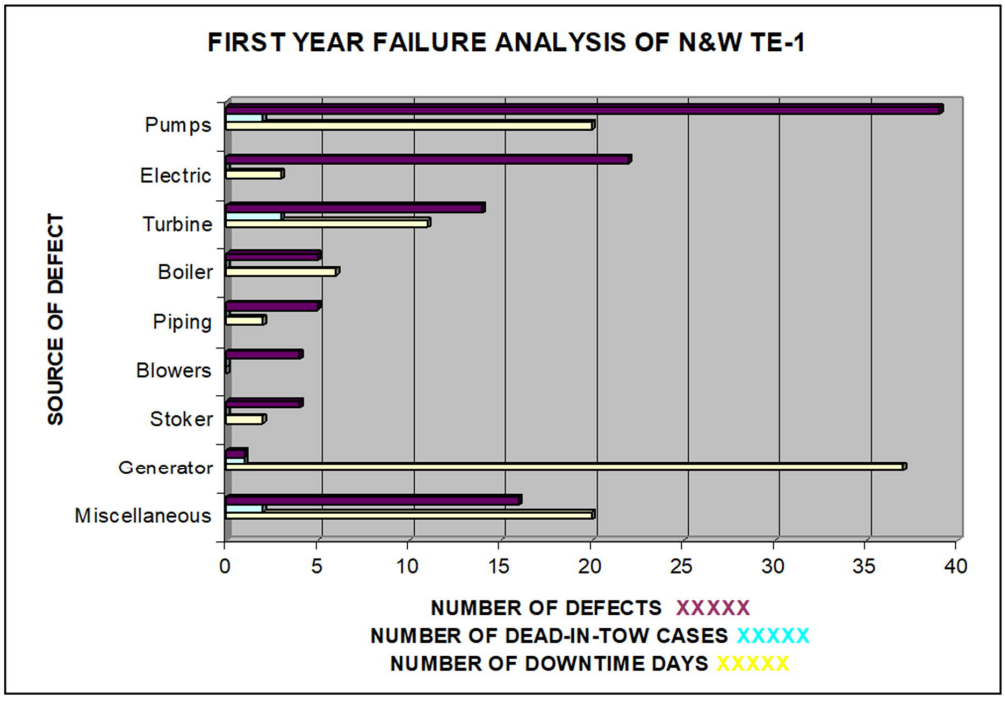

Figure 2.29: Failure analysis of the first operational year of the TE-1.

The tender constituted an additional operational disadvantage of the locomotive, its 49-meter overall length having necessitated uncoupling of the tender for turning the engine on 35-meter turntables.[140]

Up to the time of the present study, this was the world's biggest novel type of a mainline revenue service steam engine to have been built and operated. Improved design and further purchases were prospected, but a turbine damage ultimately resulted in withdrawal of the engine in 1958.[141] Table 2.10 reviews the performance of the *'TE-1'* in heavy-duty assignments within 3,5 years.

+	-
TOTAL LOCO WEIGHT WAS ADHESIVE	COMPLEX FEEDWATER SYSTEM
DIESEL-EQUIVALENT LOW-SPEED CHARACTERISTICS	NARROW ECONOMICAL POWER RANGE OF TURBINE
BOILER RESPONDED TO CHANGEABLE STEAM DEMAND	MINOR DEFECTS COULD STOP THE ENTIRE UNIT
DYNAMIC ALBEIT NON-RECOVERING BRAKES	INFERIOR TO CLASSICAL STEAM IN *GTM per HOUR*
DIESEL-EQUIVALENT RIDING QUALITIES	TURNTABLES REQUIRED UNCOUPLING OF TENDER

Table 2.10: Summary of recorded characteristic of the N&W TE-1.

2.6 Post-steam age proposals for steam locomotives

The global energy crises around the years 1973 - 1985 revived the interest in steam power in effort to reduce dependence on fossil oil as fuel. Various proposals have been projected, although none of them materialized so far. Coal prevailed as the primary alternative fuel of the proposals but has later become controversial due to its heavy global impact on greenhouse gas emissions and thus resulted in low-emission concepts of the latest projects. Due to the scope of the present study the potential relevance of projects involved with fossil fuel rather concerns the steam circuit and configuration than combusting.

2.6.1 Proposed 2200 kW direct drive steam locomotive of American Coal Enterprises (ACE)[142]

The proposed engine was called *ACE 3000* due to its nominal power of 3000 hp (*ca.* 2200 kW). It advanced to a stage of search for financing in the early 1980's, but never materialized. The ultimate cancellation in 1985 was due to *i.a.* changes in oil *vs.* coal price ratio, and to retracting of the railroad companies that earlier indicated serious interest in the project. Below characteristics of the locomotive were listed by *D. Wardale* who participated in the project.[143]

- boiler pressure 2,1 MPa,
- 2 x 2-cylinder compound configuration with conventional outside cylinders and rods,
- power rating 2237 kW continuous, 2983 kW maximum,
- maximum speed 130 km/h,
- interconnection of the two engine units by means of auxiliary coupling rods to retain a 180° angle between the engines, resulting in balanced reciprocating masses,
- firebox with *Porta's* gas producing combustion system (*GPCS)*,
- diesel tolerances in piston and cylinder liner design,
- coal replenishment and ash removal by rapid-change containers,
- predicted thermal drawbar efficiency of 0,18 maximum, and 0,15 in normal service.

Interconnection of the two engines to balance the reciprocating masses, applying diesel tolerances where feasible, and the rapid-change containers for fuel replenishment and ash disposal appear as the most interesting features from the viewpoint of the present study. The author assumes the predicted efficiency to be heavily dependent on the boiler efficiency, this in turn suffering from the entraining of coal particles inherent of stoker.[144] Assuming boiler efficiency of 0,80 for a capable coal-fired boiler vs. 0,95 for state-of-the-art oil-fired boiler, the author calculates the predicted maximum efficiency to be 0,21 instead of 0,18.

2.6.2 Proposed 2500 kW steam-electric locomotive by National Steam Propulsion Company[145]

The NSPC proposal of 1982 was called *CE-635* and originated from the same energy crisis than the ACE 3000. The design exploited a V-type 12-cylinder block of an existing diesel-electric locomotive. The block was to be modified as a double expansion steam engine with 6 high-pressure and 6 low-pressure cylinders, the generator section remaining essentially unchanged. The condenser and fuel tanks involved a support unit equipped with power trucks, so *all the weight would have been adhesive*.

In addition to the interest of several railroads the proposal was reported to have attracted the attention of Electro-Motive Division (EMD) of *General Motors Co*.[146] Lack of funding ultimately prevented the realization of the proposal, the main characteristics of which are given below:

- boiler pressure 7 MPa,
- fluidized-bed boiler with SO_x reduction,
- rated power 2574 kW, and
- predicted thermal efficiency 0,18 of the prototype but up to 0,27 of successive generations.

Assessing the viability of the predicted efficiencies is not possible without the superheat degree, not specified in the above parameters.

2.6.3 Proposed triple expansion steam-electric freight locomotive for US railroads[147]

The scarce printed information of the proposal by Mssrs. *George Carpenter* and *Robert Comyns-Carr* refers to a time frame of *ca*. 1990's and lists following characteristics:

- once-through coil type steam generator,
- 12 MPa working pressure,
- reciprocating steam engine with triple expansion as the prime mover,
- condensing steam cycle,
- nominal power of 3309 kW (4500 hp),
- electric transmission, and
- regenerative dynamic brakes.

All the qualitative characteristics of the proposal appear viable in view of the pattern locomotive and are discussed within its design in Chapter 4.

2.7 Recent and ongoing steam technology development projects

2.7.1 Automotive applications of steam technology

2.7.1.1 Steam generating in steam cars

Alan J. Haigh gives some details of *Doble* steam car of the 1930's in his book *The Design, Construction and Working of Locomotive boilers*.[148] The vehicle featured a condensing steam cycle with a coil-type monotube boiler producing steam at 5,5 MPa and 727 K. The limitations of weight resulted in a relatively modest heat exchanging surface and hence to a flue gas temperature of 555 K at exit of boiler. Consequently, the boiler efficiency remained at 0,80.[149] The coil-type boiler appears to have worked well in automotive applications.[150] Such a fact has been in a decisive role in selecting the boiler of the pattern locomotive in Chapter 4 as the boiler weight is not as critical in locomotives as in automobiles.

Ryti refers to test results of a 170-kW steam bus that started in 15-30 seconds from the ignition of the burner, the start having been immediate if less than 2 hours had elapsed of the previous run.[151]

2.7.1.2 Zero Emission Engine

A German joint project involved the *Freie Universität Berlin* and the *University of Erlangen* with a small enterprise *IAV GmbH* to creating a *Zero Emission Engine (ZEE)* in the 1990's. The engine was unveiled in 2000 and further developed until 2001, then promoted in an article of *Motortechnische Zeitschrift* and later in *VDI Bericht Nr 1565.* Steam parameters of the *unlubricated* 3-cylinder 998-cc. 50-kW engine were 5 MPa/773 K, the calculations extending to 950 K. Materials of pistons and cylinder liners were not specified in documents mentioned above, but cheramic coating has been presumed. Each cylinder had its own burner and steam generator, enabling the individual operation of any number of cylinders. A test bench brake power efficiency peaked at 0,24.[152] The concept has been exploited and further discussed within configuration of the pattern locomotive in Chapter 4.

2.7.2 Torrefied wood or *bio-coal* project[153]

Minnesota University and *Coalition for Sustainable Rail* (*CSR*) launched a joint project in 2012 to restore an ex-AT&SF (*Atchison, Topeka* & *Santa Fe Railroad)* 4-6-4 steam locomotive of 1937, and convert it to burn *bio-coal* or *torrefied wood pellets* instead of fossil fuel. *Natural Resource Research Institute* of the Minnesota University acquired a pilot plant to develop and test the torrefaction procedure, the product of which was at first tested in practice on a narrow-gauge railroad since 2016. Encouraged by the promising results, the tests were further continued in a normal gauge locomotive in 2019. The most recent information of the tests has been published in August 2019, referring to 'generally satisfactory results.' Quick lighting and hot burning were mentioned. The same report made a point of the ongoing nature of the study, the ultimate pursuit of which is a biomass pellet that burns similarly to coal but minimizes smoke and net-carbon emissions associated with the fossil fuel. As for the 4-6-4 locomotive restoration project, the engine has been externally restored and is waiting for a decision whether the restoration should be extended to operational degree. The *CSR* is a not-for-profit organisation supported by donations, while the workforce, essentially disciples of the late *L.D. Porta,* have been consulting heritage railways both in the Americas and Europe.

2.7.3 Waste heat recovery systems development

Several academic studies concerning recovery of waste heat of internal combustion engines by means of various *bottoming cycles* have been recently reported. The most interesting ones from the viewpoint of the present study are those exploiting the *Rankine* cycle, the studies of *G. Latz* at *Chalmers Technical University*, Sweden in 2013 and *Paanu et al.* at *Vaasa University*, Finland in 2012 are mentioned here. The present study exploits the *Rankine* cycle as the *principal* process and thus benefits of the maximum temperature difference of the system whereas the referred studies concern exploiting the *Rankine* cycle (or alternative cycles) as a *bottoming* cycle with a shorter temperature range and thus inevitably lower thermal efficiency as explained by *Carnot's theorem*. Nevertheless, the studies point out the potential of *Rankine* cycle to increase even the efficiency of diesel engines.

2.8 Conclusions about configurations

Rigid frames reached the limits of their dimensions by the 1930's, or at the time the diesels started to overtake steam power. The transit period both reinforced the advance of articulated concept and gave

birth to innovative departures resulting in experimental or proposed concepts. Below statements contain both general views, and opinions expressed by *connoisseurs* of steam.

1. Rigid frames limited the size, speed, and tractive force of a steam locomotive as both its size and stability called for pilot and trailing trucks while only axles within the rigid wheelbase contributed to the tractive force. Except for tank engines and truckless types with low speed, the adhesive weight of rigid frame locomotives was typically less than 40 % of the total.
2. Only multi-cylinder layouts of rigid-frame locomotives resulted in a satisfactory dynamic balance of the reciprocating masses.
3. Articulated concepts like *Mallet* and *Beyer-Garratt* involved cylinders moving in relation to the boiler and thus required flexible joints in high-pressure steam pipes prone to leakages. The pipes also caused heat losses and pressure drops.
4. *Beyer-Garratts* evidently surpassed *Mallets* as regards their adhesive weights, bi-directional operability, and speed.[154]
5. Oil-firing facilitated a cab-ahead version of the *Mallet* concept, resulting in an ergonomic layout with a perfect visibility.
6. Electric transmission, powering two swiveling trucks, proved itself in the first steam electric locomotive before the advent of diesels, in which the concept was ultimately adopted and developed, to take the shape prevailing today.
7. Three North American heavy-duty experimental steam turbine electric locomotives further supported the viability of the electric transmission as the causes of eventual failures of the engines were elsewhere.
8. Chain drives remained a curiosity in steam locomotives, but to begin with, power trucks were successfully applied, and secondly, chain drives mechanically proved themselves, even if the teething problems of oil-tightness remained unsolved during the short career of the prototypes. The steam engines of the swiveling trucks retained the disadvantage of flexible steam pipes.
9. Experimental and proposed locomotives, as well as automotive solutions, include innovative boiler constructions departing from the long horizontal tradition. Watertube boilers did prove their capabilities, regardless of remaining a curiosity during the phasing-out of steam power.

The author's conclusions of the above statements suggest selecting a configuration combining *power trucks*, a primarily *piston-type prime mover*, *electric transmission*, and a *monotube-type boiler* for the basis of the pattern locomotive design. Such a selection is expected to result in exploiting 100 % of the total weight for adhesion, location of the prime mover in an insulated compartment, a flawless transmission of power to axles, and space between the trucks accomodating a vertical boiler.

3. Efficiency of steam locomotives

3.1 Definitions of efficiency and its components

Until 1824, no theoretical approach seems to have existed about the relation between work performed and energy used by a heat engine. It was then that the French scientist *Sadi Carnot* published his consideration, even if not explicitly formulated, about the thermal efficiency of heat engines. [155]

Carnot's compatriot *Clapeyron*, a railway engineer and locomotive designer, revised and published the said consideration as formula (3.1), still re-known as *Carnot's theorem:* [156]

$$\eta_C = 1 - \frac{T_1}{T_2} \tag{3.1}$$

The formula is valid for an *ideal* heat engine where no increase of entropy takes place within the working cycle, η_C standing for its efficiency, T_1 for its lowest, and T_2 for its highest temperature [K]. Aptly called *Carnot*-efficiency, the η_C thus only depends on the maximum and minimum temperatures of the cycle. Increasing of efficiency is therefore only possible by increasing T_2 and/or decreasing T_1.

Due to its dealing with an ideal process, Carnot's theorem was an academic rather than practical assessing tool. It did, however, alert the most serious locomotive engineers to analyse the root causes of low efficiency of steam locomotives. [157] The temperature window of the latter was - and still is - narrow in comparison to stationary power plants, since

- cylinder oils typically set the upper limit for T_2 at 660 K almost to the end of steam age, [158]
- exhausting to the atmosphere practically set the minimum value of T_1 at 373 K, [159] and
- even in case condensers were used, subatmospheric pressures were not practicable. [160]

A steam locomotive is a mobile power plant consisting of the steam generator or boiler, and the steam engine. The boiler consists of flue gas side and steam side. The latter and the steam engine of the locomotive comprise the *steam cycle* comparable to a simple power plant cycle sketched in Fig. 3.1.

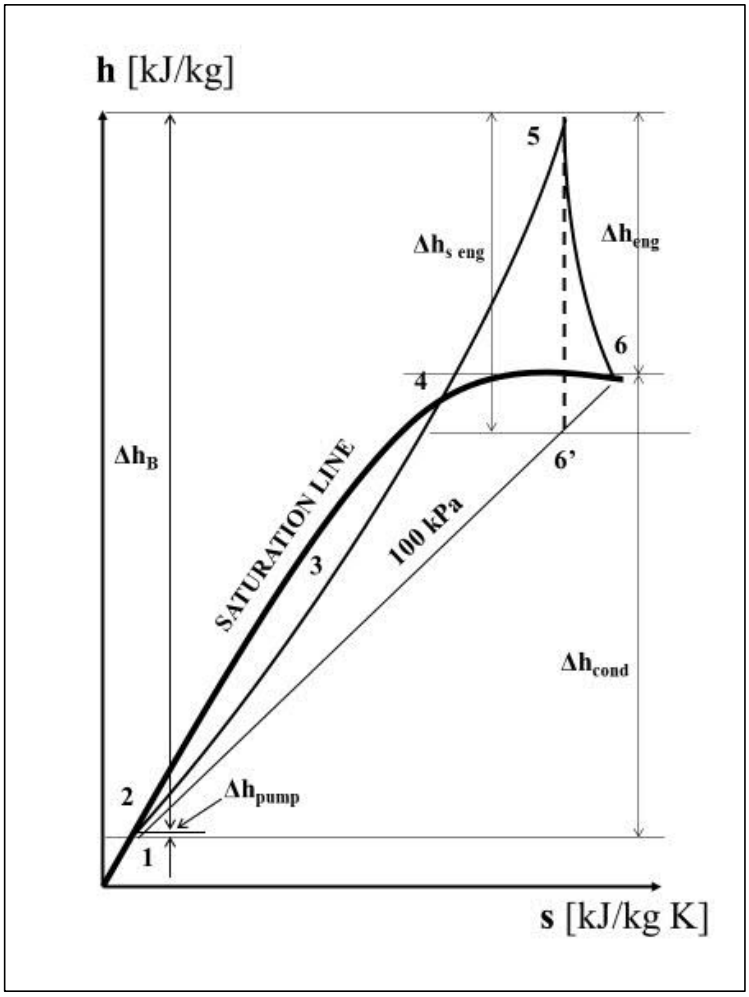

Figure 3.1: Principle of a simple power plant steam cycle.

In a power plant with condensing, the start of the cycle would take place at a subatmospheric pressure whereas a non-condensing steam locomotive exhausts into the atmosphere. Even if a condenser were fitted, it would in practice work at atmospheric pressure, to minimize leaks, and thus the pressure at point 1 would be 100 kPa, the specific enthalpy corresponding to the temperature of the feedwater. Raising the feedwater pressure to that of the boiler involves an enthalpy rise Δh_{pump} to point 2, from which the water starts evaporation at constant = boiler pressure during stage 3 until the saturation line is achieved at point 4, all the water then having been evaporated. The cycle continues by superheating the steam, still at boiler pressure, to point 5 where the steam enters the expander, *i.e.,* turbine in a power plant, or piston engine in a locomotive. The dotted line 5-6' depicts an isentropic drop of enthalpy and conforms to the ideal *Rankine* cycle, bearing the name of its inventor, the actual drop following the line 5-6. For a typical locomotive boiler with 1,6 MPa working pressure and superheat temperature of 623 K, the Δh_{pump} would be *ca.* 1,65 kJ/kg, *i.e.,* of a marginal order in relation to the 3145 kJ/kg of superheated steam, the difference between isentropic and non-isentropic rise of enthalpy in the pump thus being negligible and the pump itself being practically isentropic.[161]

According to *Ryti*, the efficiency η_{stc} of the steam cycle can be expressed in terms of enthalpy changes within the steam cycle, using the symbols of Fig. 3.1, and is obtained from formula (3.2)

$$\eta_{stc} = 1 - \frac{\Delta h_{cond}}{\Delta h_B} \tag{3.2}$$

Chapelon used to assess the performance of his modificated locomotives by comparing the efficiency of their steam cycle to the efficiency η_{Rank} of the ideal *Rankine* cycle of Formula (3.3)

$$\eta_{Rank} = 1 - \frac{\Delta h_{cond\,s}}{\Delta h_B} \tag{3.3}$$

assuming *isentropic* expansion of steam in the engine to atmospheric pressure, *i.e.,* referring to point 6' in Fig. 3.1. The message of the numerator in both formulae is that simultaneous decreasing of enthalpy of exhaust steam, and increasing temperature and thus enthalpy of feedwater, decreases the Δh_{cond} and thus increases the efficiency. Maximizing the enthalpy drop within the engine is thus an obvious target, limited by the steam temperature as was discussed above, and by the *internal isentropic efficiency* η_s of the engine. The η_s is characteristic of the type and size of the engine, big and well insulated engines attaining the best figures, and turbines typically surpassing piston engines except for power range below 1-1,5 MW.[162] *Mollier's h, s* chart is a practical tool for illustrating the impact of isentropic efficiency to the expansion stage of the steam cycle as shown in Fig. 3.2 below.

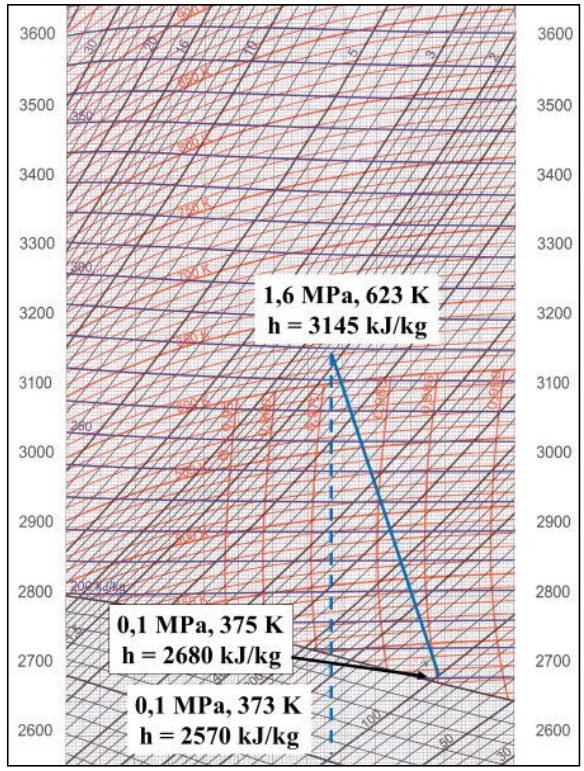

Figure 3.2: Isentropic and non-isentropic enthalpy drops in a single expansion engine.

Towards the end of steam age, typical working pressures were at least 1,6 MPa while superheat temperatures reached up to 720 K, *ca.* 660 K having become quite a common figure and contributing to increasing the isentropic efficiency to 0,90 or higher as proved in practical tests by *Chapelon* and *Porta* in their compounds, and by *Wardale* in a single expansion locomotive.[163] [164]

The dotted blue line in Fig. 3.2 shows the isentropic drop of enthalpy to the value corresponding to the atmospheric pressure (0,1 MPa) while the unbroken blue line shows the actual enthalpy drop on the constant pressure line, thus the steeper the blue line, the higher the isentropic efficiency, Fig. 3.2 yielding η_s = (3145-2680)/(3145-2570) = 0,81. The *indicated efficiency* η_{ind}, rather than *steam cycle efficiency* η_{stc}, is commonly used in the steam locomotive practice, for assessing the performance of the cylinders, taking in account the boiler efficiency η_B and the *own consumption efficiency* η_{oc} as in Formula (3.4):

$$\eta_{ind} = \eta_{stc}\eta_B\eta_{oc} \tag{3.4}$$

Efficiency of the boiler is the product of *combustion efficiency* η_{comb} and *absorption efficiency* η_{ab}:

$$\eta_B = \eta_{comb}\eta_{ab} \tag{3.5}$$

the η_{comb} being sensitive to the fuel quality as discussed further below, and the η_{ab} depending on radiation and convection of heat of flame, and of flue gasses. Both components are further discussed within the cases assessed. The overall efficiency of typical late steam age stoker-fired coal burning locomotives often remained η_B < 0,70.[165] *Chapelon* gives η_B = 0,78 for *conventional* boilers, referring to hand-fired French locomotives with advanced steam and fluegas circuits.[166] Mechanical losses of the engine are depicted by its *mechanical efficiency* η_{mech} while the *transmission efficiency* η_{tr} further reduces the *drawbar thermal efficiency* η_{db} of the locomotive to be obtained from Formula (3.6):[167]

$$\eta_{db} = \eta_{ind}\eta_{mech}\eta_{tr} \tag{3.6}$$

The drawbar thermal efficiency, on the other hand, depicts the share of chemical energy of fuel converted to drawbar work, and since power P_{db} = work input W_{db} divided by time t, and similarly for the boiler, firing rate Φ_B = fuel energy input E divided by time t, Formula (3.7) is valid:

$$\eta_{db} = \frac{W_{db}}{E_F} = \frac{P_{db}}{\Phi_B} \tag{3.7}$$

3.2 Impacts of various losses on the efficiency

The energy balance of an average single expansion steam locomotive of the 1950's, visualizing the various losses, is shown in Fig. 3.3, item 8 of which directly indicates the percentage of fuel energy converted to drawbar work and thus the drawbar thermal efficiency η_{db}.
Despite of being low at the outset, the average of 7,25 % only represents a standard attained in regular work and thus neglects, *e.g.,* shunting work of a most intermittent nature, not to mention the sources of non-productive consumption of fuel, the round-the-year figures inevitably remaining much lower.[168]

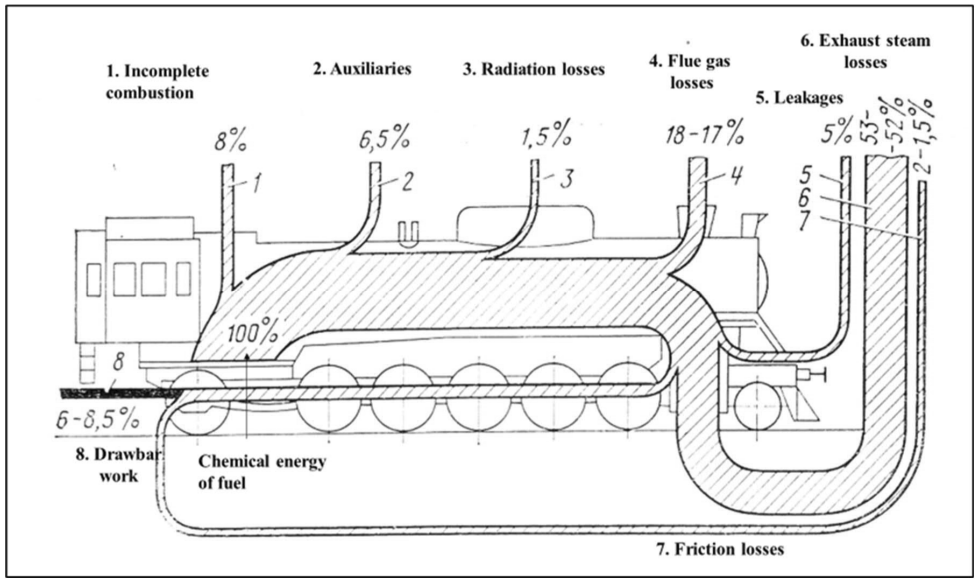

Figure 3.3: Energy balance of a 2-cylinder single expansion steam locomotive of the 1950's.[169]

The below break-up of the loss factors is the author's translation or modification of the original Soviet source of the diagram. The author has added explanations duly referring to eventual other sources.

1. The incompleteness of combustion is partially chemical, due to incorrect amount of oxygen, and partially mechanical, due to fuel particles being seized unburnt by draught within the flue gas, while many particles fall through the grate either directly or within clinker formation.
2. Auxiliary systems like stoker engines, jets for spreading the coal on the grate, water pumps or injectors to feed water into the boiler, air pumps of the brake system, generators to power the lights *etc.,* were steam powered. Most of the steam used by feedwater systems was recovered into the boiler whereas steam used by the rest of the devices was typically rejected.[170]
3. Glass wool started to replace the fragile and cancer-causing asbestos, if any insulation at all, during last decades of steam age.[171]
4. Flue gas flow and its temperature were directly proportional to the working intensity of the classical steam locomotive, the resulting heat losses being the bigger, the harder the engine worked.[172] Efforts have been made, to recover heat from flue gasses to heating feedwater and combustion air. Sulphur content of the fuel set a lower limit to the reduction of flue gas temperature, due to corrosion problems experienced within the *Franco-Crosti* concept.[173]
5. Visible steam leaks were typical of classical locomotives with lots of outside piping, hence easy to detect and rectify, whilst the *internal* leaks called for systematic testing and might amount up to 50 % of the total evaporation capacity of the boiler, most of such leaks having occurred over valve and piston rings, substantially reducing the useful work of steam.[174]
6. The share of heat loss within exhaust steam appears striking. This heat was mostly rejected as a major part of it originated from phase-transition, *i.e.*, evaporation of water. Up to 14 % of the enthalpy of exhaust steam is potentially recoverable by mixing- or surface-type feedwater heaters if fitted.[175] Recovery of the rest was not viable on a locomotive with restricted cooling capacity of carry-on condensers, cumbersome as discussed in the previous chapter. *Ryti* refers to various empirical formulae or studies about the *wall effects* within cylinders.[176] *Porta* maintains that a wall effect that is never mentioned occurs in the receiver, and that due to the non-existing

theoretical explanation even a rough estimate of the loss is unknown so far.[177] On the other hand, the losses occurring in the receiver are included in the total losses of the cylinders also taken in account in the isentropic efficiency. Even if not explicitly defined in theory, Porta reports of having recorded up to 50 % increase in steam consumption for a given work in case of poor insulation or intermittent work.[178] Porta also maintains that leaks and radiation often originate from poor construction.[179]

7. Most of the steam age locomotives featured plain rather than roller bearings, until the latter were more widely adopted during the last decades of steam, to reduce friction, to eliminate need for on-the-road lubrication, and to improve reliability.[180]
8. The share of energy converted to drawbar work. Operational statistics support the view that figures like 6,5 to 8 % only refer to average drawbar work within a trip, the consumption figures being extremely sensitive to several factors like fuel quality and skills of the crews.[181]

3.3 Efforts to increase the efficiency

The first efforts to increase the efficiency of steam engine date back to the time before *Trevithick* built the first steam locomotive, and thus also before *Carnot* published the first theoretical approach to the subject. Fg. 3.4 presents a timeline of developing of the efficiency until the 1960's as studied by *Nusselt, Forbes, and Nock*, the last one concentrating to locomotives whereas the others mainly considered the steam engines in general. The blue points thus refer to stationary engines with notably higher figures than the locomotives ever attained. Note the logarithmic scale of the vertical axis.

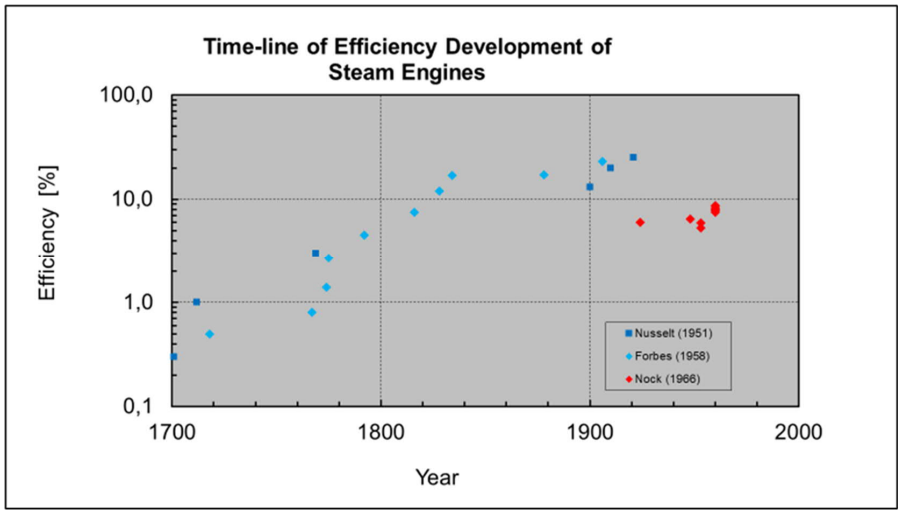

Figure 3.4: Efficiency development of steam engines over times. *Courtesy of Ph. D. Eng. T. Paloposki 2018*

Even if not shown in the graph, the first attempts to increase the efficiency of steam locomotives took place as individual efforts, covering the first century of locomotives up to the time of superheaters.[182] The second wave of development was distinctively pursued by the school of thought established by *André Chapelon* (1892-1978) in France and continued by *L. Dante Porta* (1922-2003) in Argentina, the successors of whom still keep up forwarding and developing the heritage of the two late masters.[183] The second wave thus commenced when electric locomotives already challenged steam power while diesels had not yet proved themselves. *Porta* and his closest disciple, the Briton *David Wardale,* maintain that steam power largely lost the game as railways failed to learn from *Chapelon's* message during 1929-

1932, a period appearing crucial as regards the choice of motive power policy, the diesels then having emerged as a new serious and ultimately winning challenger in the scene.[184]

No documents are available of the efficiency of *Stephenson's 'Rocket'*, but since the pressure was 0,35 MPa (gauge), the non-preheated feedwater was mechanically pumped into the boiler, and the engine exhausted into the atmosphere, the highest possible steam cycle efficiency can be calculated from Formula (3.2) of Paragraph 3.1, yielding η_{stc} = 0,026. Assuming boiler efficiency 0,5, due to modest insulation and level of heat absorption, and a mechanical efficiency of *e.g.,* 0,80, η_{db} = 0,01.

The *'Rocket'* already had 25 *firetubes* in its boiler, to increase the evaporative surface and thus the efficiency of the boiler, the contribution having been remarkable without much theoretical back-up.[185]

Exhaust steam injector is the invention in 1858 of *Henri Giffard.* Even if having appeared a technical paradox, the device proved itself, today's versions being capable of recovering up to 14 % of the energy otherwise rejected.[186] The relative impact of *10 % on the thermal efficiency* of locomotives using the device was noted, *i.e.,* assuming an efficiency of 0,07, the increased figure would be 0,077, with the result that the simple and robust injector became widely used up to the end of steam age.[187]

Double expansion or *compound* steam engines aimed at improving the operation economy by a more complete expansion, as earlier mentioned in Paragraph 2.3 discussing the concept from the point of configuration. Compounding was reported to save about 10 - 12 % of fuel and 8 - 10 % of water, the relative *impact on efficiency thus being around 10 %.*[188] On the other hand, the overall thermal efficiency of the locomotives of the late 1800's hardly attained 0,03, as again evidenced by Formula (3.2) yielding η_{stc} = 0,042 for the steam cycle, or η_{db} = 0,025 assuming η_B = 0,70 and η_{mech} = 0,80.

Superheated steam has been regarded as having changed the course of development of efficiency of steam locomotives, more than any other invention prior to 1950, as fuel savings of 10-30 % were reported during the pioneering applications of *Schmidt's* superheater in the early 1900's.[189] Having resulted in up to *30 % relative increase in efficiency,* such savings exceeded those of compounding which accordingly was largely rejected for its claimed complexity; superheaters seemed to be equal or better in improving the operation economy.[190] Such a view turned out to distinguish the mainstream constructions from the *French* and *Argentinean* practice which retained compounding in search for exploiting the benefits of *both* compounding *and* superheating, the course having lasted throughout the steam age, not only involving the steam circuit but stressing the key role of the flue gas side.[191]

Firebox is the first stage of the flue gas flow path. A typical *staybolted* firebox is shown in Fig. 3.5. The firebox of a firetube boiler typically constitutes 8,5-10 % of the total evaporative surface but due to the high temperature resulting from the direct radiation of flames, it evaporates more than 40 % of the water.[192] The *direct evaporative surface* of the firebox thus plays a key role in transferring the heat of flames to the boiler water, *i.e.,* in *absorption efficiency.* The combustion takes place in the firebox, the air traditionally being delivered from under the firegrate. The necessary draught is created by exhaust steam as was described in Chapter 1. The resulting gas velocity in the firebox of a hard-working locomotive may amount up to 30 m/s.[193] Such a gas stream has been recorded to have entrained coal particles representing 50 % of the total amount of coal fired, taking them unburnt through the tubes and chimney.[194] Lines C and D of Fig. 3.6 depict the situation, the explanation lying in the combustion air, 100% of which is delivered as primary air through the grate. For example, if the coal rate is 400 kg/m^{2}h, primary air flow is ca. 3500 kg/m^{2}h, and only 300 kg/m^{2}h of coal burns on the grate, the rest being entrained within the air flow, or lost in the ash pan. Literal citation of a comment by Mr. *E.S. Cox*, one of the most eminent British locomotive designers of the 1950's: "Whatever heights the cylinder efficiency may be developed to attain, it is always nullified at full power operation by low boiler efficiency, which can fall to 50 % and below, due to loss of unburnt fuel".[195] Report of *C.A. Brand* of the USA in

1939, cited by *Wardale*, supports the above citation as 50 % of coal fired during full power test of a Pennsylvania Railroad locomotive was lost unburnt.[196]

The phenomenon is called *carryover*, the impact of which the above citations mathematically prove to have been the worst one of the individual factors decreasing the efficiency of steam locomotives.

Fig. 3.5 gives a constructional overview of the firebox, the staybolts having been counted in thousands in the biggest American locomotive boilers, every bolt being a potential source of leakage or crack. The brick arch increases the turbulence of gas flow while the circulation tubes boost the evaporation.

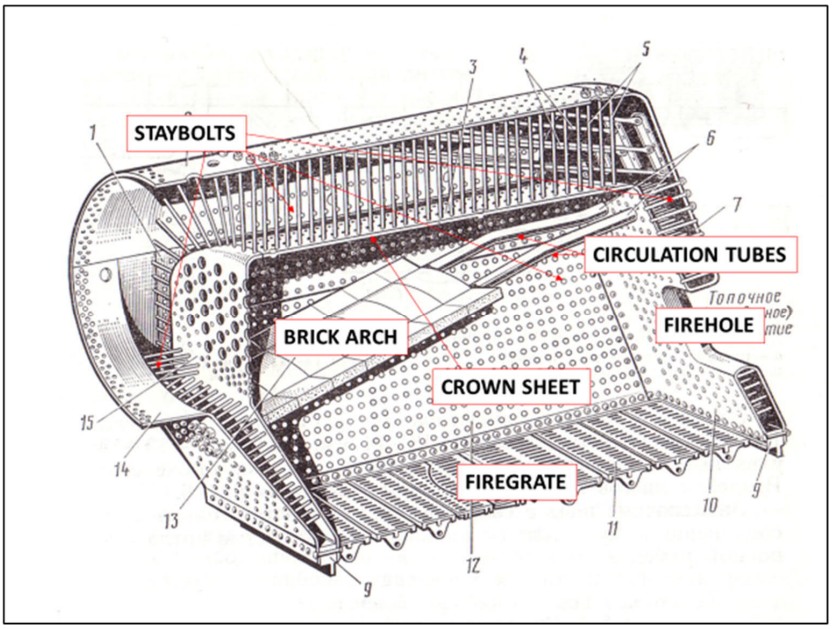

Figure 3.5: Staybolted firebox of a middle-size Russian locomotive boiler.[197]

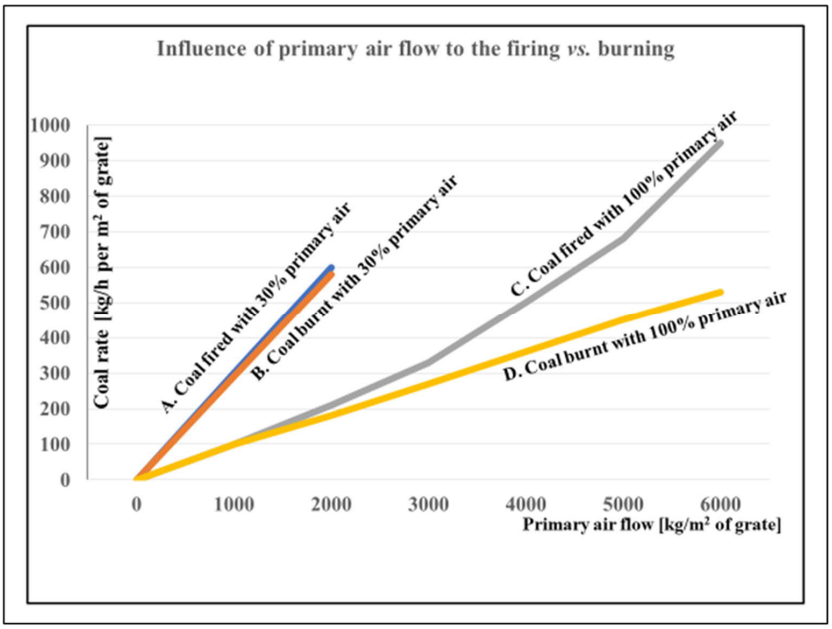

Figure 3.6: Influence of primary air in combustion.[198]

The *gasification* concept was applied for the first time in a steam tram locomotive in Birmingham as early as in 1875, for smokeless burning of coal by feeding steam under the grate.[199] The experiment was forgotten until 1949 that *Porta* built his experimental 1-metre gauge locomotive in Argentina.[200]

Porta's principal aim was to further develop the successful properties of *Chapelon's* famed *240P* compound locomotive, *i.a.* by adding an intermediate superheater and oil-extracting device between the HP and LP cylinders, starting exactly like *Chapelon*, *i.e.*, rebuilding an existing 4-6-2 type locomotive to a 4-8-0 type 4-cylinder compound.[201] On top of the two improvements mentioned, *Porta* added a pathbreaking innovation by implementing a *gas producing combustion system*, or *GPCS*.[202] The local high-ash (18 %) coal with clinkering tendency constituted a serious problem in conventional fireboxes and gave a reason for experimenting with exhaust steam, to cool the firebed to prevent clinkering, and with overfire jets of secondary combustion air, to combust the fines entrained from the firebed.[203] The principle shown in Fig. 3.7. has proved itself in several late steam age applications. Lines A and B of Fig. 3.6 depict the influence of secondary combustion air to the completeness of combustion in the *'Red Devil'* locomotive of *South African Railways* modified by *D. Wardale* in 1983.[204] The lines clearly indicate that practically all the coal fired was also combusted.

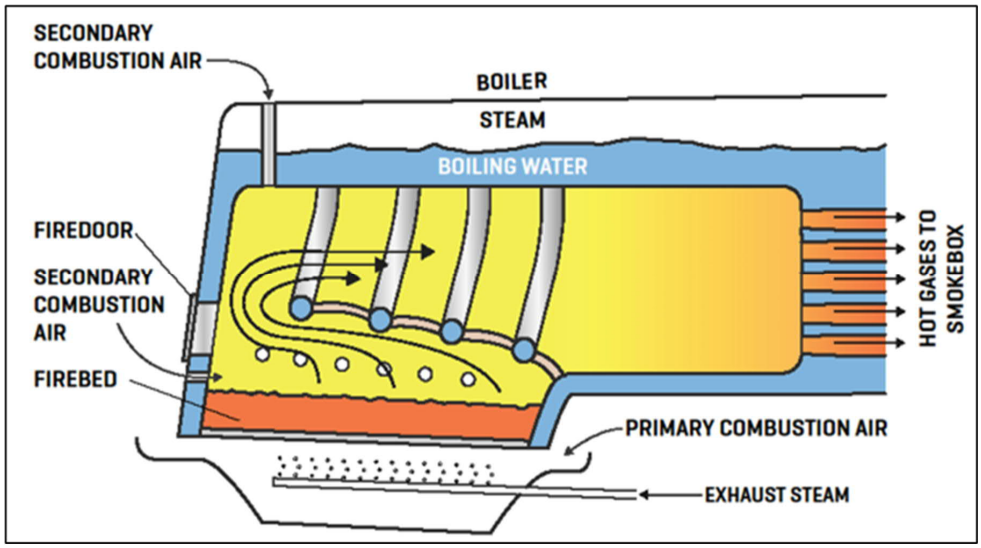

Figure 3.7: *Porta's GPCS* firebox. *Courtesy of Coalition for Sustainable Rail*

Formation of gasses within the firebed is schematically illustrated in Fig's 3.8 and 3.9. The message of Fig. 3.8 is that firebed thickness of about 15 particles is necessary for maximum formation of CO while Fig. 3.9 indicates how this formation takes place. Formation of CO_2 starts in the vicinity of the fire grate, to reach a maximum at 4-5 particles distance from the grate, whereafter more and more CO_2 is reduced to CO as the gas is flowing through the hot carbon layer. Proper amount of secondary air above the firebed is required, to efficiently combust this CO, the latent energy of which would be lost within the flue gas unless overfire air combusts the CO in the firebox. The cooling effect of steam is due to the endothermic reaction $C+H_2O$ (vapour) $\rightarrow CO+H_2$ between water vapour and the hot firebed, resulting in reduction of temperature of the latter in the immediate proximity of the grate.[205] As seen above, the steam also boosts gas formation in the firebed, resulting in both CO and H_2 in the firebox. Secondary air is then delivered in a turbulent flow above the firebed for efficient combustion of the volatiles, with simultaneous results of

- increasing combustion efficiency,
- returning the coal and other particulates entrained by draught back to the firebed, and
- reduction of emissions of CO and particulates.[206]

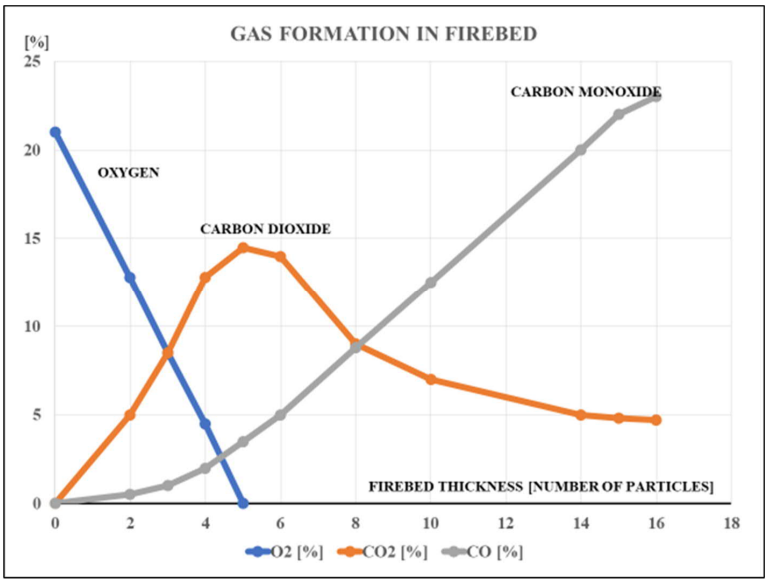

Figure 3.8: Gas formation in firebed.[207]

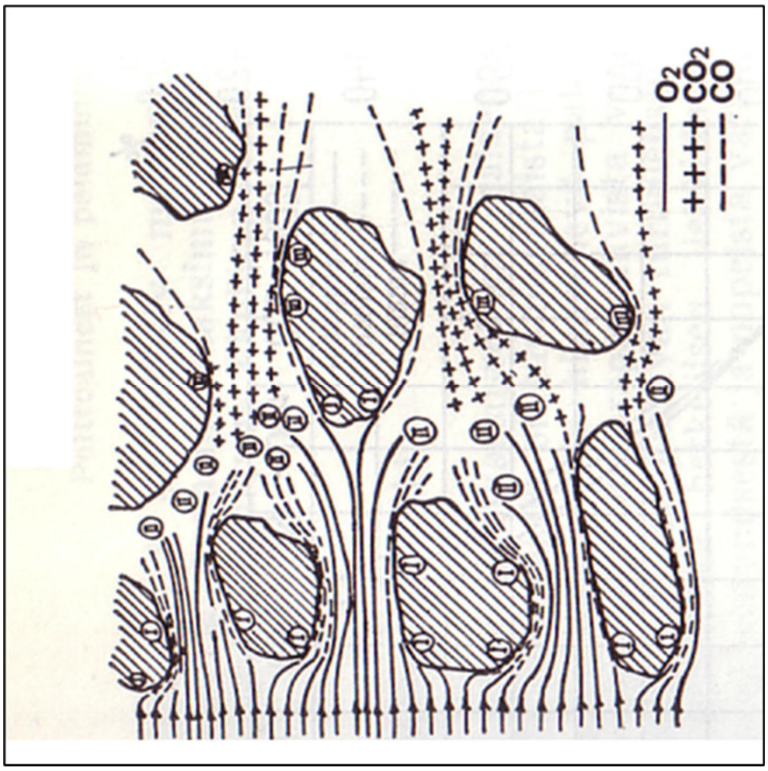

Figure 3.9: Impact of firebed thickness on the gas formation.[208]

Both in *Porta'*s own locomotive and in the *'Red Devil',* the relative increase of boiler efficiency was 20 % or more. The results are further discussed within the test summary in Paragraph 3.5. *Porta* proved the viability of the *GPCS* concept, not only in coal, but also *i.a.* biomass combustion, by introducing the system into his last project, a locomotive burning *bagasse*, remainder of sugar cane after extracting the juice. *Porta* unveiled the engine in *Havana* in 1999, 4 years before his death.[209]

Experiments with combustion of pulverized coal by *Hans Wendler* of the former *German Democratic Republic* were reported to result in a relative increase of 10 % of the efficiency of boilers burning ordinary coal, but up to 35 % compared to brown coal briquettes, more than 100 engines having been consequently fitted with the system aptly bearing *Wendler's* name.[210] Such results constituted one of several other reasons for *Wardale* to predict an efficiency of 0,85-0,86 for boilers burning *micronized* coal, ground to particle size of tens of microns.[211] He listed the potential benefits as in Table3.1.

HIGH COMBUSTION EFFICIENCY REGARDLESS OF BOILER LOAD
NO MORE FIREBED TO INFLUENCE THE ENGINE PERFORMANCE
LESS CHALLENGE FOR SKILLS AND PHYSICS OF FIREMEN
MINIMUM SENSITIVITY TO COAL QUALITY
INCREASED BOILER CAPACITY AND ENGINE POWER
SUSTAINED STEAMING CAPACITY AS NO GRATE TO SET LIMITS
NO FIRE CLEANING OR FREQUENT ASH DISPOSAL
NO SPARK ARRESTORS REQUIRED → ACCESSIBLE SMOKE BOX
ELIMINATION OF FIELD FIRE RISK
REDUCED ABRASIVE WEAR OF BOILER DETAILS
MINIMUM STANDBY OR IDLING FUEL CONSUMPTION
REDUCED EMISSIONS AT MEDIUM AND HIGH STEAMING RATES
ELIMINATION OF LOSS AND DIRT RELATED WITH LUMP COAL
IMPROVED STEAM RISING CONDITIONS AT DEPOTS
FEASIBILITY OF AUTOMATIC FIRING

Table 3.1: Predicted advantages of micronized coal combustion in locomotives.[212]

The author has edited *Wardale's* list, yet retained the points, many of them resembling the potential benefits of oil firing. In both cases, the shape of the relatively low firebox plays a significant role, as the flame path with an intense heat should not touch the tube plate or the sides of the firebox.[213] The typical location of oil burner(s) is either under the tube plate or under the firehole, the flame path of the latter case being about as in Fig. 3.10, and burners always calling for a refractory lining of the firebox.[214] The shape of the flame path became unavoidably complex, due to the inevitable brick arch and the angular shape of the firebox, but oil was widely used during the late steam age at times when heavy fuel oil prices were below those of good quality coal, this in turn having become scarce.[215]

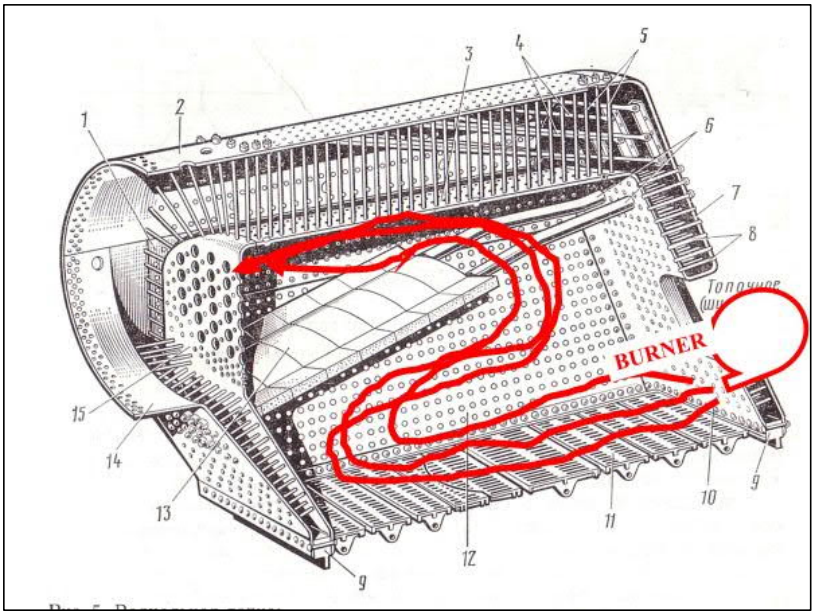

Figure 3.10: Flame path of an oil burner in a conventional firebox.

The impact of oil-burning must have been on the efficiency of *combustion* rather than of *absorption*, as the burners are efficient while oil combustion produces less flue gasses, thus reducing the velocity and turbulence of gas flow through the tubes which had to be accordingly modified.[216]

Firetubes and ***flue tubes*** constitute roughly 90 % of the evaporative surface of the boiler although their actual share of evaporation is less, or *ca.* 60 %.[217] Regarding the impact of tubes to the efficiency of the boiler, the gas flow ratio between the *fire tubes* and *flue tubes* is crucial, as the latter ones carry the superheating elements, the degree of superheat being one of the key factors of efficiency.[218] The exact impact on the efficiency thus depends on the temperature in which the steam leaves the superheater elements. Several configurations of elements were developed along the decades, resulting in justification for the statements of *Chapelon* and *Porta* who raised the steam temperature to 698 K – 723 K respectively, and for the German practice with 698 K, that such increases were technically viable.[219] [220] The impact of steam temperature on the *steam cycle efficiency*, corresponding to a rise from 623 K to 723 K, retaining all the other parameters, and using Formula (3.3), yields η_{stc} = 0,21 instead of η_{stc} = 0,15, resulting in a relative increase of the η_{stc} by *ca.* 40 %. As further discussed in Paragraph 3.5, the two reference locomotives with 723 K superheat temperature showed the best overall drawbar thermal efficiency figures found for the present study, or η_{db} = 0,09 for a 2-cylinder simple expansion and η_{db} = 0,12 for a 4-cylinder compound engine.

The lubrication system was to withstand the steam temperature. Careful studying of *diesel tribology* convinced *Porta* enough to stress that the *oil film* was to have the priority over the steam temperature, this being much lower than the gas temperature within diesel engines.[221] The traditional method of lubricating the cylinders (as used *i.a.* in Finland until the end of the steam age) by dripping cylinder oil on the valve rod and letting the *superheated* steam sweep it on its way to the cylinders, made an immediate contact of oil with steam at its hottest. [222] *Porta* developed a system, successfully applied by *Wardale,* using *saturated steam* to control the temperature of the hottest spot of the steam path within the engine, *i.e.,* the steam chest, and to safely convey the cylinder oil onto the liners, the mean temperature of which remained somewhere between the admission steam and exhaust steam.[223] *Porta* further applied diesel tribology by introducing a multi-ring practice in both valve and main cylinder pistons, thus contributing

to minimizing the leaks over the pistons to a level which, together with other leaks, totalled below 2 % of boiler evaporation in *run-down* condition, a typical average figure having been 5 % in *normal* conditions as earlier seen in Fig. 3.3 of Paragraph 3.2 while actual leaks of up to 50 % had been recorded in practical tests.[224]

Internal streamlining is a concept covering both the steam circuit and flue gas circuit. The term was launched and actively pursued by *Porta* and his followers during and after the late steam age while the practical initiator of the concept was *Chapelon* with his first rebuilds of French 4-cylinder compound locomotives from 1929 onwards. The concept still aims at reducing pressure drops within the said circuits, by means of wide steam passages and an efficient draughting system, both factors contributing to reducing *specific steam consumption* and *retaining of engine power at high speeds*.

The draught, induced in the firebox by the exhaust steam, constituted an automatic link between the evaporation and steam consumption, as already shown by *Stephenson's 'Rocket'.*[225] The results of research concerning the said link were not exploited to the full before the end of steam age, judging by the minor-scale application of efficient draught systems, or by the general opinion of sharp exhaust symbolizing power.[226] The author himself is in a position to confirm this, having heard such opinions from the mouth of *experienced steam age engine drivers*. Both theoretical and practical study of the function and significance of draughting systems date back to the mid-19th century, while the basic impact of exhaust steam on the draught was already found by *Trevithick* in his first locomotive in 1804.[227] Several *blast pipe* modifications arose from the research along the last decades of the 19th century, but the application by *Chapelon* in 1926 of the patent of *K. Kylälä*, a Finnish engine driver, resulted in a blast pipe design aptly called *KylChap front end* that soon became internationally re-known together with several brands thoroughly analyzed and described in *J. Koopmans's* thesis, the second edition of which is dated in 2014.[228] *Chapelon* demonstrated in 1929 the results of his efforts to achieve the maximum vacuum in the smokebox at the minimum back pressure in the cylinders, by comparing the appropriate figures of a *Paris-Orleans* railway locomotive before and after its modification, Fig. 3.11 showing the comparative graphs.[229] The message of the graph is that a properly designed blastpipe creates the given vacuum at a lower back pressure, thus, *e.g.,* to attain a 250 mm H_2O vacuum, the modified engine only required a back pressure of 28 kPa *vs.* the 70 kPa pressure of the original locomotive, resulting in 200 kW increase of cylinder power at 120 km/h.[230]

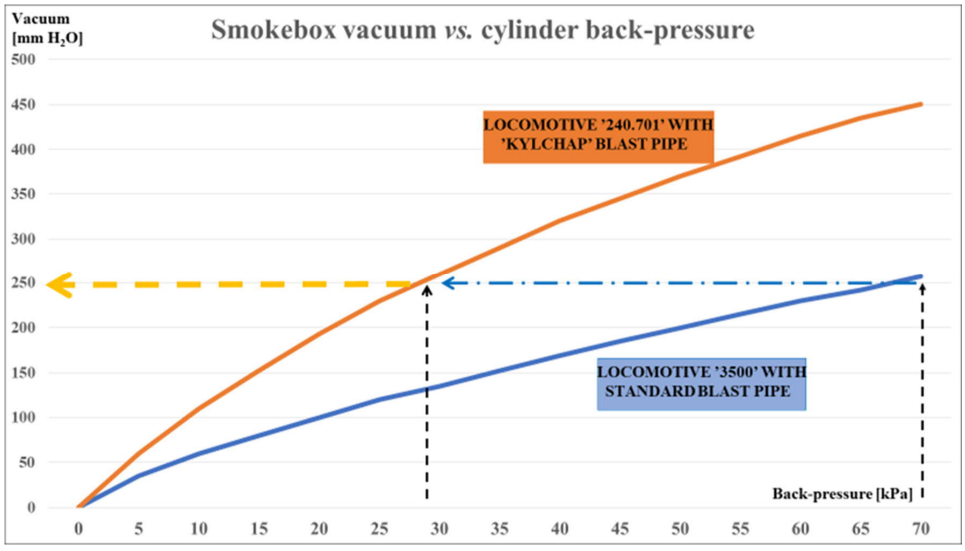

Figure 3.11: Smokebox vacuum *vs.* piston back-pressure.

The cited increase of 200 kW conforms to *Chapelon's* estimate of 100 kPa back pressure causing a power loss of 360 kW (500 hp) in a modern fast train locomotive.[231] He further calculated that since the time of *Crampton,* whose engines were famous for their good steaming at high speeds, the ratio between *steam port cross-section* and *piston area* had remained at the level of 1:10 (0,1), if not less over years, as shown in Fig. 3.12. The right-most blue column stands out in showing *Chapelon's* opting for ratio 1:5 (0,2) between areas of HP-cyl. inlet port and piston of his rebuilt *'240.701'*.[232]

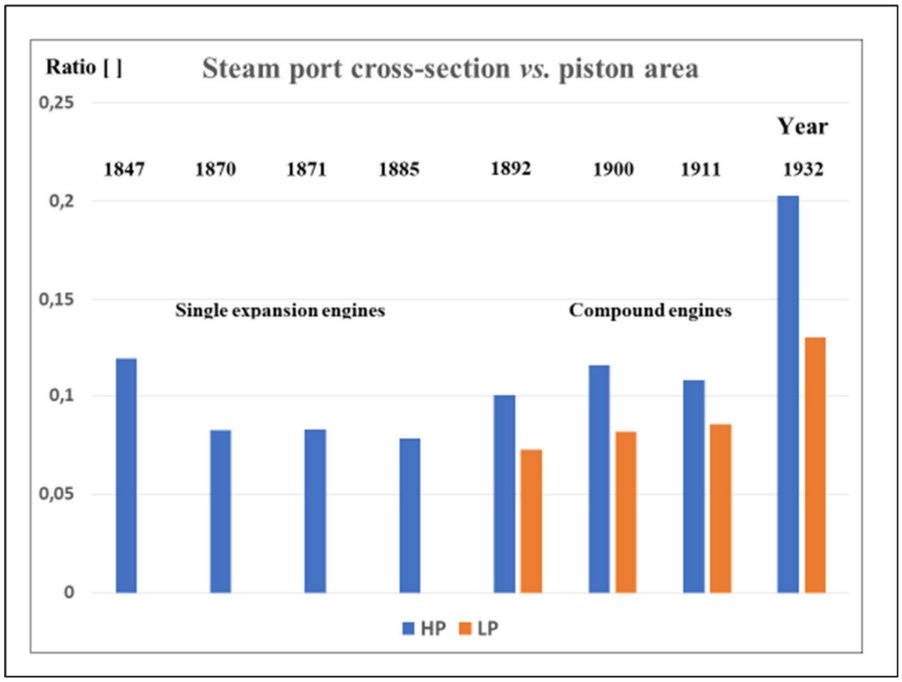

Figure 3.12: Ratio *steam port cross section vs. piston area* in fast steam locomotives over times.[233]

Increasing train speeds tended to aggravate the impact of pressure drops, as the decreasing of driving wheel diameters discussed in Paragraph 2.3 resulted in higher *rotational* speed.[234] This fact prompted *Porta* to use the term *breathing capacity* of the engine, and to apply a ratio as high as 1:4 between the steam port and piston areas of his experimental 4-cylinder compound.[235] The internal streamlining resulted in decrease of *specific steam consumption* (s.s.c), or weight of steam *per* power unit at either indicated or drawbar basis. Fig. 3.13 shows a sample of such *s.s.c*-curves, the power figures referring to *indicated hp* while the consumptions are given in *kcal.* The efficiency column on the left refers to indicated power. Regardless of the messy-looking graph, it clearly points out the principal message by showing the mainstream trend of curves without a minimum, the parabolic shape of some curves thus immediately attracting attention. Such a shape suggests a poor *breathing capacity* of the engine as it foretells of 'choking' of the engine due to pressure drops at high speeds. [236] The lowermost curves depict 4-cylinder compound locomotives with 2 MPa boiler pressure, 660 K - 670 K (387°C-397°C) steam temperature, and a streamlined steam circuit, the indicated efficiency reaching 16 % (0,16).

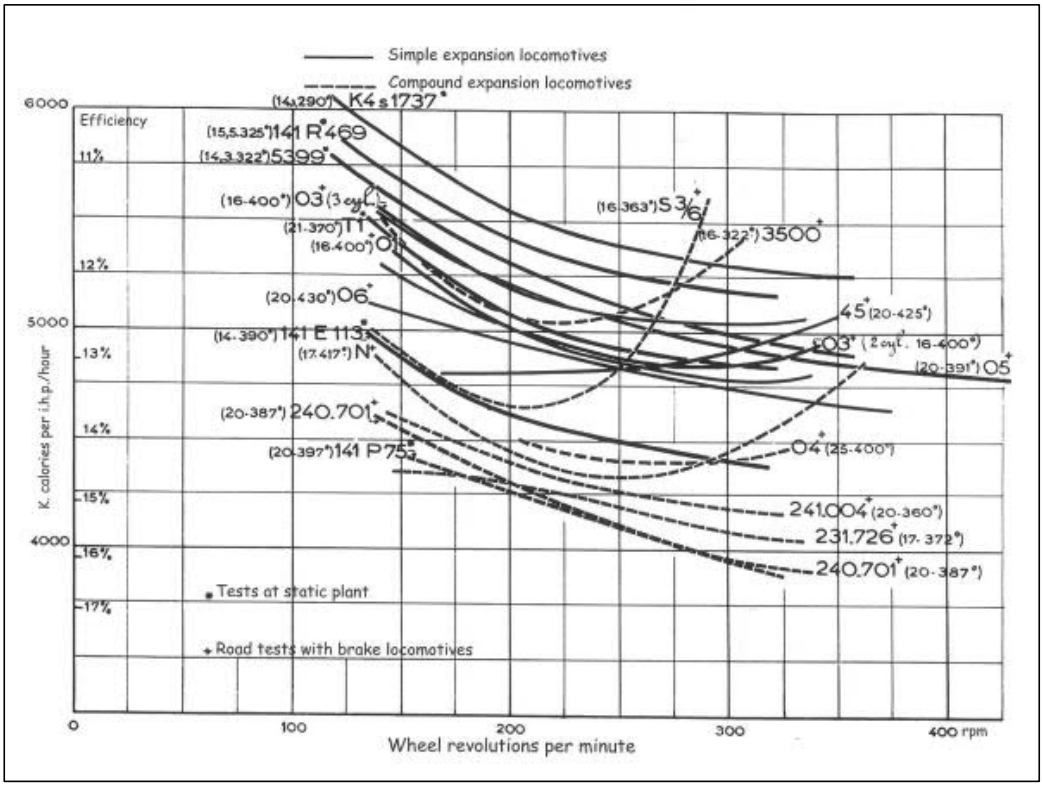

Figure 3.13: Specific steam consumption of various single expansion and compound locomotives.[237]

The dotted curves of Fig. 3.13 depict compound engines while the unbroken lines represent simple expansion engines. A typical rotational speed of a fast train steam locomotive was *ca.* 300 – 400 rpm. The graphs support following conclusions:

- even in single expansion locomotives, the specific steam consumption decreases along the rotational speed if the steam circuit and draughting system are streamlined,
- the parabolic curves suggest 'choking' of steam flow along increased rotational speed, *ie.* the passages are too tight, or contain abrupt bends or changes of cross-section,
- similar engines (curves K4 1737 *vs*. 5399 high up) attain a low and decreasing consumption after streamlining of steam circuit and draughting system,
- the specific steam consumption of a compound engine is clearly lower than that of a simple expansion engine, even if the latter were modified at a good standard.

The impact of internal streamlining on the performance of a 2-cylinder simple expansion locomotive *K4s* no. 5399 of Pennsylvania Railroad is further indicated in Fig. 3.14. The boiler pressure remained unchanged whereas the superheat temperature was raised by 30 degrees, the steam passages were streamlined, and poppet valves were substituted for the original piston valves. The parabolic shape of the steam consumption curve of the unmodified engine is conspicuous. The modified locomotive attained a 17 % higher indicated power at a 15 % lower specific steam consumption, after a relatively light modification. [238]

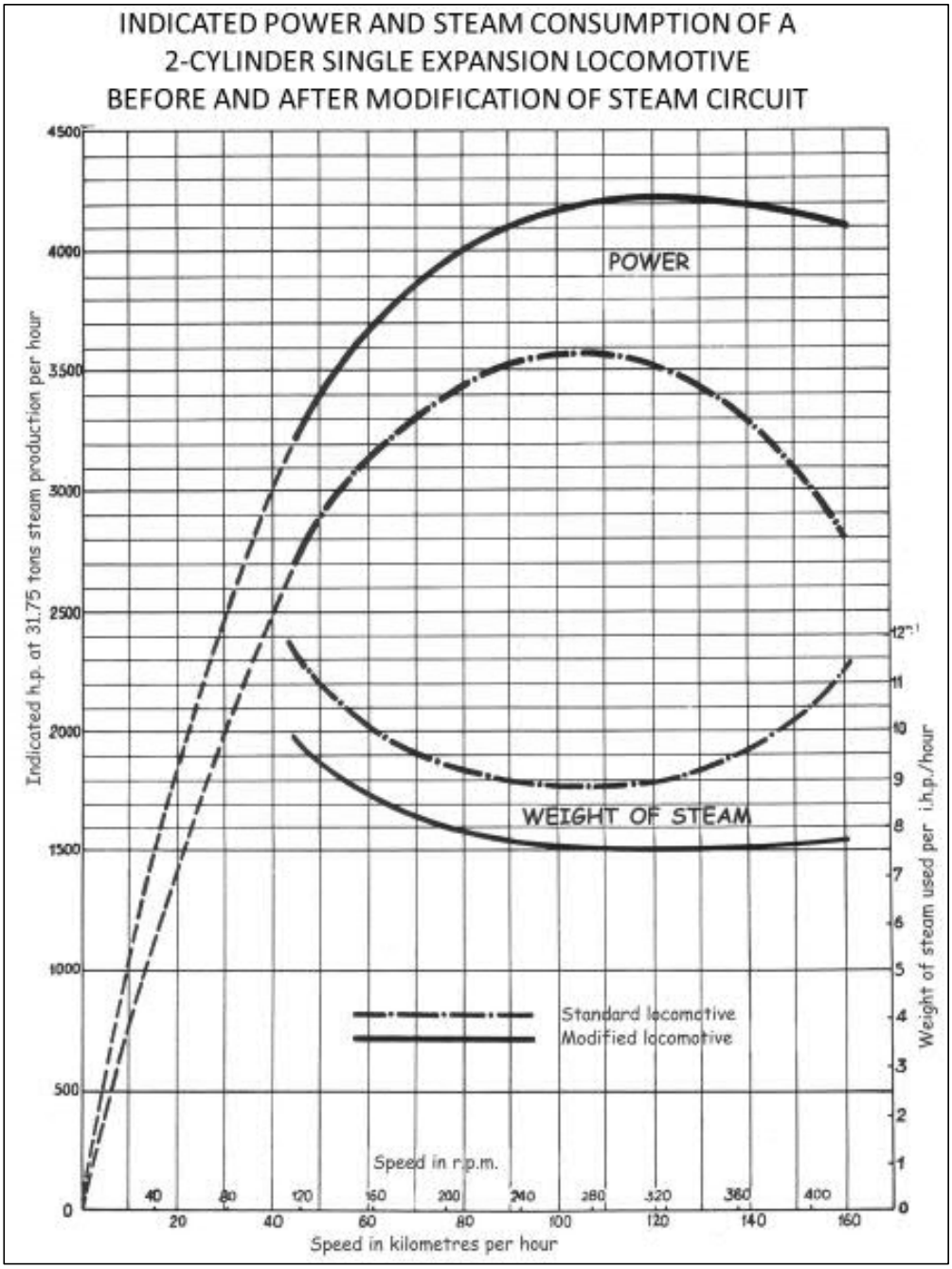

Figure 3.14: Impact of modified steam passages on power and steam consumption of *'K4s'* 5399.[239]

Fig. 3.15 depicts the impact of rotational speed [r/s] and admission ratio [%] on drawbar tractive effort in various *simple* (upper graph) and *compound* (lower graph) locomotives. The vertical axis refers to the proportion of remaining tractive effort as the speed is increased. The graph with green highlighting indicates that at a rotational speed of 6 r/s, the compound engine ① 4-8-0 with streamlined steam circuit and poppet valves still retained 95 % of its tractive effort at 30 % admission ratio.[240] The corresponding track speed of the engine was 125 km/h.

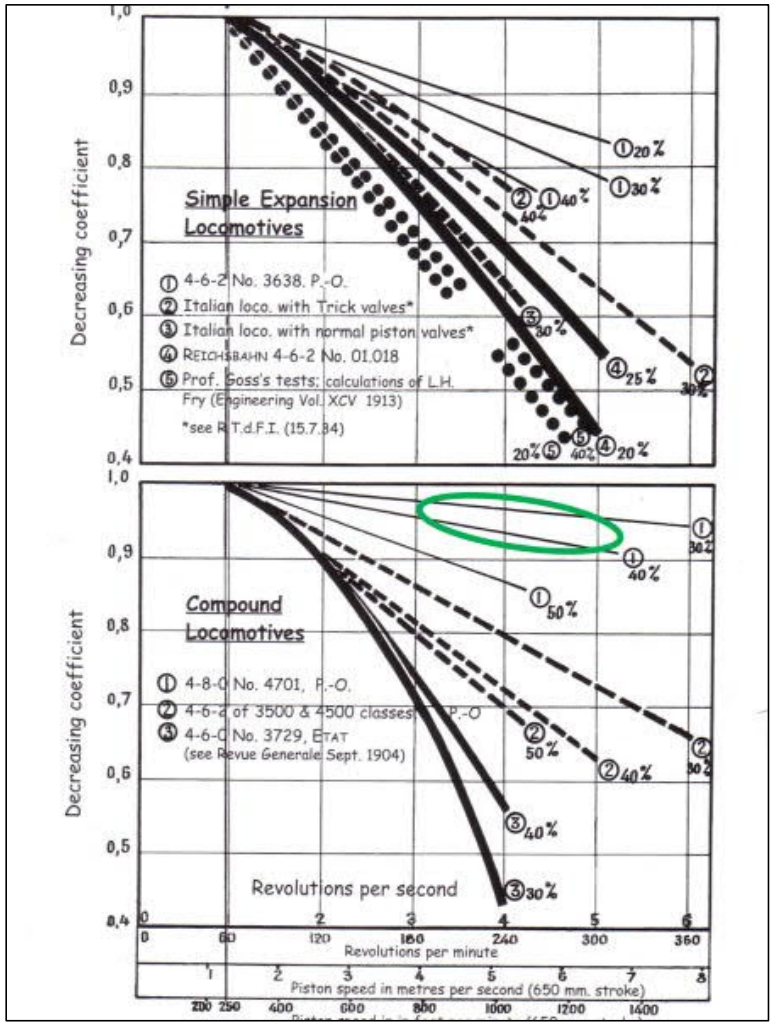

Figure 3.15: Influence of rotational speed of locomotive to its drawbar tractive effort.

3.4 Methods of testing actual efficiency

World-wide testing activity during decades has proved the sensitivity of coal-fired steam locomotives to the firing and evaporation rates, and to the quality of coal, not to speak of the skills of the crews. It is thus of vital importance that the working conditions and coal properties are specified for tests in question. Reference is made to item 1. of Fig. 3.1 in the previous chapter, a loss of 8 % having been estimated to result of incomplete burning, while losses of up to 50 % at the maximum firing rate have been recorded during actual tests with a stoker-fired locomotive of the Pennsylvania Railroad; enough for this aspect to be stressed.[241] Efficiency reports, concerning locomotives discussed below, have been obtained by three alternative testing methods:

1. stationary testing plants,
2. road tests with a brake locomotive, and
3. road tests with a dynamometer car attached to the train, or with a brake locomotive.

Stationary testing plant consists of rollers on which the driving wheels of the locomotive rest, with a built-in dynamometer to assess and record the wheelrim speed and forces. Such a device does not take in account the rolling resistance of idle axles and thus only indicates the force and speed related to the *wheelrims* of driving wheels. *Vitry* in France, and *Rugby* in England belong to the best-known plants in Europe. *Altoona* plant in the USA has also tested several locomotives delivered to Europe.

Brake locomotives are typically exploited for testing the locomotives on electrified railway lines, or on closed loops specially built for measuring purposes. Electric locomotives can be readily used for dynamic braking while a testing loop exists *i.a.* in *Sthsherbinka*, Moscow, Russia. The plant includes a laboratory, the vicinity of which speeds up test results involved with the analysis of fuel properties.

Dynamometer car tests are widely used, either by coupling the car between the locomotive and a heavy train, or by substituting a brake locomotive for the train. The dynamometer car continuously monitors and records parameters like speed, distance traversed, and drawbar pull.

3.5 Results of late- and post-steam age efficiency tests

Representative simple expansion and compound locomotives have been selected for references of actual efficiency tests summarized in Tables 3.2 and 3.3, and individually discussed as follows:

- Specifications of each locomotive are given with the accuracy obtained from available data, boiler pressures applying the *gauge* readings rather than absolute pressures which in turn have been duly exploited in calculations.
- Due to the generally low efficiency of steam locomotives, some figures have been given in three decimals, to indicate even the small advance steps, yet mainly retaining the 2-decimal practice.
- *Feedwater* temperatures, not always specified in official test reports, rely on assumptions based on figures common to steam age practice, the exhaust steam feedwater heater having been used worldwide and yielding a feedwater temperature of *ca.* 368 K while the average temperature of tank water is assumed to be 288 K.
- Drawbar power refers to the value obtained from the tender drawbar, thus taking in account the weight and the rolling resistance of the tender, even if the *power-to-weight* ratio only refers to the locomotive less tender.
- The *boiler efficiency,* if not given, has been calculated as the ratio between *evaporation rate* and *firing rate* obtained from the test data.
- The ratios between efficiencies of *calculated steam cycle* and theoretical *Rankine* cycle, and ratios between *drawbar power* and *indicated power,* respectively, are shown with the aim to assess the degree of predictability of calculations, particularly those concerning the pattern locomotive.

SIMPLE EXPANSION ENGINES					
ENGINE & RELATED DATA			BR '7MT'	SAR '26'	'Rio Turbio'
STEAM PRESSURE	p_B (g)	[MPa]	1,72	1,55	1,57
STEAM TEMPERATURE	T_{st}	[K]	663	723	693
CYL. & TYPE				2-cyl.	
DB-POWER MAX.	$P_{db\ max}$	[kW]	1300	2830	1000
WEIGHT LESS TENDER	m_{loc}	[t]	95,5	123,0	48,0
POWER-TO-WEIGHT	P_{db}/m_{loc}	[kW/t]	13,6	23,0	20,6
SPEED MAX.	v_{max}	[km/h]	145	90	50
SPEED AT TEST	v_{test}	[km/h]	100	90	50
DB-POWER AT TEST	$P_{db\ test}$	[kW]	1160	1700	368
COAL USED	LHV	[MJ/kg]	31,8	27,5	23,4
ENTHALPIES					
SUPERHEATED STEAM	h_{st}	[kg/kJ]	3270	3365	3300
EXHAUST STEAM	h_{exh}	[kg/kJ]	2730	2748	2720
WATER TO PUMP	h_{fw}	[kg/kJ]	398	398	398
WATER FROM PUMP	$h_{fw'}$	[kg/kJ]	400	400	400
TANK WATER	h_w	[kg/kJ]	62	62	62
EFFICIENCIES					
BOILER	η_B	[]	0,68	0,72	0,80
STEAM CYCLE	η_{stc}	[]	0,19	0,21	0,20
RANKINE	η_{Rank}	[]	0,23	0,23	0,22
RATIO	η_{stc}/η_{Rank}	[]	0,81	0,91	0,89
ACTUAL INDICATED	η_{ind}	[]	0,12	0,13	not given
ACTUAL DRAWBAR	η_{db}	[]	0,09	0,09	0,09
RATIO	η_{db}/η_{ind}	[]	0,79	0,65	-

Table 3.2: Performance parameters of representative simple expansion 2-cylinder locomotives.

3.5.1 Simple expansion engines

The ***British Railways*** **(BR)** ***Standard '7MT'*** class, also known as *'Britannia'*, the '7' indicating the *power class* in terms of drawbar tractive effort in *lbf* (= 4,45 N) at 80 km/h (roughly 7000 for *7MT*) and *'MT'* standing for *mixed traffic* = both freight and passenger service, was the last British steam locomotive extensively used in fast trains. Built between 1951-1953, the class incorporated *i.a.* roller bearings on all axles and rods, the permitted speed having been 145 km/h.[242] The *Standard classes* were created after the *post-war* nationalization of British railways, to replace the innumerable regional types by state-of-the-art standardized designs, the *'7MT'* having turned out to become one of the most successful of the line and having been the object of thorough tests, both on the road and at a stationary plant. Oddly enough, not a single mention of the superheat temperature of the class (or any of the *Standard* classes) has been found by the author, a most probable guess of 663 K having been applied in Table 3.2. Omitting circulator tubes from the firebox construction also seems strange, for an otherwise modern boiler.

Findings concerning the performance analysis:

- The drawbar thermal efficiency *0,092* reported by official British Railways test bulletin represents the best level reportedly attained in Europe with simple expansion 2-cylinder locomotives, only the German class *'23',* and the Russian *'ЛВ'* class having slightly surpassed the *'7MT'*, as far as known by the author.[243] [244]
- The efficiency of the *'7MT'* was sensitive to the coal quality, the figure *0,092* having been attained when combusting *South Kirkby* coal with a *calorific value* of 32,1 MJ/kg while *Blidworth* coal, 29,3 MJ/kg, only yielded *0,083*, regardless of the firing rate, suggesting a substantial *carryover* of unburnt coal, with a reported boiler efficiency of 0,68.[245]
- The *'hammer blow'* effect discussed in Fig. 2.7, had been shown to represent the lowest level on British Railways while the *'fore-and-aft'* fluctuation even caused passenger complaints, pointing out to one of the handicaps inherent to 2-cylinder engines.[246]
- By extrapolating the referred test data, *Wardale* predicts efficiencies of *0,064* and *0,060* when combusting *S. Kirkby* or *Blidworth* coal respectively, at a speed of 130 km/h.[247]

Class '26' of ***South African Railways*** (SAR) is a rebuild by *D. Wardale* of the SAR standard *25NC* locomotive originally built in 1953-1955, letters *'NC'* referring to the *non-condensing* version, as 90 units were equipped with German-built condensers to save water on the dry areas of South Africa.[248]

The modification originated from anticipated South African energy crisis suggesting extended use of steam traction, with the ultimate decision to modify a locomotive to show what could be attained in thermal efficiency, reliability, and general effectiveness by exploiting the best available know-how.[249]

Wardale based his efforts on a close and comprehensive cooperation with Porta whose know-how and expertise were exploited to the full in the modification project, the outcome of which became known as the *'Red Devil'* while it also carried a plate with the name *L.D. Porta* for a few years.

The original *'25'*- class was the heaviest and most powerful rigid-frame narrow gauge (1067 mm) locomotive ever built and was thought to represent the best standard of the time but *eg.* only gave a drawbar efficiency 0,033 at full power at 90 km/h.[250] One of the most evident explanations was the low efficiency of 0,38 of the original boiler due to the heavy carryover of unburnt coal at full power.[251] Constructional and economical restrictions prevented realizing of several projected modifications like higher boiler pressure or increasing of adhesive weight whereas the *GPCS*, an efficient draughting system, raising the steam temperature to 723 K, enlarging the steam chests, a thorough revising of cylinder tribology and numerous other items were carried out.[252]

Findings concerning the performance analysis:

- The maximum attained drawbar power was 2830 kW, or 43 % higher than the 1947 kW of the *'25NC'*, the steam temperature (723 K *vs.* 653 K) together with streamlining of both the steam and flue gas circuits evidently having contributed to the 'breathing capacity' of the engine.
- The power-to-weight ratio 23 kW/ton of the locomotive (excluding tender) was the highest one hitherto attained by a simple expansion 2-cylinder engine,[253] such a ratio being rarely achieved by present-day diesel-electric locomotives which typically exert 12-18 drawbar-kW/ton while *eg.* the Dr18 used as the reference diesel-electric locomotive in Chapter 4 attains 10 db-kW/ton.[254]
- At maximum power, the boiler efficiency was 0,65, or 70 % better than the 0,38 of the *'25NC'*, primarily due to the *GPCS* that eliminated most of the carryover of unburnt coal.

- The ratio 0,91 between efficiencies of calculated steam cycle and *Rankine* cycle implies an exceptionally high isentropic efficiency of the cylinders, resulting from both the high degree of superheat and extremely good insulation.
- The above figure also indicates in practice the impact of a high degree of superheat on reducing the gap between efficiencies of calculated and theoretical steam cycles.
- The drawbar efficiency at maximum power was 0,08, or 150 % higher than the 0,03 of the *'25NC'*.
- The ratio 0,65 between the drawbar *vs.* indicated efficiencies implies relatively high combined influence of rolling resistance and mechanical efficiency.

Rio Turbio – Rio Gallegos Railway is a 750 mm narrow gauge line of 255 km between the coal mines of Rio Turbio and the port of Gallegos, opened in 1951 until which a fleet of 50 steam-powered *Sentinel* waggons transported the coal by road.[255] The railway was built over an arid country where South-Western winds continuously blow at a speed of 100 km/h or more, with the result that hauling the 60-wagon empty train to the mines over gradients of 1:143 was actually harder than the return trip with the loaded 1700-ton train over ruling gradients of 1:333.[256] The arid conditions enabled a continuous disposal of ashes from the ash pan of the locomotives without any risk of field fire.[257] The maximum permitted speed over the line was 50 km/h. The *2-10-2* locomotives originated from a design of *Baldwin Locomotive Works* built by *Mitsubishi* for the *Rio Turbio* railway in two 10-engine batches.[258] The first batch was supposed to attain a continuous drawbar power of 700 kW but could hardly sustain 520 kW, due to clinkering of the local coal.[259] *Porta* modified three engines by raising the boiler pressure from 1,37 MPa to 1,57 MPa, the steam temperature to 693 K, introduced the *GPCS* and a *Lempor* (*Lemâitre-Porta*) draughting system after which the locomotives could develop a *continuous* drawbar power of 895 kW, peaking at 1000 kW.[260] The figures were remarkable for locomotives only weighing 48 tons less tender, and running on such a narrow track.[261] Consequently, all the said modifications were incorporated in the second batch, and during overhauls eventually built into the first batch as well.[262] The declining global interest in coal as a source of energy cut down the traffic, the small remainder being dieselized and steam power withdrawn in 1997 while revival of at least two 2-10-2's has been projected.[263]

Findings concerning the performance analysis:

- The boiler efficiency 0,80 refers to total evaporation and total coal consumption during a round trip on the 255 km line, suggesting low level of carryover due to the *GPCS*.[264]
- The drawbar efficiency 0,09 refers to total coal consumption during a return trip and to the drawbar work measured with the dynamometer car, the figure being exceptionally high, to be a sustained value.[265]
- The *'db power during test'*-figure 368 kW was the average power measured with a dynamometer car during a round trip.[266]
- The power-to-weight ratio of 20,6 kW/ton of the locomotive belongs to the highest hitherto attained, by a simple expansion 2-cylinder steam locomotive.[267]
- The ratio 0,89 between efficiencies of calculated steam cycle and *Rankine* cycle implies a high isentropic efficiency of cylinders, presumably due to 'exaggerated' insulation, and to streamlining of steam passages, resulting in small pressure drops.
- The above ratio also indicates, like the case of *'SAR 26'*, that the efficiency of the steam cycle can be brought within about 90 % of the theoretical maximum even in a simple expansion engine.

3.5.2 Compound engines

Compounding was largely abandoned in locomotives after introducing superheaters, as was discussed in Paragraph 3.3, while having been retained and developed particularly in France and Argentine as shown in Table 3.3 below.

COMPOUND ENGINES						
ENGINE & RELATED DATA			P-O '240'	'242A.1'	'Argentina'	'Y6b'
STEAM PRESSURE	p_B (g)	[MPa]	1,95	1,95	1,96	2,0
STEAM TEMPERATURE	T_{st}	[K]	678	698	723	623
CYL. & TYPE			4-cyl.	3-cyl.	4-cyl.	4-cyl. *Mallet*
DB-POWER MAX.	$P_{db\ max}$	[kW]	2647	2940	1559	4117
WEIGHT LESS TENDER	m_{loc}	[t]	109,0	148,0	68,0	277,0
POWER-TO-WEIGHT	P_{db}/m_{loc}	[kW/t]	24,3	19,9	22,9	14,9
SPEED MAX.	v_{max}	[km/h]	140	150	105	80
SPEED AT TEST	v_{test}	[km/h]	90	60	50	41
DB-POWER AT TEST	$P_{db\ test}$	[kW]	not given	1617	735	2860
COAL USED	LHV	[MJ/kg]	29,3	31,1	27,9	32,4
ENTHALPIES						
SUPERHEATED STEAM	h_{st}	[kg/kJ]	3258	3300	3360	3145
EXHAUST STEAM	h_{exh}	[kg/kJ]	2705	2705	2705	2715
WATER TO PUMP	h_{fw}	[kg/kJ]	398	398	398	398
WATER FROM PUMP	$h_{fw'}$	[kg/kJ]	400	400	400	400
TANK WATER	h_w	[kg/kJ]	62	62	62	62
EFFICIENCIES						
BOILER	η_B	[]	0,78	0,78	0,81	0,63
STEAM CYCLE	η_{stc}	[]	0,19	0,20	0,22	0,16
RANKINE	η_{Rank}	[]	0,20	0,24	0,24	0,22
RATIO	η_{stc}/η_{Rank}	[]	0,94	0,87	0,92	0,70
ACTUAL INDICATED	η_{ind}	[]	0,16	0,15	not given	not given
ACTUAL DRAWBAR	η_{db}	[]	0,10	0,10	0,12	0,08
RATIO	η_{db}/η_{ind}	[]	0,60	0,65	-	-

Table 3.3: Performance parameters of representative compound locomotives with 3-4 cylinders.

Chapelon's 'P-O 240' originated from a saturated steam 4-cylinder compound with '4-6-2' wheel system (231 in France). The conversion to a superheated engine with improved steam circuit made Chapelon and the engine famous in 1929 while the ultimate success followed 3 years later when the engine was converted to a 4-8-0 by replacing the rear truck with a fourth pair of driving wheels.

Findings concerning the performance analysis:

- Boiler efficiency 0,78 exceeded the typical 0,60 - 0,70, presumably due to the exceptionally long and narrow firebox, the thick firebed having been a precursor of gas-producing firebox.
- High superheat and good insulation are evidenced by the high ratio of actual *vs. Rankine* cycle.
- Wide steam passages and poppet valves support the above comment.
- The power-to-weight ratio 23,3 kW/t at the drawbar less tender has not been hitherto surpassed by any steam locomotive, or by great majority of diesel-electric locomotives.[268]

- The gap between indicated and drawbar efficiencies suggests a substantial impact of mechanical losses due to the 4-cylinder configuration.

Chapelon's '242.A' 3-cylinder compound locomotive, built in 1946, aimed at establishing a series of locomotives with similar cylinder layout (the *Sauvage* system earlier discussed in Fig. 2.10) but remained a sole engine due to change of electrification policy of France. Nevertheless, the concept was regarded as a success and showed properties comparable with the *P-O '240'*.

Findings concerning the performance analysis:

- High steam temperature increased the actual steam cycle efficiency even over that of the *'240'* while the rise of *Rankine* cycle efficiency was even bigger, resulting in a ratio 0,87 between the two, or somewhat lower than that of the '*P-O 240'*.
- The cylinder layout with low-pressure cylinders outside may be a partial explanation for a somewhat lower isentropic efficiency compared to the *'P-O 240'* with its inside LP cylinders, the reasoning being purely the author's own.

'Argentina' originated from a one-meter gauge 4-6-2 locomotive rebuilt by *L.D. Porta* as a 4-8-0, the obvious inspiration having been *Chapelon's P-O '240'*. The most significant innovation was the gas producing firebox as earlier stated in Paragraph 3.3.

Findings concerning the performance analysis:

- *Porta* was the first to raise the steam temperature to 723 K, resulting in actual efficiency 0,22 of the steam cycle, the best one attained by the present time, to the author's knowledge.
- A re-superheater with cylinder oil-extracting device was fitted, to raise the temperature of the LP cylinder inlet steam to 590 K, such a high degree of superheat being a novelty in LP cylinders.[269]
- The ratio 0,92 between actual and Rankine cycles seems to prove the combined impact of high degree of superheat, re-superheating, and good insulation.
- *Porta* studied the diesel engine and introduced the multi-ring concept in steam engines, both in valve chamber and in cylinders, resulting in steam-tightness, as earlier discussed.
- The impact of gas producing firebox in reducing unburnt coal shows in the efficiency 0,81 of the boiler.
- The impact of *Porta's* draughting system appears to have contributed to the high power-to-weight ratio of 22,9, or close to that of Chapelon's *'P-O 240'*.
- The drawbar thermal efficiency of 0,12 appears to reperesent the highest level attained by a steam locomotive exhausting into the atmosphere.

N&W 'Y6b' was the biggest and last true *Mallet* compound mainline steam locomotive class, the last unit of which having been retired in 1960.

Findings concerning the performance analysis:

- The Americans typically prioritized power and reliability over the thermal efficiency, hence a high boiler pressure but a conservative steam temperature.

- The boiler efficiency 0,63 seems to indicate a substantial carryover of unburnt coal as the coal used was of high quality, while stoker-firing was the only possibility in such a gargantuan boiler.
- The resulting drawbar efficiency falls in the range of a decent 2-cylinder simple expansion engine.

3.6 Conclusions about development of efficiency

3.6.1 Lessons of the past

The overall efficiency of the bulk of steam locomotives had not improved within the last decades of steam traction regardless of the potential proven both in theory and in practice. The author's view of assumed reason's suggests the following priority:

1. *Up to 40-50% losses of unburnt coal* were reported due to carryover particles.[270]
2. Prevailing lubrication methods and oils did not enable high superheat temperatures.[271]
3. Draughting systems wasted cylinder power through excessive back pressure.[272]
4. Poor or missing steam circuit streamlining resulted in substantial pressure drops.[273]
5. Inadequate knowledge of theory at *all* levels contributed to mediocre engine performance.[274]
6. Poor or missing insulation caused heat losses particularly in cylinders and steam pipes.[275]
7. Conservative design resulted in unavoidable leaks.[276]
8. Compound locomotives remained a small minority after superheating was adopted.[277]

3.6.2 Guidelines for the future

The late steam age advances, confirmed by Tables 3.2 and 3.3, support the following views:

1. Steam cycle efficiency can be brought close to that of the ideal *Rankine* cycle,
2. Properties of multi-cylinder locomotives surpass those of 2-cylinder engines regarding both the efficiency, and the technical performance.
3. Power-to-weight ratio can be made competitive with other power modalities even today.
4. The boiler is the key factor of overall thermal efficiency, forced draught potentially offering better prospect over induced draught in recovery of fluegas heat, the *Franco-Crosti* preheater offering an efficient and proven method for such a recovery to result in boiler efficiencies exceeding 0,90 even when burning solid fuel as was discussed in Paragraph 2.3.
5. Flexibility offered by liquid fuel to design of locomotive layout was proved for the first time on the Southern Pacific as early as 100 years ago, as was discussed within the *cab-forwards*.
6. Predictions of efficiencies up to 0,27 have been presented in recent proposals for future steam locomotives, as was discussed in Paragraph 2.6.
7. Hybrid concept is already emerging in diesel locomotive industry.[278]

The above aspects support the view that an efficient boiler, combined with state-of-the-art steam cycle and engine tribology, enables a thermal efficiency approaching that of a diesel-electric locomotive.

4. Proposed locomotive concept *Hs1*

4.1 Configuration

4.1.1 Basic design

Transfer from steam power to diesel and electric traction set new standards of operation and ergonomy of locomotives. Any potential novel steam power thus faces the pre-requisites resulting from such a change, Table 4.1 comprising of the author's view of the consequent aspects. Apart from items A7 and B5, the characteristics repeatedly set diesel locomotives as a comparison basis.

A. TECHNO-ECONOMICAL ASPECTS
1. COMPATIBILITY WITH DIESEL POWER IN MULTIPLE UNIT OPERATION
2. MULTIPLE UNIT OPERATION BY SINGLE (ONE PERSON) CREW
3. BI-DIRECTIONAL OPERATION
4. OPERATION RANGE COMPARABLE TO DIESEL LOCOMOTIVES
5. SERVICEABILITY COMPARABLE TO DIESEL LOCOMOTIVES
6. ERGONOMICS COMPARABLE TO DIESEL LOCOMOTIVES
7. ADAPTABILITY TO 100 % BIO-OIL COMBUSTION
B. OPERATIONAL ASPECTS
1. TRACTION PROPERTIES COMPARABLE TO DIESEL LOCOMOTIVES
2. IMPACT ON TRACKS AND ROADBED COMPARABLE TO DIESEL LOCOMOTIVES
3. START-UP AND SHUT-DOWN TIMES COMPARABLE TO DIESEL LOCOMOTIVES
4. RISK OF FIELD FIRE NOT TO EXCEED THAT OF DIESEL LOCOMOTIVES
5. MINIMUM AMOUNT OF STEAM-SPECIFIC COMPONENTS

Table 4.1: Pre-requisites for the proposed locomotive concept.[279]

The outlines of general-purpose diesel locomotives bear a world-wide similarity, marked by two power trucks and a single cab like in the Dr18 locomotive of FenniaRail shown in Fig. 4.1. The engine is a thoroughly modernized version of a Czech construction, equipped with an up-to-date Caterpillar prime mover and corresponding power electronics. Tables 4.2 and 4.3 list the main characteristics of the locomotive and are used as the basis of specifications of the pattern locomotive where applicable.

Figure 4.1: Dr18 class diesel-electric locomotive of FenniaRail, Finland; operational since 2017.
Photo: Courtesy of Sakari K Salo

Dr18		
PRINCIPAL DUTY	FREIGHT	
PRIME MOVER DIESEL	Caterpillar 3512 C HD	
TRANSMISSION	ELECTRIC	
AXLE SYSTEM	Co - Co = 3 + 3	
POWER OF PRIME MOVER	[kW]	1550
TOTAL WEIGHT	[t]	120
WEIGHT PER AXLE	[t]	20
TRACTIVE FORCE		
- AT START	[kN]	380
- CONTINUOUS MAX.	[kN]	257**)
CONSTRUCTIONAL SPEED	[km/h]	90
MINIMUM CURVE RADIUS	[m]	120 *)
LENGTH	[mm]	17 340
WIDTH	[mm]	3 140
HEIGHT	[mm]	4 624
*) AT 5 km/h MAX.		
**) AT 16 km/h		

Table 4.2: Main specifications of the Dr18 class diesel-electric locomotive.[280]

ANALYSIS OF POWER BALANCE OF Dr18	
ITEM	POWER [kW]
POWER OF DIESEL	1550
- TRACTION MOTOR COOLING	30
- COOLING OF DIESEL	41
- COMPRESSOR	43
- AUXILIARY NETWORK 3 x 400 V	2
- AUXILIARY NETWORK 24 V DC	4
- EXCITATION ALTERNATORS	5
AUXILIARY GENERATOR (η = 0,88)	142
POWER FOR TRACTION GENERATOR (η = 0,95)	1408
POWER RESERVE	26
POWER AVAILABLE FOR TRACTION	1300
TRACTION MOTORS (x 6; η = 0,90)	1170
WHEELRIM POWER (GEARBOX η = 0,98-0,99)	1158
POWER TO DRAWBAR (η = 0,99)	1146

Table 4.3: Power balance of Dr18 locomotive.[281]

4.1.2 Preliminary specifications

The pre-requisites and above reference to outlines of diesel-electric locomotives result in preliminary technical specifications shown in Table 4.4. The electric transmission has been retained. A watertube boiler has been opted as a matter of principle, as further discussed in detail in Paragraph 4.3.

For practical purposes, the pattern locomotive will be hereafter called as '*Hs1',* the letters 'Hs' standing in Finnish for 'Höyry-sähkö', translating in English as 'Steam-electric'.

OUTLINES OF THE PATTERN LOCOMOTIVE			
A. CONFIGURATION	**B. TECHNICAL PARAMETERS**		
ALL-WHEEL DRIVE	**LENGTH**	**17000**	**[mm]**
ELECTRICAL TRANSMISSION	**WIDTH**	**3150**	**[mm]**
REGENERATIVE BRAKE SYSTEM	**HEIGHT**	**5100**	**[mm]**
INSULATED PRIME MOVER COMPARTMENT	**TOTAL WEIGHT**	**130**	**[t]**
SHORT AND WIDE STEAM LINES AND PORTS	**ADHESIVE WEIGHT**	**130**	**[t]**
ELECTRONIC VALVE CONTROL	**AXLE WEIGHT MAX.**	**22**	**[t]**
BI-DIRECTIONAL OPERATION	**DRAWBAR POWER**	**ca. 1000**	**[kW]**
WELDED WATERTUBE BOILER	**D.B. TRACTIVE FORCE**	**325**	**[kN]**
LIQUID FUEL COMBUSTION SYSTEM	**CONSTRUCTIONAL SPEED**	**100**	**[km/h]**
FORCED DRAUGHT			
OIL-FREE AND CONDENSING STEAM CYCLE			

Table 4.4: Configuration and preliminary specifications of the *Hs1*.

4.2 Selection and outlines of the prime mover

4.2.1 Configuration

The opted basic configuration with electric transmission results in locating the prime mover in power compartment similar with that of a diesel-electric locomotive. The compartment does not dictate the configuration of the prime mover, opposite to conventional direct-drive steam engines with their open rod mechanisms connected to the driving wheels. Priority can thus be given to efficient insulation and compact design. Steam turbine and reciprocating steam engine constitute the two alternative expander options. The below *pro/contra* argumentation between the two was discussed in Chapter 2:

- up to 1 – 1,5 MW power range piston engines are competitive with turbines in efficiency, [282]
- efficiency of piston engines *vs.* turbines is less sensitive to partial-load operation, [283]
- existing and emerging tribological solutions enable use of unlubricated cylinders, [284]
- turbines enable complete expanding of steam, unlike piston engines in which *water hammer* may result from steam condensing on cylinder walls. [285] [286]

The above arguments support opting for a combination of the two alternatives through introducing a turbine between the low-pressure cylinder outlet and the condenser. The dimensions are selected to result in maximum power of the turbine at the maximum pressure and mass flow of the exhaust steam, *i.e.,* to correspond to the incompleteness of expansion of the piston engine at its maximum power setting. The prime mover configuration is now marked by following characteristics:

- the total power fits in the range between 1 - 1,5 MW,
- adjustability of the piston engine can be fully exploited,

- unlubricated cylinders result in oilless exhaust steam and condensate,
- regardless of the small size of the turbine it can safely exhaust into the condenser at atmospheric pressure,
- the isentropic efficiency of the turbine peaks when that of the piston engine is at its lowest,
- the mechanical efficiency of the piston engine is at its maximum when the admission ratio is high, *i.e.,* at maximum power, while the mechanical efficiency of the turbine is high throughout its power range.[287]

Keeping the total weight of the locomotive within the specifications calls for compactness and a high power-to-weight ratio of the prime mover configuration. Such characteristics are typical of *radial* piston engines, as witnessed by their popularity in aviation technology before the take-over by gas turbines. The radial concept has been reproduced in a steam-powered version sketched in Fig. 4.2. The configuration is based on the *master-and-articulated* connecting rod (abbreviated as *conrod*) system used in the aviation engines. Selecting an odd number of cylinders prevailed as the design rule throughout the radial engine era, to minimize the torsional vibrations. In the present case, a 5-cylinder layout has been opted, due to the compound configuration of the steam engine in which one of the cylinders is working at high pressure while the remaining four cylinders constitute the low-pressure section. The exhaust steam of the high-pressure cylinder is collected in the *receiver*, *i.e.,* the intermediate steam vessel feeding the four other cylinders constituting the low-pressure section. The resulting expansion ratio between high- and low-pressure sections is thus 1:4, as all the 5 cylinders have the same volume. Typical range of volume ratio between HP- and LP-cyliders of advanced French compound locomotives was 1:2,1 to 1:2,4[288]. However, at higher boiler pressures, an uneven distribution of work between HP- and LP-cylinders became evident, as was discussed in Chapter 2 about a *Yarrow*-boilered locomotive in which the modified ratio of 1:4 proved itself.[289] Selecting such a ratio for the *Hs 1* working at 5,2 MPa boiler pressure thus appears to fit into the scheme. Calculations in the end of the present chapter predict a work balance between HP *vs.* LP sections to occur at HP admission ratio $\varepsilon_{HP} = 0{,}37$, *i.e.,* close to an average power setting $\varepsilon_{HP} = 0{,}40$.

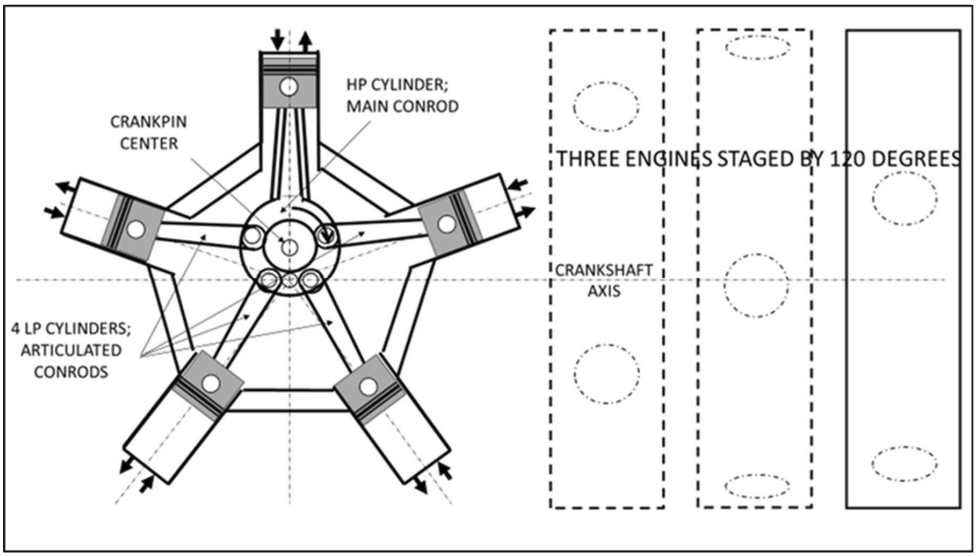

Figure 4.2: Elevation of a 5-cylinder radial engine and side view of three engines staged by 120°.

The inevitable difference of piston thrusts in HP *vs.* LP cylinders results in an uneven torque of a single 5-cylinder unit. Three units are therefore mounted in row and staged by 120°, to stabilize the torque. The staging with resulting total of 15 cylinders is illustrated in Fig. 4.3.

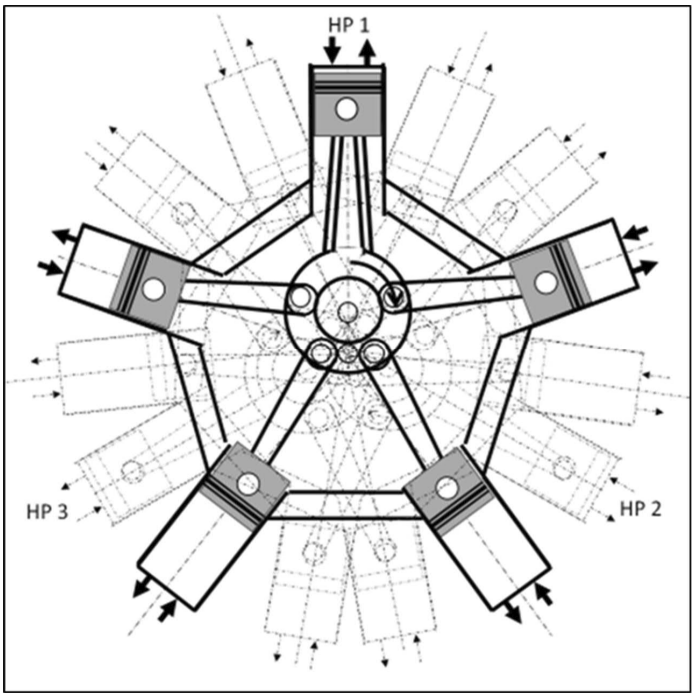

Figure 4.3: Staging of three radial engine units by 120°.

4.2.2 Preliminary design parameter calculations

a. Estimated power.

Specifications in Table 4.3 call for a drawbar power P_{db} = 1000 kW. At a given traction efficiency η_{tr}, the prime mover is thus to exert a brake power (4.1)

$$P_b = \frac{P_{db}}{\eta_{tr}} \tag{4.1}$$

at the output shaft. The η_{tr} takes in account the efficiency of the entire power chain from the prime mover to the drawbar, *i.e.,* the efficiencies of the electric and mechanical elements of the transmission and the power losses between wheelrims and the drawbar. Moreover, the prime mover must deliver the power consumed by the auxiliaries and potential leaks, all taken in account by the own consumption efficiency estimate η_{oc} = 0,96 [290], to make the locomotive work. Other items affecting the power requirement are η_{gen} = 0,95 [291] of the generator, η_{trm} = 0,95 [292] of the traction motors, and η_{trans} = 0,99 [293] of the transmission from wheelrims to the drawbar. Thus, traction efficiency η_{tr} is obtained from Formula (4.2):

$$\eta_{tr} = \eta_{oc}\eta_{gen}\eta_{trm}\eta_{trans} = 0{,}86 \tag{4.2}$$

The brake power P_b is then obtained from Formula (4.3), *i.e.*, by dividing the drawbar power by η_{tr}:

$$\boldsymbol{P_b} = \frac{\boldsymbol{P_{db}}}{\boldsymbol{\eta_{tr}}} = 1166 \text{ kW} \tag{4.3}$$

Assuming mechanical efficiency of the prime mover $\boldsymbol{\eta_{mech}} = 0{,}92$ [294], the indicated power (4.4) is

$$\boldsymbol{P_{ind}} = \frac{\boldsymbol{P_b}}{\boldsymbol{\eta_{mech}}} = 1267 \text{ kW} \tag{4.4}$$

b. Estimated steam consumption.

The interdependence of indicated power $\boldsymbol{P_{ind}}$ of an expander, and isentropic enthalpy drop Δh_s within it, is expressed by formula (4.5) [295]:

$$\boldsymbol{P_{ind}} = \boldsymbol{\eta_{s\,tot}} \dot{m} \boldsymbol{\Delta h_s} \tag{4.5}$$

Solving (4.5) for ṁ yields formula (4.6) from which the steam consumption is readily attainable if the isentropic efficiency $\boldsymbol{\eta_s}$ and steam conditions are known:

$$\dot{m} = \frac{\boldsymbol{P_{ind}}}{\boldsymbol{\eta_{s\,tot}} \boldsymbol{\Delta h_s}} \tag{4.6}$$

The combined isentropic efficiency $\boldsymbol{\eta_{s\,tot}}$ of the prime mover at maximum power assuming $\boldsymbol{\eta_{s\,comp}} = 0{,}90$ for the piston engine as attained even in some classical steam locomotives with outside cylinders and modest steam parameters as shown in Paragraph 3.4, and a conservative figure of $\boldsymbol{\eta_{s\,TB}} = 0{,}78$ for the turbine, $\boldsymbol{\eta_{s\,tot}} = 0{,}88$.[296] Steam conditions, further dealt in Chapter 4.3, are specified as 5,2 MPa and 810 K. Expansion to atmospheric pressure from such an initial state results in an isentropic enthalpy drop of 953 kJ/kg, as obtained from *Mollier h, s* chart. According to Formula (4.7), the actual enthalpy-drop is thus:

$$\boldsymbol{\Delta h_{act}} = \boldsymbol{\eta_{s\,tot}} \boldsymbol{\Delta h_s} = 842 \text{ kJ/kg} \tag{4.7}$$

Calculations in paragraph 4.2.2 yielded a target indicated power $\boldsymbol{P_{ind}} = 1267$ kW. Formula (4.6) now yields $\dot{m} = 1267/(0{,}88 \cdot 842) = 1{,}70$ kg/s for steam consumption at maximum drawbar power. This figure is applied as a preliminary criterion when dimensioning the steam generator of Paragraph 4.3.2.

4.2.3 Steam distribution system

Comparison between piston *vs*. poppet valves and eventual opting for *Caprotti* type poppet valves, the principle of which is shown in Fig. 4.4, has been based on the aspects and reported benefits of poppet valves in general, and of some specific benefits of Caprotti valves in particular:

1. The steam pressure does not work against the opening or closure of poppet valves.[297]
2. Clearance volumes of 4 – 5,5 % are attainable with poppet valves while piston valves typically require as much as 10 - 12 %.[298]
3. The weight of typical poppet valves is 4 - 5 % of correspondent piston valves that make 6 - 7 times longer travel to provide equal cross section of flow-path for the steam flow and thus cause very much bigger inertia forces than poppet valves.[299]
4. Due to their hollow construction, the *Caprotti*-type poppet valves feature both flow-by and flow-through characteristics.[300]

5. *Caprotti* valves are springless and oilless.[301]
6. Separate valve cages of the *Caprotti* valves have been proved to minimize distortions.[302]

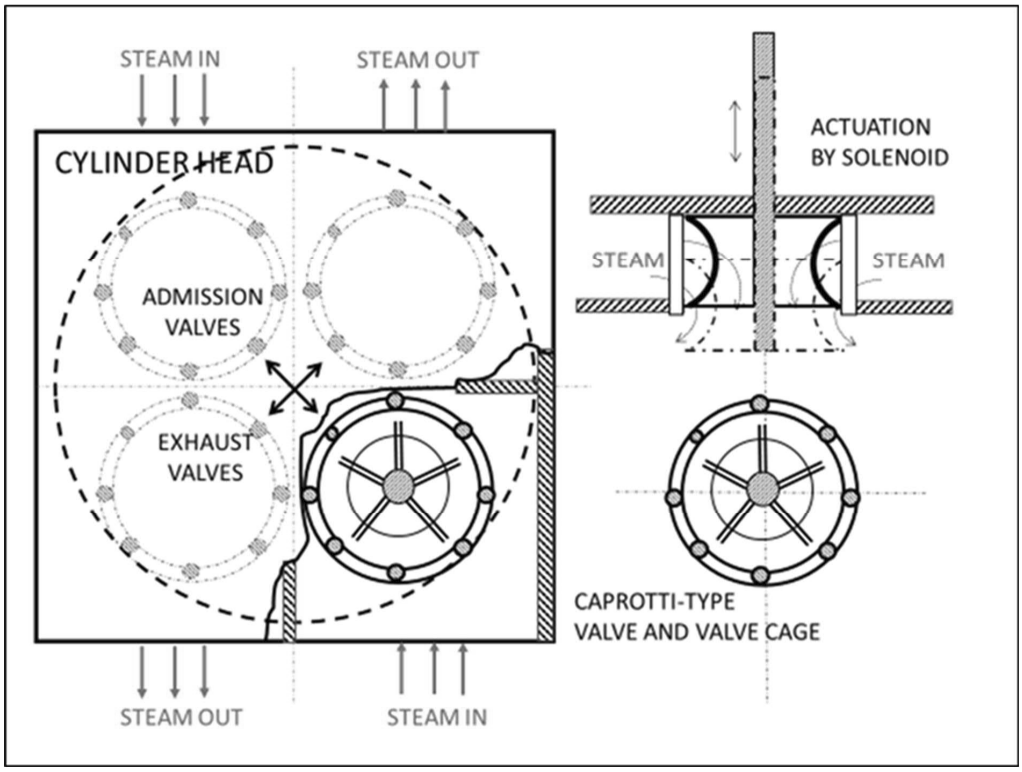

Figure 4.4: Principle of *Caprotti* valves; note the hollow center adding to the flow-path cross-section.

Fig's 4.5 – 4.8, with drawings by *courtesy of Vesa Tarula* of Kumera Corporation, show the author's proposal for modification of *Caprotti's* construction. The modified version aims at maximizing the flow-path cross-sections with consequent reduction of pressure losses. The admission valve is marked with blue, and exhaust valve with red colour. The actual steam flow within the cylinder calls for practical tests, but the aim of the valve layout is to direct the hot incoming steam along the cylinder walls to minimize their cooling while the expanded steam would exhaust through the center of the cylinder head. The two concentric valves are actuated by electrically and independently controllable power packs, only having to cope with the mass forces of the valves, opposite to ICE-type valve mechanisms in which cylinder pressure also inherently causes axial forces on valves. Somewhat less stringent material requirements are expected for steam engine valves that work in max. temperature of 810 K, compared with typical exhaust valve temperature of *ca.* 1000 K of diesel engines.[303] The camless valve control technology is in vigorous development stage by the 2020's, working ICE applications having already been introduced by at least two manufacturers.[304]

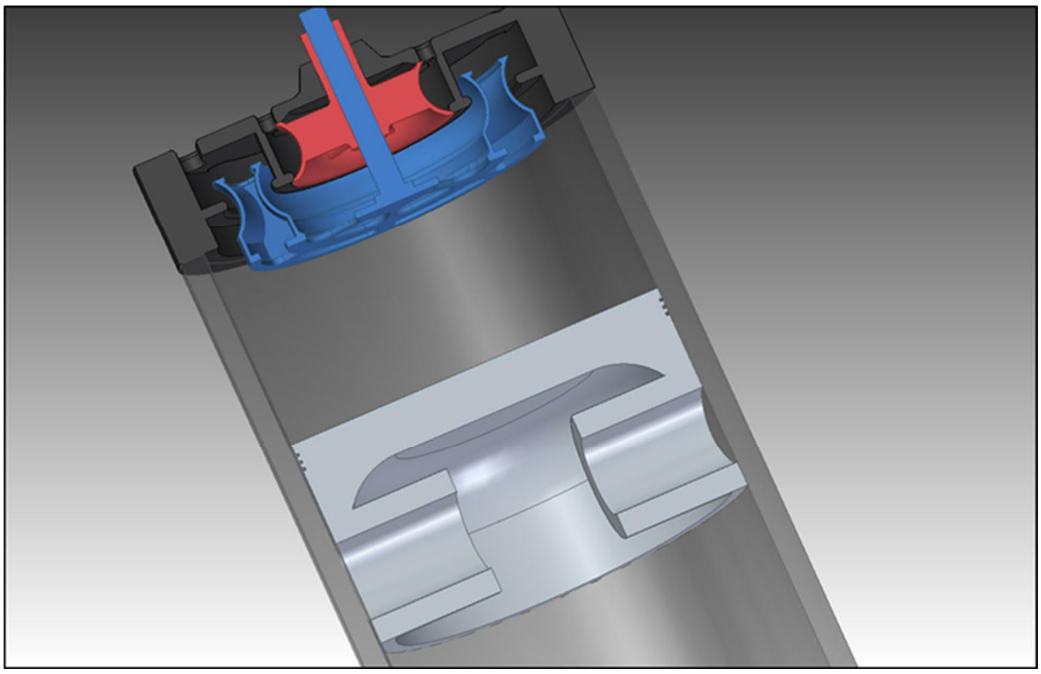

Figure 4.5: Layout of valves in cylinder head and piston in the cylinder; admission valve open, exhaust valve closed.

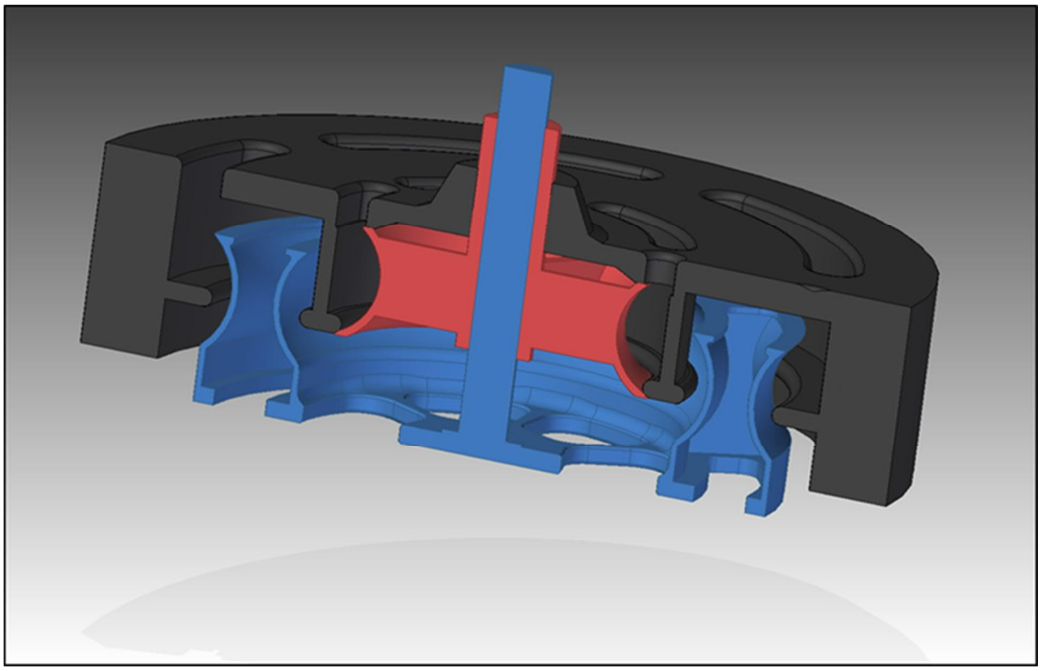

Figure 4.6: Admission valve open, exhaust valve closed.

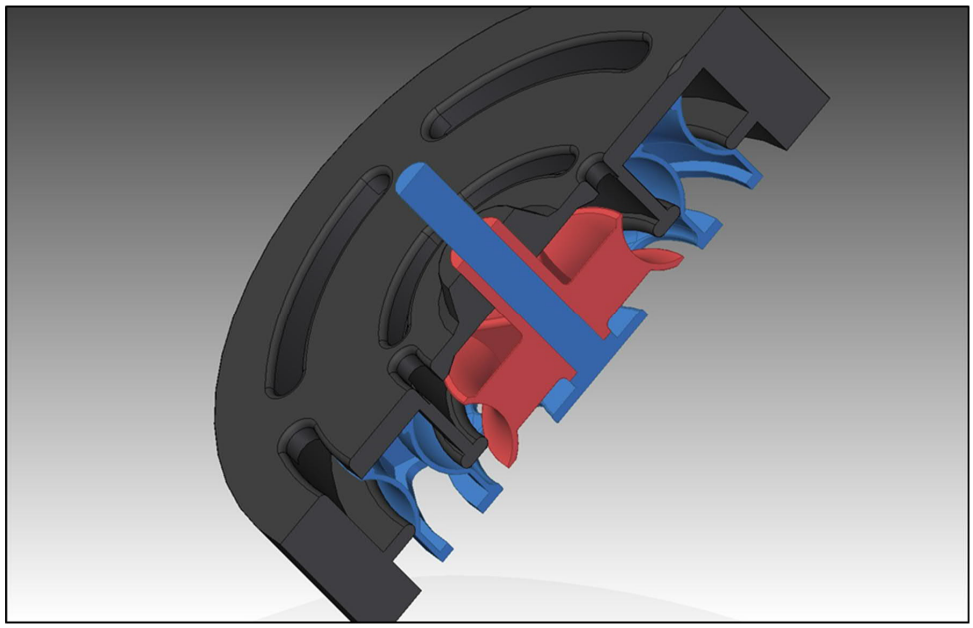

Figure 4.7: Exhaust valve open, admission valve closed.

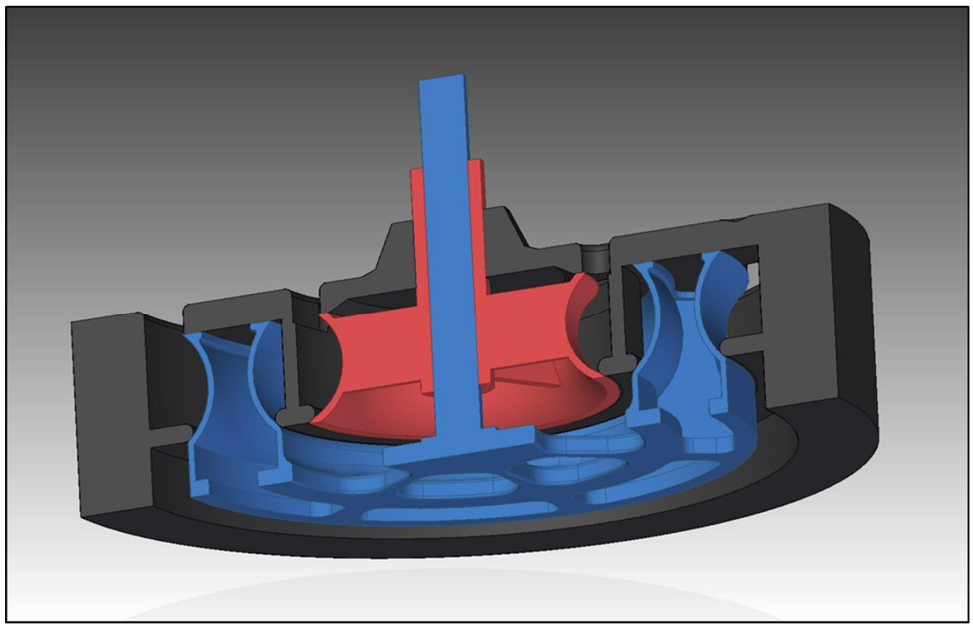

Figure 4.8: Both valves closed.

4.2.4 Tribological aspects

The ultimate tribological target feature of the prime mover design is its oil-free operation, expected to eliminate contamination of boilers and condensers, such a handicap having hampered operation with condensing locomotives, as was described in Chapter 2. The German 'Zero Emission Engine', earlier discussed in Paragraph 2.7.1.2, was demonstratedly working without cylinder lubrication. The materials were not specified in the source cited, presumably for patent-related reasons. *Ryti* refers to tests with

automotive applications using carbon rings, cheramic cylinder liners, and up to 950 K superheat temperature.[305] The reported results suggest viability of the oil-free concept, this having consequently been adopted in the pattern locomotive design. *L.D. Porta* promoted application of diesel engine tolerances and multi-ring practice even for modernization of 1st generation steam locomotives.[306] Both principles have been projected in the prime mover of the pattern locomotive, with the aim of exploiting standard components of diesel engines when feasible.

4.2.5 Transmission of power to drawbar

Power of the prime mover is electrically transmitted to the drawbar through an alternating current (AC) generator feeding AC traction motors on each axle. The infinitely variable power and speed control of the traction motors is obtained by frequency modulation. The power chain thus conforms to state-of-the-art practice of modern diesel-electric locomotives. Fig. 4.9 depicts the entire circuit.

4.2.6 Outlines of regenerative braking system

An energy recovery system has been provided, to facilitate exploiting of braking energy either by feeding it to resistors for heating feedwater, or by electrically accumulating the energy. The recovery and re-use of the braking energy involves the two-way power chain between wheelrims and the storing system, i.e., either resistors or batteries. The primary aim is to use Lithium-ion batteries that currently constitute the main type used in mobile applications.307 Lithium Iron Phosphate (LFP) battery has been opted from several alternatives for its reported affordability, safety, and reliability based on following properties:

- medium high energy density of 90 – 160 Wh/kg,
- Lithium Iron Phosphate (cathode material) occurs in nature, is inexpensive, non-toxic, and thermally stable, and is considered as
- ideal for heavy equipment and industrial environment due to withstanding abuse and a wide range of temperatures.308

According to the same source, the up to 220 Wh/kg energy density of the alternative types with Cobalt oxide content is hampered by its volatility and potential supply shortage of Cobalt as well as their thermal instability that increases the risk of overheating in potential overcharging of the batteries.
The corresponding energy flow consists of following stages:

- from wheelrims via gearbox to traction motors that work as generators in the recovery stage,
- from generators to batteries,
- from batteries to traction motors, and
- from traction motors via gearbox back to wheelrims.

Overall efficiency ηrec of the recovery cycle thus depends on efficiency of each individual stage, being their product. The gearboxes and traction motors are involved in both recovery and re-use stages. The transmission efficiency and motor efficiency thus affect in second power, or $\boldsymbol{\eta_{trans}^2}$ and $\boldsymbol{\eta_{trm}^2}$, respectively. The efficiency of combined charging/discharging cycle of batteries is depicted by ηstor. Formula (4.8) then applies:

$$\boldsymbol{\eta_{rec} = \eta_{trm}^2 \eta_{trans}^2 \eta_{stor}} \tag{4.8}$$

Specifications of Hs1 and Dr18 in 4.2.2 and Table 4.3, respectively, yield the below figures:

ηtrm = 0,95309
ηtrans = 0,98-0,99 (gearbox of Dr18)310

A recent Brazilian study predicts ηstor = 0,92.311 Applying the above parameters, Formula (4.8) yields ηrec = 0,80 – 0,81.

NB: Recent news about *e.g.,* Chinese public transport[312] and a heavy-duty Finnish off-road truck project[313] support the possibility of using supercapacitors to store the energy recovered from regenerative braking or idling, reports of the former indicating a duration of 30 s for the charging of the capacitors. In view of the results of simulated yard work further described in item 5.2.2 the technology should be feasible in such work but is listed as item 6.4.5 among the topics for further studies in Paragraph 6.4.

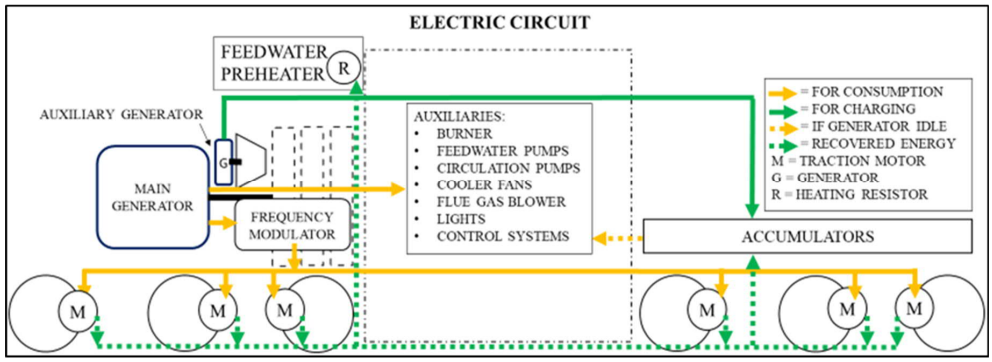

Figure 4.9: Electric transmission and energy recovery system of *Hs1*.

4.3 Generating and use of steam

4.3.1 Functional overview of the steam circuit

The steam circuit is closed, involving condensing of the exhaust steam, regardless of the selected boiler and prime mover type. Except for the blow-down feature of the boiler, or any potential leaks within the entire circuit, the cycle does not involve escape of steam into the atmosphere. Fig. 4.10 locates the focal reference points at which the key parameters are tabulated.

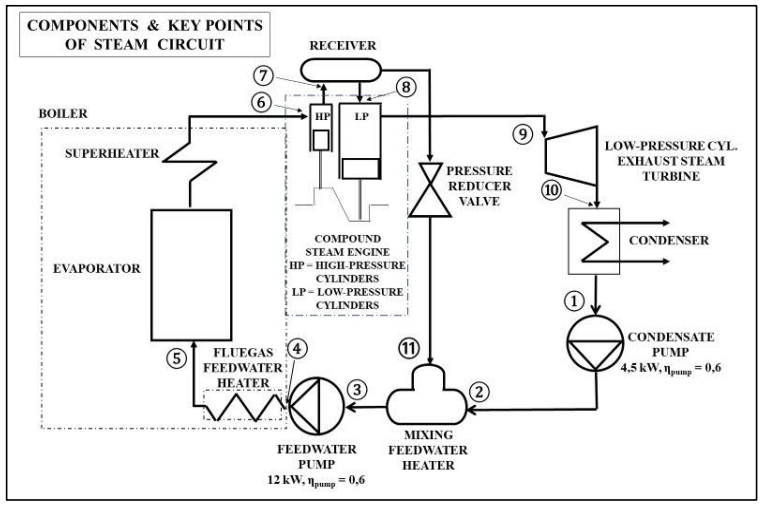

Figure 4.10: The closed-cycle steam circuit of *Hs1*.

The steam circuit is designed for 5,2 MPa working pressure with 810 K superheat temperature.

The condenser is expected to work at atmospheric pressure, or ideally at an input steam temperature of 373 K. The same temperature applies for water at condensate pump inlet and is thus the lowest temperature of the steam cycle. The condensate is pumped into a mixing feedwater heater at 1,8 MPa pressure and 480 K temperature, attained by exploiting the enthalpy of steam outlet from the receiver, *i.e.,* from the steam vessel between high- and low-pressure steam cylinders. The mixture is pumped into the evaporator at boiler pressure through fluegas heat exchanger. This stage of the cycle makes use of the *Franco-Crosti* system described in Paragraph 2.3, to bring the feedwater up to the saturation temperature corresponding to the boiler pressure. Unlike coal combustion, the practically sulphur-free bio-oil combustion is expected to avoid corrosion problems in the projected version of *Franco-Crosti* system. From the evaporator, the steam proceeds through the superheater and steam drum to the high-pressure cylinders of the compound steam engine. The expanded steam enters the receiver, big enough to stabilize the pressure of steam before passing on to low-pressure cylinders. The low-pressure cylinder exhaust steam enters a steam turbine that in turn exhausts to the condenser at close to atmospheric pressure. The phase conversion in the condenser involves such a substantial cooling air flow that recovery of the conversion energy becomes impracticable; the amount of air is too much to be used in combustion while adequate amount of cooling water cannot be carried onboard. Table 4.5 explains the key points of Fig. 4.10, subscripts referring to locations of the items in question in the circuit. Steam tables have been used for determining the parameters. The isentropic efficiency is assumed $\eta_{s\ comp} = 0{,}90$ [314] for the compound steam engine working at a high steam temperature in a well-insulated compartment, and an estimated $\eta_{s\ TB} = 0{,}78$ for the exhaust steam turbine, such a lower figure being explained by both the relatively small size of the turbine and its presumably plentiful operation at partial loads. [315] [316]

ITEM	DESCRIPTION
①	CONDENSATE INLET TO PUMP
②	CONDENSATE INLET TO MIXING PREHEATER
③	FEEDWATER INLET TO FEEDWATER PUMP
④	FEEDWATER INLET TO SURFACE PREHEATER
⑤	FEEDWATER INLET TO STEAM GENERATOR
⑥	STEAM INLET TO HIGH-PRESSURE CYLINDER
⑦	STEAM INLET TO RECEIVER
⑧	STEAM INLET TO LOW-PRESSURE CYLINDER
⑨	EXHAUST STEAM INLET TO TURBINE
⑩	EXHAUST STEAM INLET TO CONDENSER
⑪	BLEED STEAM INLET TO MIXING PREHEATER

Table 4.5: Explanation of the key points of Fig. 57.

NB: The receiver pressure 1,8 MPa corresponds to assumed average HP cylinder admission ratio $\varepsilon_{HP} = 0{,}40$ and has been pre-set as the bleed steam outlet pressure, controlled by a reducer valve.

Fig. 4.11 illustrates the physical location of various components in the steam circuit.

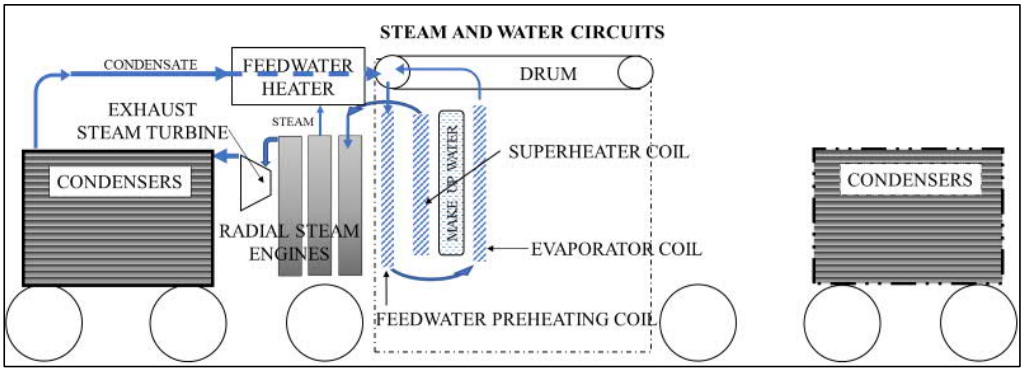

Figure 4.11: Layout of the steam circuit-related components.

From time to time, the blow-down and potential leakage losses necessitate replenishing of water in the steam circuit. A make-up water tank has been duly provided and shown in the scheme. The tank is to be filled with duly treated water since the design does not include any on-board purification system, firstly to omit complicated carry-on appliances discussed within the N&W's steam turbine experiment, and secondly, to save weight. Judging by Fig. 2.29 of Paragraph 2.3, the variety of pumps appeared as the source of most on-the-road problems of N&W's experimental locomotive.

4.3.2 Steam generator

4.3.2.1 Basic design

The below aspects, based on reports concerning experimental locomotives discussed in Chapter 2, support opting for a watertube- rather than firetube-type boiler.

1. The size of the watertube boiler is compact in relation to its steam output.[317]
2. High operation pressures are safely attainable.[318]
3. Quick response to load fluctuations has been attained even with solid fuel.[319]
4. The start-up is rapid in comparison with firetube boilers.[320]
5. State-of-the-art welding technology enables an entirely welded construction.[321]

Watertube boilers appear in several variations. The selected type is a *monotube* boiler consisting of spiral-shaped tubes arranged in concentric vertical coils as sketched in Fig. 4.12. Height of the coils made monotube boilers useless in a conventional locomotive frame construction, as maximum height was – and still is – only available where no axles or frame details prevent using the space in immediate proximity of the rail head. The proposed modification, exploiting ample-size loading gauges of railways in *e.g.,* USA, Canada, Russia, or Finland, is based on a *Mitchell*-type industrial steam generator, reportedly capable of delivering steam in 10 minutes after cold start.[322] Main differences in comparison with the original boiler are the roof- rather than floor-mounted burner, and the toroid-shape drum added by the author. The re-location of the burner aims at minimizing the risk of dirt accumulating on the burner nozzles.[323] This arrangement was also successfully applied in famous steam automobiles of *Abner Doble* until the end of their era.[324] The superheater is to provide a heating surface large enough, to result in the specified steam temperature regardless of the modest heating value of pyrolysis oil. The calculated ratio between superheating *vs.* evaporating surface of the *Hs1* is 0,71 while a typical late steam age ratio was 0,4, *i.a.* in the USA.[325]

The toroid-shape drum provides a space in its centre, to accomodate a burner of standard design and dimensions. The selected type, with a modulation ratio of 1:5, has been tested at a firing rate of 2400 kg/h of pyrolysis oil, such a capacity exceeding the predicted requirements by *ca.* 70 % as will be shown in calculations of Paragraph 4.6. [326]

The boiler location between the power trucks has become possible by re-locating the typical head-end cab of diesel-powered locomotives into the lateral centre of the locomotive, as later shown in Paragraph 4.5.

The flue gas flow of the boiler in Fig. 4.12 is depicted by red arrows. Water and steam flows also refer to the diagram of Fig. 4.11 above. The *counter-flow* principle, later depicted in Fig. 4.13, is exploited in each coil. An insulated annular make-up water tank is integrated in the boiler.

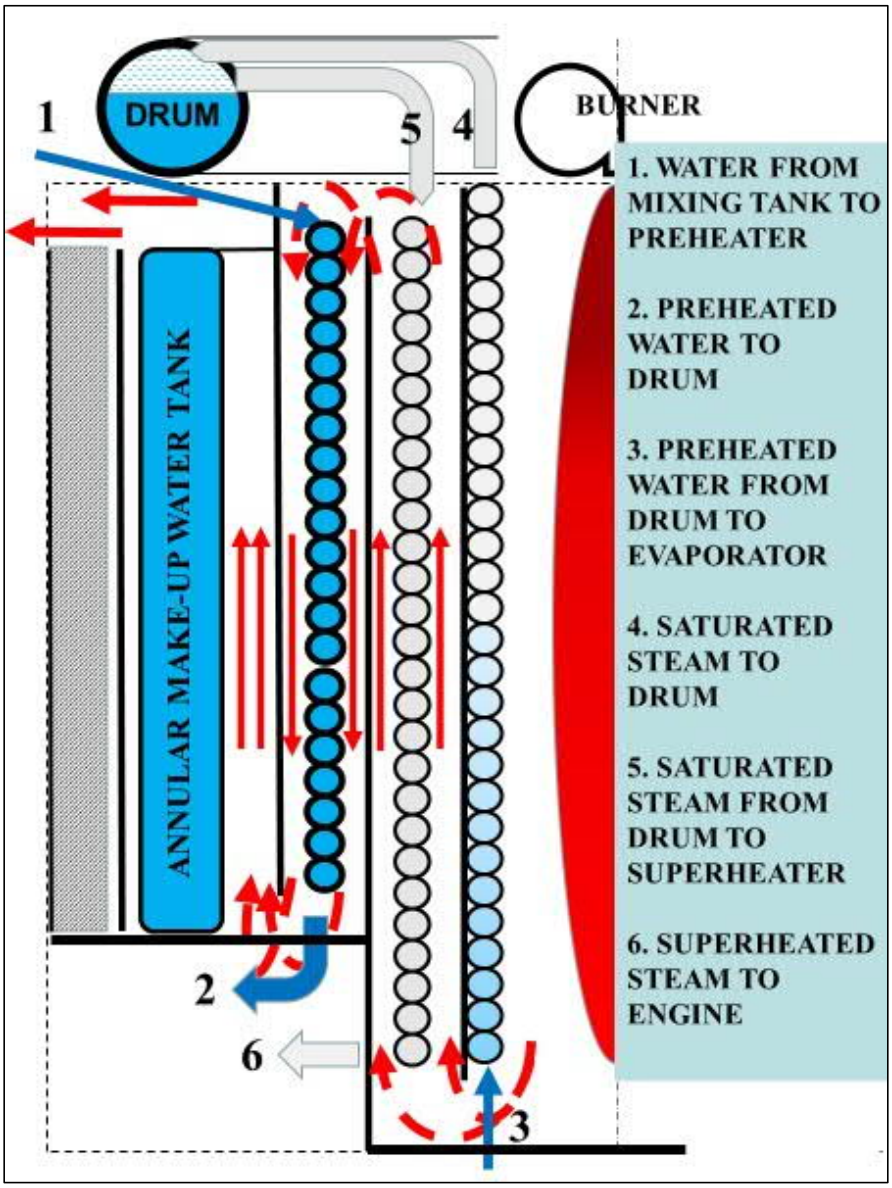

Figure 4.12: Outlines and description of the modified monotube boiler.

4.3.2.1 Steam parameters

Steaming capacity of the boiler must meet the steam demand of the prime mover at maximum continuous drawbar power P_{db}, the preliminary requirement having been calculated in Paragraph 4.2.2 to be 1,70 kg/s. This figure exactly conforms to the calculated consumption at HP cylinder admission ratio ε_{HP} = 0,60, as later shown in calculations of Paragraph 4.6A.

Selection of boiler pressure p = 5,2 MPa, and superheat temperature T_{sup} = 810 K, has been based in search for an optimum between aspects listed below, items 1. to 3. being visible in *Mollier h, s* chart as shown within the calculations, and items 4. - 6. duly pointing at references:

1. At any given pressure, the specific enthalpy of steam is directly proportional to its temperature.
2. The isotherms tend to drop rapidly towards the left, or towards isobars of higher pressures.
3. Expansion to atmospheric pressure ends up with a high humidity of the expanded steam.
4. Automotive steam engine experiments of *i.a.* Saab-Scania exploited up to 10 MPa pressures while the German Zero Emission Engine worked at 5 MPa. [327] [328]
5. Steam temperature 810 K is regarded as an upper limit in power plant applications as temperatures higher than this, call for exploiting costly special steels rather than ordinary ferritic steels. [329]
6. The viability of ceramics as coating or construction material of unlubricated cylinder liners has been proved *i.a.* by Volkswagen. [330]

The selected steam parameters result in exhaust steam conditions close to the dry saturated line. Need for expensive special steels in the construction is also avoided. The mean effective pressure of piston engine of the prime mover is kept within the same range (2,5 - 2,8 MPa) as in medium speed diesel engines. [331] All steam parameters are further discussed within the calculations of Paragraph 4.6A.

4.3.2.2 Heat transfer elements

The heat transfer elements of *Hs 1* involve both steam circuit and fluegas circuit essentially consisting of six heat exchangers related with generation or processing of steam:

a. evaporator
b. superheater
c. mixing tank feedwater preheater
d. fluegas feedwater preheater
e. condensers, and
f. combustion air preheaters.

Items a, b, d, and f exploit the fluegas heat whereas preheater c makes use of bleed steam outlet from the receiver while condensers, item e, are cooled by air from stagnation pressure or cooling fans.

Evaporator a is the innermost coil of the boiler, surrounding the furnace. Its water wall absorbs a substantial portion of the combustion heat through radiation and is supposed to evaporate all the preheated feedwater at all operating conditions.

Fig. 4.13 illustrates the working principle of typical heat exchangers involving two opposite fluid flows.

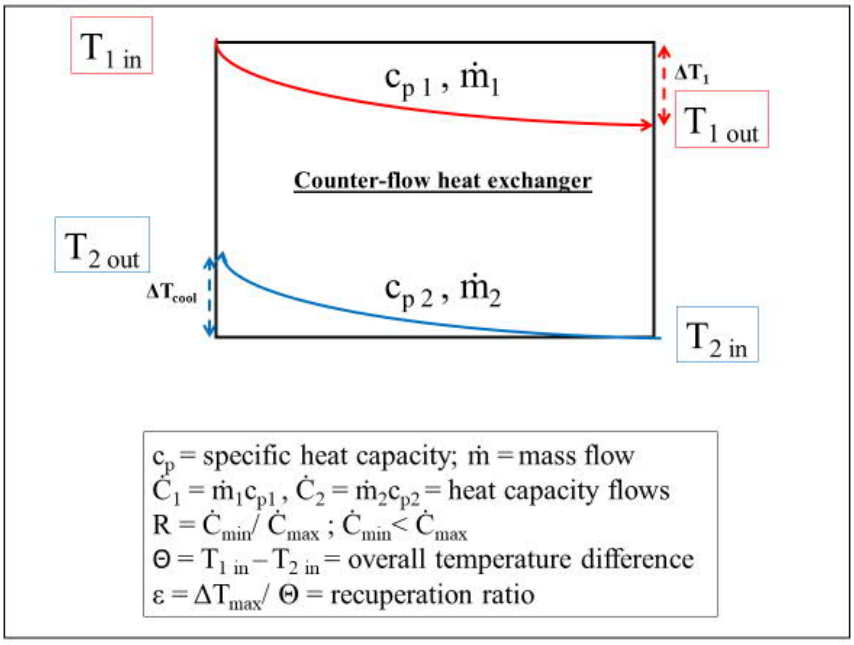

Figure 4.13: Principle of a counter-flow heat exchanger. [332]

The two flows do not mix with each other, as they are separated by tube or plate walls. The mutual order of superiority of parameters $\dot{C}$ or ΔT of each fluid is to be checked case by case as the definition of $R = \dot{C}_{min}/\dot{C}_{max}$ dictates its being < 1. The comparative quality of the exchanger in relation to an ideal exchanger is expressed by the recuperation ratio $\varepsilon < 1$. In an ideal heat exchanger, both fluids would end up with the initial temperatures of opposite fluids, resulting in $\varepsilon = 1$. [333]

The conductance G of the heat exchanger characterises its ability to transfer heat from one fluid to another.

4.4 Selection of fuel

4.4.1 Arguments supporting use of liquid fuel

Opting for liquid rather than solid type of fuel is supported by following constructional aspects:

1. Designs of both *frame* and *boiler* constructions become more flexible as liquid fuel is delivered to the burner *via* pipelines rather than *via* mechanical conveyors, thus enabling integration of tanks with the frame structure, in optimum locations.
2. Roof-mounting of the burner is expected to secure its flawless operation as eventual fuel droplets or dirt might disturb the function of the sensitive nozzles in case of floor-mounting. [334]
3. Light-up and shut-off of the burner can be readily performed anytime.
4. Higher energy density of fuel contributes to controlling the total weight of the locomotive.
5. Eventual bio-oil combustion only requires minor modifications to standard fossil oil burners. [335]

The primary aim of using bio-oil for fuel has been retained throughout the study, while all calculations also cover light fuel oil (LFO) as an alternative with proven characteristics. The alternative fuel is to test the viability of the concept, regardless of eventual complications in availability or use of bio-oils.

4.4.2 Properties of pyrolysis oil

Fast pyrolysis bio-oils, later referred as PYR, belong to fuels recently studied within extensive tests and pilot plants of industrial scale.[336] These oils have been proved to work well, provided that their special properties are taken in account.[337] Combustion tests indicate that the NO_x emissions mainly originate from fuel-bound nitrogen. Particulate emissions are typically incombustible matter and may be higher than in combusting of fossil fuels.[338] Table 4.6 shows some properties of PYR compared with those of heavy (HFO) and light (LFO) fuel oil.

Property	Standard	Typical bio-oils	Heavy fuel oil	Light fuel oil
Solid matter %	ASTM D 7579	< 0,5		
pH	ASTM E 70	2 - 3		
Water content w-%	ASTM E 203	20 - 30	~ 0	~ 0
Viscosity (40 °C) mm^2/s	EN ISO 3104, ASTM D 445	15 - 35[1]	max 180/420 50 °C	2,0 - 4,5
Density (15 °C) kg/dm^3	EN ISO 12185, ASTM D 4052	1,10 - 1,30[1]	max 0,99/0,995	max 0,845
Acid figure (TAN) mg KOH/g	ASTM D 664	70 - 100		
LHV (As received) MJ/kg	DIN 51900, ASTM D 240	13 - 18[1]	min 40,6	42,6
Ash content w-%	EN ISO 6245	0,01 - 0,1[2]	max 0,08	max 0,01
Residual C (MCR, CCR) w-%	ASTM D 4530, ASTM D 189	17 - 23		
C w-% dry matter	ASTM D 5291	50 - 60		
H w-% dry matter	ASTM D 5291	7 - 8		
N w-% dry matter	ASTM D 5291	< 0,4	0,4	0,02
S w-% dry matter	EN ISO 20846, ASTM D 5453	< 0,05	max 1,0	max 0,001
O w-% dry matter	calculational	35 - 40		
Na+K+Ca+Mg w-% dry matter	EN ISO 16476	< 0,06		
Cl ppm	ISO 8754, ASTM D 4294	< 75		
Flame point °C	EN ISO 3016, EN ISO 9038 ASTM D 93B	40 -110[3]	min 65	min 60

[1] Depending of water content

[2] Metals, when getting oxidized within ash formation, may result in excessive ash content, *i.e.* , more ashes than dry matter

[3] Method of determining the flame point does not apply for pyrolysis oils

Table 4.6: Various properties of fast pyrolysis oil vs. HFO and LFO.[339]

Table 4.7 lists further aspects supporting the potential use of PYR as locomotive fuel.

1. PYROLYSIS OIL PRODUCTION NEITHER COMPETES WITH FOOD PRODUCTION OF LAND AREA NOR INVOLVES FELLING TREES FOR FUEL USE SINCE FOREST RESIDUE CONSTITUTES BOTH FEEDSTOCK AND FUEL OF THE OIL PRODUCTION PROCESS.
2. TECHNO-ECONOMICALLY THE BIO-OIL PRODUCTION PROCESS HAS BEEN PROVED TO BE COMPETITIVE WITHIN THE FIELD IF INTEGRATED INTO A COMBINED HEAT AND POWER (CHP) PRODUCTION PLANT. (Energy&Fuels, Aug. 2015)
3. PYROLYSIS OIL MAY BE USED AS SUCH IN EXTERNAL COMBUSTION APPLICATIONS WHEREAS ITS USE IN INTERNAL COMBUSTION ENGINES WOULD REQUIRE FURTHER REFINING.
4. IN COMPARISON WITH SOLID BIOMASS THE COMBUSTION OF PYROLYSIS OIL IS EASIER TO CONTROL AND AUTOMATE, AND ITS VOLUME-BASED ENERGY DENSITY IS HIGHER.
5. FAST PYROLYSIS IS A SUBJECT OF ONGOING STUDIES AND TESTS, TO PROMOTE USE OF RENEWABLE SOURCES OF ENERGY AS SUBSTITUTES FOR HEAVY FUEL OIL (HFO) WITH THE AIM OF BOTH CLEANER ENVIRONMENT AND REDUCED DEPENDENCE ON IMPORTED FUEL.
6. A 50 000 t/a CAPACITY PYROLYSIS OIL PILOT PLANT WAS STARTED IN FINLAND IN 2013 IN THE VICINITY OF ABUNDANT SOURCES OF FOREST RESIDUE, ENABLING A SHORT SUPPLY CHAIN.
7. TESTING FACILITIES OF THE PLANT MATCH WITH THE POWER RANGE DEALT IN THE STUDY.

Table 4.7: Arguments supporting use of PYR for locomotive fuel.

4.4.3 Outlines of PYR production

A relevant potential for PYR to replace fossil oil, *e.g.,* in Finland, lies in the abundance of forest residue. This constitutes a sulphur-free source of energy that can be used for both *feedstock* and *fuel* in a process where the pyrolyzer is integrated in a combined heat and power (CHP) plant. The heat transfer within the pyrolyzer involves a flow of hot sand as seen in Fig. 4.14. Consequently, the oil contains abrasive particles. These do not appear to have caused any uncontrollable problems in external combustion applications whereas further refining is required, should the PYR be used for fuel in internal combustion engines. Fig. 4.14 gives an overview of a CHP-integrated pyrolyzer.

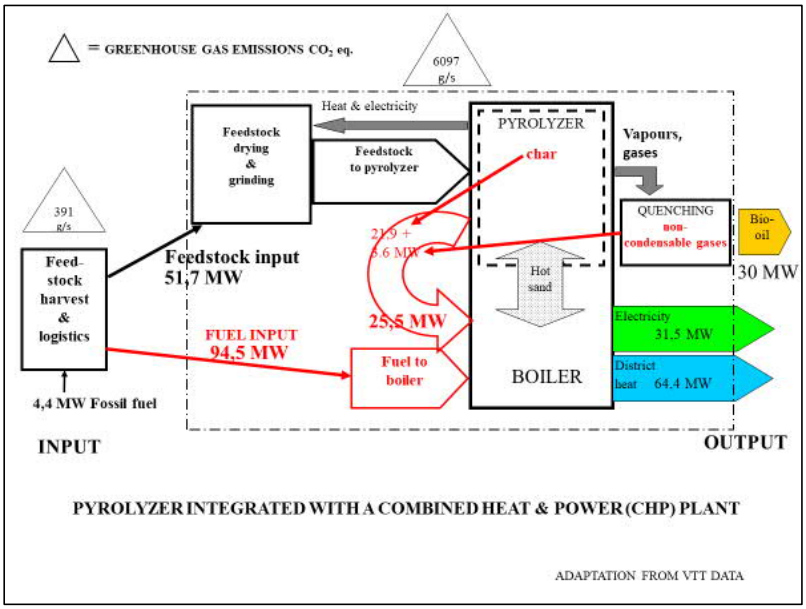

Figure 4.14: Pyrolysis oil production process as integrated in a CHP power plant. [340]

4.4.4 Outlines of the gas flow circuit

Fig. 4.15 illustrates a schematic layout of the components involved in gas flow circuit.

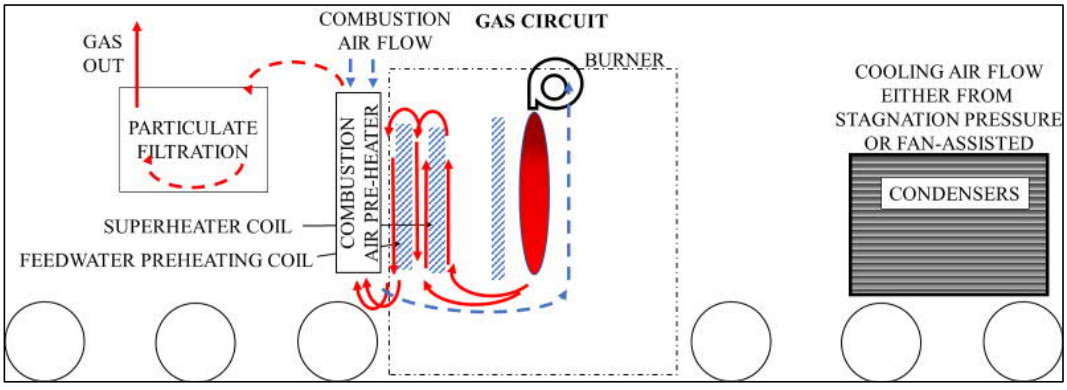

Figure 4.15: Fluegas circuit of *Hs1*.

4.5 Resulting ultimate outlines of the *Hs1*

4.5.1 Superstructure and layout

The overall appearance of the locomotive is sketched in Fig. 4.16. The power trucks exactly conform to those of an existing diesel-electric locomotive, the *Dr18* discussed within all the further comparisons. The centrally located cab has two air-conditioned operator's compartments, elevated for optimum visibility. The external layout is fully symmetrical, both functionally and from the driver's point of view. The hoods are identical outwards whereas the insides deviate from each other, one end comprising of the power compartment and the other end housing *i.a.* fuel and water tanks, battery packs, and electrical appliances.

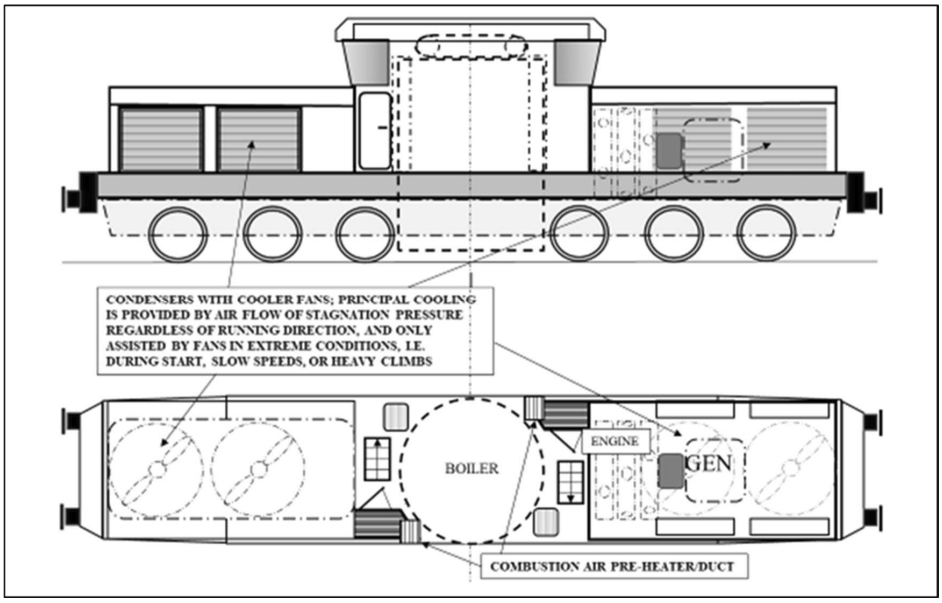

Figure 4.16: Overall layout of *Hs1*.

4.5.2 Elements of steam generating system

Opting 1,7 m for the inside diameter of the furnace, as discussed in further calculations of Paragraph 4.6B, defines the convective surface in four of the heat exchangers. The surface area of combustion air preheaters has been independently specified. All the relevant surfaces are further compiled in Table B19 of Paragraph 4.6B.

a. Furnace
   The water wall of the furnace is assumed to evaporate the preheated feedwater even at the maximum capacity of the boiler. The circular shape of the furnace is to avoid blind corners and thus to maximize its heat transfer capacity. The required evaporative surface on one side and the geometrical limitations of the locomotive on the other side define the optimum inside diameter of the boiler. Maximum height is set by loading profiles of railways.
b. Superheater
   The superheater is to provide adequate heating surface while excessive superheating must be prevented. The preventing system is to exploit water jets, *i.e.,* a system commonly used in

industrial applications, but the detailed configuration of the system is omitted from the scope of the study.

c. Mixing tank feedwater preheater
   Steam outlet from receiver is exploited for heating of condensate before it is pumped to the fluegas heat exchanger and further to the boiler. The outlet steam is called bleed steam, its pressure being limited to 1,8 MPa by a control valve. The mixing tank preheater increases the steam cycle efficiency.

d. Flue gas feedwater preheater
   The outermost coil of the boiler in Fig. 4.12 constitutes the flue gas feedwater preheater aiming at heating the feedwater up to the saturation temperature 539 K of steam at boiler pressure. Preheating is to ensure start of evaporation once the feedwater enters the water wall of the furnace.

e. Combustion air preheater
   The aim of the air preheater is to recover maximum amount of the remaining heat of the fluegas after its exit from feedwater preheater. Traditionally, corrosion has been the limiting factor of reducing the fluegas temperature. Practically sulphur-free fluegas from pyrolysis oil combustion is predicted to mitigate, if not eliminate the said limitation. Due to eventual condensation of fluegas, 398 K exit temperature has been projected for the fluegas side of the preheater. The resulting combustion air temperatures have been applied in the combustion calculations. The locomotive is assumed to operate in moderate climatic conditions, the typical range of temperature falling between -25 ^{o}C and + 25 ^{o}C. The upper limit has been used in the calculations for cooling air inlet temperature. Speed of 25 m/s has been used, to find out the pressure and fan power required, should the air flow be created by fans. The air preheater is a plate-type heat exchanger divided in two sections, placed symmetrically around the boiler, to facilitate identical air flow regardless of the running direction. Fig's 4.17 and 4.18 show the arrangement.

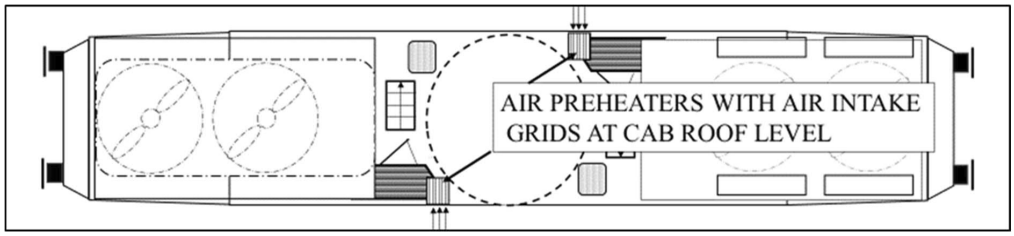

Figure 4.17: Arrangement and layout of combustion air preheaters onboard the locomotive.

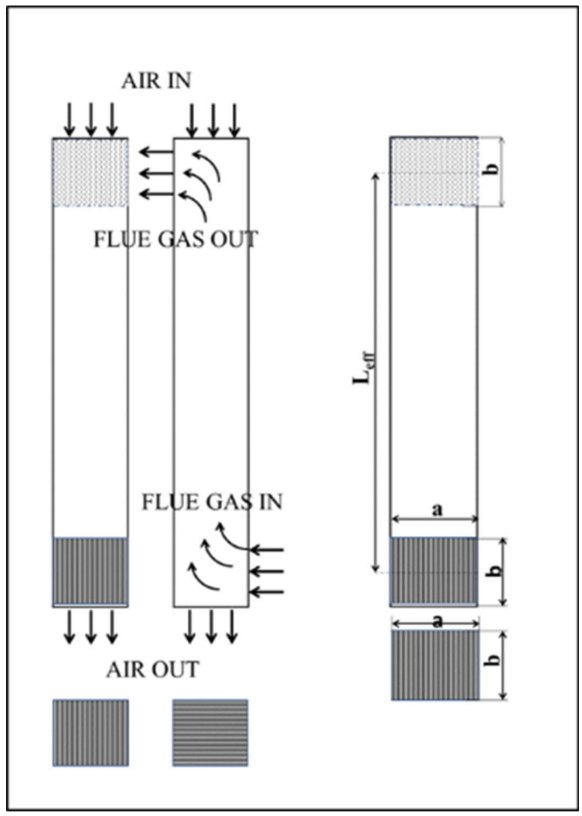

Figure 4.18: Configuration of combustion air preheaters.

f. Condensers

The turbine completes the working cycle of the prime mover by exhausting to air-cooled condensers. These aim to exploit *stagnation pressure* caused by the movement of the locomotive, to build up the coolig air flow. During start, or when climbing uphill, less stagnation pressure is available, and the air flow must be created by fans. Both ends of the locomotive have air intake grids that can be closed, similar grids being mounted over the fan casings. If fans are required, the fan grids are opened, and front grid closed, to ensure that the air flow only takes place through the condensers, and *vice versa*. Fig. 4.19 shows the layout and components of the condensing system. Calculation of the cooling capacity essentially consists of a multi-stage iterating process and involves complex dual-phase considerations. Summary of the detailed spread sheet calculations of Ph. Lic. (Eng.) *Kari Saari* of Aalto University are shown in appropriate section of Paragraph 4.6B, *by courtesy of Mr Saari.*

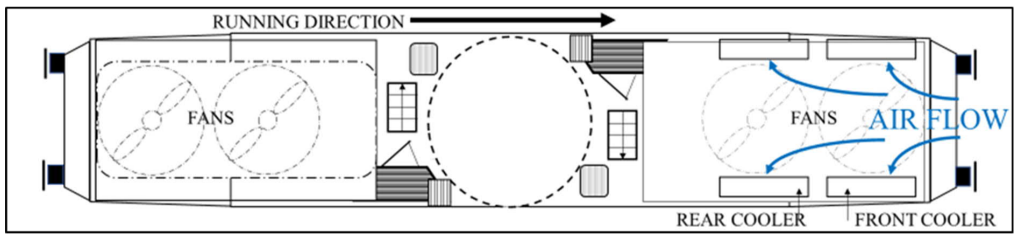

Figure 4.19: Functional layout of the condensers.

4.5.3 Mass considerations

A comparison between masses of diesel- *vs.* steam-specific components is required to ensure that the total mass of *Hs 1* does not substantially exceed that of the reference locomotive *Dr18*, the prime mover of the latter remaining the only major diesel-specific component as the electric transmission and power trucks are similar in both engines. The weight of the steam-powered 15-cylinder radial engine is estimated to be of the same order than the 12-cylinder V-type diesel engine. Boiler specifications of Appendix B predict a mass of *ca.* 20 t while the total mass of condensers, mostly built of aluminium, is estimated to be 4 t. Fuel tanks with a projected capacity of 5 t are integrated in the self-supporting lightweight frame construction. The projected carry-on water volume is 4,5 m^3. With the energy density 0,14 kWh/kg applied in item 4.2.6, a battery package of 6 tons results in a capacity of 840 kWh. Adding such a package weight to the fuel and water weight, the mass of steam-specific components of the *Hs 1* would thus add about 40 t to the 120-t weight of the *Dr18*, resulting in a total locomotive mass of *ca.* 160 t. On the other hand, the mass of the *Dr18* appears to have been made high on purpose, as the available tractive effort is directly proportional to the adhesive weight and is thus most desirable in heavy haul. Comparing the ratio 9,5 kW of drawbar power *per* ton of locomotive mass of the *Dr18* with *e.g.,* the 15,5 kW/t of a *Dr13* class *Alstom*-built diesel-electric locomotive, proves the potential of building the power of the *Dr18* in up to 60 % = 45 t less weight.[341] Such a reduction matches with the predicted additional weight of the *Hs 1,* its design weight 130 t providing an additional 10-t margin. Paragraph 3.4 proved that the best representatives of late steam age locomotives attained a power-to-weight ratio of 23 kW/t less tender, implying roughly 16 kW/t, tender included. The *Hs1* is an equivalent of the latter case with its carry-on tanks while its power-to-weight ratio is 8 kW/t, *i.e.*, on the safe side with an ample margin.

4.6 Calculations of the *Hs1*

Assessing the power of the prime mover and the capacity of heat exchanger units aim at ensuring the capability of all functional elements of the locomotive. Calculations refer to spread sheets with back-up of formulae and input data of Appendices A and B.

A. Prime mover calculations

Power calculations are based on assessing enthalpy drops within the prime mover by using the basic dimensions and steam parameters given in tables of Appendix A, Tables A1 and A2 being repeated below, to clarify the critical points of the steam circuit, and the key parameters.

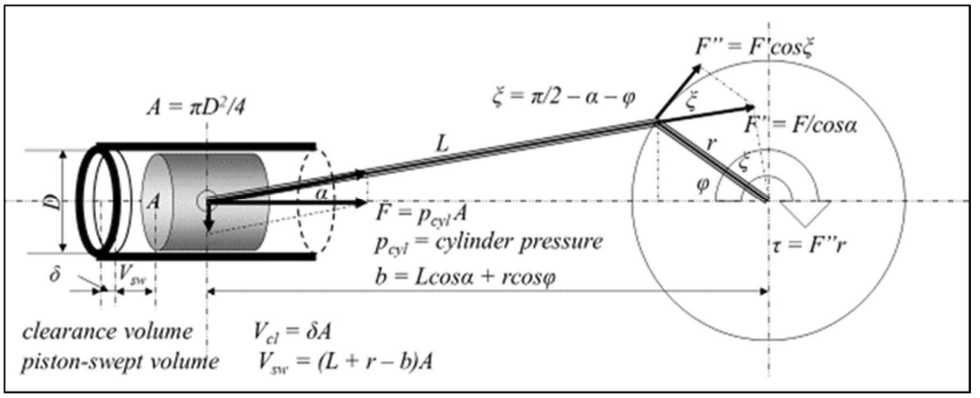

Figure A1: Dimensions and trigonometry of the prime mover cylinders.

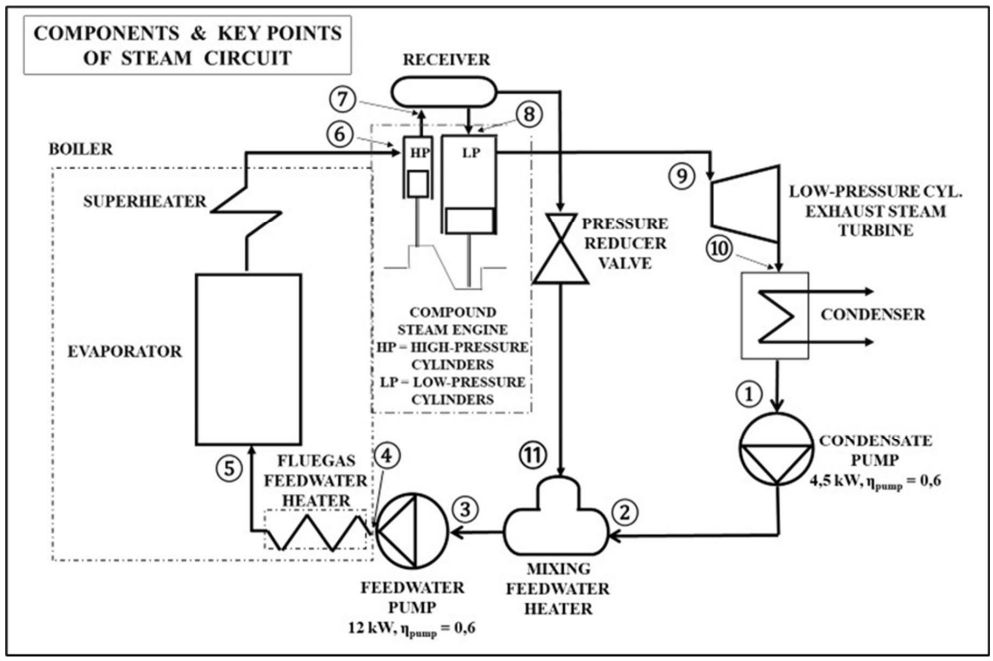

Figure A2: Diagram of steam circuit of the *Hs1*.

PRIME MOVER PARAMETERS			
A. Fixed parameters			
Cylinder diameter	D	0,20	[m]
Piston area	A	0,03	[m^2]
Crank radius	r	0,14	[m]
Piston stroke s = 2r	s	0,28	[m]
Connecting rod length	L	0,5	[m]
Crank-to-connecting-rod ratio	r / L	0,28	[ ]
Displacement V_{disp} = As	V_{disp}	0,0088	[m^3]
Clearance volume:			
- proportional	V_{prop}	6	[%]
- actual	V_{cl}	0,00053	[m^3]
Number of engine units	N_{eng}	3	[ ]
Number of cylinders per engine unit	N_{cyl}	5	[ ]
Number of HP cylinders per engine unit	N'_{HP}	1	[ ]
Total number of HP cylinders	N_{HP}	3	[ ]
Number of LP cylinders per engine unit	N'_{LP}	4	[ ]
Total number of LP cylinders	N_{LP}	12	[ ]
Rotational speed	n	7,5	[r/s]
Piston speed	w_p	4,2	[m/s]
Mechanical efficiency	η_{mech}	0,92	[ ]
B. Parameters depending on crank angle			
Momentary piston-swept volume of cylinder	V_{SW}	**Fig.4.20**	[m^3]
Momentary total volume of cylinder	V_{tot}	$V_{SW}+V_{cl}$	[m^3]

Table A1: Technical data of the prime mover.

STEAM CYCLE PARAMETERS			
Boiler pressure (abs)	p_B	5,2	[MPa]
Boiler efficiency	η_B	0,95	[ ]
Own consumption efficiency	η_{oc}	0,96	[ ]
Temperature of superheated steam at boiler pressure	T_{sup}	810	[K]
Temperature of feedwater at boiler pressure	T_{fw}	539	[K]
Specific enthalpy of preheated feedwater at 539 K	h_5	1166	[kJ/kg]
Specific enthalpy of superheated steam at boiler pressure	h_B	3518	[kJ/kg]
Specific entropy of superheated steam at boiler pressure	s_{sup}	7067	[J/kgK]
Specific enthalpy of evaporation at boiler pressure	l	1627	[kJ/kg]
Specific enthalpy of water at feedwater pump inlet	h_3	884	[kJ/kg]
Specific enthalpy of feedwater at boiler inlet	h_4	887	[kJ/kg]
Condenser pressure (abs)	p_{cond}	0,1	[MPa]
Specific enthalpy of water at condensate pump inlet	h_1	418	[kJ/kg]
Specific enthalpy of water at inlet of mixing feedw. tank	h_2	420	[kJ/kg]
Density of superheated steam at boiler pressure	ρ_{HP}	14,4	[kg/m^3]
Isentropic index of high-pressure steam	κ_{HP}	1,27	[ ]
Isentropic index of low-pressure steam	κ_{LP}	1,30	[ ]
Isentropic efficiency of compound steam engine	$\eta_{s\,comp}$	0,90	[ ]
Isentropic efficiency of exhaust steam turbine	$\eta_{s\,TB}$	0,78	[ ]

Table A2: Principal steam parameters of the prime mover.

The HP-cylinder admission ratio ε_{HP} = 0,60 corresponds to full power of the prime mover and is primarily applied both in the calculations and further in the simulated operations. The full power also sets the power requirements for feedwater and condensate pumps, the efficiencies of both having been predicted to be $\boldsymbol{\eta_{pump}}$ = 0,60 and the powers obtained from Formulae (4.1) - (4.3):

$$\Delta \boldsymbol{h_{pump\,s}} \approx \boldsymbol{\nu \Delta p_{pump}} \qquad (4.1)^{342}$$

$$\boldsymbol{P_{pump\,s}} = \dot{m} \Delta \boldsymbol{h_{pump\,s}} \qquad (4.2)^{343}$$

$$\boldsymbol{P_{pump\,act}} = \frac{\boldsymbol{P_{pump\,s}}}{\boldsymbol{\eta_{pump\,s}}} \qquad (4.3)^{344}$$

$\Delta h_{pump\,s}$ = isentropic rise of enthalpy within the pump, ν = specific volume of water at mean temperature of water in pump, Δp_{pump} = rise of pressure in pump, $\dot{m}$ = mass flow of water in pump, $P_{pump\,s}$ = power of isentropic pump, $P_{pump\,act}$ = actual power consumption of pump, and $\eta_{pump\,s}$ = isentropic efficiency of pump. Selected steam circuit parameters yield Δp_{cond} = 1,68 MPa for the condensate pump and Δp_{fw} = 3,42 MPa for the feedwater pump. Specific volume of water is obtained from tables: ν_{cond} = 0,001105 m^3/kg and ν_{fw} = 0,001228 m^3/kg.[345] Mass flows are taken from Table A11 calculated in Paragraph 4.6, yielding $\dot{m}_{cond}$ = 1,43 kg/s and $\dot{m}_{fw}$ = 1,70 kg/s. For the given parameters, spread sheet calculations yield powers $P_{pump\,cond}$ = 4,5 kW for the condensate pump and $P_{pump\,fw}$ = 12,0 kW, or a total of 16,4 kW ≈ 1,3 % of the indicated power 1252 kW of the prime mover, the combined power loss of the pumps being ≈ 0,5 %. The rest of the calculations follows the sequence below:

a. Generate expansion graph corresponding to the maximum HP-cylinder admission ratio.
b. Determine the corresponding enthalpy drop within HP-cylinders.

c. Determine the steam consumption.
d. Determine affordable LP-cylinder admission ratio to use up all HP-cylinder exhaust steam.
e. Generate expansion graph corresponding to above admission ratio, to determine the resulting exhaust steam pressure and other steam conditions.
f. Determine the corresponding enthalpy drop within LP-cylinders.
g. Determine enthalpy-drop within the exhaust steam turbine.
h. Determine steam mass flows in different sections of the prime mover.
i. Determine indicated power of the prime mover sections.
j. Determine brake power P_b of the prime mover.
k. Determine the brake efficiency of the prime mover.

Calculation procedure

a. Plot high-pressure cylinder steam expansion curve corresponding to admission ratio $\varepsilon_{HP} = 0{,}60$. Apply pre-set dimensions of the prime mover in Fig. A1 and Table A1, and parameters of the steam cycle in Table A2 above, and Tables A3, A4 in Appendix A.

Parameters of the hyperbolic expansion curve satisfy Formula (A.1) and its conversion (A.2). To obtain the total cylinder volume V_{tot} in Formula (A.3) the clearance volume V_{cl} must be added to swept volume V_{SW} which in turn is a function of crank angle φ in Formula (A.4). The clearance volume plays a significant role in the expansion, although its steam consumption is negligible as the space is always filled with steam, due to compression stage. The end point of the admission line belongs to the expansion curve as earlier described in Paragraph 2.2. The constant C_{HP} is thus determined. Fig. A3 depicts interdependence between the crank angle and the HP-cylinder events, the illustrated case showing that *e.g.*, for $\varepsilon_{HP} = 0{,}40$, the admission is cut off at crank angle 71^0.

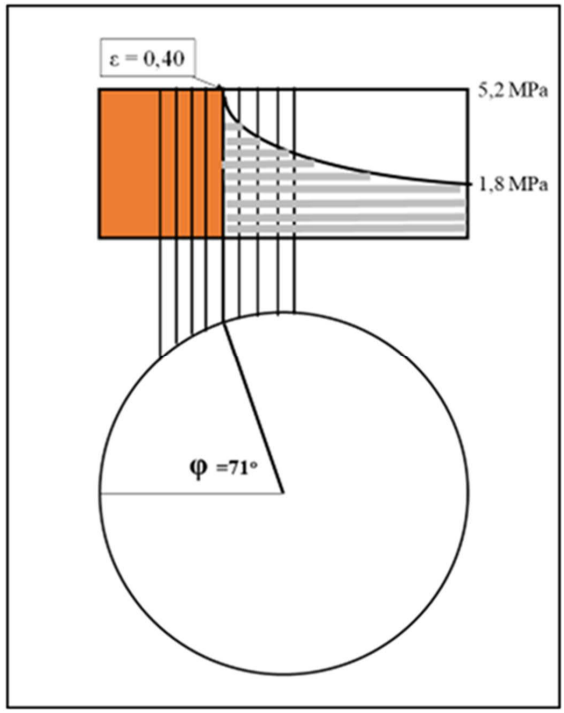

Figure A3: Dependence between crank angle φ and admission ratio ε.

Steam tables give isentropic index κ_{HP} = 1,27 for steam at HP-cylinder inlet conditions 5,2 MPa and 810 K.

$$p_6 V_{tot}^{\kappa_{HP}} = C_{HP}{}_{-}{}^{346} \quad \text{(A.1)}$$

$$p_6 = \frac{C_{HP}}{V_{tot}^{\kappa_{HP}}} \quad \text{(A.2)}$$

$$V_{tot} = V_{sw} + V_{cl} \quad \text{(A.3)}$$

$$V_{SW} = (L + r - (r cos\varphi + L cos\left(arcsin\frac{r sin\varphi}{L}\right)))A^{347} \quad \text{(A.4)}$$

b. Determine enthalpy drop and steam parameters at exit of HP cylinders.

The procedure consists of following steps:

- check the specific enthalpy, entropy, and temperature of inlet steam,
- obtain exhaust steam pressure and specific enthalpy according to admission ratio ε_{HP} = 0,60,
- calculate the resulting isentropic enthalpy drop and correct it to the actual one by means of the selected isentropic efficiency $\eta_{s\,comp}$ = 0,90 of the compound engine,
- find the point of exhaust steam isobar to comply with the actual enthalpy drop, and
- check the density and temperature of steam according to its actual specific enthalpy.

The above sequence, including similar process of determining enthalpy drop within the low-pressure cylinders and exhaust steam turbine, is graphically depicted in *Mollier h, s* chart of Fig. A4.

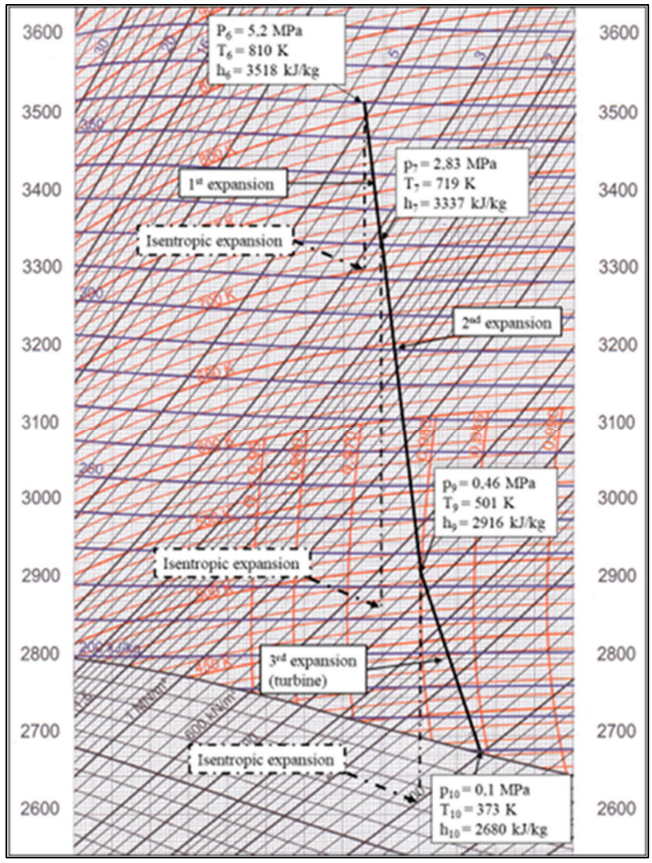

Figure A4: Enthalpy drops of prime mover at all stages of expansion, plotted at *Mollier h, s* chart.

Steam tables have been exploited for obtaining accurate readings for specific enthalpies, entropies, temperatures, and densities used in the calculations.
Formulae (A.5), (A.6), and (A.7) have been used for calculating the parameters:

$$\boldsymbol{\Delta h_{HP\,s} = h_6 - h_{7s}} \tag{A.5}$$

$$\boldsymbol{\Delta h_{HP} = \eta_{comp} \Delta h_{HP\,s}} \tag{A.6}$$

$$\boldsymbol{h_7 = h_6 - \Delta h_{HP}} \tag{A.7}$$

h_6 specific enthalpy of steam leaving the boiler and entering HP cylinders,
p_7 pressure of high-pressure cylinder exhaust steam,
$T_{7\,s}$ actual temperature of high-pressure cylinder exhaust steam,
ρ_7 density of high-pressure cylinder exhaust steam,
$h_{7\,s}$ specific enthalpy of high-pressure cylinder exhaust steam after isentropic expansion,
s_7 specific entropy of high-pressure cylinder exhaust steam after isentropic expansion,
$\Delta h_{HP\,s}$ isentropic enthalpy drop in high-pressure cylinders,
Δh_{HP} actual enthalpy drop in high-pressure cylinders,
h_7 actual specific enthalpy of high-pressure cylinder exhaust steam.

The resulting enthalpy drops, and steam parameters have been compiled in Table A6 of Appendix A. Subscripts refer to appropriate key points of steam circuit.

c. Determine steam consumption at cylinder admission ratio ε_{HP} = 0,60.

Steam consumption of the prime mover is equal to mass flow of steam from boiler to high-pressure cylinders, or $\dot{m}_6$ of the steam circuit in Fig. A2. Admission ratio ε_{HP} = 0,60 presets the $\dot{\mathbf{m}}_6$ according to formula (A.8):

$$\dot{m}_6 = N_{HP} n \rho_6 \varepsilon_{HP} V_{tot} \tag{A.8}$$

where parameters are derived from Tables A1 and A2. Density $\rho_6 = \rho_{HP}$ since the inlet steam comes directly from the boiler. The resulting steam consumption is 1,70 kg/s as also noted in Appendix A.

NB: Clearance volume V_{cl} has been neglected when calculating the steam consumption, as the space is always filled with steam trapped in the cylinder, due to compression stage as was explained in 2.2.

d. Determine affordable low-pressure cylinder admission ratio ε_{LP} when ε_{HP} = 0,60.

Calculations aim at adjusting ε_{LP} to exactly use up the amount of steam exhausted from HP cylinders. However, the LP cylinder inlet mass flow $\dot{\mathbf{m}}_8 < \dot{\mathbf{m}}_7$ by the bleed steam mass flow $\dot{\mathbf{m}}_{11}$ taken from the receiver. Due to 1^0 increments between crank angles, the tabulated *vs.* calculated ε's may not exactly match, and therefore the closest $\varepsilon_{tab} < \varepsilon_{calc}$ is applied in subsequent calculations. Formula (A.9) is applied for the calculation, the resulting ε_{calc} = 0,205 also shown in Table 8 of Appendix A. The steam parameters $\dot{\mathbf{m}}_8$, ρ_8 at exit of HP cylinders also apply for LP cylinder inlet steam:

$$\varepsilon_{calc} = \frac{\dot{m}_8}{n \rho_8 N_{LP} V_{disp}} \tag{A.9}$$

In this case, the calculated ε_{calc} exactly matches with the tabulated ε_{tab} as evidenced by the corresponding column of the spread sheet, although not shown in the text.

e. Plot low-pressure cylinder steam expansion curve corresponding to admission ratio ε_{LP} = 0,20.

The procedure is identical with item a., only the LP steam parameters having been substituted for the HP parameters, resulting in Formula (A.10):

$$p_8 V_{tot}^{\kappa_{LP}} = C_{LP} \tag{A.10}$$

f. Determine enthalpy drops, and steam parameters at exit of LP cylinders.

The procedure is identical with item b., only the LP steam parameters having been substituted for the HP parameters, resulting in Formulae (A.11) - (A.13):

$$\Delta h_{LP\,s} = h_8 - h_{9\,s} \tag{A.11}$$

$$\Delta h_{LP} = \eta_{s\,comp} \Delta h_{LP\,s} \tag{A.12}$$

$$\boldsymbol{h_9 = h_8 - \Delta h_{LP}} \tag{A.13}$$

The resulting parameters, as derived from the spread sheets, are shown in Table A9 of Appendix A.
The exit parameters of LP cylinders are applied as input parameters for the exhaust steam turbine.

g. Determine enthalpy drops within the exhaust steam turbine.

The procedure is identical with that of item f., only the turbine parameters having been substituted for the LP parameters, yielding Formulae (A.14) – (A.16):

$$\boldsymbol{\Delta h_{TB\,s} = h_9 - h_{10\,s}} \tag{A.14}$$

$$\boldsymbol{\Delta h_{TB} = \eta_{s\,TB} \Delta h_{TB\,s}} \tag{A.15}$$

$$\boldsymbol{h_{10} = h_9 - \Delta h_{TB}} \tag{A.16}$$

The resulting parameters are shown in Table A10 of Appendix A.

h. Determine mass flows of steam in each section of prime mover at $\varepsilon_{HP} = 0{,}60$.

Equals signs in (A.17) and (A.18) are valid, since the circuit of Fig. A2 is closed:

$$\boldsymbol{\dot{m}_1 = \dot{m}_2 = \dot{m}_8 = \dot{m}_9 = \dot{m}_{10}} \tag{A.17}$$

$$\boldsymbol{\dot{m}_3 = \dot{m}_4 = \dot{m}_5 = \dot{m}_6 = \dot{m}_7} \tag{A.18}$$

Mass balance of mixing feedwater preheater tank yields interdependence (A.19):

$$\boldsymbol{\dot{m}_4 = \dot{m}_2 + \dot{m}_{11};\ \dot{m}_2 = \dot{m}_4 - \dot{m}_{11}} \tag{A.19}$$

The below formula (A.20) follows from energy balance of the preheater tank:

$$\dot{m}_4 h_4 = (\dot{m}_4 - \dot{m}_{11}) h_2 + \dot{m}_{11} h_{11} \tag{A.20}$$

Solving (A.20) for bleed steam mass flow $\dot{m}_{11}$ yields formula (A.21):

$$\boldsymbol{\dot{m}_{11} = \frac{\dot{m}_4 (h_4 - h_2)}{(h_{11} - h_2)}} \tag{A.21}$$

Resulting mass flows are tabulated in Table 11 of Appendix A.

i. Determine indicated power of each section of the prime mover.

Indicated power as a function of mass flow and isentropic enthalpy drop has been earlier discussed in Chapter 4.2.2. Formula (A.22) [348] below shows the basic formulation of the relation of the terms,

$$\boldsymbol{P_{ind} = \eta_s \dot{m} \Delta h_s} \tag{A.22}$$

the same applying for each section of the prime mover. The corresponding enthalpy-drops and mass flows yield Formulae (A.23) - (A.25), the isentropic efficiency already having been taken in account:

$$\boldsymbol{P_{ind\ HP}} = \dot{m}_6 \boldsymbol{\Delta h_{HP}} \tag{A.23}$$

$$\boldsymbol{P_{ind\ LP}} = \dot{m}_8 \boldsymbol{\Delta h_{LP}} \tag{A.24}$$

$$\boldsymbol{P_{ind\ TB}} = \dot{m}_8 \boldsymbol{\Delta h_{TB}} \tag{A.25}$$

The resulting indicated powers are listed in Table A12 of Appendix A. The combined indicated power of the prime mover is 1252 kW, *i.e.*, 15 kW less than the preliminary 1267 kW calculated in Paragraph 2.2. The difference of 1,2 % results from accurate calculations and is regarded as acceptable.

Fig. A5 is a graphical summary of the indicated power of each section of the prime mover *vs.* $\boldsymbol{\varepsilon_{HP}}$.

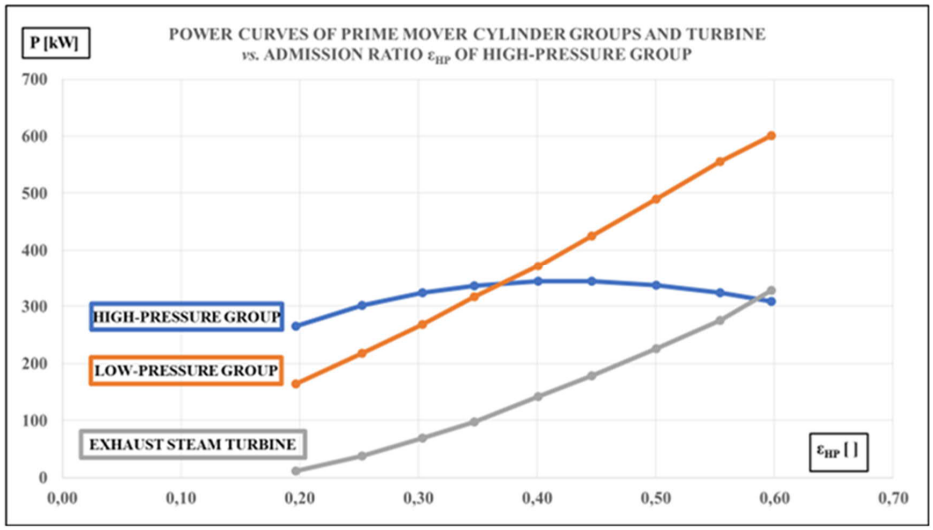

Figure A5: Indicated power of prime mover sections *vs.* ε_{HP}.

The power balance between HP and LP sections of the prime mover occurs at $\boldsymbol{\varepsilon_{HP}} = 0{,}37$. The evidence of incomplete expansion of the piston engine at high admission ratios is obviated by the increasing share of the turbine of the total power. Decreasing power of the HP group at high admission ratios is due to the increasing back pressure of the receiver, this in turn increasing the power of the LP group.

j. Determine brake power $\boldsymbol{P_b}$ (A.26) of the prime mover available for traction, by applying predicted mechanical efficiency $\boldsymbol{\eta_{mech}} = 0{,}92$, and own consumption efficiency $\boldsymbol{\eta_{oc}} = 0{,}96$:

$$\boldsymbol{P_b} = \boldsymbol{\eta_{mech}} \boldsymbol{\eta_{oc}} \boldsymbol{P_{ind}} \tag{A.26}$$

The $\boldsymbol{\eta_{mech}}$ and $\boldsymbol{\eta_{oc}}$ are based on sources earlier cited in Paragraph 2.2. The resulting $\boldsymbol{P_b} = 1106$ kW, as also noted in Table A13 of Appendix A.

k. Determine efficiencies of the prime mover.

Formula (A.27) [349] defines the efficiency η_{stc} of the steam cycle, the reduction term taking in account the effect of mass flows $\dot{m}_1$ and $\dot{m}_4$, as only $\dot{m}_1$ (from which the bleed steam flow $\dot{m}_{11}$ has been reduced) involves condensing while $\dot{m}_4$ represents the entire mass flow going through the boiler:

$$\eta_{stc} = 1 - \frac{\dot{m}_1(h_{10}-h_1)}{\dot{m}_4(h_6-h_4)} \tag{A.27}$$

At full power, *i.e.,* at ε_{HP} = 0,60, the resulting η_{stc} = 0,28. For a comparison, the ideal *Rankine* cycle efficiency at the default steam parameters would be η_{Rank} = 0,30, the ratio η_{stc}/η_{Rank} thus being 0,93.

Indicated efficiency η_{ind} in Formula (A.28) takes in account the predicted efficiency η_B = 0,95 of the boiler,

$$\eta_{ind} = \eta_B \eta_{stc} \tag{A.28}$$

The resulting calculated η_{ind} = 0,27 as noted in Table A14 of Appendix A.

Brake efficiency η_b in Formula (A.29) takes in account the own consumption and mechanical losses:

$$\eta_b = \eta_{mech}\eta_{oc}\eta_{ind} \tag{A.29}$$

With predicted parameters η_{mech} = 0,92, and η_{oc} = 0,96, Formula (A.29) yields η_b = 0,23.
The overall efficiency of the locomotive is discussed within the simulation results in Chapter 5.

B. Calculation of the steam generating system

The calculations aim at ensuring an adequate capacity of all heat exchangers involved in generation and recovery of steam, and in recovery of enthalpy of the flue gas, corresponding to steam demand of the prime mover operating at continuous full power. Fuel data of calculations for both pyrolysis oil and light fuel oil combustion have been provided by *D. Tech. T. Paloposki of Aalto University.* Both fuels have been discussed, to test the feasibility of the locomotive concept in case of potential problems concerning availability or properties of bio-oils. Identical pattern of calculations has been applied for both types of fuel. The convection area calculations aim at a reasonable margin, to cover the uncertainty of calculations, and to make a provision for the eventual accumulation of scale or dirt on the surfaces. Preheating of feedwater has been projected by applying two successive methods, the first one exploiting power plant practice, by using bleed steam to heat the condensate before pumping it under boiler pressure into the second preheater, this in turn recovering the heat of flue gas. The aim is to bring the feedwater up to 539 K, or the saturation temperature at boiler pressure. Such a system resembles the *Franco-Crosti* concept discussed in Paragraph 2.3. The proposed arrangement should be viable in combusting sulphur-free fuel, thus avoiding the inherent corrosion problems of *Franco-Crosti* boilers.

A water spray system, similar with power plant applications, has been projected to prevent excessive superheating, although the detail planning has been excluded from the scope of the study.

The nature of the calculations is iterative, as the thermodynamic properties of fluids depend on temperatures which thus tend to oscillate, due to the iteration. The below sequence has been applied:

a. Determining of dimensions and combustion parameters of the furnace.
b. Determining and tabulation of heat exchanger parameters.
c. Discussing outlines of condenser calculations, not executed by the author.

d. Results of calculations.

Calculation procedure

a. Determining the dimensions and combustion parameters of the furnace.

The boiler should be capable of increasing enthalpy of steam flow $\dot{m}_{st}$ by the amount of Δh_B assuming efficiency η_B of the boiler, resulting in Formula (B.1):

$$\Phi_B = \frac{\dot{m}_{st}\Delta h_B}{\eta_B} \tag{B.1}$$

Mass flow $\dot{m}_F$ of fuel required to attain the thermal power $\Phi_{B\,req}$ is obtained from Formula (B.2)

$$\dot{m}_F = \frac{\Phi_{B\,req}}{LHV_{act}} \tag{B.2}$$

where LHV_{act} is the lower heating value of fuel. The evaporative surface A_{ev} of the furnace is obtained from Formula (B.3) where D_{fb} is the nominal inside diameter and u_{fb} the height of the furnace, both dimensions referring to the boiler specifications of Appendix B:

$$A_{ev} = ½\pi^2 D_{fb} u_{fb} \tag{B.3}$$

NB: The term ½π takes in account the shape of the evaporator wall, made up of a spiral tube, the wall surface being configured by the inside wall of the tube coil, the effective height thus being $½\pi u_{fb}$. The second π involved in the formula refers to the circumference of the evaporator coil πD_{fb}.

Experimental Formula (B.4)[350] called *Hudson–Orrok* equation has been applied in assessing the furnace conditions. The formula, reportedly suitable for lump coal, pulverized coal, or oil combustion, was used as a design tool for late steam age locomotive boilers.

$$\zeta = \frac{1}{1+\lambda_{air}\frac{\sqrt{\frac{\Phi_F}{10^6 A_{ev}}}}{\psi}} \tag{B.4}$$

At the time of introducing the formula, the SI dimensions, nowadays prevalent, were not established yet, hence the use of [kcal] instead of [kJ] in the terminology explained below:

ζ [] = fraction of thermal input into the furnace absorbed by heating surface
λ [] = excess air factor in combustion; λ_{air} = 1,15 has been selected for both PYR and LFO.
Φ_F [kcal/h] = rate of heat release, or thermal input into the furnace
A_{ev} [m^2] = heating (evaporative) surface of the furnace
ψ [$kcal^{0,5}h^{-0,5}m^{-1}$] = 0,46 (experimental constant).

NB: The ζ and A_{ev} of Formula (B.4) were substituted for the original symbols μ and H by the author who also added the ψ, to mark the plain constant 0,46 [$kcal^{0.5}/m^{-0.5}$] of the original formula.

Definition of the term ζ implies that the thermal power Φ_{fb}, or the rate of heat release absorbed by the heating surface of the furnace, is obtained from Formula (B.5):

$$\boldsymbol{\Phi_{fb} = \zeta \Phi_F} \tag{B.5}$$

The heat release rate $\boldsymbol{\Phi_{req}}$ in the furnace required for evaporating the mass flow $\boldsymbol{\dot{m}_{fw}}$ of feedwater at full power is obtained from Formula (B.6), $\boldsymbol{Q_{ev}}$ being the heat of evaporation:

$$\boldsymbol{\Phi_{req} = \dot{m}_{fw} Q_{ev}} \tag{B.6}$$

Volume $\boldsymbol{V_{fb}}$ of the furnace follows from boiler dimensions as expressed in Formula (B.7):

$$\boldsymbol{V_{fb} = ¼ \pi D_{fb}^2 u_{fb}} \tag{B.7}$$

The ratio of the thermal power, *i.e.,* the rate of heat release, to the volume of the furnace should satisfy condition (B.8) in combustion of PYR, due to the slower droplet burning times and larger flame size in comparison with corresponding figures in mineral oil combustion where the heat release rate is typically 0,8 - 1 MW/m^3: [351]

$$\boldsymbol{q_{fb} = \frac{\Phi_F}{V_{fb}}} < 0{,}8 \text{ MW/m}^3 \tag{B.8}$$

The selected parameters result in $\boldsymbol{q_{fb}}$ = 0,64, *i.e.*, condition (B.8) is satisfied.
The initial temperature $\boldsymbol{T_0}$ of flue gas leaving the furnace is obtained via energy balance (B.9) equating the fraction (1- ζ) of the firing rate not absorbed by the furnace, and the thermal power within the flue gas flow exiting the furnace, since the temperature $\boldsymbol{T_{ex\,fg}}$ of flue gas exiting the furnace has been fixed:

$$\boldsymbol{\bar{c}_{p\,fg} \dot{m}_{fg} \left(T_0 - T_{ex\,fg} \right) = (1 - \zeta) \Phi_F} \tag{B.9}$$

Solving (B.9) for T_0 yields Formula (B.10):

$$\boldsymbol{T_0 = \frac{(1-\zeta)}{\bar{c}_{p\,fg} \dot{m}_{fg}} \Phi_F + T_{ex\,fg}} \tag{B.10}$$

Substituting figures stated within definition of Formulae B.1 – B.10 to the corresponding terms yields Table B6 of Appendix B, the below list of calculated parameters being an excerpt of the table:

$\boldsymbol{\zeta}$ [] = 0,508
$\boldsymbol{A_{ev}}$ [m^2] = 31,9
$\boldsymbol{V_{fb}}$ [m^3] = 8,6
$\boldsymbol{T_o}$ [K] = 1240
$\boldsymbol{\Phi_{ev}}$ [kW] = 2767
$\boldsymbol{\Phi_{fb}}$ [kW] = 2821

b. Calculation procedure for obtaining the heat exchanger parameters.

Calculations of superheater, flue gas preheater of feedwater, and combustion air preheater are based on heat transfer from flue gas to another fluid, *i.e.,* to water, steam, or air. The calculation pattern and formulae thus apply for each one of the cases and consists of determining of the below parameters:

- Inlet temperature $\boldsymbol{T_{in}}$ [K] of both fluids.

- Exit temperatures $\boldsymbol{T_{out}}$ [K] of both fluids.
- Mean specific heat capacity $\boldsymbol{\bar{c}_{p\,i}}$ [kJ/kgK] of both fluids.
- Mass flow $\boldsymbol{\dot{m}_i}$ [kg/s] of both fluids.
- Heat capacity flow $\boldsymbol{\dot{C}_i}$ [kW/K] of both fluids.
- Temperature difference $\boldsymbol{\Delta T_i}$ [K] of both fluids.

Calculations then yield the below properties for each heat exchanger:

- Temperature range **θ** [K]
- Heat capacity flow ratio **R** []
- Recuperation rate **ε** []
- Dimensionless conductance **Z** []
- Required conductance $\mathbf{G_{req}}$ [kW/K]
- Required convective surface A_{req} [m^2]
- Actual (calculated) conductance G_{act} [kW/K]
- Provided convective surface A_{prov} [m^2]

Energy balance of each exchanger, applying definitions and parameters tabulated in Appendix B, is expressed by Formula (B.11)[352]:

$$\dot{m}_{fg}\bar{c}_{p\,fg}(T_{fg\,in} - T_{fg\,out}) = \dot{m}_{fl}\bar{c}_{p\,fl}(T_{fl\,out} - T_{fl\,in}) \quad \text{(B.11)}$$

Exit temperature of flue gas from the previous exchanger upstream the flue gas circuit is used as inlet temperature $\boldsymbol{T_{in\,fg}}$ of the exchanger in question. Solving (B.11) for $\boldsymbol{T_{fg\,out}}$ yields Formula (B.12):

$$T_{fg\,out} = T_{fg\,in} - \frac{\dot{m}_{fl}\bar{c}_{p\,fl}}{\dot{m}_{fg}\bar{c}_{p\,fg}}(T_{fl\,out} - T_{fl\,in}) \quad \text{(B.12)}$$

Mean specific heat capacities of both fluids involved are assumed to correspond to mean temperatures of the fluids within the heat exchanger, obtained from corresponding tables of Appendix B. Formula (B.13) applies for both fluids:

$$\bar{T} = \frac{T_{in}+T_{out}}{2} \quad \text{(B.13)}$$

Heat capacity flows $\boldsymbol{\dot{C}_i}$ on both sides of the heat exchanger are defined by Formula (B.14)[353] where the subscript $_i$ is to be duly substituted for the one referring to the fluid in question:

$$\dot{C}_i = \dot{m}_i\bar{c}_{p\,i} \quad \text{(B.14)}$$

The ratio $\boldsymbol{R}$ of the heat capacity flows involved in each heat exchanger is expressed as in (B.15)[354];

$$R = \frac{\dot{C}_{min}}{\dot{C}_{max}} < 1 \quad \text{(B.15)}$$

i.e., the numerator is always the smaller one of the heat-capacity flows.

Temperature difference on both sides of the heat exchanger is expressed as in (B.16)[355]

$$\boldsymbol{\Delta T_i = T_{max\,i} - T_{min\,i}} \tag{B.16}$$

where the subscript $_i$ is to be duly substituted for the one referring to the fluid in question. Temperature range $\boldsymbol{\theta}$ of the heat exchanger is defined as the difference between the highest and lowest temperature involved in the fluid flows, as expressed by Formula (B.17) [356]:

$$\boldsymbol{\theta = T_{max} - T_{min}} \tag{B.17}$$

The recuperation rate $\boldsymbol{\varepsilon}$ is defined as the ratio between the bigger one of the temperature differences (B.17) and the overall temperature range (B.18) as expressed in formula (B.18)[357]:

$$\boldsymbol{\varepsilon = \frac{(\Delta T)_{max}}{\theta}} \tag{B.18}$$

The dimensionless conductance $\boldsymbol{Z}$ is now obtained from Formula (B.19)[358], all factors being defined:

$$\boldsymbol{Z = \frac{1}{1-R} log_e \frac{1-R\varepsilon}{1-\varepsilon}} \tag{B.19}$$

The required conductance of the heat exchanger is defined by Formula (B.20)[359]:

$$\boldsymbol{G_{req} = Z\dot{C}_{min}} \tag{B.20}$$

On both sides of the heat exchanger, the corresponding actual conductances $\boldsymbol{G_i}$ are obtainable from Formula (B.21) [360] where $\boldsymbol{\alpha_i}$ = heat transfer coefficient and $\boldsymbol{A_i}$ = the area of convective surface:

$$\boldsymbol{G_i = \alpha_i A_i} \tag{B.21}$$

The subscript $_i$ is to be duly substituted for the one referring to the fluid in question. Heat transfer coefficient $\boldsymbol{\alpha}$ is defined by formula (B.22) [361] where $\boldsymbol{Nu}$ = Nusselt number, $\boldsymbol{\lambda}$ = thermal conductivity of fluid, and $\boldsymbol{D_h}$ = hydraulic diameter of the flow channel:

$$\boldsymbol{\alpha = \frac{Nu\lambda}{D_h}} \tag{B.22}$$

The general definition for hydraulic diameter $D_h = 4A/l$ where A = cross section and l = circumference of flow path, but as $\boldsymbol{D_h}$ of a round tube equals its diameter D, and as $A = \delta l$ where $\delta << l$, the hydraulic diameter may be approximated as in Formula (B.23) [362]:

$$\boldsymbol{D_h \approx 2\delta} \tag{B.23}$$

Within turbulent flow, which is the target in all cases involved, the *Dittus-Boelter* Formula, (B.24) [363] defines $\boldsymbol{Nu}$ as follows,

$$\boldsymbol{Nu = 0,023 Re^{0,8} Pr^{0,3}} \tag{B.24}$$

where $\boldsymbol{Re}$ = *Reynolds number*, fluid properties and channels defining it as in Formula (B.25) [364],

$$\boldsymbol{Re} = \frac{\boldsymbol{\rho w D_h}}{\boldsymbol{\eta}} \tag{B.25}$$

while $\boldsymbol{Pr}$ stands for *Prandtl number* of fluid flow and is defined as (B.26) [365]:

$$\boldsymbol{Pr} = \frac{\boldsymbol{c_{p\,i}\eta_i}}{\boldsymbol{\lambda_i}} \tag{B.26}$$

where specific heat capacity $\boldsymbol{c_{p\,i}}$, dynamic viscosity $\boldsymbol{\eta_i}$, and thermal conductivity $\boldsymbol{\lambda_i}$ are obtained from appropriate tables of Appendix B. Volumetric fluid flow is obtained from Formula (B.27)

$$\boldsymbol{\dot{V}_i} = \frac{\dot{\mathrm{m}}_i}{\boldsymbol{\rho_i}} \tag{B.27}$$

where subscript $_i$ is to be duly substituted for the appropriate fluid mass flow $\dot{\mathbf{m}}$ and density $\boldsymbol{\rho}$, the latter being obtained from corresponding table in Appendix B. The fluid velocity $\boldsymbol{w_i}$ in a channel with cross section $\boldsymbol{A_i}$ is obtained from Formula (B.28):

$$\boldsymbol{w_i} = \frac{\dot{\mathrm{m}}_i}{\boldsymbol{\rho_i A_i}} \tag{B.28}$$

The subscript $_i$ is to be duly substituted for the one referring to the fluid in question.
Actual overall conductance $\boldsymbol{G_{tot}}$ depends on the conductances of each side of the heat-exchanger according to Formula (B.29) [366]:

$$\boldsymbol{G_{tot}} = \frac{\boldsymbol{G_1 G_2}}{\boldsymbol{G_1 + G_2}} \tag{B.29}$$

Combining (B.21) and (B.29) yields Formula (B.30) [367] for the required convective surface $\boldsymbol{A_{req}}$:

$$\boldsymbol{A_{req}} = \boldsymbol{G}\frac{\boldsymbol{\alpha_1 + \alpha_2}}{\boldsymbol{\alpha_1 \alpha_2}} \tag{B.30}$$

In each case, $\boldsymbol{A_{prov} > A_{req}}$ is the target, subscript ‚$_{\mathbf{prov}}$' standing for *provided*.

c. Outlines of condenser calculations

The calculations involving complex dual-phase considerations have been excuted by Ph. Lic. *Kari Saari* of Aalto University, and shown by his courtesy in detail in spread sheets supporting the current outlines, albeit only shown in limited detail in the text.

The pattern locomotive is assumed to operate in moderate climatic conditions, with typical range of temperature between -25 °C and + 25 °C. The upper limit has been used in the calculations for cooling air inlet temperature, stagnation pressure being assumed to induce the basic cooling air flow as often as possible. A speed of 90 km/h, or 25 m/s, has been used for reference, to specify the pressure and fan power required in case the air flow should be created by fans.

The calculations essentially consist of a multi-stage iterating process, the principal condition of which involves equating the thermal powers at both sides of the heat exchanger, *i.e.,* the condenser. Thermal power expressed by heat capacity flow at the *air side* is depicted by formula (B.31)[368],

$$\boldsymbol{\Phi_{air}} = \dot{m}_{air}\bar{c}_{p\,air}\boldsymbol{\Delta T} \tag{B.31}$$

and by conductance at *condensing steam side* as in Formula (B.32)[369]:

$$\boldsymbol{\Phi_{cond}} = \boldsymbol{G_{tot}dT_{log}} = \boldsymbol{G_{tot}}\frac{(T_{cond}-T_1)-(T_{cond}-T_2)}{log_e\frac{T_{cond}-T_1}{T_{cond}-T_2}} \tag{B.32}$$

Key parameters used by Mr *Saari* are shown in Tables *KS 1* and *KS 2*.

SYMBOL	DEFINITION	DIM.
T_1	COOLING AIR INTAKE TEMPERATURE	[°C]
T_{cond}	CONDENSING TEMPERATURE OF STEAM	[°C]
T_2	COOLING AIR EXIT TEMPERATURE	[°C]
	- ITERATED, BASED ON THE CONDITION $\Phi_{air} = \Phi_{cond}$	
Φ_{air}	THERMAL POWER OF COOLING AIR	[kW]
$\dot{m}_{air}$	MASS FLOW OF COOLING AIR	[kg/s]
$c_{p\,air}$	MEAN SPECIFIC HEAT CAPACITY OF COOLING AIR	[kJ/kg°C]
$\Delta T=T_2-T_1$	TEMPERATURE RISE OF COOLING AIR	[°C]
Φ_{cond}	THERMAL POWER OF CONDENSING STEAM	[kW]
G_{tot}	OVERALL CONDUCTANCE	[kW]
dT_{log}	LOGARITHMIC TEMP. DIFFERENCE BETW. T_{cond} and T_{air}	[]

Table *KS 1*: Parameters exploited in calculation Formulae (B.31, B.32).

INPUT DATA, DIMENSIONS, AND PARAMETERS				
DESCRIPTION	**SYMBOL**	**VALUE**	**DIMENSION**	**REMARKS**
AIR INTAKE GRID				
- WIDTH	b_{grid}	2	[m]	
- HEIGHT	u_{grid}	2	[m]	
- DEPTH	L_{grid}	0,2	[m]	
GRID SPACING	δ_{grid}	0,1	[m]	
THICKNESS OF FINS (SMOOTH PLATE)	g_{grid}	0,002	[m]	
HYDRAULIC DIAMETER	$D_{h\,grid}$	0,2	[m]	
RATIO A/A_0	$\delta/(\delta+g)$	0,98	[]	
SPEED OF LOCOMOTIVE	U	25	[m/s]	
AIR SPEED AFTER GRID	U_{red}	24,5	[m/s]	INFLUENCE OF GRID
				APPEARS MARGINAL
DIMENSIONS OF CONDENSER UNITS				
- NUMBER	N_{cond}	4	[]	
- WIDTH	b_{cond}	1,8	[m]	
- HEIGHT	u_{cond}	2	[m]	
- DEPTH	L_{cond}	0,2	[m]	
SPACING OF FINS	δ_{cond}	0,003	[m]	
HYDRAULIC DIAMETER	$D_{h\,cond}$	0,006	[m]	
THICKNESS OF FINS	g_{cond}	0,0005	[m]	
NUMBER OF FINS	N_g	571	[]	PER CONDENSER UNIT
TOTAL AREA OF FINS	A_g	411	[m^2]	- " -
AIR FLOW CROSS SECTION	A_{cond}	3,1	[m^2]	- " -
PHYSICAL PROPERTIES OF AIR				
TEMPERATURE AT INTAKE	T_1	298	[K]	
DYNAMIC VISCOSITY AT INTAKE	η_{air}	1,8E-05	[kg/m s]	
HEAT CONDUCTIVITY AT INTAKE	λ_{air}	0,026	[W/m K]	
DENSITY AT INTAKE	ρ_{air}	1,17	[kg/m^3]	
TEMPERATURE AT EXIT FROM CONDENSERS	T_2	339,8	[K]	FIRST GUESS
MEAN TEMPERATURE	$\bar{T}_{air}$	318,9	[K]	
MEAN DENSITY	$\bar{\rho}_{air}$	1,09	[kg/m^3]	
MEAN DYNAMIC VISCOSITY	$\bar{\eta}_{air}$	1,9E-05	[kg/ms]	
MEAN HEAT CONDUCTIVITY	$\bar{\lambda}_{air}$	0,027	[W/mK]	
MEAN SPECIFIC HEAT CAPACITY	$\bar{c}_{P\,air}$	1,007	[kJ/kgK]	

Table *KS 2*: Input parameters of condenser calculations.

d. Results of calculations.

1. Furnace: Results of furnace calculations were presented within the appropriate procedure.
2. Superheater:

Flue gas side			**PYR**	**LFO**
Inlet temperature	T_{in}	[K]	1240	1226
Exit temperature	T_{out}	[K]	782	716
Specific heat capacity	$\bar{c}_{p\,fg}$	[kJ/kgK]	1,30	1,25
Mass flow of flue gas	$\dot{m}_{fg}$	[kg/s]	2,55	2,38
Heat capacity flow	$\dot{c}_{fg}$	[kW/K]	3,31	2,97
Temperature difference	ΔT_{fg}	[K]	458	510
Steam side			**PYR & LFO**	
Inlet temperature	T_{sat}	[K]	539	
Exit temperature	T_{sup}	[K]	810	
Specific heat capacity	$\bar{c}_p$	[kJ/kgK]	3,30	
Mass flow of steam	$\dot{m}_{st}$	[kg/s]	1,70	
Heat capacity flow	$\dot{c}_{st}$	[kW/K]	5,60	
Temperature difference	ΔT_{st}	[K]	271	
Resulting superheater parameters			**PYR**	**LFO**
Temperature range	Θ	[K]	701	687
Heat capacity flow ratio	R	[ ]	0,59	0,53
Recuperation rate	ε	[ ]	0,65	0,74
Dimensionless conductance	Z	[ ]	1,40	1,93
Required conductance	G_{req}	[kW/K]	4,6	5,8
Required convective surface	A_{req}	[m^2]	**75**	**75**
Actual conductance	G_{act}	[kW/K]	4,90	6,07
Provided convective surface	A_{prov}	[m^2]	**80**	

Table B16: Resulting superheater characteristics.

Tables B16a – B16d support calculations for Table B16.

Superheater PYR, flue gas side									
$\bar{T}_{fg}$	p_{fg}	$\dot{m}_{fg}$	$\bar{\rho}_{fg}$	$\dot{V}_{fg}$	d_{sup}	D_{tube}	δ_{sup}	D_h	w_{fg}
[K]	[MPa]	[kg/s]	[kg/m^3]	[m^3/s]	[m]	[m]	[m]	[m]	[m/s]
1011	0,1	2,55	0,34	7,45	2,6	0,050	0,015	0,030	30,9
$\bar{\eta}_{fg}$	$\bar{\lambda}_{fg}$	Pr_{fg}	Re_{fg}	Nu_{fg}	α_{fg}	A_{req}	u_{sup}	A_{prov}	G_{fg}
[kg/m s]	[W/m K]	[ ]	[ ]	[ ]	[W/m^2K]	[m^2]	[m]	[m^2]	[W/K]
0,000041	0,0679	0,77	7825	28	63	75,2	3,7	80	4999

Table B16a: Calculation parameters of superheater in PYR combustion, flue gas side.

Superheater PYR, steam side									
$\overline{T}_{st}$	p_{st}	$\overline{\rho}_{st}$	$\overline{\eta}_{st}$	$\overline{\lambda}_{st}$	Pr_{st}	D_{tube}	w_{st}	$\dot{m}_{st}$	$\dot{V}_{st}$
[K]	[MPa]	[kg/m^3]	[kg/m s]	[W/m K]	[ ]	[m]	[m/s]	[kg/s]	[m^3/s]
675	5,2	20,40	0,000024	0,0598	1,35	0,050	43,3	1,70	0,08
Re_{st}	Nu_{st}	α_{st}	A_{prov}	G_{st}					
[ ]	[ ]	[W/m^{2}K]	[m^2]	[W/K]					
1790126	2527	3055	80	2E+05					

Table B16b: Calculation parameters of superheater in PYR combustion, steam side.

Superheater LFO, flue gas side										
$\overline{T}_{fg}$	p_{fg}	$\dot{m}_{fg}$	$\overline{\rho}_{fg}$	$\dot{V}_{fg}$	d_2	D_{tube}	d_{tube}	δ_{sup}	D_h	w_{fg}
[K]	[MPa]	[kg/s]	[kg/m^3]	[m^3/s]	[m]	[m]	[m]	[m]	[m]	[m/s]
971	0,1	2,38	0,36	6,66	2,6	0,050	0,057	0,011	0,022	37,7
$\overline{\eta}_{fg}$	$\overline{\lambda}_{fg}$	Pr_{fg}	Re_{fg}	Nu_{fg}	α_{fg}	A_{req}	u_{sup}	A_o	A_{prov}	G_w
[kg/m s]	[W/m K]	[ ]	[ ]	[ ]	[W/m^{2}K]	[m^2]	[m]	[m^2]	[m^2]	[kW/K]
0,000040	0,0644	0,77	7497	27	78	75	3,7	79,6	80	6226

Table B16c: Calculation parameters of superheater in LFO combustion, flue gas side.

NB: The channel width δsup has been reduced by 4 mm, to create adequate turbulence.

Superheater LFO, steam side									
$\overline{T}_{st}$	p_{st}	$\overline{\rho}_{st}$	$\overline{\eta}_{st}$	$\overline{\lambda}_{st}$	Pr_{st}	D_{tube}	w_{st}	$\dot{m}_{st}$	$\dot{V}_{st}$
[K]	[MPa]	[kg/m^3]	[kg/m s]	[W/m K]	[ ]	[m]	[m/s]	[kg/s]	[m^3/s]
675	5,2	20,40	0,000024	0,0598	1,35	0,05	43,3	1,70	0,08
Re_{st}	Nu_{st}	α_{st}	A_{prov}	G_{st}					
[ ]	[ ]	[W/m^{2}K]	[m^2]	[kW/K]					
1790126	2527	3055	80	2E+05					

Table B16d: Calculation parameters of superheater in LFO combustion, steam side.

3. Feedwater preheater:

Flue gas side			**PYR**	**LFO**
Inlet temperature	T_{in}	[K]	782	716
Exit temperature	T_{out}	[K]	623	538
Specific heat capacity	$\bar{c}_{p\,fg}$	[kJ/kgK]	1,20	1,15
Mass flow	$\dot{m}_{fg}$	[kg/s]	2,55	2,38
Heat capacity flow	$\dot{C}_{fg}$	[kW/K]	3,06	2,73
Temperature difference	ΔT_{fg}	[K]	159	178
Water side			**PYR & LFO**	
Inlet temperature	T_{in}	[K]	480	
Exit temperature	T_{out}	[K]	539	
Specific heat capacity	$\bar{c}_{p\,w}$	[kJ/kgK]	4,81	
Mass flow	$\dot{m}_{w}$	[kg/s]	1,70	
Heat capacity flow	$\dot{C}_{w}$	[kW/K]	8,17	
Temperature difference	ΔT_{w}	[K]	60	
Resulting feedwater preheater parameters			**PYR**	**LFO**
Temperature range	Θ	[K]	302	236
Heat capacity flow ratio	R	[ ]	0,37	0,33
Recuperation rate	ε	[ ]	0,53	0,75
Dimensionless conductance	Z	[ ]	0,85	1,66
Required conductance	G_{req}	[kW/K]	2,6	4,5
Required convective surface	A_{req}	[m^2]	**48**	**71**
Actual conductance	G_{act}	[kW/K]	3,94	4,72
Provided convective surface	A_{prov}	[m^2]	**73**	

Table B17: Resulting feedwater preheater characteristics.

Tables B17a – B17d support calculations for Table B17.

Feedwater heater PYR, flue gas side								
$\bar{T}_{fg}$	p_{fg}	ρ_{fg}	η_{fg}	λ_{fg}	Pr_{fg}	d_h	w_{fg}	$\dot{m}_{fg}$
[K]	[MPa]	[kg/m³]	[kg/m s]	[W/mK]	[ ]	[m]	[m/s]	[kg/s]
702	0,1	0,49	0,000032	0,0496	0,76	0,03	20,5	2,63
$\dot{V}_{fg}$	Re_{fg}	Nu_{fg}	α_{fg}	δ_{preh}	d_{preh}	A_{fg}	G_{fg}	
[m³/s]	[ ]	[ ]	[W/m²K]	[ ]	[ ]	[m²]	[W/K]	
5,34	9629	33	54	0,015	2,8	73,5	3963	

Table B17a: Calculation parameters of feedwater preheater in PYR combustion, flue gas side.

Feedwater heater PYR, water side								
$\bar{T}_w$	p	$\bar{\rho}_w$	$\bar{\eta}_w$	$\bar{\lambda}_w$	Pr_w	D_w	w_w	$\dot{m}_w$
[K]	[MPa]	[kg/m^3]	[kg/m s]	[W/mK]	[ ]	[m]	[m/s]	[kg/s]
510	5,2	820,7	0,000113	0,6320	0,86	0,05	1,1	1,70
$\dot{V}_w$	Re_w	Nu_w	α_w	d_{preh}	A_{req}	A_{prov}	G_w	
[m^3/s]	[ ]	[ ]	[W/m^{2}K]	[m]	[m^2]	[m^2]	[W/K]	
0,002	386056	648	8273	2,8	48	73	607833	

Table B17b: Calculation parameters of feedwater preheater in PYR combustion, water side.

Feedwater heater LFO, flue gas side								
$\bar{T}_{fg}$	p_{fg}	$\bar{\rho}_{fg}$	$\bar{\eta}_{fg}$	$\bar{\lambda}_{fg}$	Pr_{fg}	D_h	w_{fg}	$\dot{m}_{fg}$
[K]	[MPa]	[kg/m^3]	[kg/m s]	[W/mK]	[ ]	[m]	[m/s]	[kg/s]
627	0,1	0,55	0,000029	0,0449	0,75	0,022	22,6	2,38
$\dot{V}_{fg}$	Re_{fg}	Nu_{fg}	α_{fg}	δ_{preh}	d_{preh}	A_{preh}	G_{fg}	
[m^3/s]	[ ]	[ ]	[W/m^{2}K]	[ ]	[ ]	[m^2]	[W/K]	
4,30	9369	32	65	0,011	2,8	73,5	4757	

Table B17c: Calculation parameters of feedwater preheater in LFO combustion, flue gas side.

NB: The flue channel width δ_{preh} has been reduced by 4 mm, to attain adequate turbulence.

Feedwater heater LFO, water side								
$\bar{T}_w$	p_w	$\bar{\rho}_w$	$\bar{\eta}_w$	$\bar{\lambda}_w$	Pr_w	D_w	w_w	$\dot{m}_w$
[K]	[MPa]	[kg/m^3]	[kg/m s]	[W/mK]	[ ]	[m]	[m/s]	[kg/s]
510	5,2	821	0,000113	0,6320	0,86	0,05	1,1	1,70
$\dot{V}_w$	Re_w	Nu_w	α_w	d_{preh}	A_{req}	A_{prov}	G_w	
[m^3/s]	[ ]	[ ]	[W/m^{2}K]	[m]	[m^2]	[m^2]	[W/K]	
0,002	386056	648	8273	2,8	71	73	607833	

Table B17d: Calculation parameters of feedwater heater in LFO combustion, water side.

4. Combustion air preheater:

Flue gas side			**PYR**	**LFO**
Inlet temperature	T_{in}	[K]	623	538
Exit temperature	T_{out}	[K]	398	398
Mean specific heat of air	$\bar{C}_{p\,fg}$	[kJ/kgK]	1,14	1,10
Mass flow of air	$\dot{m}_{fg}$	[kg/s]	2,55	2,38
Heat capacity flow of air	$\dot{C}_{fg}$	[kW/K]	2,90	2,62
Temperature difference of air	ΔT_{fg}	[K]	225	140
Air side			**PYR**	**LFO**
Inlet temperature	T_{in}	[K]	298	298
Exit temperature	T_{out}	[K]	581	457
Mean specific heat of air	$\bar{C}_{p\,air}$	[kJ/kgK]	1,03	1,02
Mass flow of air	$\dot{m}_{air}$	[kg/s]	2,24	2,27
Heat capacity flow of air	$\dot{C}_{air}$	[kW/K]	2,30	2,31
Temperature difference of air	ΔT_{air}	[K]	283	159
Resulting combustion air heater parameters			**PYR**	**LFO**
Temperature range	Θ	[K]	325	240
Heat capacity flow ratio	R	[ ]	0,79	0,88
Recuperation rate	ε	[ ]	0,87	0,66
Dimensionless conductance	Z	[ ]	4,24	1,76
Required conductance	G_{req}	[kW/K]	9,8	4,1
Required convective surface	A_{req}	[m^2]	**207**	**90**
Actual conductance	G_{act}	[kW/K]	10,20	9,76
Provided convective surface	A_{prov}	[m^2]	**216**	

Table B18: Resulting combustion air preheater characteristics.

Tables B18a – B18d support calculations for Table B18.

Combustion air preheater PYR, flue gas side									
$\bar{T}$	**p**	$\dot{m}$	$\bar{\rho}_{fg}$	$\dot{V}_{fg}$	b_1	b_2	L_{fin}	t_{fin}	a_1
[K]	[MPa]	[kg/s]	[kg/m^3]	[m^3/s]	[m]	[m]	[m]	[m]	[m]
510	0,1	2,55	0,68	3,76	0,50	0,50	1,3	0,0005	0,42
a_2	δ_{fin}	n_{fin1}	n_{fin2}	A_{min1}	A_{min2}	A_1	A_2	D_h	**w**
[m]	[m]	[ ]	[ ]	[m^2]	[m^2]	[m^2]	[m^2]	[m]	[m/s]
0,42	0,002	199	199	0,08	0,08	108	108	0,004	22,6
$\bar{\eta}_{fg}$	$\bar{\lambda}_{fg}$	**Pr**	**Re_1**	**Re_2**	**Nu**	**α**	A_{req}	**G**	
[kg/m s]	[W/m K]	[ ]	[ ]	[ ]	[ ]	[W/m^2K]	[m^2]	[W/K]	
0,000025	0,0376	0,75	2459	2459	11	102	207	22138	

Table B18a: Calculation parameters of air preheater in PYR combustion, flue gas side.

Combustion air preheater PYR, air side									
$\overline{T}_{air}$	p_{air}	$\dot{m}_{air}$	$\overline{\rho}_{air}$	$\dot{V}_{air}$	b_1	b_2	L_{air}	t_{fin}	a_1
[K]	[MPa]	[kg/s]	[kg/m^3]	[m^3/s]	[m]	[m]	[m]	[m]	[m]
439	0,1	2,24	0,79	2,82	0,50	0,50	1,3	0,0005	0,42
a_2	δ_{fin}	n_{fin1}	n_{fin2}	A_{min1}	A_{min2}	A_1	A_2	D_h	w
[m]	[m]	[ ]	[ ]	[m^2]	[m^2]	[m^2]	[m^2]	[m]	[m/s]
0,42	0,002	199	199	0,08	0,08	108	108	0,004	33,9
$\overline{\eta}$	$\overline{\lambda}$	Pr	Re_1	Re_2	Nu	α	A_{req}	G	
[kg/m s]	[W/m K]	[ ]	[ ]	[ ]	[ ]	[W/m^{2}K]	[m^2]	[W/K]	
0,000025	0,0360	0,70	2191	2191	10	88	207	18931	

Table B18b: Calculation parameters of air preheater in PYR combustion, air side.

Combustion air preheater LFO, flue gas side									
$\overline{T}_{fg}$	p_{fg}	$\dot{m}_{fg}$	$\overline{\rho}_{fg}$	$\dot{V}_{fg}$	b_{fg1}	b_{fg2}	L_{fg}	δ_{fg}	a_{fg1}
[K]	[MPa]	[kg/s]	[kg/m^3]	[m^3/s]	[m]	[m]	[m]	[m]	[m]
468	0,1	2,41	0,74	3,24	0,50	0,50	1,3	0,0005	0,42
a_{fg2}	δ_{fin}	$n_{fin\ fg1}$	$n_{fin\ fg2}$	$A_{min\ fg1}$	$A_{min\ fg2}$	A_{fg1}	A_{fg2}	D_h	w_{fg}
[m]	[m]	[ ]	[ ]	[m^2]	[m^2]	[m^2]	[m^2]	[m]	[m/s]
0,42	0,002	199	199	0,08	0,08	108	108	0,004	19,5
$\overline{\eta}_{fg}$	$\overline{\lambda}_{fg}$	Pr_{fg}	$Re_{fg\ 1}$	$Re_{fg\ 2}$	Nu_{fg}	α_{fg}	A_{fg}	G_{fg}	
[kg/m s]	[W/m K]	[ ]	[ ]	[ ]	[ ]	[W/m^{2}K]	[m^2]	[kW/K]	
0,000024	0,0353	0,74	2448	2448	11	95	45	20578	

Table B18c: Calculation parameters of air preheater in LFO combustion, flue gas side.

Combustion air preheater LFO, air side									
$\overline{T}_{air}$	p_{air}	$\dot{m}_{air}$	$\overline{\rho}_{air}$	$\dot{V}_{air}$	b_{air1}	b_{air2}	L_{air}	δ_{air}	a_{air1}
[K]	[MPa]	[kg/s]	[kg/m^3]	[m^3/s]	[m]	[m]	[m]	[m]	[m]
377	0,1	2,27	0,93	2,46	0,50	0,50	1,3	0,0005	0,42
a_{air2}	$\delta_{fin\ air}$	$n_{fin\ air1}$	$n_{fin\ air2}$	$A_{min\ air1}$	$A_{min\ air2}$	A_{air1}	A_{air2}	D_h	w_{air}
[m]	[m]	[ ]	[ ]	[m^2]	[m^2]	[m^2]	[m^2]	[m]	[m/s]
0,42	0,002	199	199	0,08	0,08	108	108	0,004	29,6
$\overline{\eta}_{air}$	$\overline{\lambda}_{air}$	Pr_{air}	Re_{air1}	Re_{air2}	Nu_{air}	α_{air}	A_{req}	G_{air}	
[kg/m s]	[W/m K]	[ ]	[ ]	[ ]	[ ]	[W/m^{2}K]	[m^2]	[W/K]	
0,000022	0,032	0,70	2486	2486	11	86	90	18559	

Table B18d: Calculation parameters of air preheater in LFO combustion, air side.

5. Condenser:

Table *KS 3* presents a summary of the condenser calculations. The total cooling power of 3100 kW is attained by the air flow caused by stagnation pressure at locomotive speed of 25 m/s and ambient temperature of 25 °C, or 298 K.

STAGNATION PRESSURE WITHOUT BLOWERS		
Input data		
Item	**Value**	**Dimension**
Air flow velocity	18,6	[m/s]
Axial deviation of air flow in front cooler	32	[deg]
Axial deviation of air flow in rear cooler	36	[deg]
Final temperature of air flow:		
- Front coolers	66,8	[°C]
- Rear coolers	64,2	[°C]
Steam side heat transfer coefficient check:		
Calculated	13130	[W/m²K]
Input	13100	[W/m²K]
Resulting cooling power		
Front coolers		
Total stagnation pressure	365	[Pa]
Pressure drop	361	[Pa]
Heat flow by conductance	799	[kW]
Heat capacity flow: $\dot{C} = \dot{m}c_p\Delta T$	800	[kW]
Rear coolers		
Total stagnation pressure	365	[Pa]
Pressure drop	363	[Pa]
Heat flow by conductance	751	[kW]
Heat capacity flow: $\Phi = \dot{m}c_p\Delta T$	750	[kW]
Total cooling power	**3100**	**[kW]**

Table *KS 3*: Cooling characteristics of the condensers with air flow from stagnation pressure.

Table *KS 4* shows the required cooling power at various admission ratios ε_{HP} of the prime mover.

ε_{HP}	Δh_{cond}	$\dot{m}_9$	Φ_{cond}
[ ]	[kJ/kg]	[kg/s]	[kW]
0,20	2246	0,46	1035
0,25	2249	0,59	1336
0,30	2252	0,72	1613
0,35	2255	0,82	1853
0,40	2258	0,95	2149
0,45	2260	1,06	2399
0,50	2263	1,19	2701
0,55	2266	1,32	2999
0,60	2269	1,43	3244

Table *KS 4*: Required cooling power *vs.* cylinder admission ratio.

NB: Table *KS 4* indicates that the maximum cooling power attained through air flow from stagnation pressure is slightly less than the required cooling power at maximum power of prime mover. It is to be noted that the full fan-assisted cooling capacity of the rear end of the locomotive is available. Moreover, in moderate climatic conditions, the cooling air temperature is normally expected to stay under 25ºC = 298 K.

A summary of the results of all the heat echanger calculations is shown in Table B19.

CAPACITY OF STEAM GENERATING SYSTEM			
FURNACE	**THERMAL POWER []**		
	REQUIRED		PROVIDED
	2767		**2821**
MIXING TANK FEEDWATER PREHEATER	**FEEDWATER TEMPERATURE []**		
	REQUIRED		ATTAINED
	PYR	LFO	
	539	539	**539**
FLUEGAS HEAT EXCHANGERS	**CONVECTIVE SURFACES [m^2]**		
	REQUIRED		PROVIDED
	PYR	LFO	
SUPERHEATER	75	75	**80**
FLUEGAS FEEDWATER PREHEATER	48	71	**73**
COMBUSTION AIR PREHEATER	207	90	**216**
CONDENSER	**COOLING POWER [kW]**		
	REQUIRED		ATTAINED
	3244		**3100**

Table B19: Summary of calculations of heat exchangers involved in generating of steam.

5. Predicted performance of locomotive *Hs1*

5.1 Performance in view of calculations

5.1.1 Prime mover

Calculations of paragraph 4.6.A predict a brake efficiency $\eta_b = 0{,}23$ for the prime mover at full power, *i.e.*, at $\varepsilon_{HP} = 0{,}60$. The prediction is in harmony with the test results of the German 'Zero Emission Engine' project reported by *VDI Bericht 1565* in 2001 and earlier discussed in Paragraph 2.7.1.2. The 'ZEE' was a 50-kW engine and worked at steam parameters 5 MPa / 773 K *vs.* 5,2 MPa / 810 K of the *Hs 1,* a brake efficiency $\eta_b = 0{,}24$ having been attained in a test bench. There is no mention about inclusion or obmission of the own consumption efficiency in the results of the 'ZEE' while the present prime mover calculations do include it. Considering that the efficiency of steam engines increases along the size,[370] and that minimizing of incomplete expansion of the prime mover by using the exhaust steam turbine has been projected, the predicted $\eta_b = 0{,}23$ may be regarded as a conservative figure. Moreover, full power has been applied in all the simulations whereas most of the tests of the locomotives in Paragraph 3.5 refer to maximum *efficiency* rather than to maximum *power*.

5.1.2 Flue gas circuit as a whole

Combustion data of Table B3 in Appendix B specifies a firing rate 5547 kW of the boiler, combustion air being preheated to 581 K as predicted by air preheater calculations, and assuming efficiency 0,995 of the oil burner.[371] The predicted efficiency of the boiler is $\eta_B = 0{,}95$. The heat power rejected within exhausted fluegas is 278 kW = 5 % of the firing rate, supporting the prediction of $\eta_B = 0{,}95$. A firetube boiler, burning solid fuel with induced draught unavoidably resulting in some unburnt fuel, and with a *Franco-Crosti* preheater, was calculated to attain $\eta_B = 0{,}91$ as mentioned in Paragraph 3.6. An oil burner with $\eta_{burn} = 0{,}995$, *i.e.*, almost *nil* unburnt oil, and controlled draught thus further supports attaining $\eta_B = 0{,}95$ in a watertube boiler with an advanced application of *Franco-Crosti* preheater.

5.1.3 Individual elements of the steam generating system

a. Furnace
   The evaporative surface of the combustion chamber waterwall at selected boiler dimensions is $A_{ev} = 31{,}9\ m^2$. The volume of the combustion chamber is $V_{fb} = 8{,}6\ m^3$. Calculations in Paragraph 4.6.2 yield an available thermal power $\Phi_{abs} = 2821$ kW of the evaporator based on the heat absorbed by the water wall at the firing rate $\Phi_F = 5547$ kW, this in turn having been deducted from the maximum steaming capacity at predicted boiler efficiency. The required thermal power is $\Phi_{req} = 2767$ kW. Thus, $\Phi_{req} < \Phi_{abs}$ with a margin of 54 kW, or 2 %.

b. Superheater
Ample dimensions of superheater have been aimed at, to secure an adequate superheating capacity, as large superheaters proved themselves in practice during the steam age. Typical European ratio between evaporative and superheating surfaces used to be *ca.* 3:1, but ratios up to 2:1 were applied in late steam age classes, with a positive impact on the efficiency.[372]
The provided heating surface of the superheater at opted dimensions is A_{sup} = 80 m^2. Calculations in Paragraph 4.6.2 require a heating surface A_{req} = 75 m^2 at maximum steaming rate in both PYR and LFO combustion, the latter case necessitating a 4 mm reduction in flue channel width, to increase the turbulence and thus the corresponding heat transfer. In both cases, $A_{req} > A_{prov}$ with a 6 - 7 % margin.

c. Mixing tank feedwater preheater
The mixing tank involves an intermediate steam outlet from the receiver. The steam is mixed with the condensate, pumped into the tank. Capacity of the mixing tank feedwater preheater has been pre-determined by fixing the pressure of the bleed steam.

d. Fluegas feedwater preheater
The opted boiler dimensions provide a heating surface A_{preh} = 73 m^2 for the preheater. The calculated requirements for heating surfaces at maximum steaming rate are A_{req} = 48 m^2 in PYR combustion, and 71 m^2 in LFO combustion. Thus, $A_{req} < A_{preh}$ with margins of 25 m^2/52 % and 2 m^2/3 %.

e. Combustion air preheater
The provided heat exchanging surface of the combustion air preheater is A_{prov} = 216 m^2. The target exit temperature of the fluegas has been set at 398 K while the air inlet is assumed to take place at ambient temperature of 298 K. To attain the target temperature of flue gas at maximum steaming capacity, calculations of Paragraph 4.6.B require cooling surfaces A_{req} = 207 m^2 and 87 m^2 in PYR *vs.* LFO combustion, respectively. Thus, $A_{req} < A_{prov}$ with margins of 9 m^2/4 % and 90 m^2/140 % respectively. Increasing or decreasing the size of the preheater is relatively easy, as the device is not tied with dimensions of other appliances.

f. Condenser
At maximum power, the prime mover calculations in Paragraph 4.6.B indicate a required cooling power Φ_{req} = 3244 kW. Assuming ambient temperature 298 K and stagnation pressure at speed of 25 m/s, the calculations predict a cooling power Φ_{cond} = 3100 kW. In this case $\Phi_{req} > \Phi_{cond}$. The cooling fans of the rear end of the locomotive provide the additional capacity, if necessary, as the fans of both ends are designed to generate an air flow matching the stagnation pressure at maximum speed of the locomotive.

5.1.4 Selection of efficiency-related constants and their impact on the calculated results

The relations between various factors of efficiency have already been dealt within the calculations, the below factors being variables treated as fixed constants after being selected. The other components of efficiency are not independent and thus result from calculations.

5.1.4.1 η_s = internal isentropic efficiency

This is a component-specific constant separately predicted in the present study for cylinders of the prime mover as η_{comp}, the subscript standing for *compound*, and for exhaust steam turbine as η_{TB}, the subscript standing for *turbine*. Citing *Ryti*, η_{comp} is 0,81 – 0,88 for a compound steam engine for steam parameters 1,2 MPa, 593 K and back pressure 100 kPa.[373] On the other hand, such parameters were substantially exceeded in late steam age locomotives by e.g., *Chapelon* whose test results from a 4-cylinder compound locomotive imply $\eta_s > 0{,}90$ with steam parameters 2,1 MPa, 673 K.[374] Consequently, $\eta_{comp} = 0{,}90$ has been opted for the Hs1 working at 5,2 MPa, 810 K, such parameters thus appearing conservative rather than optimistic.

Ryti further reminds that $\eta_{TB} > \eta_{comp}$ for big turbines but η_{TB} decreases in smaller turbines. The exhaust steam turbine of the *Hs1* is rather small, $\eta_{TB} = 0{,}78$ having been therefore opted, corresponding the average figure for a simple expansion steam engine working at steam parameters 1,2 MPa, 593 K.

To study the impact of $\eta_{comp} = 0{,}90$ *vs.* 0,88 the author calculated the difference between consequent prime mover brake powers, obtaining 1108 kW *vs.* 1081 kW, or 2,4 % for a 2,2 % decrease of η_{comp}, *i.e.*, almost linear within small changes.

5.1.4.2 η_{mech} = mechanical efficiency

Mechanical efficiency of steam engines used to be separately given for horizontal or vertical engines, the best figures having been 0,92 and 0,95 respectively, according to *Ryti* who also makes a point of big turbines approaching 1.[375] The author has opted $\eta_{mech} = 0{,}92$ for the *Hs1*, the radial engine prime mover consisting of three separate units and a turbine. Considering the absence of crossheads and slide bars as well as the projected needle bearing application to the 1-throw crankshafts and connecting rods the predicted $\eta_{mech} = 0{,}92$ appears to the author as a safe figure. The brake power of the prime mover is *directly proportional* to the mechanical efficiency.

5.1.4.3 η_B = boiler efficiency

Boiler efficiency was shown in Chapter 3 to have been the key factor of low efficiency of steam locomotives while its being the product of two factors was dealt within the calculations of Chapter 4 and further dealt below. The highest $\eta_B = 0{,}91$ of the steam age was predicted for a firetube boiler with a *Franco-Crosti* preheater but without any combustion air preheater as referred in Chapter 3. The opted boiler configuration of the Hs1 involves a 2-stage preheating of feedwater and an air pre-heater to raise the temperature of combustion air up to *ca.* 500 K, hence the predicted $\eta_B = 0.95$. The thermal efficiency of the locomotive is *directly* proportional to its boiler efficiency.

5.1.4.4 η_{comb} = combustion efficiency

This is the first factor of η_B and depicts the share of heat release of combustion from the fuel energy. As was described in Chapter 3 the classic locomotive boilers suffered from both mechanical and chemical losses within the combustion as the draught would entrain fuel particles unburnt and the amount of combustion air was difficult to adjust. Burners with controlled flame and air feed enable a manufacturer to guarantee combustion efficiencies as high as $\eta_{comb} = 0{,}995$.[376] Together with η_{ab} the η_{comb} directly affects the boiler efficiency.

5.1.4.5 η_{ab} = absorption efficiency

The absorption efficiency of classic locomotive boilers was heavily dependent on the power setting due to the induced draught as was discussed in Chapter 3. In contrast, the controlled forced draught of the oil burmer enables a better adjustment of the flue gas flow and absorption of heat to the boiler surfaces and finally to the air preheater. A figure in the range of $\eta_{ab} = 0{,}95$ is peredicted for the *Hs1*.
Together with η_{comb} the η_{ab} directly affects the boiler efficiency.

5.1.4.6 η_{oc} = own consumption efficiency

In comparison with classic locomotives the own consumption of the *Hs1* is on one hand reduced by the better boiler efficiency, less demand of both fuel and water, and less demand of compressed air due to dynamic braking, and on the other hand increased by momentary need of fans to cool the condensers in case the air flow from stagnation pressure is not sufficient. The net effect is predicted to be on the reduction side, a prediction η_{oc} = 0,96 of the steam age supporting such a view.[377] The efficiency of the locomotive is *directly* proportional to η_{oc}.

5.1.4.7 η_{gen} = generator efficiency

The prediction η_{gen} = 0,95 is based on product information of ABB.[378] As a part of power transmission, the η_{gen} has a *direct* impact to the overall efficiency of the locomotive.

5.1.4.8 η_{trm} = traction motor efficiency

The prediction η_{trm} = 0,95 is based on product information of ABB.[379] As a part of power transmission, the η_{trm} has a *direct* impact to the overall efficiency of the locomotive.

5.1.4.9 η_{rec} = efficiency of system to recover the braking energy

The predicted η_{rec} = 0,80 as discussed within item 4.2.6. assuming the energy was stored in batteries. The η_{rec} contributes to the overall efficiency η_{db} of the locomotive, the impact of η_{rec} being shown by Formula (5.1)

$$\eta_{db} = \frac{W_{db}+\eta_{rec}W_b}{E_{cons}} \tag{5.1}$$

W_{db} = drawbar work, W_b = braking work, and E_{cons} = energy consumed. Recovery of braking energy is further explained in item 5.2.1 of Paragraph 5.2.

5.1.4.10 Isentropic indexes κ_{HP} and κ_{LP}

The isentropic indexes are not free variables but depend on steam parameters, *i.e.,* pressure and temperature and are thus different for inlet steam of high-pressure *vs.* low-pressure cylinders. Spirax-Sarco steam tables have been used for the *Hs1* as they readily specify appropriate figures.

5.2 Description of simulations

Operational characteristics of the pattern locomotive and the reference diesel-electric locomotive have been compared by exploiting a simulation program developed within the study. The simulations cover both yard and road operations, the latter having been extended to a classical steam locomotive, to create a picture of the advance since the end of the steam age. Three versions of the basic program have been exploited:

1. Road test simulation in a freight train on an actual railroad
2. Yard work test simulation on level track
3. Road test simulation in a local passenger train on level track

The structure of the program remains identical in all the three versions except that the gradient resistance is omitted from the level track tests, and that increments of 1 meter are applied in the level track versions instead of the already short 10-meter increments of the depicted actual railroad. The shorter the

increments, the smoother the graphs depicting forces, accelerations, and speeds involved with the simulations, although the same formulae apply.

Main objectives of the simulations are to predict the traction properties of *Hs 1* in typical assignments for a general-purpose locomotive, and its drawbar thermal efficiency. The focus of simulations is on freight and shunting duties while also performance in light local passenger trains with frequent stops has been studied. Comparative data is collected from the diesel electric locomotive *Dr18*. The freight train simulation is also performed with a classical Finnish *Tr1* class steam locomotive for comparison.

Mass and resistances of the equipment constitute the starting point of all the simulations. Table C1 is valid for the above cases 1. and 2. while only the train weight is different (100 t) in case 3. Rolling resistance factor $\boldsymbol{\mu_r}$ refers to *Ivalo: Höyryveturit ja niiden hoito,* p. 556, 557. Air resistance factor $\boldsymbol{k_{air}}$ and area $\boldsymbol{A_{air}}$ exposed to air resistance are estimates of the author, based on the relatively non-streamlined shape, and calculated cross section of the rolling stock, and assessed by comparing the simulated data with actual performance data for the *Dr18,* made available for the author by *Fennia Rail Oy*, *i.e.*, the owner of the locomotive.

Track and train parametres			
Train weight a) freight	m_{Tf}	[t]	800
Train weight b) passenger	m_{Tp}	[t]	100
Rolling resistance factor	μ_r	[ ]	0,0016
Drag coefficient a) Hs1	k_{air}	[ ]	0,80
Air density	ρ_{air}	[kg/m^3]	1,29
Area exposed to air resistance			
- Locomotive coefficient	0,12	[m^2/t]	15,6
- Train coefficient a) freight	0,04	[m^2/t]	32
- Train coefficient b) passenger	0,04	[m^2/t]	4
-Area total a) freight Hs1	A_{air}	[m^2]	47,6
-Area total b) freight Dr18			46,4
-Area total c) freight Tr1			50,8
-Area total d) passenger Hs1			19,6
-Area total e) passenger Dr18			18,4
Gradient factor: as tabulated in track profile			

Table C1: Train parameters valid for all the test locomotives of on-the-road simulations.

5.2.1 On-the-road freight trains

The former 78 km trunk line between Jyväskylä and Haapamäki has been opted for the test bed of on-the-road simulations. The track profile is shown in Fig. C1 both in actual and in condensed form.

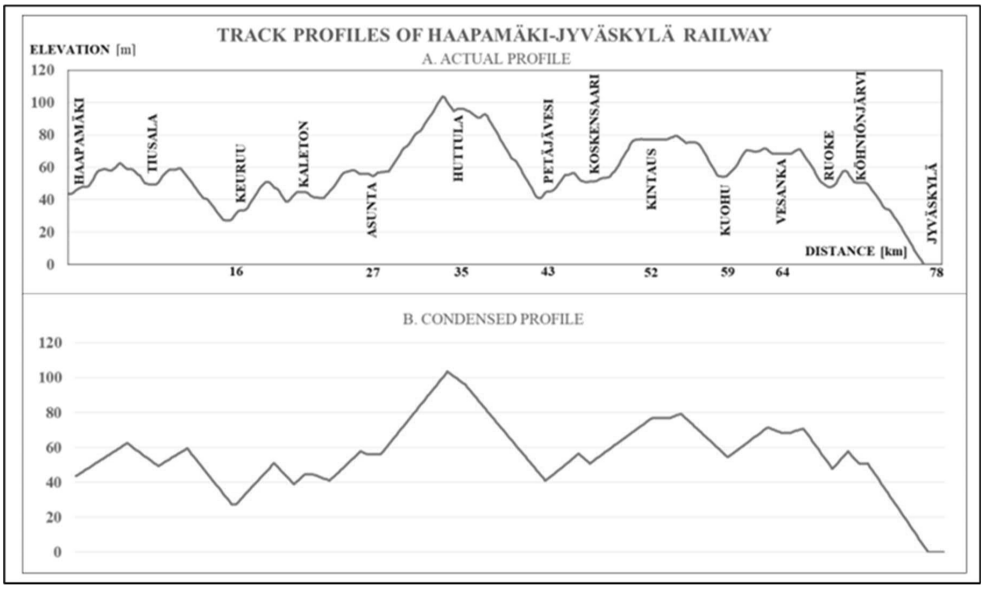

Figure 5.1: Track profile of the railroad between Haapamäki and Jyväskylä.

There are lengthy ascents and descents of up to 1:80 (1,25 %), and a speed limit of 80 km/h due to sharp curves or track conditions. The route has remained unelectrified after losing its former position as a trunk line after by-pass lines were built. Timetables of the once heavy traffic have been exploited in creating database of a simulation program. The profile has been condensed, to eliminate shorter than 500 m grades, and plotted at 10 m increments over the entire route length. Elevations have been given by setting the elevation of Jyväskylä (80,5 m from sea level) as zero point.

The locomotives have been simulated with an 800-t freight train from Haapamäki to Jyväskylä and back, at non-stop schedules over the entire route.

Opting for 800-t train weight is based on the rated maximum tonnage over the route for the classical *Tr1*, or one of the locomotives to be simulated for comparison, such a train being relatively heavy for a branch line with the illustrated profile even today.

The two-way trip is to compensate the impact of the substantial difference between elevations of the terminus stations, to avoid distortions potentially caused by recovered, re-used, and stored energy to the efficiency comparison.

Basically, the drawbar power of *Dr18* is adjusted to match the maximum drawbar power of *Hs 1* whenever the power is on, except for two occasions:

1. at start, care must be paid to avoid slipping, as the wheelrim force would exceed the adhesion limit 325 kN if maximum power is applied below *ca.* 3 m/s speed as shown below for *Hs 1*:

$$\boldsymbol{F = P_{db}/v} = 976 \text{ kW}/3 \text{ m/s} = 325 \text{ kN} \qquad \text{(C.0)}$$

2. in case of exploiting recovered energy of the *Hs 1*, the selected drawbar tractive force may fluctuate within a couple of kilometers of travel, the tractive force of *Dr18* being adjusted accordingly.

Power is generally cut off after reaching the summit if a downhill immediately follows the climb. Cutting off the power enables turning off burner of the *Hs 1* and implies idling of the engine of *Dr18*.

Brakes are only applied to observe the speed limits, or to bring the train to stop at the destination. The former case involves equating the brake force with the default train resistances while braking to stop is performed by applying a suitable brake force. In case of dynamic braking, *i.e.,* using the electric brake of the locomotive only, the *Dr18* specifications define 120 kN as the maximum brake force. Such a maximum is also applied in exploiting the energy recovery system of *Hs1* in which the traction *motors* work as *generators* to charge the accumulators when dynamic brakes are applied. Efficiency of the entire electromechanical system has been assumed to be $\eta_{rec} = 0{,}80$, by exploiting the most efficient generator and traction motors with efficiencies of *ca.* 0,96, and frequency modulators of a similar efficiency range. The recovered energy is re-used at the first possible occasion.

The classical *Tr1,* quite a heavy hand-fired steam locomotive, is operated according to steam age practice, avoiding excessive physical stress to the fireman. The last engines were built with roller bearings, thus contributing to uniformity in comparing the train resistances within the simulations.

Figure 5.2: Tr1 1096, the last-built (1957) steam locomotive of the Finnish State Railways.
Photo: Courtesy of Sakari K Salo.

Distance		Elevation	Rolling resistance $F_r = \mu_r(m_{loc} + m_T)g$			Gradient resistance $F_g = \beta_g(m_{loc} + m_T)g$			Air resistance $F_{air} = ½k\rho_{air}A_{air}v^2$			Train resistance $F_T = F_r + F_g + F_{air}$		
[km]		[m]	[kN]			[kN]			[kN]			[kN]		
			Hs1	Dr18	Tr1	Hs1	Dr18	Tr1	Hs1	Dr18	Tr1	Hs1	Dr18	Tr1
0,0	Haapamäki	43,59	14,6	14,4	15,0	0	0	0	0	0	0	14,6	14,4	15,0
0,01		43,63				37,35	36,94	38,43	0,02	0,02	0,01	52,0	51,8	53,5
0,02		43,67				37,35	36,94	38,43	0,14	0,14	0,11	52,1	51,9	53,6
0,03		43,71				37,35	36,94	38,43	0,20	0,19	0,23	52,1	52,0	53,7
0,04		43,75				37,35	36,94	38,43	0,23	0,22	0,29	52,2	52,0	53,7
0,05		43,79				37,35	36,94	38,43	0,25	0,25	0,34	52,2	52,0	53,8
0,06		43,84				37,35	36,94	38,43	0,28	0,27	0,39	52,2	52,1	53,8
0,07		43,88				37,35	36,94	38,43	0,30	0,30	0,44	52,2	52,1	53,9
0,08		43,92				37,35	36,94	38,43	0,33	0,32	0,49	52,3	52,1	53,9
0,09		43,96				37,35	36,94	38,43	0,35	0,35	0,54	52,3	52,1	54,0
0,10		44,00				37,35	36,94	38,43	0,38	0,37	0,58	52,3	52,2	54,0

Figure 5.3: Resistances of locomotive and train during the first 100 meters at start from Haapamäki.

The gradient factor $\boldsymbol{\beta_g}$ is the tangent of the gradient angle and expressed as (C.1) where $\boldsymbol{\Delta u_g}$ is the vertical and $\boldsymbol{\Delta s_g}$ the horizontal distance between the beginning and end of the gradient:

$$\boldsymbol{\beta_g = \frac{\Delta u_g}{\Delta s_g}} \tag{C.1}$$

Table C1 and the locomotive specifications of spread sheets and Appendix C, are taken in account in calculating the resistances (C.2) – (C.5).

Rolling resistance [kN]:

$$\boldsymbol{F_r = \mu_r(m_{train} + m_{loc})g} \tag{C.2}$$

Gradient resistance [kN]:

$$\boldsymbol{F_g = \beta_g(m_{train} + m_{loc})g} \tag{C.3}$$

Air resistance [kN]:

$$\boldsymbol{F_{air} = k_{air}\rho_{air}A_{air}v_{loc}^2 g} \tag{C.4}$$

Train resistance [kN]:

$$\boldsymbol{F_{train} = F_r + F_g + F_{air}} \tag{C.5}$$

Power setting of the *Hs 1* and Dr18 refers to the percentage of applied power to the maximum power. In the *Tr1* the power setting refers to the admission ratio $\boldsymbol{\varepsilon}$ of the cylinders. There is no explicit relation between $\boldsymbol{\varepsilon}$ and the power, but as the driving wheels of classical steam locomotives are directly coupled in the cylinders, the steam consumption is directly proportional to both $\boldsymbol{\varepsilon}$ and the distance travelled. The power is thus indirectly obtainable through energy consumed and work performed.

Momentary drawbar power [kW]:

$$\boldsymbol{X_P = \frac{P_{set}}{P_{max}}} \tag{C.6}$$

Tractive force $\boldsymbol{F_{db}}$ in the drawbar follows from the well-known dependence $\boldsymbol{P = Fv}$ between momentary power $\boldsymbol{P_{db}}$ and speed $\boldsymbol{v}$:

$$\boldsymbol{F_{db} = \frac{P_{db}}{v_{loc}}} \tag{C.7}$$

On level track, the gradient resistance is zero whereas on open road typically all the resistances decrease the drawbar tractive force, except in a downgrade where the gradient resistance turns negative. Fig. 5.4 depicts the relations between individual resistances in the vicinity of the summit of the *Huttula* hill half-way the trip, enhancing the key role of gradients in the resistance formation.

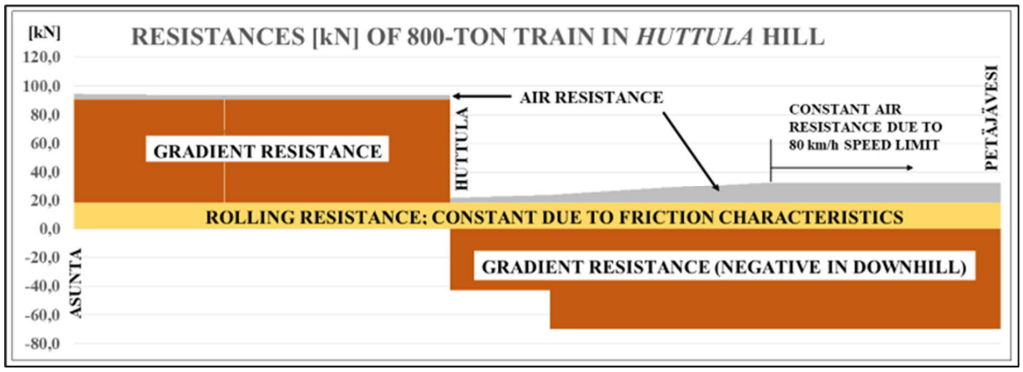

Figure 5.4: Components of train resistance during climb and descent of a hill.

In Fig. 5.4, the conspicuous step in the right-hand section of the gradient resistance graph depicts the steepening of the descent at the corresponding point.

At any given point of observation, the force to accelerate the train is obtained from Formula (C.8):

$$\boldsymbol{F_a = F_{db} - F_T} \tag{C.8}$$

The resulting momentary acceleration [m/s^2] is expressed by equation (C.9) following from Newton's second law, or $\boldsymbol{F = ma}$:

$$\boldsymbol{a = \frac{F_a}{m_{loc}+m_T}} \tag{C.9}$$

Tractive force [kN]			Acceleration [m/s^2]			Momentary train speed [km/h]			Brake force [kN]		
Hs1	Dr18	Tr1	Hs1	Dr18	Tr1	Hs1	Dr18	Tr1	Hs1	Dr18	Tr1
90	89	86	0	0	0	39,2	39,3	37,5	0	0	0
90	89	86	0	0	0	39,2	39,3	37,5	0	0	0
90	89	86	0	0	0	39,2	39,3	37,5	0	0	0
90	89	86	0	0	0	39,2	39,3	37,5	0	0	0
90	89	86	0	0	0	39,2	39,3	37,4	0	0	0
90	89	86	0	0	0	39,2	39,3	37,4	0	0	0
90	89	86	0	0	0	39,2	39,3	37,4	0	0	0
90	89	86	0	0	0	39,2	39,3	37,4	0	0	0
90	89	86	0	0	0	39,2	39,3	37,3	0	0	0
90	89	86	0	0	0	39,3	39,4	37,4	0	0	0
0	0	0	0,027	0,028	0,028	39,4	39,5	37,5			
0	0	0	0,027	0,028	0,028	39,5	39,6	37,6			
0	0	0	0,027	0,028	0,028	39,6	39,7	37,7			
0	0	0	0,027	0,028	0,028	39,7	39,8	37,8			
0	0	0	0,027	0,028	0,028	39,8	39,9	37,9			
0	0	0	0,027	0,028	0,028	39,9	39,9	38,0			
0	0	0	0,027	0,028	0,027	39,9	40,0	38,1			
0	0	0	0,027	0,028	0,027	40,0	40,1	38,2			
0	0	0	0,027	0,028	0,027	40,1	40,2	38,3			
0	0	0	0,027	0,028	0,027	40,2	40,3	38,4			

Figure 5.5: Ascent (pink) ends and turns to descent (green); power is turned off but speed increases.

Power setting			Drawbar power			Tractive force			Acceler. force			Acceleration		
$X_P = \frac{P_{set}}{P_{max}}$		$X_P = \varepsilon_{set}$	P_{db}			$F_{db} = \frac{P_{db}}{v}$			$F_a = F_{db} - F_T$			$a = \frac{F_a}{m_{loc} + m_T}$		
[%]			[kW]			[kN]			[kN]			[m/s^2]		
Hs1	**Dr18**	**Tr1**	**Hs1**	**Dr18**	**Tr1**	**Hs1**	**Dr18**	**Tr1**	**Hs1**	**Dr18**	**Tr1**	**Hs1**	**Dr18**	**Tr1**
30	**30**	**85**	**300**	**300**	**77**	**300**	**300**	**155**	**285**	**286**	140	**0,05**	**0,05**	**0,05**
11,5	**9,8**	**85**	**112**	**112**	**324**	**112**	**112**	**155**	**47**	**47**	**101**	**0,05**	**0,05**	**0,11**
13,5	**11,5**	**60**	**132**	**132**	**403**	**54**	**54**	**137**	**47**	**47**	**83**	**0,05**	**0,05**	**0,09**
14,4	**12,3**	**60**	**141**	**141**	**455**	**50**	**50**	**137**	**47**	**47**	**83**	**0,05**	**0,05**	**0,09**
15,2	**13,0**	**60**	**149**	**149**	**494**	**49**	**49**	**137**	**47**	**47**	**83**	**0,05**	**0,05**	**0,09**
16,0	**13,6**	**60**	**156**	**156**	**528**	**49**	**49**	**137**	**47**	**47**	**83**	**0,05**	**0,05**	**0,09**
16,7	**14,3**	**60**	**163**	**163**	**560**	**49**	**49**	**137**	**47**	**47**	**83**	**0,05**	**0,05**	**0,09**
17,4	**14,9**	**60**	**170**	**170**	**590**	**48**	**48**	**137**	**47**	**47**	**83**	**0,05**	**0,05**	**0,09**
18,1	**15,4**	**60**	**177**	**177**	**619**	**48**	**48**	**137**	**47**	**47**	**83**	**0,05**	**0,05**	**0,09**
18,7	**16,0**	**60**	**183**	**183**	**645**	**48**	**48**	**137**	**47**	**47**	**83**	**0,05**	**0,05**	**0,09**
100	**85,1**	**60**	**977**	**975**	**671**	**248**	**248**	**137**	**196**	**196**	**83**	**0,21**	**0,21**	**0,09**

Figure 5.6: Power setting and resulting changes in forces and acceleration.

Speed [m/s] after acceleration, within the incremental distance specified, follows from the known formula $\boldsymbol{v = v_0 + at}$ written as (C.10):

$$\boldsymbol{v_{incr} = v_0 + at_{incr}} \tag{C.10}$$

Time [s] to travel the incremental distance is obtained from formula (C.11) following from the known equation $\boldsymbol{s = v_0 t + \frac{at^2}{2}}$ by solving it for t and applying momentary speed and acceleration:

$$\boldsymbol{t_{incr} = \frac{-v_0 + \sqrt{v_0^2 - 2as}}{a}} \tag{C.11}$$

Drawbar work [MJ] is obtained from equation (C.12) following from the known formula $\boldsymbol{W = Fs}$ and calculated for each increment to be summed for any distance:

$$\boldsymbol{W_{db} = F_{db} s} \tag{C.12}$$

Momentary train speed						Time to traverse 10 m			Brake force			Drawbar work		
$v = v_0 + at$						$t = \frac{-v_0 \pm \sqrt{v_0^2 - 2as}}{a}$			F_b			$W_{db} = F_{db}s$		
[m/s]			[km/h]			[s]			[kN]			[MJ]		
												Σ		
												2109	2101	2123
Hs1	**Dr18**	**Tr1**	**Hs1**	**Dr18**	**Tr1**	**Hs1**	**Dr18**	**Tr1**	**Hs1**	**Dr18**	**Tr1**	**Hs1**	**Dr18**	**Tr1**
1	**1**	**0,5**	**3,6**	**3,6**	**1,8**	**28,3**	**28,3**	**15**	**0**	**0**	**0**	**3,0**	**3,0**	**1,5**
2,4	**2,4**	**2,1**	**8,7**	**8,7**	**7,5**	**8,3**	**8,3**	**9,8**				**1,1**	**1,1**	**1,5**
2,8	**2,8**	**2,9**	**10,2**	**10,2**	**10,6**	**4,0**	**4,0**	**4,4**				**0,5**	**0,5**	**1,4**
3,0	**3,0**	**3,3**	**10,9**	**10,9**	**12,0**	**3,4**	**3,4**	**3,2**				**0,5**	**0,5**	**1,4**
3,2	**3,2**	**3,6**	**11,5**	**11,5**	**13,0**	**3,2**	**3,2**	**2,9**				**0,5**	**0,5**	**1,4**
3,4	**3,4**	**3,9**	**12,1**	**12,1**	**13,9**	**3,1**	**3,1**	**2,7**				**0,5**	**0,5**	**1,4**
3,5	**3,5**	**4,1**	**12,6**	**12,6**	**14,7**	**2,9**	**2,9**	**2,5**				**0,5**	**0,5**	**1,4**
3,7	**3,7**	**4,3**	**13,2**	**13,2**	**15,5**	**2,8**	**2,8**	**2,4**				**0,5**	**0,5**	**1,4**
3,8	**3,8**	**4,5**	**13,7**	**13,7**	**16,3**	**2,7**	**2,7**	**2,3**				**0,5**	**0,5**	**1,4**
3,9	**3,9**	**4,7**	**14,2**	**14,2**	**17,0**	**2,6**	**2,6**	**2,2**				**0,5**	**0,5**	**1,4**
4,5	**4,5**	**4,9**	**16,1**	**16,1**	**17,6**	**2,4**	**2,4**	**2,1**				**2,5**	**2,5**	**1,4**

Figure 5.7: Use of speed, time, brake force, and drawbar work formulae at start from zero speed.

For locomotive *Hs1*, in which the prime mover is rotating at constant velocity, the mass flow $\dot{m}_{st}$ of steam is taken to be directly proportional to preset power, and thus to the corresponding steam flow $\dot{m}_{st\ max}$ earlier calculated in the prime mover chapter. The resulting total mass of steam is then the sum of consumption *per* each increment of distance, defined by mass flow and time of power on. Due to the properly insulated prime mover working in a warm and well-insulated compartment, the *wall effect* of cylinders is assumed to remain negligible and thus cause *nil* steam consumption. Formula (C.13) then applies:

$$m_{st} = \Sigma t_{incr} \frac{P_{set}}{P_{max}} \dot{m}_{st\ max} \tag{C.13}$$

For the classical steam locomotive *Tr1,* the incremental steam consumption is directly proportional to the number of revolutions of driving wheels within 10-m increment, the admission taking place four times *per* revolution in a 2-cylinder engine, the admission ratio ε_{set} determining the admitted volume $\varepsilon_{set} V_{disp}$, and density ρ_{st} the mass of steam. The resulting mass of steam consumed is thus obtained from Formula (C.14), in which the χ is a factor taking in account the eventual impact of *wall effect* by adding 5 % to the calculated consumption:

$$m_{st} = 4\Sigma\chi\varepsilon_{set} \frac{s_{incr}}{\pi D_{dr}} V_{disp} \rho_{st} \tag{C.14}$$

where V_{disp} is the displacement of one cylinder and D_{dr} the diameter of the driving wheels.
Energy consumption of the *Hs1* and *Tr1* is calculated according to formula (C.15), *via* steam consumption during the time to travel the incremental distance, the specific enthalpy-rise Δh_{st} of steam in the boiler, and the boiler efficiency η_B:

$$E_{tot} = \frac{m_{st} \Delta h_{st}}{\eta_B} \tag{C.15}$$

The overall energy consumption of a diesel locomotive depends on its *specific fuel consumption,* or fuel consumed per kWh of work, and of its consumption at idling, as a diesel engine is rarely stopped during operation exept for lengthy stand-still periods. The preliminary specific consumption figures refer to Wärtsilä Diesel Product Information given by the 7th Locomotive Depot of St. Petersburg where Wärtsilä *6L20* engines are used in *ТЭМ18В* class diesel-electric locomotives.[380] Figures of this relatively modern engine have been compared to results obtained from actual tests with *Dr18* locomotives in changeable road conditions, including climbs and descents within 300 km's of route length.[381] Tests during 2017 of the *Dr18* equipped with *Caterpillar 3512 C HD* engine do not specify idling consumption figures but rather concentrate on overall consumption per kilometer. Comparisons with figures obtained from simulated runs of the present study, exploiting the above mentioned Wärtsilä engine data, showed < 2 % deviation from those given by the actual road tests of *Dr18*. Thus, a specific consumption *s.f.c.* = 190 g/kWh referring to indicated power, and idling consumption of *10 kg/h*, have been exploited. The *Dr18* specifications give a transmission efficiency $\eta_{tr} = 0{,}74$, resulting in a specific consumption of 257 g/kWh at the drawbar basis.[382] Formula (C.16) then gives the total fuel consumption as this is calculated for every 10-meter increment by taking in account the time of traversing over each increment. If power is cut off, the first term on the right side is zero.

$$E_{tot} = (X_P t_{run} \dot{m}_{F\,run} + t_{idle} \dot{m}_{F\,idle}) Q_F \qquad \text{(C.16)}$$

where subscripts *run* and *idle* refer to specific running and idling consumptions, respectively.
Energy [MJ] recovered by braking of *Hs1* is obtained from Formula (C.17), a version of the known formula $W = Fs$, equating the recovered energy with negative work done by braking force F_b and taking in account the efficiency η_{rec} of the recovery system comprising of the traction motors working both as generators and motors, and of charging the accumulators:

$$E_{rec} = \eta_{rec} F_b s_{incr} \qquad \text{(C.17)}$$

The recovered energy is thus re-usable without further considerations of efficiency of recovery.

Energy consumption						Energy recovered		Cumulative time		
Steam				Fuel		$E_{rec} = \eta_{rec} F_b s$		$t_{cum} = \Sigma t_{incr}$		
$m_{st} = \Sigma t_{incr} \frac{P_{set}}{P_{max}} \dot{m}_{st\,max}$		$m_{st} = 4\Sigma\chi\epsilon_{set} \frac{s_{incr}}{\pi D_{dr}} V_{disp} \rho_{st}$		$E_{tot} = (X_P t_{run} \dot{m}_{F\,run} + t_{idle} \dot{m}_{idle}) Q_F$		[MJ]		[min]		
$E_{tot} = \frac{m_{st} \Delta h_{st}}{\eta_B}$				[MJ]	[MJ]					
[kg]	[MJ]	[kg]	[MJ]	idle	work	Stored	Used	Σ		
3182	8811	8310	29984	324	6113	374	285	88	88	84
Hs1		Tr1		Dr18 only		Hs1 only		Hs1	Dr18	Tr1
14,4	40,0	7,9	32	0,0	0,6	0,0	0,0	0,5	0,5	0,3
1,6	4,5	7,9	32	0,0	0,1			1,0	1,0	0,6
0,9	2,5	5,6	23	0,0	0,0			1,1	1,1	0,7
0,8	2,3	5,6	23	0,0	0,0			1,2	1,2	0,8
0,8	2,3	5,6	23	0,0	0,0			1,2	1,2	0,8
0,8	2,3	5,6	23	0,0	0,0			1,3	1,3	0,9
0,8	2,3	5,6	23	0,0	0,0			1,3	1,3	0,9
0,8	2,3	5,6	23	0,0	0,0			1,4	1,4	1,0
0,8	2,3	5,6	23	0,0	0,0			1,4	1,4	1,0
0,8	2,3	5,6	23	0,0	0,0			1,5	1,5	1,1
4,1	11,3	5,6	23	0,0	0,2			1,5	1,5	1,1

Figure 5.8: Energy consumption of the test locomotives and energy recovery of *Hs1*.

Tractive force [kN]			Acceleration [m/s²]			Momentary train speed [km/h]			Brake force [kN]		
Hs1	Dr18	Tr1	Hs1	Dr18	Tr1	Hs1	Dr18	Tr1	Hs1	Dr18	Tr1
-43	-43	-44	0	0	0	80,0	80,0	80,0	43	43	44
-43	-43	-44	0	0	0	80,0	80,0	80,0	43	43	44
-43	-43	-44	0	0	0	80,0	80,0	80,0	43	43	44
-43	-43	-44	0	0	0	80,0	80,0	80,0	43	43	44
-43	-43	-44	0	0	0	80,0	80,0	80,0	43	43	44
-43	-43	-44	0	0	0	80,0	80,0	80,0	43	43	44
-43	-43	-44	0	0	0	80,0	80,0	80,0	43	43	44
-43	-43	-44	0	0	0	80,0	80,0	80,0	43	43	44
-43	-43	-44	0	0	0	80,0	80,0	80,0	43	43	44
-43	-43	-44	0	0	0	80,0	80,0	80,0	43	43	44
34	30	0	-0,042	-0,047	-0,079	80,0	79,9	79,9			
34	30	0	-0,042	-0,047	-0,079	79,9	79,8	79,8			
34	30	0	-0,042	-0,047	-0,079	79,8	79,8	79,6			
34	30	0	-0,042	-0,047	-0,079	79,8	79,7	79,5			
34	30	0	-0,042	-0,047	-0,079	79,7	79,6	79,4			
34	30	0	-0,042	-0,046	-0,079	79,6	79,5	79,3			
34	30	0	-0,042	-0,046	-0,079	79,5	79,5	79,1			
34	30	0	-0,042	-0,046	-0,079	79,5	79,4	79,0			
34	30	0	-0,042	-0,046	-0,079	79,4	79,3	78,9			
34	30	0	-0,042	-0,046	-0,079	79,3	79,2	78,7			

Figure 5.9: Braking in downgrade at constant speed; energy recovery and re-use in *Hs1.*

The drawbar thermal efficiency η_{db} is calculated from formula (C.18) where W_{db} is drawbar work, and E_{rec} the recovered and stored energy, and E_F the fuel energy consumed. The formula applies for any type of locomotive.

$$\eta_{db} = \frac{W_{db}+E_{rec}}{E_F} \quad \text{(C.18)}$$

Table 5.1 presents a summary of simulated on-the-road tests. The shaded rows with bold figures show the travel times, and the drawbar thermal efficiencies attained. The stored energy has been added to the drawbar work when calculating the overall thermal efficiency of *Hs 1* as discussed above.

SIMULATION WITH 800-TON FREIGHT TRAIN AT MAXIMUM SPEED OF 80 KM/H						
Item	**Symbol**	**Definition**	**Dimension**	**Total distance: 156 km** Performance data:		
				Hs 1	**Dr18**	**Tr1**
Travel time	t_{tot}	Formulae described within calculations	**[min]**	**174**	**174**	**174**
Average speed	v_{av}		[km/h]	54	54	54
Drawbar work	W_{db}		[MJ]	4548	4531	4522
Steam consumption						
- mass	m_{st}		[kg]	6560		17856
- energy	E_{st}		[MJ]	17700		64425
Energy consumption total	E_F		[MJ]	17700	13792	68671
- productive	E_{work}		[MJ]	17700	13187	64425
- non-productive	E_{idle}		[MJ]	0	606	4246
LHV of fuel used	LHV_F		[MJ/kg]	14,7	40,7	28,0
Fuel consumption	m_F		[kg]	1203	339	2453
Energy recovered	E_{rec}		[MJ]	944		
" re-used within trip	E_{r-u}		[MJ]	787		
" stored	E_{stor}		[MJ]	157		
" related to drawbar work	E_{rec}/W_{db}		[%]	20,8		
" related to energy used	E_{rec}/E_F		[%]	5		
Drawbar thermal efficiency	η_{db}	$\eta_{db} = (W_{db} + E_{stor})/E_{tot}$	**[]**	**0,27**	**0,33**	**0,07**

Table 5.2: Summary of simulated on-the-road freight train tests.

5.2.2 Yard work

Working at level track is assumed for practical reasons, as track yards are generally built with negligible gradients. The yard test program thus only takes in account the rolling resistance and air resistance of trains. Increments of one meter have been applied in plotting the simulation program, to maximize the accuracy of simulating the start and stop of trains.

The main aim of simulating yard work is to assess the potential for energy recovery during shunting moves that involve incessant alternation of accelerating and braking of trains. Traffic regulations of *e.g.,* Finnish railways set a speed limit of 40 km/h in so called short turnouts typical at stations and track yards.[383] However, shunting duties within large marshalling yards also typically include serving regional industries, often calling for delivery of trains *via* main line at higher than yard speeds. For such purposes, a maximum of 70 km/h has been opted for the simulation and applied in Fig. 5.11 where *Hs 1* is shown accelerating an 800-t train to speed and braking to stop. Acceleration takes *ca.* 3,5 km and braking *ca.* 1,2 km when applying the dynamic brakes of the locomotive at 120 kN brake force. Such a force is selected as it is specified as the maximum for *Dr18* diesel-electric locomotives in dynamic braking. The engine often moves without train, such a case being included in simulations.

Track and train parametres			
Train weight: freight	m_{Tf}	[t]	1000
			800
			600
			400
			200
			0
Train weight: passenger	m_{Tp}	[t]	100
Rolling resistance factor	μ_r	[ ]	0,0016
Drag coefficient	k_{air}	[ ]	0,80
Air density	ρ_{air}	[kg/m^3]	1,29
Area exposed to air resistance			
- Locomotive coefficient		[m^2/t]	0,12
- Train coefficient freight			0,04
- Train coefficient passenger			0,04
Locomotive Hs1		[m^2]	15,6
Locomotive Dr18		[m^2]	14,4
Freight car area exposed to air resistance:			
1000-ton train		[m^2]	40
800 t			32
600 t			24
400 t			16
200 t			8
Locomotive alone			0
100-ton local passenger train		[m^2]	4
-Area total: freight Hs1	A_{air}	[m^2]	55,6
			47,6
			39,6
			31,6
			23,6
			15,6
-Area total: freight Dr18	A_{air}	[m^2]	54,4
			46,4
			38,4
			30,4
			22,4
			14,4
-Area total: passenger Hs1	A_{air}	[m^2]	19,6
-Area total: passenger Dr18			18,4

Table 5.3: Track and train parameters valid for yard tests on level track.

Distance	Rolling resistance		Air resistance									
from start	$F_r = \mu_r(m_{loc} + m_T)g$		$F_{air} = ½k\rho_{air}A_{air}v^2$									
[km]	[kN]		[kN]									
	14,6/14,4 kN re. **800 t**											
	11,5/11,3 kN re. **600 t**											
	8,3/8,2 kN re. **400 t**											
	5,2/5,0 kN re. **200 t**											
	2,0/1,9 re. **Loco alone**		**800 t**		**600 t**		**400 t**		**200 t**		**Loco alone**	
	Hs 1	**Dr18**	**Hs1**	**Dr18**	**Hs1**	**Dr18**	**Hs1**	**Dr18**	**Hs1**	**Dr18**	**Hs1**	**Dr18**
0,0	14,6	14,4										
0,001	11,5	11,3	0,01	0,01	0,01	0,00	0,00	0,00	0,00	0,00	0,00	0,00
0,002	8,3	8,2	0,02	0,02	0,06	0,06	0,08	0,08	0,04	0,04	0,12	0,13
0,003	5,2	5,0	0,03	0,03	0,10	0,10	0,12	0,12	0,06	0,06	0,18	0,19
0,004	2,0	1,9	0,03	0,03	0,12	0,11	0,13	0,13	0,07	0,07	0,19	0,20
0,005			0,04	0,04	0,13	0,13	0,14	0,14	0,08	0,08	0,21	0,22
0,006			0,05	0,05	0,14	0,14	0,15	0,15	0,09	0,08	0,22	0,23
0,007			0,06	0,06	0,15	0,15	0,16	0,16	0,09	0,09	0,24	0,25
0,008			0,08	0,08	0,16	0,16	0,17	0,17	0,10	0,10	0,25	0,26
0,009			0,09	0,09	0,17	0,16	0,18	0,18	0,11	0,11	0,26	0,27
0,010			0,11	0,10	0,18	0,17	0,19	0,18	0,12	0,12	0,28	0,29

Figure 5.10: Air resistance at start with different train weights.

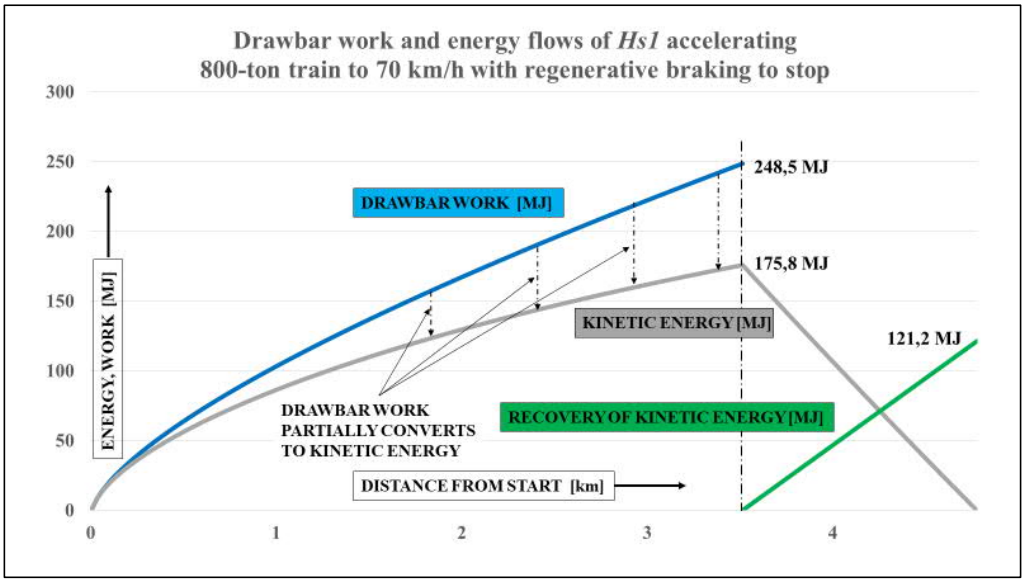

Figure 5.11: Drawbar work, conversion, and recovery of energy during acceleration and braking.

Performance parameters of the *Hs 1* and *Dr18* are listed in Tables 5.4 and 5.5, respectively. The term W_a indicates the drawbar work and E_F the fuel energy required to perform the work. Efficiency η_0 applies for the *Hs 1* in case no braking energy recovery takes place. The recovered and stored energy is expressed by E_{rec}, or from energy generated by braking as earlier explained in Paragraph 5.2.1. The E_{rec}

has been added to W_a when calculating drawbar thermal efficiency η_{db} since E_{rec} was built up during the acceleration by the drawbar work W_a at energy input E_F.

PERFORMANCE DATA OF *Hs 1*					
v_0	W_a	E_F	η_0	E_{rec}	η_{db}
[km/h]	[MJ]	[MJ]	[ ]	[MJ]	[ ]
20	**15**	**70**	**0,21**	**10**	**0,36**
30	**35**	**168**	**0,21**	**23**	**0,35**
40	**65**	**314**	**0,21**	**41**	**0,34**
50	**108**	**518**	**0,21**	**63**	**0,33**
60	**166**	**798**	**0,21**	**90**	**0,32**
70	**247**	**1188**	**0,21**	**122**	**0,31**

Table 5.4: Level track performance data of the *Hs1*.

The energy recovery terms do not apply to the *Dr18* and have thus been omitted from Table 5.5 whereas the idling energy E_{idle} has been included.

PERFORMANCE DATA OF Dr18				
v_0	W_a	E_{idle}	E_F	η_{db}
[km/h]	[MJ]	[MJ]	[MJ]	[ ]
20	**15**	**4**	**47**	**0,31**
30	**34**	**6**	**106**	**0,32**
40	**64**	**9**	**195**	**0,33**
50	**106**	**11**	**319**	**0,33**
60	**163**	**13**	**487**	**0,34**
70	**242**	**15**	**718**	**0,34**

Table 5.5: Level track performance data of the *Dr18*.

Fig's 5.12 – 5.17 show graphs of comparative simulations between *Hs1* and *Dr18* performing the same task. Efficiency of *Hs1* in case of working without any recovery of braking energy is shown by the dotted green line whereas the regenerative braking depicted by the unbroken green line depicts the efficiency attained by the *Hs1* with regenerative brakes.

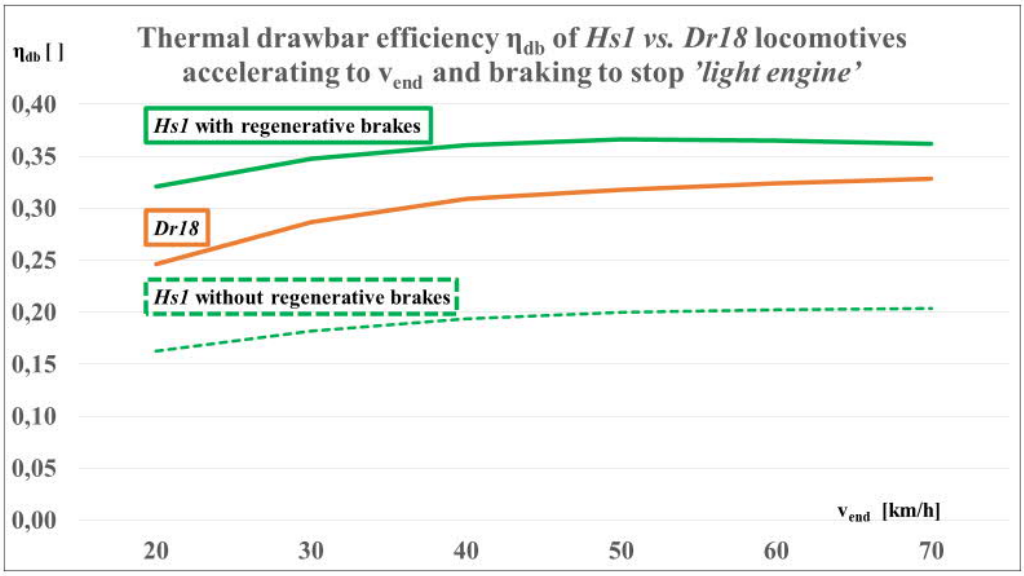

Figure 5.12: Test with locomotive only, from start to various speeds and braking to stop.

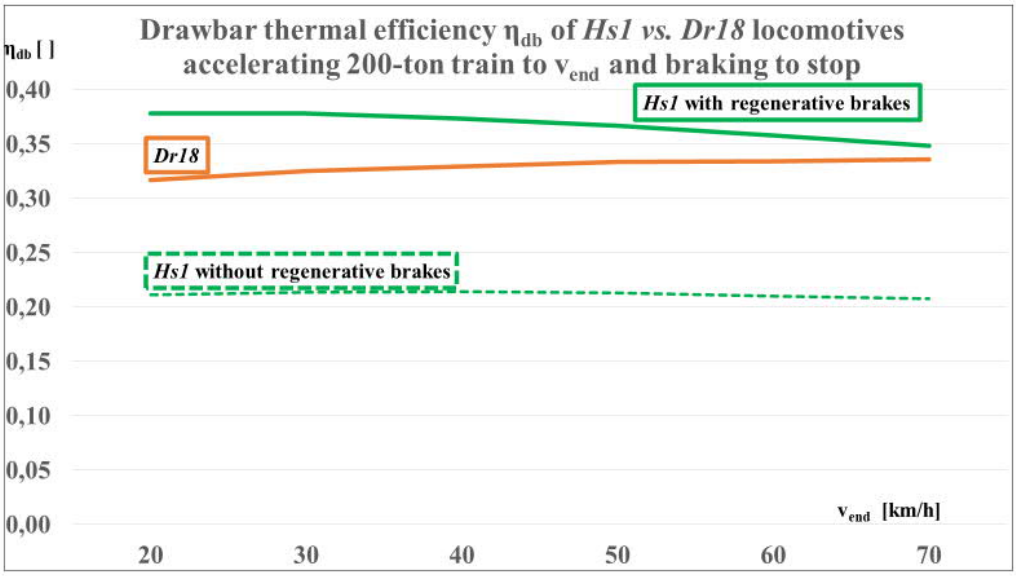

Figure 5.13: Test with a 200-t train from start to various speeds and braking to stop.

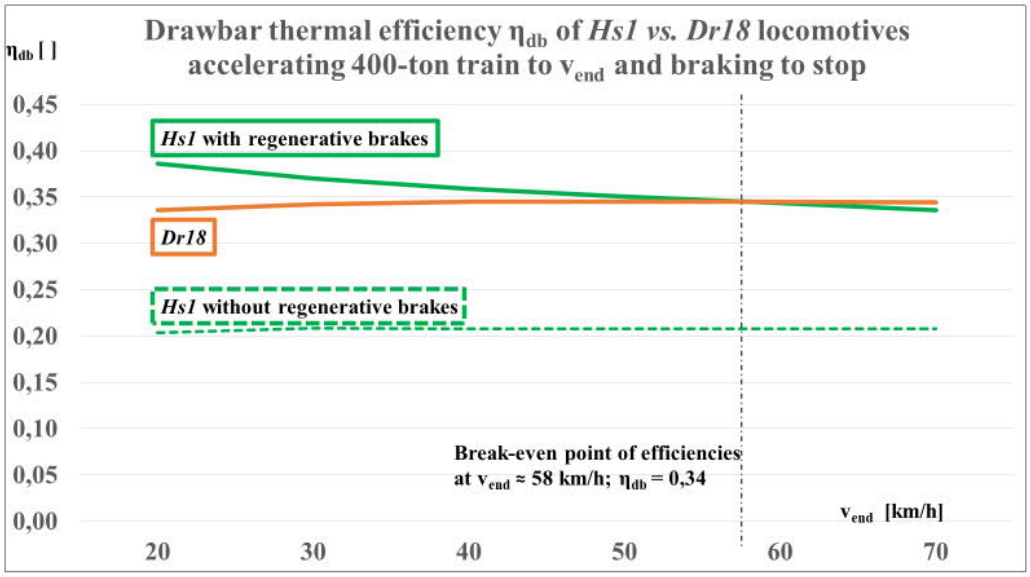

Figure 5.14: Test with a 400-t train from start to various speeds and braking to stop.

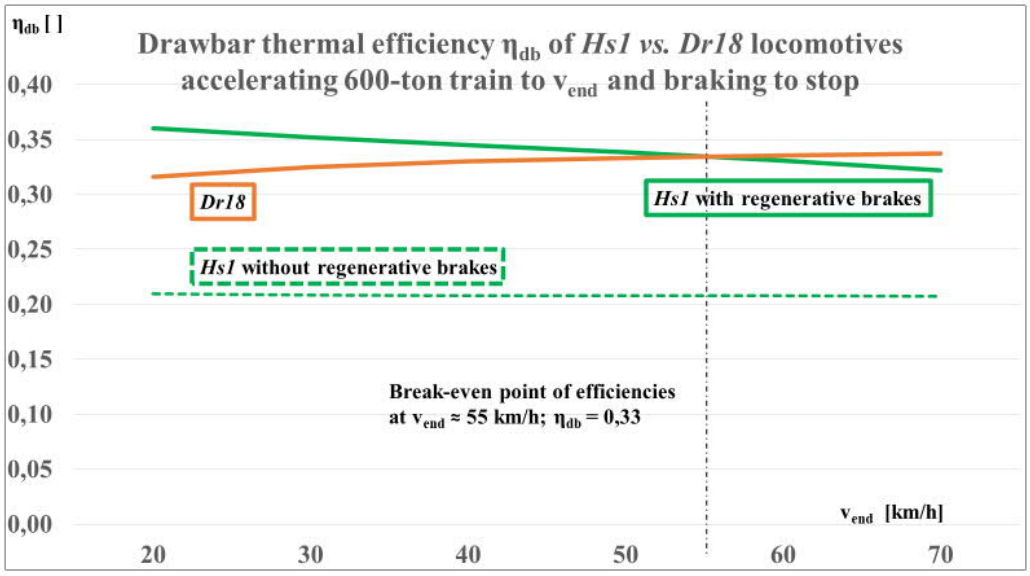

Figure 5.15: Test with a 600-t train from start to various speeds and braking to stop.

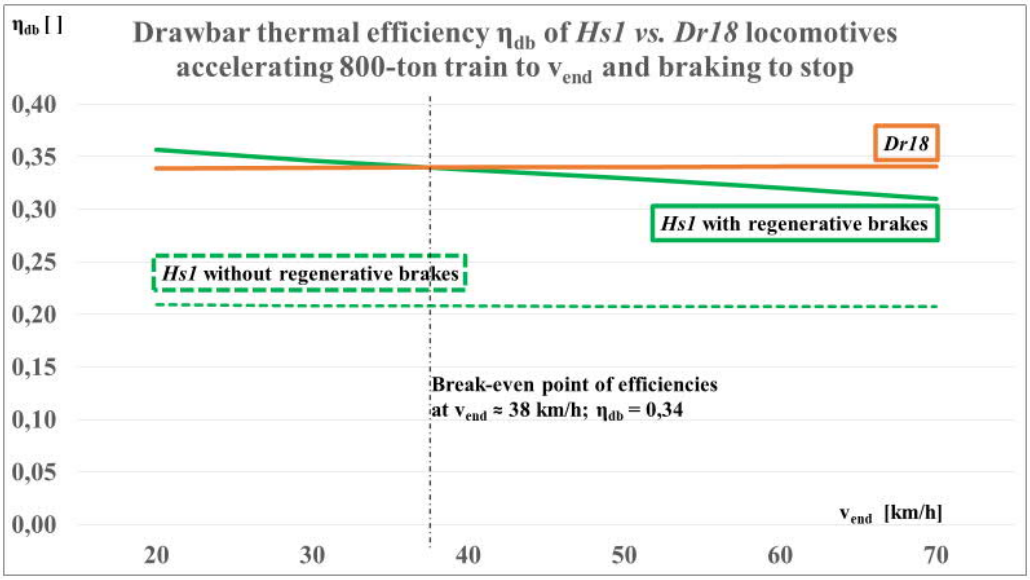

Figure 5.16: Test with an 800-t train from start to various speeds and braking to stop.

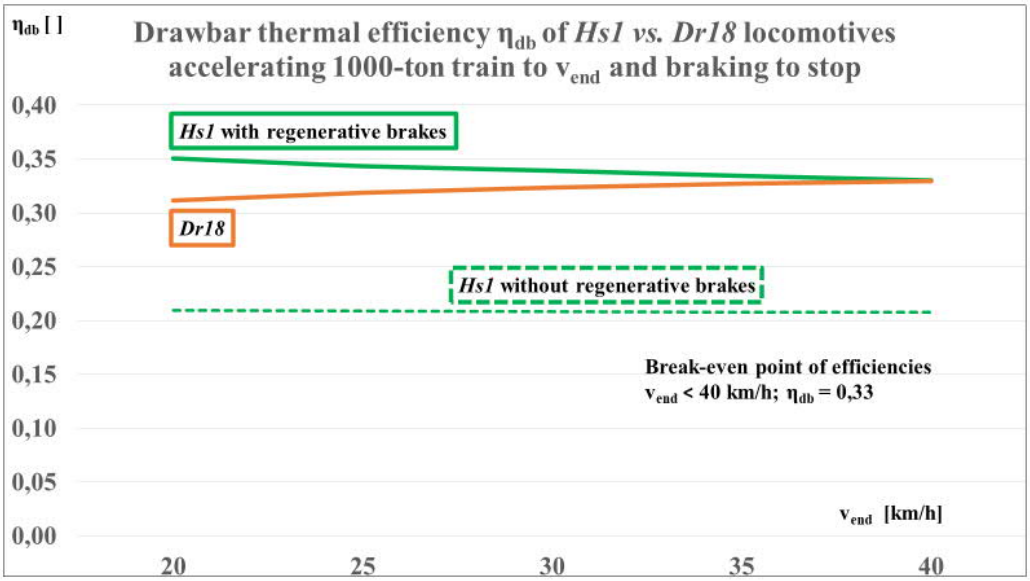

Figure 5.17: Test with a 1000-t train from start to various speeds and braking to stop.

5.2.3 Local passenger trains

Operation of 100-t (2 coaches) passenger trains has been simulated in a comparative test between the *Hs 1* and *Dr18*. Fig. 5.19 and Table 5.6 present graphical and tabulated summaries of the test, respectively. In Table 5.6, target speed has been set to the maximum of both locomotives. The first case implies braking, once the speed is attained, while the second case involves a travel of 5000 m. Stops of 30 seconds are included in the calculations. The stops affect the idling consumption of the Dr18.

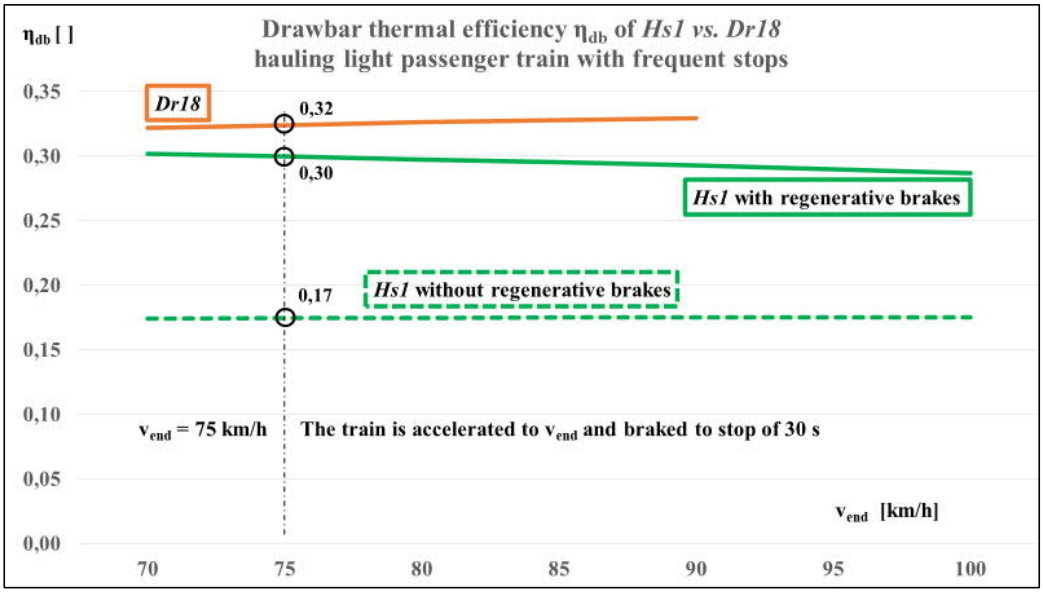

Figure 5.18: Comparison of *Hs 1* and *Dr18* in a local train with frequent stops; v_{end} refers to the speed attained before the brakes are applied, a stop of 30 s being included in the efficiency calculations.

ITEM			Hs 1		Dr18	
DRAWBAR WORK	W_{db}	[MJ]	105	115	76	107
ENERGY CONSUMED	E_F	[MJ]	601	744	229	320
ENERGY RECOVERED	E_{rec}	[MJ]	67	67	-	-
THERMAL EFFICIENCY	η_{db}	[ ]	**0,29**	**0,24**	**0,33**	**0,33**
START-TO-STOP DISTANCE	s_{tot}	[m]	2806	5000	1683	5000
TOTAL TIME	t_{tot}	[min]	3,2	4,6	2,4	4,6
AVERAGE SPEED	v_{av}	[km/h]	52,2	65,9	41,5	64,6

Table 5.6: *Hs1* vs. *Dr18* hauling a 100-t local passenger train.

5.3 Performance in view of the simulation results

5.3.1 Results of simulated tests

5.3.1.1 On-the-road freight train simulations

Table 5.2 of paragraph 5.2.1 predicts the test engines to attain following drawbar thermal efficiencies:

Hs 1: **0,27**
Dr18: **0,33**
Tr1: **0,07**

The same table indicates that the recovery of braking energy amounts in 19 % of the drawbar work and 5 % of the energy consumption of the *Hs 1.* The ratio between the two figures is in harmony with the drawbar efficiency, as the *Sr2* class electric locomotives of Finnish Railways suggest an average of 15 % feed-back of the energy taken from the catenary, by virtue of regenerative braking.[384] Assuming efficiency of 0,9 (*i.e.,* more than three times that of the *Hs 1*) for electric locomotives, the ratio 5 % *vs.* 15 %, or 1:3, appears to make sense about the energy recovery predictions of the *Hs 1*.

At full power, the *Dr18* proves the supremacy of diesel *vs.* steam traction in long-haul service, as the diesel shows up the more efficient the harder it works.

Regardless of its low idling consumption (*ca.* 5 % of the full power consumption)[385] the diesel is predicted to consume non-productive fuel for an amount of 13 % related to the drawbar work. The profile of the route accounts most of the idling, since all the locomotives are running with closed throttle for about 50 % of the total travel time.

The efficiency of 0,07 predicted for the *Tr1* by the simulation is in harmony with the figures discussed in Chapter 3 (*e.g.,* Fig. 3.3), essentially due to moderate admission ratios applied in the simulation. High admission ratios would result in fierce draft and unburnt coal particles which in turn would further worsen the efficiency of the locomotive as was discussed in Chapter 3.

Table 5.2 further indicates that the energy of coal consumed by the Tr1 when the throttle is closed, is equal to 60 % of the drawbar work, as the fire grate cannot be turned off like a burner because the fire should be maintained in stand-by condition anyway.

The travel times and resulting average speeds of the engines at the total route length of 156 km:

Hs 1:	t_{tot} = 2,9 h, v_{av} = 54 km/h
Dr18:	t_{tot} = 2,9 h, v_{av} = 54 km/h
Tr1:	t_{tot} = 2,9 h, v_{av} = 54 km/h

The schedule of the simulated runs is substantially faster than the late steam age freight schedules based on studies on the footplate where the nature of work on a hand-fired steam locomotive has been taken in account.

The fuel analysis within calculations of Appendix B indicated that wet flue gas of LFO contains twice as much CO_2 per kg of fuel burnt as fluegas of pyrolysis oil, partially because the latter requires *ca.* 50 % less oxygen in combustion.[386] Due to the difference (42,7 MJ/kg_F *vs.* 15 MJ/kg_F) in heating values of the two fuels, the actual mass flow of pyrolysis oil is 2,8 times that of LFO for a given thermal power. Lower thermal efficiency of the *Hs 1* adds to the difference and further to the resulting CO_2 emissions. Regardless of the carbon neutrality being an issue of debate, combustion of LFO involves releasing CO_2 of fossil origin whereas combustion of pyrolysis oil does not.

The higher nitrogen emissions of the *Hs 1* mainly originate from fuel bound N_2 in combustion of pyrolysis oil as the lower temperature of combustion reduces the formation of thermal nitrogen oxides.[387] As a whole, defining the mechanism of formation of nitrogen compounds is complex, and has been excluded from the scope of the study.

5.3.1.2 Yard work simulations

Fig's 5.12 - 5.18, together with Tables 5.4 - 5.6, indicate the contrasting efficiency curves of *Hs 1 vs. Dr18* along increase of target speeds of the simulation. The brake-even point of the drawbar thermal efficiencies of the two locomotives moves towards higher speeds when the train weight is decreased, η_{db} **= 0,33** being attained by both locomotives handling an 800-t train at a speed of *ca.* 37 km/h, or close to the speed limit of typical shunting operations. Variations are within η_{db} = 0,31 – 0,35 over the whole speed range simulated, as indicated by the graphs. The engines thus appear quite equal performers in yard work. The contrast of *Hs1* compared to classic steam is particularly notable, as the efficiency of the latter was at its worst in shunting duties, due to the intermittent nature of the work that prevented the engine from warming up, resulting in thermal losses while idling times further increased the non-productive fuel consumption.[388]

5.3.1.3 Local passenger train simulations

Fig. 5.18 and Table 5.6 sum up the comparison between *Hs 1* and Dr18 hauling a 100-ton local train. Drawbar thermal efficiency of *Hs 1* is **0,24** *vs.* **0,33** of Dr18 at average speed of 65 km/h while the short distance hauls raise the efficiency of *Hs1* to **0,29**, the **0,33** of the Dr18 being unchanged. Calculations indicate a competitive efficiency for the *Hs 1* at shorter stopping intervals, albeit with substantial decreasing of average speed, rendering such intervals rather irrelevant.

6. Conclusions and recommendations

6.1 Late steam age in retrospective

Discussion of the study about characteristics and performance of late steam age locomotives had its principal focus on the period started by *André Chapelon's* pioneering development project in 1929 and extending to the most recent proposals for exploiting steam power in locomotives or automotive applications. Diesel-electric locomotive has been regarded as the principal reference and competitor.

The discussion supports conclusions listed below.

1. Locomotives rebuilt by *Chapelon* from 1929 onwards demonstratedly improved both technical and thermodynamical performance of the contemporary steam locomotives by up to 100 % in power output and efficiency.
2. Development of the diesel-electric locomotive gradually made it a serious and ultimately winning competitor of steam, despite *Chapelon's* simultaneous achievements.
3. Due to the cumbersome equipment and oil remnants in the exhaust steam, condensing the steam was exploited to alleviate fresh-water problems rather than to improve the thermodynamics of steam locomotives.
4. Draughting systems constituted a substantial problem since the very first steam locomotive, the extremities having been weak draught with poor steaming, or fierce draught with entrained unburnt fuel particles and excessive back pressure in cylinders.
5. Even the most modern articulated steam locomotives featured a low ratio of adhesive *vs.* total weight, not to mention the case of rigid-frame locomotives.
6. Regardless of its advance steps the *Stephensonian* steam locomotive retained its inherent characteristic of rejecting most of the enthalpy of exhaust steam.
7. Reciprocating components caused a variety of harmful forces.
8. Lubrication of open rod mechanisms caused spill-out of lubricants into the environment.
9. Working environment on classical steam locomotives rarely attract contemporary engine crews.
10. Keen interest in heritage trains, on the other hand, is expected to result in continuous restoration activity, with a substantial potential of benefitting from latest advances in steam technology.

6.2 The 21st century steam locomotive *vs.* the research questions

6.2.1 What would be the optimum mechanical configuration?

General-purpose diesel-electric locomotives appear to make a relevant reference when configuring an up-to-date technology steam locomotive. Characteristics appreciated by users of such locomotives have been included in configuring the author's view of the 21st century steam locomotive. Firstly, the proposal aims at avoiding the handicaps inherent of classical steam locomotives and discussed in the previous

chapters, and secondly, at exploiting to the full the proven or promising characteristics of recent steam engine projects, the resulting configuration being reproduced below.

1. All-wheel drive.
2. Bi-directional operation.
3. Compact design.
4. Flexibility in single or multiple-unit operation.
5. Watertube boiler with high steam temperature and roof-mounted burner.
6. Short and wide steam passages to minimize pressure drops and thermal losses.
7. Bio-oil combustion to reduce overall CO_2 emissions.
8. Maximum thermal insulation of boiler and power compartments.
9. Reciprocating compound engine with single-size cylinders.
10. Poppet valves to reduce pressure drops in steam inlet and outlet.
11. Exhaust steam turbine to minimize influence of incomplete expansion.
12. Regenerative brakes to electrically recover the braking energy.
13. Condensing steam cycle.
14. Maximum exploiting of cooling air flow from stagnation pressure.
15. *Franco-Crosti* concept to exploit the fluegas in preheating feedwater and combustion air.
16. Fuel and water tanks integrated in the light-weight frame construction.

Electric transmission together with up-to-date accumulator technologies enables recovery of braking energy in a way not viable before, as efficiency of both the generators and the traction motors are about to exceed 0,95 while the charging capacity of battery packs is around 0,5 MJ/kg. Opting for a monotube type steam generator enables a start-up from cold state within 10 minutes while steaming is immediate at start of the burner when the boiler is in steam. Applying light-weight construction enables adjusting the total mass of the locomotive within limits set by eventual axle weight restrictions, and to attain power-to-mass ratios matching those of diesel electric locomotives.

6.2.2 What would be the efficiency?

The predictions are limited to transitory, rather than to around-the-year drawbar thermal efficiency. Figures between 0,18 and 0,36 are predicted. The lowest figure applies to operation in light work without any recovery of braking energy. Such cases are not supposed to occur if all appliances are in normal condition. The highest figures are attainable when frequent applying of brakes is necessary, either in yard work or at downhills.
Efficiency of electric motors is regulated by EU legislation within IE classes 1 to 4, the IE4 being subject to reach the level of 0,96 by 2023 in the relevant power range, *i.e.,* 175 kW.[389] Motors of IE4 class are for sale already, according to *i.a. Siemens.*[390] ABB reports of attaining generator efficiency of 0,969 in diesel-electric locomotives in the power range of 1 to 3 MW, *i.e.,* fit for the present case.[391] The potential efficiency of the entire power chain from prime mover to the drawbar is thus expected to develop favourably in near future.

6.3 Utopy or opportunity?

Paragraph 1.1 implies that diesel-electric locomotives constitute the basis of comparative judgement as the scope of the study only deals with the motive power options of non-electrified railroads. The relative efficiency *percentages* have been calculated by comparing the simulation results in question.

6.3.1 Judgement by projected and simulated characteristics

The configuration and predicted performance of the *Hs 1* is technically viable in view of calculations analyzed in Paragraph 5.2, indicating a reasonable capacity margin of the projected constructional elements. Boiler pressures as high as twice the one opted for the *Hs1* have shown their viability in automotive applications as was discussed in Paragraph 2.7, also referring to superheat temperatures of 950 K having been tested in steam cars. The steam parameters opted for the *Hs1* thus provide potential of raising them in future developments, enhancing the view of *opportunity*. On-the-road simulations predict the *Hs1* to fall 18 % behind the *Dr18* in relation to the efficiency of the latter whereas yard work with a wide range of train weights at typical shunting operation speeds turns the scale *level* with the *Dr18*, or even 9 % in favour of the *Hs1* at its best. Simulations of regional passenger trains suggest a strong dependent of efficiency of the *Hs1* of the stopping frequency due to the impact of recovery of braking energy, this inevitably remaining small-scale due to light trains. The gentle efficiency curve of a diesel engine makes it the better performer, the harder it works. Thus, in local trains the *Hs1* is predicted to fall 12 – 27 % behind the *Dr18* in terms of relative efficiency.
The *Hs1* thus turns out to be more of an *opportunity* at regions with marshalling yards and ample resources of biomass, in vicinity of power plants using forest residue for feedstock and fuel. The carbon neutrality of bio-oil thus produced is a potential proponent for the locomotive.[392]

The *Hs1* would appear as an *utopy* where electricity is an abundant resource, while no biomass is available in the vicinity, for transport costs of fuel with a low energy density tend to eat up its benefits.

6.3.2 Review of *Hs1* in terms of SWOT analysis

An assessment in Fig. 6.1 of strengths, weaknesses, opportunities, and threats provides an aspect for weighing the question about the viability of the *Hs1* in comparison to diesel locomotives.

STRENGTHS	WEAKNESSES
GREEN ENERGY DIESEL-COMPATIBLE CHARACTERISTICS IMMEDIATE AVAILABILITY AT START REGENERATIVE BRAKING LOW NOISE LEVEL LITTLE OR NO IDLING	MULTI-TECHNICAL CONFIGURATION EFFICIENCY WITHOUT REGENERATIVE BRAKING IS BELOW DIESEL LEVEL CLEANLINESS DEMAND OF FEEDWATER
OPPORTUNITIES	**THREATS**
ADAPTABILITY TO OTHER BIOFUELS RAISING OF STEAM PARAMETERS SCALING-UP BENEFITS OF MODULARITY	EMISSIONS AND EMISSION REGULATIONS TEETHING PROBLEMS OF NOVEL CONSTRUCTIONS AVAILABILITY OF COMPETENT CREWS

Figure 6.1: SWOT analysis of *Hs1*.

STRENGTHS

Green energy:
This aspect is an asset over diesels in case the latter are using fossil fuel.

Diesel-compatible characteristics:
The transmission elements are similar with those of diesel-electric locomotives, multiple unit operation also coupled with the latter being facilitated.

Immediate availability at start:
The accumulators of the *Hs1* enable operation during the start-up of the steam generator which only takes *ca.* 10 minutes from cold state.[393]

Regenerative braking:
This aspect is an asset over diesels as far as the latter are not equipped with a similar system.

Low noise level:
The difference to a same-power diesel engine is about 20 dB.[394]

Little or no idling:
The boiler burner may be shut-off any time there is no need of steam, the re-start of steam generation being immediate within 2 h from shut-off.[395]

WEAKNESSES

Multi-technical configuration:
The locomotive is a combination of technologies involved with steam, electrics, and electronics, including some sophistication of tribology. All have been proved in practice while the last mentioned contain novel applications potentially demanding research and development.

Efficiency without regenerative braking is below diesel level:
The drawbar thermal efficiency of the locomotive as such, *i.e.,* without recovery of braking energy, is 0,21 at full power, or 64 % of the reference diesel-electric and 50 % of a modern steam power plant.

Cleanliness demand of feedwater:
High-pressure watertube boilers preferably use treated feedwater to prevent corrosion and scale.[396]

OPPORTUNITIES

Adaptability to other biofuels:
Change of oil type may require burner modifications while fluegas flows potentially require re-calculation of flue channels of heat-exchangers to ensure sufficient turbulence as shown by the actual calculations concerning the alternative combustion of LFO in the study.

Raising of steam parameters:
Both locomotive and automotive solutions have been tested at 10 MPa pressure and the latter with up to 950 K steam temperature, such parameters offering potential for a substantial increasing of efficiency. Even 7 MPa and 810 K would yield *ca.* **0,24** drawbar efficiency assuming 0,95 for boiler efficiency and 0,90 for the combined efficiency of own consumption and transmission.[397] *NB*: These figures do *not* include potential recovery of braking energy.

Scaling-up benefits of modularity:
The modular construction of the *Hs1* enables *e.g.,* doubling the drawbar power by configuring a bigger unit from existing components.

THREATS

Emissions and emission regulations:
The exact formation of emissions of PYR combustion in the application discussed is unknown as stated within the limitations of the study. Since no large-scale PYR power plants exist so far, the future regulations also constitute an unknown factor. On the other hand, purification of particulates reperesents a proven technology, and due to relatively low temperature of combustion the nitrogen compounds are not expected to cause any serious obstacles.

Teething problems of novel constructions:
Novel-type valves and tribology of the prime mover are expected to constitute the principal technical challenge of the *Hs1*. Both might be mitigated by laboratory tests prior to assembly, and by applying conventional components in the meantime.

Availability of competent crews:
Legislation concerning pressure vessels specifies requirements for the skills and know-how of crews operating and maintaining the appropriate equipment, the steam technology potentially constituting a bottleneck in training. Cooperation with heritage railways might alleviate such a potential problem.

6.4 Topics calling for further research

6.4.1 Pressure drops in valves

The proposed version of poppet valves has not been tried yet but is expected to reduce pressure drops, defining of which call for practical tests.

6.4.2 Thermal losses in cylinder walls of the prime mover of the *Hs1*

The scientific efforts of explaining the losses known as *wall effects* were started by *Nusselt* in 1916.[398] *Porta* further studied the subject and came up with his model shortly before his death in 2003, fractions of his model having been published in 2006.[399] The rest of his findings are currently in the process of *posthumous* publishing but by the time of submitting the present thesis (June 2021) more than 20 Technical Papers of *Porta* were still waiting to be published.[400] The phenomenon called *missing quantity*, *i.e.*, the combined losses of wall effect and steam leaking past the pistons, reportedly caused more than 50 % *extra* or non-productive steam consumption in saturated steam engines as also confirmed by *Ryti* who pointed out the lack of explicit theory of the losses in question. Neither of the two men lived to see Porta's theory published. *Porta* predicted a 5 % loss level to be attainable as noted in 2015 by D. Wardale in his plan supported by *Porta'*s own predictions for an advanced technology *Stephensonian* steam locomotive still featuring outside cylinders.[401] The prime mover concept of the author's *Hs1* with superb thermal insulation and an enclosed power compartment is expected to reduce the said losses to a negligible level but is proposed for a topic of both theoretical and practical research.

6.4.3 Emissions

Emissions of CO_2 and NO_x constitute a research issue generally regarded as a crucial topic in view of protection of environment.

6.4.4 Life Cycle Assessment of the *Hs1*

An LCA requires detail planning of the locomotive with component and material specifications as well as reliable data for assessing the combustion products of the fuel used.

6.4.5 Potential of supercapacitors

Supercapacitors are reported to attain a rapid, or 30-second charging time to full capacity with a recovery/re-use efficiency of $\eta_{rec} = 0{,}85$ in a rail application of public transportation.[402] The feasibility of the technology in yard work of shunting locomotives and in road service of freight train locomotives is recommended as a topic of further research.

Endnotes

[1] British Standard Class 8 Locomotive. Latest editing 2021-07-12. Wikipedia [online]. [viewed 2017-02-01].
[2] Global Power Plant Efficiency Analysis. 2016-12-05. General Electric Co. [online]. [viewed 2021-01-20].
[3] [ibid].
[4] Wardale, David: The Red Devil and other tales from the age of steam, p. 43.
[5] [ibid] p. 44.
[6] [ibid].
[7] [ibid] p. 46.
[8] [ibid] p. 496.
[9] [ibid] p. 471.
[10] Solomon, Brian: The Heritage of North American Steam Railroads, p. 170.
[11] Sarjovaara, Teemu. 2015. Studies on Heavy-Duty Engine Fuel Alternatives. Doctoral thesis.
[12] Chapelon, André: La Locomotive a Vapeur, p. 27; Porta, L.D.: Advanced Steam Locomotive Development, p. 86; Wardale, David: The Red Devil and other tales from the age of steam, p. 24.
[13] Porta, L.D.: Advanced Steam Locomotive Development, p. 51, 52.
[14] Heilmann steam-electric locomotives. 2020-11-26. Wikipedia [online]. [viewed 2021-04-11].
[15] Early diesel locomotives and railcars in Europe. 2021-10-09. Wikipedia [online]. [viewed 2021-01-20].
[16] Wardale, David: The Red Devil and other tales from the age of steam. Citation of L.D. Porta, p. 513-518.
[17] Allen, Geoffrey: Railways of the 20th Century, p. 101-104.
[18] Wardale, David: The Red Devil and other tales from the age of steam, p. 365-367.
[19] [ibid] p. 490, 491.
[20] [ibid] p. 365, 366.
[21] [ibid] p. 410.
[22] Link&Motion. 2019. Annual bulletin of Coalition for Sustainable Rail & University of Minnesota.
[23] Worldwide rail electrification remains at high volume. 2021-02-19. RAILWAY PRO [online]. Available from: https://www.railwaypro.com/wp/worldwide-rail-electrification-remains-at-high-volume/ [viewed 2021-04-11].
[24] [ibid]
[25] Global Power Plant Efficiency Analysis. 2016-12-05. General Electric Co. [online]. [viewed 2021-01-20].
[26] Wardale, David: The Red Devil and other tales from the age of steam, p. 43.
[27] Global Power Plant Efficiency Analysis. 2016-12-05. General Electric Co. [online]. [viewed 2021-01-20].
[28] Wardale, David: The Red Devil and other tales from the age of steam, p. 44, 46.
[29] Nock, O.S.: The British Steam Railway Locomotives, p. 272.
[30] Wardale: The Red Devil and other tales from the age of steam, p. 52.
[31] Chapelon, André: La Locomotive a Vapeur, p. 21.
[32] [ibid] p. 21. *Marc Seguin* of France got a patent for the concept in December 1827.
[33] [ibid] p. 21. *Trevithick* got a patent for piping the exhaust steam to the chimney of a stationary boiler in 1802.
[34] Ryti: Koneoppi Osa 1 p. 251.
[35] [ibid].
[36] Ivalo: Höyryveturit ja niiden hoito, p. 240.
[37] [ibid] p. 241, 271.
[38] Chapelon, André: La Locomotive a Vapeur, p. 66, 67.
[39] [ibid] p. 209.
[40] [ibid] p. 59.
[41] Sampson: The DUMPY Book of Railways of the World, p. 44, 46, 47.
[42] Drury, George H.: Guide to North American Steam Locomotives, p. 398.
[43] Makarov: Parovozyi Serii Э (Class Э Steam locomotives), p. 38.
[44] Nock, O.S.: The British Steam Railway Locomotives, p. 219.
[45] [ibid].
[46] Chapelon, André: La Locomotive a Vapeur, p. 334.
[47] [ibid] p. 380.
[48] [ibid].
[49] Maedel, K-E. [et al.]: Deutsche Dampflokomotiven, p. 108.
[50] [ibid] p. 148.
[51] Chapelon, André: La Locomotive a Vapeur, illustrations on p. 283, 297.

[52] [ibid] p. 343.
[53] Nock, O.S.: The British Steam Railway Locomotives, p. 218.
[54] Drury, George H.: Guide to North American Steam Locomotives, p. 194.
[55] Newton, Louis M.: Rails Remembered, Vol. 4., Tale of a Turbine, p. 709.
[56] Boyd, Stephen: The Steam Locomotive, p. 118.
[57] Wardale, David: The Red Devil and other tales from the age of steam, p. 373, 374, 375.
[58] [ibid] p. 371-375.
[59] Whitehouse, P.: Ånglok från hela världen, p. 72.
[60] Futej, Gerald M.: 100 Years Against the Mountains, p. 4.
[61] Garratt, Colin D.: Masterpieces in Steam, p. 50
[62] Chapelon, André: La Locomotive a Vapeur, p. 552
[63] [ibid]
[64] [ibid] p. 603
[65] Nock, O.S.: The British Steam Railway Locomotives, p. 262, 265
[66] Franco-Crosti boilers. 2021-08-15. Wikimedia [online]. [viewed 2021-09-21].
[67] [ibid].
[68] Rakow, W.A.: Russische und sowjetische Dampflokomotiven, p. 196.
[69] [ibid].
[70] Girdlestone, Phil: Camels and Cadillacs, p. 87.
[71] [ibid] p. 58, 59.
[72] [ibid] p. 62-66.
[73] [ibid] p. 62.
[74] [ibid] p. 87.
[75] Karlsson, Lars Olov: Ånglok vid Sveriges normalspåriga enskilda järnvägar, p. 104.
[76] Ryti, Henrik: Koneoppi, Osa 1, p. 254, 255.
[77] Ljungström's Biography at the Swedish National Museum of Science and Technology.
[78] Karlsson, Lars Olov: Ånglok vid Sveriges normalspåriga enskilda järnvägar, p. 103.
[79] [ibid] p. 98.
[80] Nock, O.S.: The British Steam Railway Locomotive 1925-1965, p. 112.
[81] Information acquired by the author in 2009 at the Railway Museum of Grängesberg, Sweden.
[82] Nock, O.S.: The British Steam Railway Locomotive 1925-1965, p. 111 – 117.
[83] [ibid].
[84] Karlsson, Lars Olov: Ånglok vid Sveriges normalspåriga enskilda järnvägar, p. 98 - 105.
[85] Maedel, K-E. [et al.]: Deutsche Dampflokomotiven, p. 261.
[86] Maedel, K-E. [et al.]: Deutsche Dampflokomotiven, p. 260.
[87] Nock, O.S.: The British Steam Railway Locomotive 1925-1965, p. 111- 117.
[88] Newton, Louis M.: Rails remembered, Vol. 4, Tale of a Turbine, graph on p. 720.
[89] Drury, George H.: Guide to North American Steam Locomotives, p. 394.
[90] [ibid].
[91] Maedel, K-E. [et al.]: Deutsche Dampflokomotiven, p. 258, 259.
[92] [ibid].
[93] Ivalo, Mikko: Höyryveturit ja niiden hoito, p. 288.
[94] Nock, O.S.: The British Steam Railway Locomotive 1925-1965, p. 108.
[95] [ibid] p. 107.
[96] [ibid] p. 109.
[97] [ibid] Fig. 158.
[98] Rakow, W.A.: Russische und Sovjetische Dampflokomotiven, p. 264.
[99] [ibid] p. 265.
[100] [ibid].
[101] [ibid] p. 263.
[102] [ibid] p. 264 – 267.
[103] [ibid].
[104] [ibid] p. 267.
[105] [ibid] p. 264 – 267.
[106] Nock, O.S.: The British Steam Railway Locomotives, p. 173, 174.
[107] [ibid] p. 265.
[108] Shepherd, Ernie: Bulleid and the Turf Burner, p. 23.
[109] [ibid] p. 20.
[110] Chapelon, André: La Locomotive a Vapeur, p. 606.
[111] Maedel, K-E. [et al.]: Deutsche Dampflokomotiven, p. 262.
[112] [ibid].
[113] [ibid] p. 263.

[114] [ibid].
[115] Maedel, K-E.: Dampflokomotiven – geliebt und unvergessen, p. 84.
[116] [ibid].
[117] Heilmann steam-electric locomotives. Latest editing 2020-11-26. Wikipedia [online]. [viewed 2021-04-11].
[118] [ibid].
[119] [ibid].
[120] [ibid].
[121] [ibid].
[122] The author enquired the issue in 2015 of a high-rank former official of GE, and of R&D staff of the B&W.
[123] Klein, Maury: Union Pacific, p. 374.
[124] Huddleston, Eugene L.: The Genesis, Design and Performance of C&O Steam Turbine-Electric Class M-1. National Railway Bulletin, Vol. 68, 5/2003.
[125] Klein, Maury: Union Pacific, p. 374.
[126] GE Steam Turbine Locomotives. Latest editing 2021-09-04. Wikipedia [online]. [viewed 2019-01-20].
[127] [ibid]
[128] Huddleston, Eugene L.: The Genesis, Design and Performance of C&O Steam Turbine-Electric Class M-1. National Railway Bulletin, Vol. 68, 5/2003.
[129] GE Steam Turbine Locomotives. Latest editing 2021-09-04. Wikipedia [online]. [viewed 2019-01-20].
[130] Newton, Louis M.: Rails remembered, Vol.4, Tale of a Turbine, p. 907.
[131] [ibid] p. 732.
[132] [ibid] p. 713.
[133] [ibid] p. 721.
[134] [ibid] p. 717.
[135] [ibid] p. 787.
[136] [ibid] the database compiled by the author, based on Newton's notes.
[137] [ibid] p. 723-727.
[138] [ibid] p. 757.
[139] [ibid] p. 885-888.
[140] [ibid] p. 791.
[141] [ibid] p. 900.
[142] Adam Harris in the Addenda to English edition of Chapelon: La Locomotive a Vapeur, p. 624, 625.
[143] Wardale, David: The Red Devil and other tales from the Age of Steam, p. 376, 377.
[144] [ibid] p. 79, 80, 82.
[145] The National Steam Propulsion Company proposition. Updated 2019-01-25. Ultimate Steam page [online]. Available from: www.trainweb.org [viewed 2017-12-19].
[146] [ibid].
[147] Chapelon, André: La Locomotive a Vapeur, cover paper.
[148] Haigh, Alan J.: The Design, Construction and Working of Locomotive Boilers, p. 87, 88.
[149] Ryti, Henrik: Koneoppi, Osa 1. p. 273.
[150] Haigh, Alan J.: The Design, Construction and Working of Locomotive Boilers, p. 87, 88.
[151] [ibid] p. 273, 274.
[152] VDI-Bericht 1565, Zero Emission Engine, Berlin 2001.
[153] Information letter from the Coalition for Sustainable Rail to their donors, Aug. the 21st 2019.
[154] Chapelon, André: La Locomotive a Vapeur, p. 478.
[155] Carnot, Sadi: Reflections on the Motive Power of Fire etc 1824. English translation 1960.
[156] Jotuni, Pertti [et al.]. Tekniikan käsikirja 2, p. 610.
[157] Chapelon, André: La Locomotive a Vapeur, p. 27.
[158] Ryti, Henrik: Koneoppi, Osa 1, p. 256.
[159] Porta, L.D.: Advanced Steam Locomotive Development, p. 77.
[160] Chapelon, André: La Locomotive a Vapeur, p. 72, 74.
[161] Jotuni, Pertti [et al.] Tekniikan käsikirja 2, p. 628.
[162] Ryti, Henrik: Koneoppi, Osa 1, p. 254, 255.
[163] Chapelon: La Locomotive a Vapeur, p. 605.
[164] Wardale, David: The Red Devil and other tales from the age of steam, p. 277.
[165] [ibid] p. 81.
[166] Chapelon, André: La Locomotive a Vapeur, p. 581.
[167] Ryti, Henrik: Koneoppi, Osa 1, p. 256.
[168] Wardale, David: The Red Devil and other tales from the age of steam, p. 44.
[169] Prozorov, N.K. [et al.]: Parovozy - Ustroystvo, rabota i remont (Steam locomotives – Construction, function, and maintenance), p. 8.
[170] The author's own observations on domestic and several foreign railways.
[171] Porta, L.D.: Advanced Steam Locomotive Development, p. 54-56.

[172] Ivalo, Mikko: Höyryveturit ja niiden hoito, p. 163, 164, 165.
[173] Chapelon, André: La Locomotive a Vapeur, p. 606.
[174] Porta, L.D.: Advanced Steam Locomotive Development, p. 93.
[175] Ivalo, Mikko: Höyryveturit ja niiden hoito, p. 87.
[176] Ryti, Henrik: Koneoppi, Osa 1, p. 267.
[177] Porta, L.D.: Advanced Steam Locomotive Development, p. 88.
[178] [ibid] p. 93.
[179] [ibid] p. 86, 92.
[180] Girdlestone, Phil: Camels and Cadillacs, p. 51.
[181] Wardale, David: The Red Devil and other tales from the age of steam, p. 496, 497.
[182] Chapelon, André: La Locomotive a Vapeur, p. 34-36.
[183] Carpenter, George W. Editor of the English version of Chapelon, André: La Locomotive a Vapeur.
[184] Wardale, David: The Red Devil and other tales from the age of steam, p. 279.
[185] Maedel, K-E. [et al.]: Deutsche Dampflokomotiven, p. 18.
[186] Ivalo, Mikko: Höyryveturit ja niiden hoito, p. 87.
[187] Chapelon, André: La Locomotive a Vapeur, p. 116.
[188] Ivalo, Mikko: Höyryveturit ja niiden hoito, p. 287.
[189] Chapelon, André: La Locomotive a Vapeur, p. 53, 54.
[190] [ibid] p. 56.
[191] Porta, L.D.: Advanced Steam Locomotive Development, p. 86.
[192] Ivalo, Mikko: Höyryveturit ja niiden hoito, p. 156.
[193] Wardale, David: The Red Devil and other tales from the age of steam, p. 82.
[194] [ibid].
[195] Porta, L.D.: Advanced Steam Locomotive Development, p. 37.
[196] Wardale, David: The Red Devil and other tales from the age of steam, p. 80.
[197] Prozorov, N.K. [et al.]: Parovozy - Ustroystvo, rabota i remont (Steam locomotives – Construction, function, and maintenance), p. 17.
[198] [ibid] p. 88, adaptation by the author.
[199] van Zeller, Peter: Addition to Chapelon, André: La Locomotive a Vapeur, p. 627.
[200] [ibid].
[201] [ibid].
[202] [ibid].
[203] [ibid].
[204] Wardale, David: The Red Devil and other tales from the age of steam, p. 88, adaptation by the author.
[205] van Zeller, Peter: Addition to Chapelon, André: La Locomotive a Vapeur, p. 627.
[206] [ibid].
[207] Jotuni, Pertti [et al.]: Tekniikan käsikirja 2, p. 551, adaptation by the author based on graph of Kurki-Suonio.
[208] [ibid] p. 550.
[209] Porta, L.D.: Advanced Steam Locomotive Development, p. 5.
[210] Maedel, K-E. [et al.]: Deutsche Dampflokomotiven, p. 275.
[211] Wardale, David: The Red Devil and other tales from the age of steam, p. 337, 338.
[212] [ibid], modification by the author.
[213] Haig, Alan J.: The Design, Construction and Working of Locomotive Boilers, p. 102.
[214] [ibid].
[215] Nock, O.S.: The British Steam Railway Locomotives, p. 190.
[216] Haig, Alan J.: The Design, Construction and Working of Locomotive Boilers, p. 102.
[217] Ivalo, Mikko: Höyryveturit ja niiden hoito, p. 156.
[218] Chapelon, André: La Locomotive a Vapeur, p. 54
[219] [ibid] p. 55.
[220] Porta, L.D.: Advanced Steam Locomotive Development, p. 9.
[221] [ibid] p. 87.
[222] Ivalo, Mikko: Höyryveturit ja niiden hoito, p. 396 - 398.
[223] Wardale, David: The Red Devil and other tales from the age of steam, p. 176.
[224] Porta, L.D.: Advanced Steam Locomotive Development, p. 20, 97.
[225] Chapelon, André: La Locomotive a Vapeur, p. 21.
[226] Porta, L.D.: Advanced Steam Locomotive Development, p. 88.
[227] Koopmans, Jan J.G: The fire burns much better…200 years of steam locomotive exhaust research, p. 25.
[228] [ibid] p. 102.
[229] Chapelon, André: La Locomotive a Vapeur, p. 125; adaptation modified by the author.
[230] [ibid] p. 128.
[231] [ibid].
[232] [ibid] p. 129.

[233] [ibid] p. 129; adaptation by the author of Chapelon's graph.
[234] [ibid] p. 128; adaptation by the author from data attached to Chapelon's graph..
[235] Porta, L.D.: Advanced Seam Locomotive Development, p. 8.
[236] Chapelon, André: La Locomotive a Vapeur, p. 137-140.
[237] [ibid] p. 180.
[238] [ibid] p. 172.
[239] [ibid].
[240] [ibid] p. 134.
[241] [ibid] p. 80.
[242] Nock, O.S.: The British Steam Railway Locomotives, p. 222, 223, 228.
[243] Wardale, David: The Red Devil and other tales from the age of steam, p. 492.
[244] Rakow, W.A.: Russische und Sovjetische Dampflokomotiven, p. 229.
[245] Wardale, David: The Red Devil and other tales from the age of steam, p. 492.
[246] Carpenter, George: Addenda to Chapelon, André: La Locomotive a Vapeur, p. 554.
[247] Wardale, David: The Red Devil and other tales from the age of steam, p. 492.
[248] Girdlestone, Phil: Camels and Cadillacs, p. 107-110.
[249] [ibid] p. 107.
[250] Wardale, David: The Red Devil and other tales from the age of steam, p. 144.
[251] [ibid] p. 151.
[252] [ibid] p. 273.
[253] General Electric AC6000CW. 2021. American-Rails.com [online]. Available from: https://www.american-rails.com/ge.html [viewed 2021-04-11].
[254] Coalition of Sustainable Rail, Link&Motion Bulletin 2014.
[255] [ibid].
[256] [ibid].
[257] [ibid].
[258] Porta, L.D.: Advanced Steam Locomotive Development, p. 17.
[259] Wardale, David: The Red Devil and other tales from the age of steam, p. 23.
[260] [ibid].
[261] [ibid].
[262] [ibid].
[263] Coalition of Sustainable Rail, Link&Motion Bulletin 2014.
[264] Porta, L.D.: Advanced Seam Locomotive Development, p. 20.
[265] Wardale, David: The Red Devil and other tales from the age of steam, p. 22.
[266] [ibid].
[267] [ibid].
[268] Wardale, David: The Red Devil and other tales from the age of steam, p. 273.
[269] Porta, L.D.: Advanced Seam Locomotive Development, p. 9.
[270] Chapelon, André: La Locomotive a Vapeur, p. 450.
[271] Porta, L.D.: Advanced Seam Locomotive Development, p. 87.
[272] [ibid] p. 27.
[273] Porta, L.D.: Advanced Steam Locomotive Development, p. 65.
[274] Wardale, David: The Red Devil and other tales from the Age of Steam, p. 506.
[275] [ibid] p. 62.
[276] Porta, L.D.: Advanced Steam Locomotive Development, p. 92.
[277] Phillipson: Steam Locomotive Design; Data and Formulae, p. 361.
[278] HybridShunter 400 reacts to the current trends in the design of shunting locomotives. 2021. CZ LOKO a.s. [online]. [viewed 2021-04-06].
[279] Wardale, David: The Red Devil and other tales from the Age of Steam, p. 52, supplemented by the author.
[280] Tikkanen, P. [et al.]: Rautatieliikenteen käyttövoimat tavaraliikenteessä.
[281] Radovan Sláčal: The Power Balance of Locomotive Dr18. CZ LOCO a.s. Report 8082-110-00.
[282] Ryti, Henrik: Koneoppi, Osa 1, p. 254, 255.
[283] [ibid].
[284] VDI Bericht 1565; Zero Emission Engine, Berlin 2001.
[285] Ryti, Henrik: Koneoppi, Osa 1, p. 264.
[286] Ivalo, Mikko: Höyryveturit ja niiden hoito, p. 228.
[287] Ryti, Henrik: Koneoppi, Osa 1, p. 254.
[288] Chapelon, André: La Locomotive a Vapeur, p. 64
[289] Nock, O.S.: The British Steam Railway Locomotive 1925-1965, p. 106-109.
[290] [ibid] p. 501.
[291] Synchronous generators for diesel-electric locomotives. 2018. ABB Product note [online]. [viewed 2019-01-20].

[292] Hämäläinen, Mika. 2020. Oikosulkumoottori on ahtaalla. Metallitekniikka, Vol. 11. Helsinki (Finland): Alma Talent.
[293] Radovan Sláčal. 2017. The Power Balance of Locomotive Dr18. CZ LOCO a.s. Report 8082-110-00.
[294] Ryti, Henrik: Koneoppi, Osa 1, p. 255.
[295] Wardale, David: The Red Devil and other tales of the Age of Steam, p. 272; modification of formula by the author.
[296] Calculated by the author from enthalpy drops resulting from assumed values of $\eta_{s\ comp}$ and $\eta_{s\ TB}$.
[297] Chapelon, André: La Locomotive a Vapeur, p. 70.
[298] Ryti, Henrik: Koneoppi, Osa 1, p. 261.
[299] Chapelon, André: La Locomotive a Vapeur, p. 70.
[300] Caprotti Valve Gear. 2021-04-11. Available from: https://en.wikipedia.org/wiki/Caprotti_valve_gear/ [viewed 2019-01-20].
[301] Nock, O.S.: The British Steam Railway Locomotive 1925-1965, p. 229, 230.
[302] [ibid].
[303] Sarkar, S., J. Gharte: Diesel Engine Out Exhaust Temperature Modeling, p. 21.
[304] Camcon develops valvetrains that reduce emissions and improve performance of passenger cars. March 2019. Camcon Auto Ltd [online]. Available from: https://camcon-automotive.com [viewed 2020-01-20] and Koenigsegg Gemera Geneva unveiling. 2020-03-03. Freevalve AB [online]. Available from: https://www.freevalve.com [viewed 2020-04-11].
[305] Ryti, Henrik: Koneoppi, Osa 1, p. 264.
[306] Porta, L.D.: Advanced Steam Locomotive Development, p. 87.
[307] What is the Energy Density of a Lithium-Ion battery? Fluxpower.com [viewed 2021-09-24].
[308] [ibid].
[309] Hämäläinen, Mika. 2020. Oikosulkumoottori on ahtaalla. Metallitekniikka Vol. 11. Helsinki (Finland): Alma Talent.
[310] Radovan Sláčal. 2017. The Power Balance of Locomotive Dr18. CZ LOCO a.s. Report 8082-110-00.
[311] Mayrink, S. Jr. [et al.]. 2020. Regenerative Braking for Energy Recovering in Diesel-Electric Freight Trains.
[312] Super Capacitor Technology Leading the Charge for Public transport. 2019. Global Opportunity Explorer [online]. [viewed 2021-09-21].
[313] Maailman tehokkain kuorma-auto Sisu Polar Hybrid. Ammattilehti.fi [online]. [viewed 2021-10-10].
[314] Ryti: Koneoppi, Osa 1, p. 256 gives $\eta_s = 0{,}88$. Several test engines in Chapter 3 attained $\eta_s \geq 0{,}90$.
[315] [ibid] p. 256.
[316] [ibid] p. 254.
[317] GE Steam Turbine Locomotives. Latest editing 2021-09-04. Wikipedia [online]. [viewed 2019-01-20].
[318] [ibid].
[319] Newton, Louis M.: Rails remembered Vol.4, Tale of a Turbine, p. 723-727.
[320] [ibid].
[321] Haig, Alan: Locomotive Boilers for the 21st Century, p. 33.
[322] Näretie, V. [et al.]: Höyrytekniikka, Kattilat ja koneet, p. 66, 67.
[323] Raiko, Risto [et al.]: Poltto ja palaminen, p. 446.
[324] Haig: Locomotive Boilers for the 21st Century, p. 33.
[325] Dixon, Thomas W. Jr. [et al.]: LIMA Super Power Steam Locomotives, p. 106.
[326] Tests carried out at Fortum/Metso pilot plant in 2013, as reported by Matti Kytö, Valmet.
[327] Saab steam car and Ranotor. Latest editing 2021-10-04. Wikipedia [online]. [viewed 2019-09-19].
[328] VDI Bericht 1565, Zero Emission Engine, Berlin, 2001.
[329] Jotuni, Pertti [et al.]: Tekniikan käsikirja 2, p. 630.
[330] Enginion steam cell. Latest editing 2021-10-04. Wikipedia [online]. Available from: https://en.wikipedia.org/wiki/Steam_car [viewed 2021-04-11].
[331] Wärtsilä 20 Product Guide 2019: Section 3.3.1.
[332] Lampinen, Markku: Lämmönsiirtimien mitoitus, p. 19. Adaptation of the author.
[333] Lampinen, Markku: Lämmönsiirtimien mitoitus, p. 55.
[334] Raiko, Risto [et al.]: Poltto ja palaminen, p. 446.
[335] Lehto, Jani [et al.]: Fuel oil quality and combustion of fast pyrolysis bio-oils. VTT Publication 87, p. 53.
[336] The start-up tests of a 50 000 t/a capacity plant of Fortum Power in Joensuu, Finland, were completed in 2016.
[337] Lehto, Jani [et al.]: Fuel oil quality and combustion of fast pyrolysis bio-oils. VTT Julkaisu 87, p. 3, 4.
[338] [ibid] p. 54-56.
[339] Alakangas, Eija [et al.]: Suomessa käytettävien polttoaineiden ominaisuuksia. VTT Julkaisu 258, p. 184.
[340] Onarheim, Kristin [et al.]: Technoeconomic Assessment of a Fast Pyrolysis Bio-oil Production. Energy & Fuels, Aug. 2015. Adaptation of the author.
[341] Eonsuu, Tapio [et al.]: Suomen veturit, osa 2: Moottorikalusto, p. 39.
[342] Jotuni, Pertti [et al.]: Tekniikan käsikirja 2, p. 628.

[343] [ibid].
[344] [ibid] p. 629.
[345] Kotiaho, Voitto [et al.]: Termodynamiikan ja lämmönsiirto-opin taulukoita, p. 28, 30, 31.
[346] Ryti, Henrik: Koneoppi, Osa 1, p. 258.
[347] [ibid] p. 109; adaptation by the author.
[348] Wardale, David: The Red Devil and other tales of the Age of Steam, p. 272. Formula modified by the author.
[349] Jotuni, Pertti [et al.]: Tekniikan käsikirja 2, p. 629. Adaptation by the author.
[350] Porta, L.D.: Selection of Papers, Vol. 3, p. 83.
[351] Lehto, Jani [et al.]: Fuel oil quality and combustion of fast pyrolysis bio-oils. VTT Publication 87, p. 53.
[352] Kotiaho, Voitto [et al.]: Termodynamiikan ja lämmönsiirto-opin taulukoita, p. 55.
[353] [ibid].
[354] [ibid].
[355] [ibid].
[356] [ibid].
[357] [ibid].
[358] Lampinen, Markku [et al.]: Lämmönsiirtimien mitoitus, p. 62.
[359] [ibid].
[360] [ibid] p. 54.
[361] [ibid] p. 55.
[362] Kotiaho, Voitto [et al.]: Termodynamiikan ja lämmönsiirto-opin taulukoita, p. 2.
[363] Lampinen [et al.]: Lämmönsiirtimien mitoitus, p. 55.
[364] [ibid] p. 54.
[365] Kotiaho, Voitto [et al.]: Termodynamiikan ja lämmönsiirto-opin taulukoita, p. 2.
[366] Lampinen, Markku [et al.].: Lämmönsiirtimien mitoitus, p. 55.
[367] [ibid].
[368] [ibid] p. 145.
[369] [ibid].
[370] Ryti, Henrik: Koneoppi, Osa 1, p. 255.
[371] Wakabayashi, Daimo & Mark McGouldrick: Innovative High Efficiency Oil Burner Proves to Solve Many Environmental Challenges in Well Test Applications. 2020-01-13. OnePetro [online]. Available from: https://doi.org/10.2523/IPTC-19734-MS [viewed 2020-04-11].
[372] Rakow, W.A.: Russische und sowjetische Dampflokomotiven, p. 231.
[373] Ryti, Henrik: Koneoppi, Osa 1, p. 256.
[374] Chapelon, André: La Locomotive a Vapeur, p. 606.
[375] Ryti, Henrik: Koneoppi, Osa 1, p. 255.
[376] Wakabayashi, Daimo & Mark McGouldrick: Innovative High Efficiency Oil Burner Proves to Solve Many Environmental Challenges in Well Test Applications. 2020-01-13. OnePetro [online]. Available from: https://doi.org/10.2523/IPTC-19734-MS [viewed 2020-04-11].
[377] Wardale, David: The Red Devil and other tales from the Age of Steam, p. 501.
[378] Traction motors. 2020. ABB Product Guide [online]. [viewed 2020-01-20].
[379] [ibid].
[380] Rossiyskie Zheleshnyie Dorogi, Chastj 1: Tehnicheskie opisanie lokomotivy TƏM18B (Russian Railways, Part 1. Technical data of locomotive TƏM18B) p. 6.
[381] Tikkanen, P. [et al.]: 2018. Rautatieliikenteen käyttövoimat tavaraliikenteessä.
[382] Radovan Sláčal. 2017. The Power Balance of Locomotive Dr18. CZ LOCO a.s. Report 8082-110-00.
[383] Liikenneviraston ohjeita 22/2012, RATO 4: Vaihteet, p. 4.
[384] Readings taken from traction records of Sr2 locomotives by the author.
[385][385] Rossiyskie Zheleshnyie Dorogi, Chastj 1: Tehnicheskie opisanie lokomotivy TƏM18B (Russian Railways, Part 1. Technical data of locomotive TƏM18B) p. 9.
[386] Lehto, Jani [et al.]: Fuel oil quality and combustion of fast pyrolysis bio-oils. VTT Publication 87, p. 53.
[387] [ibid] p. 54.
[388] Porta, L.D.: Advanced Steam Locomotive Development, p. 55, 61.
[389] Hämäläinen, Mika: Oikosulkumoottori on ahtaalla. Metallitekniikka Vol. 11 2020.
[390] [ibid].
[391] Synchronous generators for diesel-electric locomotives. 2018. ABB Product note [online]. [viewed 2019-01-20].
[392] Partanen [et al.].: Suomi öljyn jälkeen, p. 199, 200.
[393] Näretie [et al.]: Höyrytekniikka, Kattilat ja koneet, p. 66, 67.
[394] Ryti, Henrik: Koneoppi, Osa 1, p. 270.
[395] [ibid] p. 273.
[396] [ibid] p. 271.
[397] [ibid] p. 272.

[398] Porta, L.D.: Advanced Steam Locomotive Development, p. 55, 56.
[399] Ryti, Henrik: Koneoppi, Osa 1, p. 265, 266, 267.
[400] Porta, L.D.: Selection of Papers. Introduction.
[401] Wardale, David: The 5 AT Fundamental Design Calculations, p. 46.
[402] Super Capacitor Technology Leading the Charge for Public transport. March 2019. Global Opportunity Explorer [online]. [viewed 2021-09-21].

References

A. Printed publications

Alakangas, Eija & Markus Hurskainen & Jaana Laatikainen-Luntama & Jaana Korhonen. 2016. Suomessa käytettävien polttoaineiden ominaisuuksia. (Properties of fuels used in Finland). Publication 258. Espoo (Finland): Teknologian tutkimuskeskus VTT Oy. 259 pages. ISBN 978-951-38-8418-5.

Allen, Geoffrey Freeman. 1983. Railways of the Twentieth Century. London (Great Britain): Sidgwick and Jackson Ltd. 256 pages. ISBN 0 283 98769 3.

Borman, Gary L. & Kenneth W. Ragland. 1998. Combustion Engineering. Singapore: WCB McGraw-Hill. 613 pages. ISBN 0-07-115978-9.

Boyd, Jim. 2002. The Steam Locomotive. New York (USA): Metro Books. (Printed in China). 144 pages. ISBN 1-5866-3613-8.

Buschmann, G. & H. Clemens & M. Hoetger & B. Mayr. 2001. Der Dampfmotor – Entwicklungsstand und Marktchansen. Motortechnische Zeitschrift 62. Frankfurt am Main (Germany): Springer Verlag.

Chapelon, André. 2000. La Locomotive a Vapeur. English edition. Barrow Farm (Great Britain): Camden Miniature Steam Services. 631 pages. ISBN 0-9536523-0-0.

Dixon Thomas W. Jr. & Kevin Kohls. 2010. LIMA Super Power Steam Locomotives. Forest (VA, USA): TLC Publishing Inc. 143 pages. ISBN 9780939487967.

Drury, George H. 2002. Guide to North American Steam Locomotives. 4th printing. Waukesha (WIS, USA): Kalmach Publishing Co. 448 pages. ISBN 0-89024-206-2.

Eonsuu, Tapio & Pekka Honkanen & Eljas Pölhö. 1995. Suomen veturit 2. Moottorikalusto. (Locomotives of Finland 2. Motorized equipment). Helsinki (Finland): Elokuvan Maailma ay. 128 pages. ISBN 952.5060-02-0.

Futej, Gerald. 2005. 100 Years Against the Mountains.West Chester (PA, USA): Greenhill Station Productions. 72 pages. ISBN 0-9768044-0-9.

Garratt, Colin D. 1973. Masterpieces in Steam. London (Great Britain): Blandford Press Ltd. 204 pages. ISBN 0 7137 0637 6.

Girdlestone, Phil. 2014. Camels and Cadillacs. Malmö (Sweden): Frank Stenvalls Förlag. 159 pages. ISBN 978-91-7266-185-1.

Haigh, Alan J. 2003. Locomotive Boilers for the Twenty-first Century. Caernarvon (Great Britain): XPRESS Publishing Co. 64 pages. IBSN 978-1-901056-47-1.

Haigh, Alan J. 2010. The design, construction and working of locomotive boilers. 3rd edition. Caernarvon (Great Britain): XPRESS Publishing Co. 112 pages. ISBN 978-1-901056-39-6.

Hovi, Ilkka. 2007. The KYL of 'KYLCHAP' Front End for Steam Locomotives. CHIME Vol. 145. London (Great Britain): Sir Nigel Gresley Locomotive Preservation Trust Ltd.

Huddleston, Eugene. 2003. The Genesis, Design and Performance of C&O Steam Turbine-Electric Class M-1. National Railway Bulletin Vol. 68/5. Philadelphia (USA): The National Railway Historical Society. ISSN 0885-5099.

Hämäläinen, Mika. 2020. Oikosulkumoottori on ahtaalla (Induction motor facing hard times). Metallitekniikka, Vol. 11. Helsinki (Finland): Alma Talent.

Ivalo, Mikko. 1953. Höyryveturit ja niiden hoito (Steam locomotives). 3rd printing. 596 pages. Porvoo (Finland): Werner Söderström OY.

Jotuni, Pertti & Henrik Ryti & Otto Pöyhönen. 1969. Tekniikan käsikirja 2 (Technical handbook). 8th printing. Jyväskylä (Finland): K.J. Gummerus. 779 pages.

Karlsson, Lars Olov. 2013. Ånglok vid Sveriges normalspåriga enskilda järnvägar, Del 2. Malmö (Sweden): Frank Stenvalls Förlag. 278 pages. ISBN 978-91-7266-187-5.

Klein, Maury. 2006. Union Pacific, Vol. II. Minnesota (USA): University of Minnesota Press. 654 pages. ISBN 100-8166-4460-8.

Koopmans, Jan. 2014. The fire burns much better. 3rd edition. Barrow Farm (Great Britain): Camden Miniature Steam Services. 490 pages. ISBN-13: 978-1-909358-05-8.

Kotiaho, W. & M. Lampinen & A. Seppälä. 2004. Termodynamiikan ja lämmönsiirto-opin taulukoita (Tables of thermodynamics). Espoo (Finland): Teknillinen korkeakoulu, Raportti 136. 61 pages. ISBN 951-22-7259-8.

Lampinen, Markku J. 2005. Lämmönsiirtimien mitoitus (Dimensions of heat exchangers). Espoo (Finland): Helsinki University of Technology. Julkaisu 145. 480 pages. ISBN 951-22-7557-0.

Lehto, J., Anja Oasmaa, Yrjö Solantausta, Matti Kytö, D. Chiaramonti. 2013. Fuel oil quality and combustion of fast pyrolysis bio-oils. Espoo (Finland): Teknologian tutkimuskeskus VTT. Julkaisu 87. 79 pages. ISBN 978-951-38-7929-7.

Link&Motion. 2014, 2019. Annual bulletin of Coalition for Sustainable Rail & University of Minnesota for members of CSR.

Maedel, K-E. 2011. Dapflokomotiven–geliebt und unvergessen. Königswinter (Germany): HEEL Verlag. 112 pages. ISBN 978-3-86852-534-2.

Maedel, K-E. & A.B. Gottwaldt. 1994. Deutsche Dampflokomotiven. Berlin (Germany): Transpress. 318 pages. ISBN 3-344-70912-7.

Makarov, Leonid Lvovich. 2004. Parovozy Serii Э (Class Э Steam locomotives). Moscow (Russia): OAO Rossiyskie Zheleznyie Dorogi (Russian Railways Co.). 287 pages. ISBN 5-93574-021-4.

Newton, Louis M. 1999. Rails remembered, Vol. 3. Roanoke (VA, USA): Progress Press. 114 pages. Library of Congress Card Number 92-93856.

Newton, Louis M. 2002. Rails remembered, Vol. 4, Tale of a Turbine. Roanoke (VA, USA): Progress Press. 211 pages. Library of Congress Card Number 92-92856.

Nock, O.S. 1966. The British Steam Railway Locomotive 1925-1965. London (Great Britain): Ian Allan Ltd. 276 pages. ISBN 0 7110 0125 1.

Näretie, Veikko & Esko Arpalahti. 1972. Höyrytekniikka: Kattilat ja koneet (Steam engineering. Boilers and engines). Helsinki (Finland): Otava. ISBN 951-1-00009-8.

Onarheim, Kristin & J. Lehto, & Y. Solantausta. 2015. Technoeconomic Assessment of a Fast Pyrolysis Bio-oil Production Process Integrated to a Fluidized Bed Boiler. Energy&Fuels Aug. 2015. Washington DC (USA): ACS Publications.

Onarheim, Kristin & Y. Solantausta & J. Lehto. 2015. Process Simulation Development of Fast Pyrolysis of Wood Using Aspen Plus. Energy&Fuels Aug. 2015. Washington DC (USA): ACS Publications.

Partanen, R. & H. Paloheimo & H. Waris. 2016. Suomi öljyn jälkeen (Finland after oil). Helsinki (Finland): Into Kustannus Oy. ISBN 978-952-264-561-6.

Phillipson, E.A. 2004. Steam Locomotive Design, Data and Formulae. 2nd printing. Barrow Farm (Great Britain): Camden Miniature Steam Services. 444 pages. ISBN 0-9536523-9-4.

Pischinger, R. & G. Krassnig & G. Taučar & Th. Sams. 1989. Thermodynamik der Verbrennungskraftmaschine. Wien (Austria)/New York (USA): Springer Verlag. ISBN 3-211-82105-8.

Porta, L.D. 2006. Advanced Steam Locomotive Development. Barrow Farm (Great Britain): Camden Miniature Steam Services. 99 pages. ISBN 978-09547131-5-7.

Porta, L.D. 2021. Selection of Papers. Vol. 3. Edinburg (Great Britain): Advanced Steam Traction Trust. 281 pages. ISBN 978-1-63752-204-2.

Prozorov, N. & M. Vigdorchik & E. Grebenkin. 1986. Parovozy – ustroystvo, rabota i remont. (Steam locomotives – construction, function, and maintenance). Moscow (USSR): Transport. 368 pages. UDK 629.422+621.133 (075.32).

Raiko, R. & J. Saastamoinen & M. Hupa & I. Kurki-Suonio. 2002. Poltto ja palaminen (Combustion and burning). 2nd printing. Jyväskylä (Finland): Gummerus Kirjapaino Oy. 750 pages. ISBN 951-666-604-3.

Rakow, W.A. 1988. Russische und Sovjetische Dampflokomotiven. 327 p. Berlin (Germany): Transpress. ISBN 3-344-00413-1.

Rossiyskie Zheleshnyie Dorogi, Chastj 1. 2014. Tehnicheskie opisanie lokomotivy TЭM18B (Russian Railways, Part 1. Technical data of locomotive TЭM18B).

Ryti, Henrik. 1983. Koneoppi, Osa 1. Staattiset koneet (Text book of engines. Part 1. Static engines). 3. painos. Espoo (Finland): Otakustantamo. 410 pages. ISBN 951-671-141-3.

Sampson, Henry. 1955. The DUMPY Book of Railways of the World. London (Great Britain): Purnell & Sons. 285 pages.

Sarjovaara, Teemu. 2015. Studies on Heavy-Duty Engine Fuel Alternatives. Doctoral thesis. Helsinki (Finland): Aalto University. 117 pages. ISBN 978-952-60-6560-1.

Sarkar, Sudip & Jayesh Gharte. 2017. Diesel Engine Out Exhaust Temperature Modelling. Gothenburg (Sweden): Chalmers University of Technology. 61 pages. ISSN 1652-8557.

Shepherd, E. 2004. Bulleid and the Turf Burner. Southampton (Great Britain): KRB Publications. 99 p. ISBN 095403585.

Sláčal, Radovan. 2017. The Power balance of locomotive Dr18. Česka Třebová (Czech Republik): CZ LOKO a.s. Report 8082-110-00. 3 pages.

Solomon, Brian. 2001. The Heritage of North American Steam Railroads. Pleasantville (NY, USA): The Reader's Digest Association (Printed in Italy). 256 p. ISBN 0-7621-0327-2.

Tikkanen, P. & Saara Haapala. 2018. Rautatieliikenteen käyttövoimat tavaraliikenteessä (Motive power in railway freight transport). Helsinki (Finland): Liikennevirasto. Tutkimuksia ja selvityksiä 16/2018. 24 pages.

VDI. 2001. Zero Emission Engine. Berlin (Germany): Verein Deutscher Ingenieuren. VDI Bericht 1565.

Wardale, David: 2013. The Red Devil and other tales from the age of steam. 2nd printing. Barrow Farm (Great Britain): Camden Miniature Steam Services. 522 p. ISBN 978-1-909358-01-0.

Wardale, David. 2015. The 5AT Fundamental Design Calculations. Edinburg (Great Britain): The Advanced Steam Traction Trust. 556 p. ISBN 978-1-942748-13-7.

Whitehouse, P.B. 1978. Ånglok från hela världen. Stockholm (Sweden): Interpublishing AB. 96 pages. ISBN 91-85500-08-9.

B. Electronic data sources

British Standard Class 8 Locomotive. Latest editing 2021-07-12. Wikipedia [online]. Available from: https://en.wikipedia.org/wiki/BR_Standard_Class_8/ [viewed 2017-02-01].

Camcon develops valvetrains that reduce emissions and improve performance of passenger cars. March 2019. Camcon Auto Ltd (Great Britain) [online]. Available from: https://camcon-automotive.com [viewed 2020-01-20]

Caprotti Valve Gear. Latest editing 2021-04-11. Wikipedia [online]. Available from: https://en.wikipedia.org/wiki/Caprotti_valve_gear/ [viewed 2019-01-20].

GE AC6000CW Diesel-electric locomotive. 2021. American-Rails.com (USA) [online]. Available from: https://www.american-rails.com/ge.html [viewed 2021-04-11].

GE Steam Turbine Locomotives. Latest editing 2021-09-04. Wikipedia [online]. Available from: https://en.wikipedia.org/wiki/GE_steam_turbine_locomotives. [viewed 2019-01-20].

Global Power Plant Efficiency Analysis. 2016-12-05. General Electric Co [online]. Available from: https://allafrica.com/download/main/main/idatcs/00101343:4d0ed2cd3673606823f3a0c7a6e48dff.pdf [viewed 2021-01-20].

Early diesel locomotives and railcars in Europe. Latest editing 2021-10-09. Wikipedia [online]. Available from: https://en.wikipedia.org/wiki/Diesel_locomotive [viewed 2021-01-20].

Enginion steam cell. Latest editing 2021-10-04. Wikipedia [online]. Available from: https://en.wikipedia.org/wiki/Steam_car [viewed 2021-04-11].

Franco-Crosti boilers. Latest editing 2021-08-15. Wikimedia [online]. Available from: https://commons.wikimedia.org/wiki/Category:Franco-Crosti_boilers [viewed 2021-09-21].

Heilmann steam-electric locomotives. Latest editing 2020-11-26. Wikipedia [online]. Available from: https://second.wiki/wiki/jean-jacques_heilmann [viewed 2021-04-11].

HybridShunter 400 reacts to the current trends in the design of shunting locomotives. 2021. CZ LOKO a.s. [online]. Available from: https/czloko.com/products/lokomotivy-1/hybridshunter-400-2.htm. [viewed 2021-04-06].

Koenigsegg Gemera Geneva unveiling. 2020-03-03. Freevalve AB (Sweden) [online]. Available from: https://www.freevalve.com [viewed 2020-04-11].

Maailman tehokkain kuorma-auto Sisu Polar Hybrid 1140 hv (The most efficient truck of the world). 2017-05-18. Ammattilehti.fi (Finland) [online]. Available from: www.ammattilehti.fi/uutiset.html?a2200=96385 [viewed 2021-10-10].

Regenerative Braking System in Rail Applications. 2014-02-23. Updated 2019-12-10. ConnectorSupplies.com (USA) [online]. Available from:

https://connectorsupplies.com/regenerative-braking-systems-rail-applications/ [viewed 2021-09-20].

Saab steam car and Ranotor. Latest editing 2021-10-04. Wikipedia [online]. Available from: https://en.wikipedia.org/wiki/Steam_car [viewed 2019-09-19].

Super Capacitor Technology Leading the Charge for Public transport. 2019-03-19. Global Opportunity Explorer (China) [online]. Available from: http://goexplorer.org/super-capacitor-techno-logy-leading-the-charge-for-public-transport/ [viewed 2021-09-21].

Synchronous generators for diesel-electric locomotives. 2018. ABB Product note [online]. Available from: https://library.e.abb.com/public/a716daac8d4147aa156f4da9ac4c203/Product%20note%20Rail%20tractiongenerator_new%20brand%20lug2018.pdf [viewed 2019-01-20].

The National Steam Propulsion Company proposition. Updated 2019-01-25. Ultimate Steam page. Trainweb.org [online]. Available from: www.trainweb.org [viewed 2017-12-19].

Wabtec unveils heavy-haul battery-electric locomotive FLXdrive. 2021-09-13. Railway Technology (Great Britain) [online]. Available from: https://www.railway-technology.com/news/wabtec-battery-electric-locomotive-flexdrive/ [viewed 2021-09-21].

What is the Energy Density of a Lithium-Ion Battery? 2020-09-21. Fluxpower.com (Vista, CA, USA) [online]. Available from: https://www.fluxpower.com/blog/what-is-the-energy-density-of-lithium-ion-battery [viewed 2021-09-24].

Wakabayashi, Daimo & Mark McGouldrick. 2020-01-13. Innovative High Efficiency Oil Burner Proves to Solve Many Environmental Challenges in Well Test Applications. OnePetro [online]. Available from: https://doi.org/10.2523/IPTC-19734-MS [viewed 2020-04-11].

Worldwide rail electrification remains at high volume. 2021-02-19. Railwaypro.com [online]. Available from: https://www.railwaypro.com/wp/worldwide-rail-electrification-remains-at-high-volume/ [viewed 2021-04-11].

Appendix A. Tables for prime mover calculations

a. Tabulated calculation parameters:

PRIME MOVER PARAMETERS			
A. Fixed parameters			
Cylinder diameter	D	0,20	[m]
Piston area	A	0,03	[m^2]
Crank radius	r	0,14	[m]
Piston stroke s = 2r	s	0,28	[m]
Connecting rod length	L	0,5	[m]
Crank-to-connecting-rod ratio	r / L	0,28	[ ]
Displacement V_{disp} = As	V_{disp}	0,0088	[m^3]
Clearance volume:			
- proportional	V_{prop}	6	[%]
- actual	V_{cl}	0,00053	[m^3]
Number of engine units	N_{eng}	3	[ ]
Number of cylinders per engine unit	N_{cyl}	5	[ ]
Number of HP cylinders per engine unit	N'_{HP}	1	[ ]
Total number of HP cylinders	N_{HP}	3	[ ]
Number of LP cylinders per engine unit	N'_{LP}	4	[ ]
Total number of LP cylinders	N_{LP}	12	[ ]
Rotational speed	n	7,5	[r/s]
Piston speed	w_p	4,2	[m/s]
Mechanical efficiency	η_{mech}	0,92	[ ]
B. Parameters depending on crank angle			
Momentary piston-swept volume of cylinder	V_{SW}	**Fig.4.20**	[m^3]
Momentary total volume of cylinder	V_{tot}	$V_{SW}+V_{cl}$	[m^3]

Table A1: Technical data of the prime mover

STEAM CYCLE PARAMETERS			
Boiler pressure (abs)	p_B	5,2	[MPa]
Boiler efficiency	η_B	0,95	[ ]
Own consumption efficiency	η_{oc}	0,96	[ ]
Temperature of superheated steam at boiler pressure	T_{sup}	810	[K]
Temperature of feedwater at boiler pressure	T_{fw}	539	[K]
Specific enthalpy of preheated feedwater at 539 K	h_5	1166	[kJ/kg]
Specific enthalpy of superheated steam at boiler pressure	h_B	3518	[kJ/kg]
Specific entropy of superheated steam at boiler pressure	s_{sup}	7067	[J/kgK]
Specific enthalpy of evaporation at boiler pressure	l	1627	[kJ/kg]
Specific enthalpy of water at feedwater pump inlet	h_3	884	[kJ/kg]
Specific enthalpy of feedwater at boiler inlet	h_4	887	[kJ/kg]
Condenser pressure (abs)	p_{cond}	0,1	[MPa]
Specific enthalpy of water at condensate pump inlet	h_1	418	[kJ/kg]
Specific enthalpy of water at inlet of mixing feedw. tank	h_2	420	[kJ/kg]
Density of superheated steam at boiler pressure	ρ_{HP}	14,4	[kg/m^3]
Isentropic index of high-pressure steam	κ_{HP}	1,27	[ ]
Isentropic index of low-pressure steam	κ_{LP}	1,30	[ ]
Isentropic efficiency of compound steam engine	$\eta_{s\ comp}$	0,90	[ ]
Isentropic efficiency of exhaust steam turbine	$\eta_{s\ TB}$	0,78	[ ]

Table A2: Principal steam parameters of the prime mover

ITEM	DESCRIPTION
①	CONDENSATE INLET TO PUMP
②	CONDENSATE INLET TO MIXING PREHEATER
③	FEEDWATER INLET TO FEEDWATER PUMP
④	FEEDWATER INLET TO SURFACE PREHEATER
⑤	FEEDWATER INLET TO STEAM GENERATOR
⑥	STEAM INLET TO HIGH-PRESSURE CYLINDER
⑦	STEAM INLET TO RECEIVER
⑧	STEAM INLET TO LOW-PRESSURE CYLINDER
⑨	EXHAUST STEAM INLET TO TURBINE
⑩	EXHAUST STEAM INLET TO CONDENSER
⑪	BLEED STEAM INLET TO MIXING PREHEATER

Table A3: Description and parameters of the steam circuit.

b. Tabulated intermediate results.

ε_{HP}	h_1	h_2	h_3	h_4	h_5	h_6	h_7	h_8	h_9	h_{10}	h_{11}
[ ]	[kJ/kg]	[kJ/kg]	[kJ/kg]	[kJ/kg]	[kJ/kg]	[kJ/kg]	[kJ/kg]	[kJ/kg]	[kJ/kg]	[kJ/kg]	[kJ/kg]
0,60	418	420	884	887	1166	3518	3332	3332	2904	2677	3332

Table A4: Specific enthalpies at key points of the steam circuit at ε_{HP} = 0,60.

φ_{deg}	V_{tot}	ε	p at ε_{HP}=0,60
0	0,001	0,000	5,20
.	.	.	.
76	0,004	**0,446**	5,20
77	0,005	0,455	5,20
78	0,005	0,464	5,20
79	0,005	0,473	5,20
80	0,005	0,482	5,20
81	0,005	0,491	5,20
82	0,005	**0,500**	5,20
83	0,005	0,509	5,20
84	0,005	0,518	5,20
85	0,005	0,527	5,20
86	0,005	0,536	5,20
87	0,005	0,545	5,20
88	0,005	**0,554**	5,20
89	0,005	0,563	5,20
90	0,006	0,571	5,20
91	0,006	0,580	5,20
92	0,006	0,589	5,20
93	0,006	**0,597**	5,20
94	0,006	0,606	5,11
.	.	.	.
180	0,009	1,000	**2,83**

Table A5: Dependence between φ, V_{tot}, ε_{HP}, and p.

ε_{HP}	$p_7 = p_8$	$T_7 = T_8$	s_7	$\rho_7 = \rho_8$	T_{7s}	h_{7s}	$\Delta h_{HP\,s}$	$\eta_{s\,comp}$	Δh_{HP}	$h_7 = h_8$
[ ]	[MPa]	[K]	[kJ/kg K]	[kg/m^3]	[K]	[kJ/kg]	[kJ/kg]	[ ]	[kJ/kg]	[kJ/kg]
0,60	2,83	717	7067	8,8	708	3312	206	0,90	185	3332

Table A6: Enthalpy drop and steam parameters at ε_{HP} = 0,60 at exit of HP cylinders.

ε_{HP}	$\dot{m}_6$
[ ]	[kg/s]
0,60	1,70

Table A7: Steam consumption of prime mover at ε_{HP} = 0,60.

ε_{HP}	ε_{calc}	ε_{tab}	κ_{LP}
0,60	0,205	0,205	1,30

Table A8: Affordable ε_{LP} at ε_{HP} = 0,60; isentropic index κ_{LP} = 1,30 conforms to steam tables.

ε_{LP}	p_8	s_8	T_8	ρ_8	h_8	p_9	T_9	$h_{9\,s}$	$\Delta h_{LP\,s}$	$\eta_{s\,comp}$	Δh_{LP}	h_9
0,205	2,83	7095	717	8,8	3332	0,47	495	2856	476	0,90	429	2904

Table A9: Enthalpy drop and steam parameters at inlet and exit of LP cylinders at ε_{LP} = 0,20, resulting from ε_{HP} = 0,60.

ε_{HP}	ε_{LP}	h_9	p_{TB}	T_9	h_s	$\Delta h_{TB\,s}$	Δh_{TB}	s_9	h_{10}	p_{cond}	$\eta_{s\,TB}$
[ ]	[ ]	[kJ/kg]	[MPa]	[K]	[kJ/kg]	[kJ/kg]	[kJ/kg]	kJ/kgK	[kJ/kg]	[MPa]	[ ]
0,60	0,20	2904	0,47	495	2613	291	227	7219	2677	0,1	0,78

Table A10: Enthalpy drop and steam parameters of the exhaust steam turbine at ε_{HP} = 0,60.

ε_{HP}	$\dot{m}_1$	$\dot{m}_2$	$\dot{m}_3$	$\dot{m}_4$	$\dot{m}_5$	$\dot{m}_6$	$\dot{m}_7$	$\dot{m}_8$	$\dot{m}_9$	$\dot{m}_{10}$	$\dot{m}_{11}$
[ ]	[kg/s]	[kg/s]	[kg/s]	[kg/s]	[kg/s]	[kg/s]	[kg/s]	[kg/s]	[kg/s]	[kg/s]	[kg/s]
0,60	1,43	1,43	1,70	1,70	1,70	1,70	1,70	1,43	1,43	1,43	0,27

Table A11: Steam mass flows at ε_{HP} = 0,60 at all observation points of the steam circuit.

ε_{HP}	Δh_{HP}	$\dot{m}_6$	P_{HP}	Δh_{LP}	$\dot{m}_8$	P_{LP}	Δh_{TB}	$\dot{m}_9$	P_{TB}	ΣP_{ind}
[ ]	[kJ/kg]	[kg/s]	[kW]	[kJ/kg]	[kg/s]	[kW]	[kJ/kg]	[kg/s]	[kW]	[kW]
0,60	185	1,70	315	429	1,43	613	227	1,43	324	1252

Table A12: Indicated powers of HP-, LP-, and turbine sections at ε_{HP} = 0,60.

ε_{HP}	P_b
[ ]	[kW]
0,60	1106

Table A13: Brake power of the prime mover at ε_{HP} = 0,60.

ε_{HP}	η_{stc}	η_{B}	η_{ind}	η_{mech}	η_{oc}	η_{b}
[ ]	[ ]	[ ]	[ ]	[ ]	[ ]	[ ]
0,60	0,28	0,95	0,27	0,92	0,96	0,23

Table A14: Efficiencies at ε_{HP} = 0,60.

Appendix B. Tables for heat exchanger calculations

Dimensions and parameters exploited in the steam and flue gas circuit calculations in spread sheets. Numbers of tables and formulae conform to those used in the spread sheets.

Cross section and arrangement of functional elements of the boiler and toroid drum including symbols of the basic dimensions are shown in Fig's B1 - B2. The dimensions used in determining the basic characteristics of the boiler are specified in Tables B1 - B6.

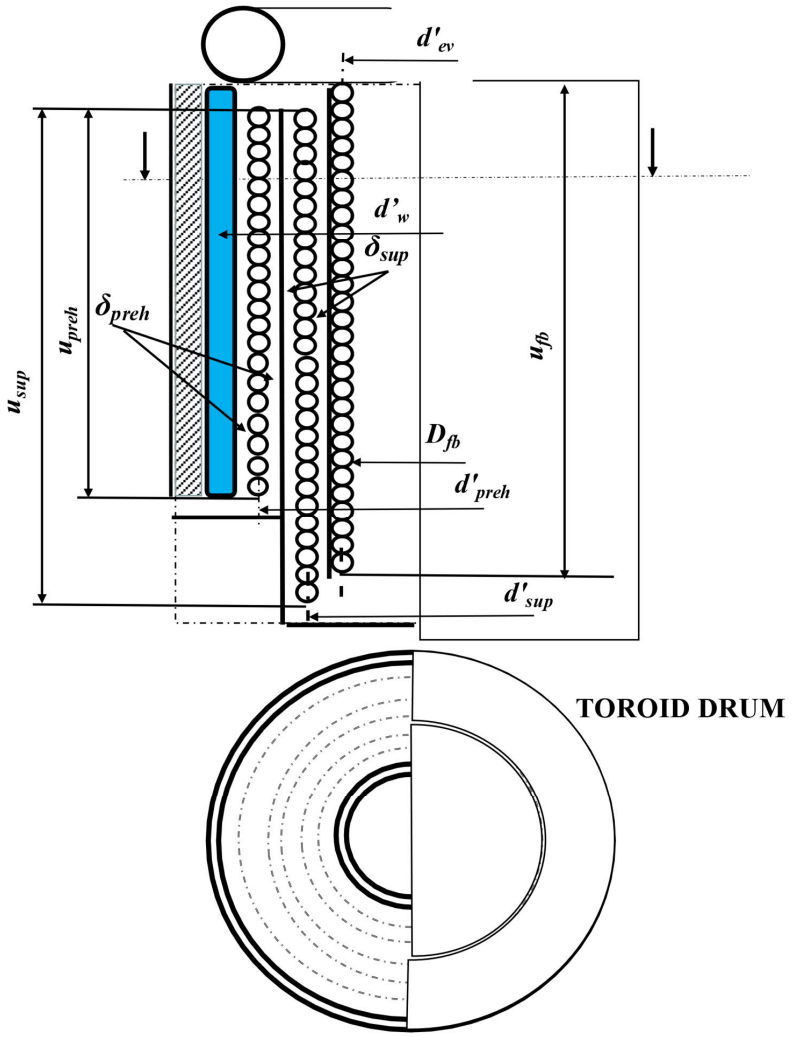

Figure B1: Layout and overall structural dimensions of the boiler of the *Hs 1*.

A. Basic constructional dimensions										
Boiler configuration from outside towards center						Coil tube dimensions			Plates	
Item	Symbol	Cumul. ø	Coil c/c ø	Increment	dim.	length	mass	volume$_w$	area	mass
						[m]	[kg]	[m^3]	[m^2]	[kg]
Casing sheet	d_B	***2,85***		0,003	[m]				35,8	838
Insulation		2,84		0,05	[m]					
Casing sheet	D_{ins}	***2,74***		0,003	[m]				34,4	806
Flue channel	δ_{preh}	2,73		***0,015***	[m]					
Preheater coil	d_{preh}	2,70	***2,76***	0,057	[m]	411	2357	0,79		
Flue channel	δ_{preh}	2,59		***0,015***	[m]					
Separation wall		2,56		0,008	[m]				21,7	1355
Flue channel	δ_{sup}	2,53		***0,015***	[m]					
Superheater coil	d_{sup}	2,50	***2,56***	0,057	[m]	521	2988	1,00		
Flue channel	δ_{sup}	2,47		***0,015***	[m]					
Separation wall		2,45		0,008	[m]				20,8	1299
Insulation		2,25		0,100	[m]					
Water tank wall		2,24		0,005	[m]				19,0	741
Water space		2,04		0,100	[m]			2,5		
Water tank wall		2,03		0,005	[m]				17,2	672
Insulation		1,83		0,100	[m]					
Casing sheet		1,83		0,003	[m]				15,5	363
Evaporator coil	D_{fb}	***1,70***	1,76	0,057	[m]	368	2109	0,71		
Toroid overall diam.	d_{tor}	***2,10***			[m]			0,33		987
Toroid c/c	d'_{tor}	***1,50***			[m]					
Toroid inside	D_{tor}	***0,60***			[m]					
Total length of coil tubes					[m]	1301				
Mass of coils and toroid					[kg]		7453			
Volume of coils & tank					[m^3]			5,3		
Total area of boiler plates					[m^2]				164,5	
Mass of plates					[kg]					6073
Mass of burner					[kg]					690
Total mass of boiler and tank in working order					[kg]					19540

Table B1: Basic dimensions of boiler of *Hs1*.

B. Tube coil and material properties			
Item	symbol	dimension	value
Wall thickness of toroid	δ_{tor}	[m]	0.015
Wall thickness of coil tubes	δ_{tube}	[m]	0.004
Specific gravity of coil tubes	m_{tube}	[kg/m]	5.73
Inside diameter of coil tubes	D_{tube}	[m]	0.050
Height of evaporator coil	u_{ev}	[m]	3.8
Height of preheater coil	u_{preh}	[m]	2.7
Height of superheater coil	u_{sup}	[m]	3.7
Specific gravity of steel	ρ_{steel}	[kg/m^3]	7800

Table B2: Material specifications of boiler unit.

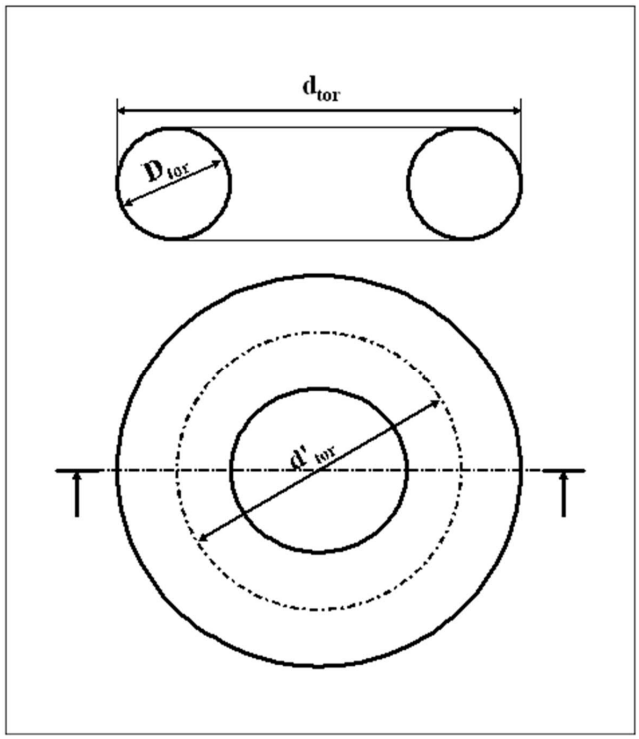

Figure B2: Toroid drum.

Steam circuit parameters				
Item	symbol	dimension	fixed	calculated
Boiler pressure p_B	p_B	[MPa]	5,2	
Superheat temperature	T_{sup}	[K]	810	
Specific enthalpy of superheated steam	h_{sup}	[kJ/kg]	3518	
Specific heat capacity of superheated steam	$c_{p\ sup}$	[kJ/kgK]	2,33	
Temperature of water at condensate pump intake	T_{cond}	[K]	373	
Specific enthalpy of condensate at pump intake	h_{cond}	[kJ/kg]	418	
Pressure of mixing preheater tank	$p_{w\ mt}$	[MPa]	1,8	
Temperature of water in mixing preheater tank	$T_{w\ mt}$	[K]	480	
Specific heat capacity of water in mixing preheater tank	$c_{p\ w\ mt}$	[kJ/kgK]	4,55	
Specific enthalpy of water at feedwater pump inlet	h_{fw}	[kJ/kg]	1166	
Temperature of water at evaporator inlet	T_{fw}	[K]	539,3	
Specific enthalpy of water at evaporator inlet	h_{fw}	[kJ/kg]		1170
Specific enthalpy of saturated steam at boiler pressure	$h_{sat\ st}$	[kJ/kg]	2793	
Heat of evaporation at boiler pressure	Q_{ev}	[kJ/kg]	1627	
Specific heat capacity of feedwater at evaporator inlet	$c_{p\ fw}$	[kJ/kgK]	5,06	
Mean specific heat capacity of feedwater	$\bar{c}_{p\ fw}$	[kJ/kgK]		4,81
Mean specific heat capacity of steam in superheater	$\bar{c}_{p\ sup}$	[kJ/kgK]		3,30
Evaporation rate of boiler	$\dot{m}_{ev}$	[kg/h]	6120	
Steaming rate (mass flow of steam = mass flow of water)	$\dot{m}_{st}$	[kg/s]	1,70	
Specific enthalpy rise within steam circuit	Δh_{tot}	[kJ/kg]		3100
Thermal power required for steam generating at ε_{HP} = 0,60	$\boldsymbol{\Phi_{st}}$	[kW]		5270
Predicted boiler efficiency	η_B	[ ]	0,95	
Gross thermal power required of the boiler	$\boldsymbol{\Phi_B}$	[kW]		5547

Table B3: Input parameters of steam circuit

Other fixed parameters, independent of fuel type			
Item	symbol	dimension	value
Ambient temperature = air intake temperature	$T_{air\ in}$	[K]	298
Flue gas temperature at exit of flue gas circuit	$T_{fg\ exit}$	[K]	398
Flue gas pressure	p_{fg}	[MPa]	0,1
Intake air pressure	p_{air}	[MPa]	0,1
Target maximum flow velocity of water in tubes	w_w	[m/s]	1,1
Gas constant	R	[J/mol K]	8,314
Molar mass of dry air	M_{da}	[kg/mol]	0,029
Molar mass of water vapor	M_v	[kg/mol]	0,018

Table B4: Various input parameters independent of fuel type

Fuel-dependent input parameters			PYR		LFO	
Item	symbol	dimension	fixed	calculated	fixed	calculated
Lower heating value of fuel	LHV	[kJ/kg]	15017		42721	
Efficiency of combustion in burner	η_{burn}	[ ]	0,995		0,995	
Heat release per kg of fuel in combustion	Q_F	[kJ/kg$_F$]		14167		40304
Mass of air per kg of fuel in stoichiometric combustion	m_{stoich}	[kg/kg$_F$]		5,0		14,4
Mass flow of air in stoichiometric combustion	$\dot{m}_{air\ stoich}$	[kg/s]		1,95		1,98
Excess air factor	λ_{air}	[ ]	1,15		1,15	
Mass of excess air per kg of fuel at selected λ_{air}	$m_{exc\ air}$	[kg/kg$_F$]		0,75		2,17
Mass flow of excess air	$\dot{m}_{exc\ air}$	[kg/s]		0,29		0,30
Mass flow of air in combustion with excess air	$\dot{m}_{comb\ air}$	[kg/s]		2,24		2,27
Temperature of flue gas at exit of combustion chamber	T_0	[K]		1240		1226
Temperature rise of combustion air without preheating	$\Delta T_{air\ amb}$	[K]		942		928
Temperature of preheated combustion air	$T_{comb\ air}$	[K]		581		457
Temperature rise of preheated combustion air	$\Delta T_{comb\ air}$	[K]		659		769
Specific heat capacity of preheated combustion air	$c_{p\ comb\ air}$	[kJ/kgK]		1,05		1,03
Specific heat capacity of air at T_0	$c_{p\ air\ max}$	[kJ/kgK]		1,19		1,19
Mean specific heat capacity of air within $T_{air\ in}$ - T_0	$\bar{c}_{p\ air\ tot}$	[kJ/kgK]		1,10		1,10
Reduction of LHV of fuel due to heating of excess air	ΔLHV	[kJ/kg$_F$]		779		2214
Reduced LHV of fuel	LHV_{red}	[kJ/kg]		14238		40507
Addition of heat release per kg of fuel by preheated air	ΔQ_F	[kJ/kg$_F$]		460		457
Resulting LHV of fuel with preheated combustion air	LHV_{act}	[kJ/kg$_F$]		14698		40964
Mass flow of fuel without preheated air	$\dot{m}_{F\ amb}$	[kg/s]		0,39		0,14
Mass flow of fuel with preheated combustion air	$\dot{m}_{F\ act}$	[kg/s]		0,38		0,14
Mass flow of flue gas with preheated combustion air	$\dot{m}_{fg\ act}$	[kg/s]		2,55		2,38
Reduction of flue gas enthalpy per kg of evaporated steam	$\Delta h_{fg\ ev}$	[kJ/kg$_{st}$]		1627		1627
Specific enthalpy of flue gas at exit of furnace	$h_{fg\ ex\ fb}$	[kJ/kg]		12539		38677
Overall temperature drop of flue gas	$\Delta T_{fg\ tot}$	[K]		842		828
Mean specific heat capacity of flue gas within fg-circuit	$\bar{c}_{p\ fg\ tot}$	[kJ/kgK]		1,23		1,19
Specific mass flow of wet flue gas from fuel combusted	$\dot{m}_{fg}$	[kg/kg$_F$]	6,75		17,60	
Specific heat capacity of flue gas at exit of fg-circuit	$c_{p\ fg\ exit}$	[kJ/kgK]		1,10		1,08
Mass flow of wet flue gas without preheating of air	$\dot{m}_{fg\ amb}$	[kg/s]		2,63		2,41
Mean specific heat capacity of flue gas exiting fg-circuit	$\bar{c}_{p\ fg\ exit}$	[kJ/kgK]		1,09		1,07

Table B5: Fuel-dependent input parameters

Symbol	Dimension	Variable	Calculus	Formula
ζ	[ ]		**0,508**	(B.4)
λ_{air}	[ ]	**1,15**		
Φ_F	[kcal/h]	**4765928**		
"	[kW]		**5547**	(B.6)
A_{ev}	[m^2]		**31,9**	(B.3)
ψ	[$kcal^{0,5}h^{-0,5}m^{-1}$]	**0,46**		
D_{ev}	[m]	**1,7**		
u_{ev}	[m]	**3,8**		
$\dot{m}_{fg}$	[kg/s]	**2,63**		
$c_{p\,fg}$	[kJ/kgK]	**1,23**		
T_0	[K]		**1240**	(B.10)
T_{exit}	[K]	**398**		
Φ_{ev}	[kW]		**2767**	$\dot{m}_{st}Q_{ev}$
Φ_{fb}	[kW]		**0**	(B.5)
V_{fb}	[m^3]		**8,6**	$¼\pi D_{ev}^2 h$
q_{fb}	[MW/m^3]		**0,64**	Φ_F/V_{fb}

Table B6: Key dimensions and parameters of furnace.

1. Fluid properties

Properties of flue gas, water, steam, and air *vs.* temperature are shown in Tables B7 – B15. Tables B7 & B8 deal with flue gas composition based on calculation program, courtesy of *T. Paloposki* of *Aalto University.* Properties of the components shown in Tables B9 - B11 were cited from VDI Heat Atlas either directly or by linear interpolation as also the air properties in Tables B12 - B13. *Spirax-Sarco* steam tables were used for determining water and steam properties in Tables B14 - B15. Green and brown colours refer to mean temperatures of flue gas within each heat exchanger, in PYR and LFO combustion, respectively. *NB:* Due to the iteration process, the temperature figures may oscillate within one degree, the change of the respective parameters being negligible.

Wet flue gas of pyrolysis oil combustion with stoichiometric and excess air												
Air factor	Moles = n_i		Mole fraction		Molecular mass		Mass		Mass fraction		Volume	
1,15	[kmol/kg_F]		[ ]		[kg/kmol]		[kg/kg_F]		[ ]		[Nm^3/kg_F]	
	Stoich.	+exc.air	Stoich.	+exc.air			Stoich.	+exc.air	Stoich.	+exc.air	Stoich.	+exc.air
CO_2	0,03	0,03	0,16	0,14	44,01		1,49	1,49	0,25	0,22	0,76	0,76
SO_2	0	0	0	0	0		0	0	0	0	0	0
N_2	0,14	0,16	0,65	0,67	28,01		3,81	4,38	0,64	0,65	3,05	3,51
H_2O	0,04	0,04	0,19	0,17	18,02		0,70	0,70	0,12	0,10	0,87	0,87
O_2	0,00	0,01	0,00	0,02	32,00		0,00	0,18	0,00	0,03	0,00	0,12
TOT.	0,21	0,23	1	1			6,00	6,75	1	1	4,68	5,26

Table B7: Predicted composition of flue gas in PYR combustion.

Wet flue gas of light fuel oil (LFO) combustion with stoichiometric and excess air												
Air factor	Moles		Mole fraction		Molec. mass		Mass		Mass fraction		Volume	
1,15	[kmol/kg$_F$]		[ ]		[kg/kmol]		[kg/kg$_F$]		[ ]		[Nm^3/kg$_F$]	
	Stoich.	+exc. air	Stoich.	+exc. air			Stoich.	+exc. air	Stoich.	+exc. air	Stoich.	+exc. air
CO_2	0,07	0,07	0,13	0,12	44,01		3,14	3,14	0,20	0,18	1,60	1,60
SO_2	0,00	0,00	0,00	0,00	64,06		0,00	0,00	0,00	0,00	0,00	0,00
N_2	0,40	0,45	0,74	0,75	28,01		11,07	12,73	0,72	0,72	8,85	10,18
H_2O	0,07	0,07	0,13	0,11	18,02		1,23	1,23	0,08	0,07	1,53	1,53
O_2	0,00	0,02	0,00	0,03	32,00		0,00	0,50	0,00	0,03	0,00	0,35
TOT.	0,53	0,61	1	1			15,4	17,6	1	1	12,0	13,7

Table B8: Predicted composition of flue gas in LFO combustion.

Dynamic viscosity and thermal conductivity *vs.* temperature										
	CO_2		SO_2		N_2		$H_2O_{(g)}$		O_2	
T	$\eta\cdot10^{-6}$	$\lambda\cdot10^{-3}$	$\eta\cdot10^{-6}$	$\lambda\cdot10^{-3}$	$\eta\cdot10^{-6}$	$\lambda\cdot10^{-3}$	$\eta\cdot10^{-6}$	$\lambda\cdot10^{-3}$	$\eta\cdot10^{-6}$	$\lambda\cdot10^{-3}$
[K]	[kg/s m]	[W/m K]	[kg/s m]	[W/m K]	[kg/s m]	[W/m K]	[kg/s m]	[W/m K]	[kg/s m]	[W/m K]
373	18,58	22,23	16,30	14,00	20,90	31,00	12,28	24,77	24,10	32,90
383	19,03	23,04	16,74	14,50	21,28	31,60	12,67	25,63	24,54	33,68
467	22,77	29,86	20,44	18,70	24,47	36,64	15,95	32,85	28,24	40,23
473	23,04	30,35	20,70	19,00	24,70	37,00	16,18	33,37	28,50	40,70
495	23,93	32,12	21,56	20,10	25,47	38,10	17,08	35,60	29,38	42,31
510	24,53	33,32	22,14	20,85	26,00	38,85	17,70	37,11	29,98	43,40
573	27,07	38,39	24,60	24,00	28,20	42,00	20,29	43,49	32,50	48,00
627	29,05	42,55	26,52	26,73	29,90	44,71	22,54	49,55	34,55	51,78
673	30,74	46,09	28,15	29,06	31,34	47,01	24,45	54,71	36,30	55,00
686	31,18	47,03	28,59	29,71	31,71	47,66	24,99	56,29	36,78	55,85
702	31,72	48,20	29,12	30,50	32,17	48,46	25,64	58,24	37,37	56,89
773	34,13	53,37	31,50	34,00	34,20	52,00	28,57	66,89	40,00	61,50
873	37,28	60,26	34,70	38,70	36,90	56,60	32,62	79,89	43,50	67,50
971	40,15	66,66	37,71	43,16	39,44	60,74	36,47	93,29	46,73	72,69
973	40,21	66,79	37,78	43,25	39,49	60,82	36,55	93,56	46,80	72,80
995	40,82	68,15	38,42	44,23	40,02	61,72	37,39	96,68	47,55	73,88
1011	41,24	69,08	38,86	44,89	40,38	62,33	37,96	98,80	48,06	74,61
1073	42,99	72,97	40,70	47,70	41,90	64,90	40,37	107,72	50,20	77,70
1173	45,71	78,78	43,40	51,90	44,10	68,60	44,08	122,18	53,40	82,00
1273	48,12	84,48	46,00	55,98	46,10	72,00	47,66	136,7	56,50	85,80

Table B9: Dynamic viscosity and thermal conductivity *vs.* temperature of components of flue gas

Specific heat capacity c_p *vs.* temperature					
T	CO_2	SO_2	N_2	$H_2O_{(g)}$	O_2
[K]	[kJ/kgK]				
298	0,84	0,62	1,04	1,86	0,92
373	0,92	0,66	1,04	1,89	0,93
383	0,92	0,67	1,04	1,89	0,94
467	0,99	0,71	1,05	1,94	0,96
473	1,00	0,71	1,05	1,94	0,96
495	1,01	0,72	1,06	1,95	0,97
510	1,02	0,73	1,06	1,96	0,97
573	1,06	0,76	1,07	2,00	0,99
627	1,09	0,77	1,08	2,03	1,01
673	1,11	0,79	1,09	2,06	1,02
686	1,12	0,79	1,09	2,07	1,03
702	1,13	0,80	1,10	2,08	1,03
773	1,16	0,81	1,12	2,13	1,05
873	1,20	0,83	1,14	2,20	1,07
971	1,23	0,85	1,16	2,27	1,09
973	1,23	0,85	1,16	2,27	1,09
995	1,23	0,85	1,17	2,29	1,09
1011	1,24	0,85	1,17	2,30	1,09
1073	1,25	0,86	1,18	2,34	1,10
1173	1,28	0,86	1,20	2,41	1,11
1273	1,29	0,88	1,22	2,48	1,12

Table B10: Specific heat capacity vs. temperature of components of flue gas

η and λ *vs.* temperature of flue gas					c_p and ρ *vs.* temperature of flue gas			
	PYR		LFO		PYR		LFO	
T	η	λ	η	λ	c_p	ρ	c_p	ρ
[K]	[kg/s m]	[W/m K]	[kg/s m]	[W/m K]	[kJ/kgK]	[kg/m^3]	[kJ/kgK]	[kg/m^3]
298					1,08		1,06	
373	2,0E-05	0,03	2,0E-05	0,03	1,10	0,93	1,08	0,93
383	2,0E-05	0,03	2,0E-05	0,03	1,10	0,90	1,08	0,91
467	2,3E-05	0,03	2,4E-05	0,04	1,13	0,74	1,10	0,74
473	2,4E-05	0,04	2,4E-05	0,04	1,13	0,73	1,10	0,73
495	2,4E-05	0,04	2,5E-05	0,04	1,14	0,70	1,11	0,70
510	2,5E-05	0,04	2,5E-05	0,04	1,14	0,68	1,11	0,68
573	2,7E-05	0,04	2,8E-05	0,04	1,16	0,60	1,13	0,61
627	2,9E-05	0,04	2,9E-05	0,04	1,18	0,55	1,15	0,55
673	3,1E-05	0,05	3,1E-05	0,05	1,20	0,51	1,16	0,52
686	3,1E-05	0,05	3,1E-05	0,05	1,20	0,50	1,17	0,51
702	3,2E-05	0,05	3,2E-05	0,05	1,21	0,49	1,17	0,49
773	3,4E-05	0,05	3,4E-05	0,05	1,23	0,45	1,19	0,45
873	3,7E-05	0,06	3,7E-05	0,06	1,26	0,40	1,22	0,40
971	3,9E-05	0,07	4,0E-05	0,06	1,29	0,36	1,25	0,36
973	4,0E-05	0,07	4,0E-05	0,06	1,29	0,36	1,25	0,36
995	4,0E-05	0,07	4,0E-05	0,07	1,30	0,35	1,25	0,35
1011	4,1E-05	0,07	4,1E-05	0,07	1,30	0,34	1,26	0,34
1073	4,2E-05	0,07	4,2E-05	0,07	1,32	0,32	1,27	0,32
1173	4,5E-05	0,08	4,5E-05	0,07	1,34	0,29	1,30	0,30
1273	4,7E-05	0,08	4,7E-05	0,08	1,36	0,27	1,31	0,27

Table B11: Resulting key properties *vs.* temperature of flue gas

Properties of air; moisture 0,7% abs., p = 0,1 MPa						
	dry air	vapor	humid air	dry air	vapor	humid air
T	η			λ		
[K]	[kg/s m]			[W/m K]		
273	1,7E-05	9,1E-06	1,7E-05	2,4E-02	-	-
298	1,9E-05	9,9E-06	1,8E-05	2,6E-02	1,9E-02	2,6E-02
373	2,2E-05	1,2E-05	2,2E-05	3,2E-02	2,4E-02	3,2E-02
377	2,2E-05	1,3E-05	2,2E-05	3,2E-02	2,4E-02	3,2E-02
439	2,5E-05	1,5E-05	2,5E-05	3,6E-02	3,0E-02	3,6E-02
472	2,6E-05	1,6E-05	2,6E-05	3,8E-02	3,3E-02	3,8E-02
473	2,6E-05	1,6E-05	2,6E-05	3,8E-02	3,3E-02	3,8E-02
573	3,0E-05	2,1E-05	3,0E-05	4,4E-02	4,3E-02	4,4E-02
579	3,0E-05	2,1E-05	3,0E-05	4,5E-02	4,4E-02	4,5E-02
673	3,3E-05	2,5E-05	3,3E-05	5,0E-02	5,5E-02	5,0E-02
773	3,7E-05	2,9E-05	3,6E-05	5,6E-02	6,7E-02	5,6E-02

Table B12: Dynamic viscosity and thermal conductivity vs. temperature of air

Properties of air; moisture 0,7% abs., p = 0,1 MPa									
T	$c_{p\ dry\ air}$	$c_{p\ vapour}$		x	p_{da}	p_{vapour}	$\rho_{dry\ air}$	ρ_{vapour}	ρ_{air}
[K]	[kJ/kgK]			kg_{H2O}/kg_{da}	[MPa]		[kg/m^3]		
273	1,003	1,859	1,009	0,007	0,099	0,001	1,263	0,014	1,278
298	1,004	1,864	1,010				1,157	0,013	1,171
373	1,010	1,890	1,016				0,925	0,010	0,935
377	1,011	1,892	1,017				0,915	0,010	0,925
439	1,019	1,923	1,026				0,786	0,009	0,795
472	1,024	1,939	1,031				0,731	0,008	0,739
473	1,024	1,940	1,031				0,729	0,008	0,737
573	1,045	1,999	1,051				0,602	0,007	0,609
579	1,046	2,003	1,053				0,597	0,007	0,603
673	1,068	2,064	1,075				0,513	0,006	0,518
1173	1,170	2,411	1,179				0,294	0,003	0,297
1225	1,177	2,446	1,186				0,282	0,003	0,285
1273	1,184	2,478	1,193				0,271	0,003	0,274

Table B13: Specific heat capacity and density vs. temperature of air

Properties of water in preheaters					
T	p_w	η_w	λ_w	$\bar{c}_{p\ w}$	ρ_w
[K]	[MPa]	[kg/s m]	[W/m K]	[kJ/kgK]	[kg/m^3]
539				5,06	
510	5,2	0,000113	0,63	4,81	820,7
480				4,55	

Table B14: Properties vs. temperature of water in preheaters.

Properties of steam in superheater					
T	p	η	λ	c_p	ρ
[K]	[MPa]	[kg/s m]	[W/m K]	[kJ/kgK]	[kg/m^3]
539				4,26	26,4
674,5	5,2	0,00002	0,06	3,30	20,4
810				2,33	14,4

Table B15: Properties vs. temperature of steam in superheater.

Appendix C. Track and locomotive data for simulations

Track and train parametres			
Train weight a) freight	m_{Tf}	[t]	800
Train weight b) passenger	m_{Tp}	[t]	100
Rolling resistance factor	μ_r	[ ]	0,0016
Drag coefficient a) Hs1	k_{air}	[ ]	0,80
Air density	ρ_{air}	[kg/m^3]	1,29
Area exposed to air resistance			
- Locomotive coefficient	0,12	[m^2/t]	15,6
- Train coefficient a) freight	0,04	[m^2/t]	32
- Train coefficient b) passenger	0,04	[m^2/t]	4
-Area total a) freight Hs1	A_{air}	[m^2]	47,6
-Area total b) freight Dr18			46,4
-Area total c) freight Tr1			50,8
-Area total d) passenger Hs1			19,6
-Area total e) passenger Dr18			18,4
Gradient factor: as tabulated in track profile			

Table C1: Track and train parameters.

Parametres of locomotive Hs 1			
Locomotive weight	m_{loc}	[t]	130
Adhesive weight	m_{adh}	[t]	130
Adhesion factor	μ_{adh}	[ ]	0,26
Permitted speed	v_{max}	[m/s]	27,8
Indicated power of prime mover	P_{ind}	[kW]	1252
Mechanical efficiency	η_{mech}	[ ]	0,92
Efficiency of auxiliaries	η_{aux}	[ ]	0,96
Brake power	P_b	[kW]	1106
Generator efficiency	η_{gen}	[ ]	0,95
Traction motor efficiency	η_{trm}	[ ]	0,95
Transmission efficiency	η_{trans}	[ ]	0,98
Traction efficiency	η_{tr}	[ ]	0,78
Drawbar power	P_{db}	[kW]	977
Drawbar tractive force	F_{db}	[kN]	325
Steam consumption at ε_{HP} = 0,60	? $_{st\ max}$	[kg/s]	1,70
Specific enthalpy of HP inlet steam	h_6	[MJ/kg]	3,52
Specific enthalpy of HP exhaust at ε_{HP}=0,60	h_7	[MJ/kg]	3,35
- " - of steam at mixing preheater inlet	h_2	[MJ/kg]	0,42
- " - at flue gas fw-preheater inlet	h_4	[MJ/kg]	0,89
Predicted boiler efficiency	η_B	[ ]	0,95
Efficiency of braking energy recovery system	η_E	[ ]	0,80
Lower heating value (LHV) of fuel	LHV_F	[MJ/kg]	14,7

Table C2: Parameters of locomotive *Hs 1.*

Parametres of locomotive Dr18			
Total weight	m_{loc}	[t]	120
Adhesive weight	m_{adh}	[t]	120
Adhesion factor	μ_{adh}	[ ]	0,31
Permitted speed	v_{max}	[m/s]	25,0
Brake power of prime mover	P_b	[kW]	1550
Efficiency of auxiliaries	η_{aux}	[ ]	0,9
Generator + rectifier efficiency	η_{gen}	[ ]	0,94
Traction motor efficiency	η_{trm}	[ ]	0,90
Transmission efficiency	η_{trans}	[ ]	0,97
Traction efficiency	η_{tr}	[ ]	0,74
Drawbar power	P_{db}	[kW]	1146
Drawbar tractive force	F_{db}	[kN]	365
Specific fuel consumption at indicated basis	? $_{F\ ind}$	[kg/kWh]	0,19
Specific fuel consumption at drawbar basis	? $_{F\ db}$	[kg/kWh]	0,26
Fuel consumption at idling	? $_{F\ idle}$	[kg/h]	10
Lower heating value of fuel	LHV_F	[MJ/kg]	40,7

Table C3: Parameters of locomotive *Dr18*.

Parametres of locomotive Tr1			
Total weight	m_{loc}	[t]	157
Adhesive weight	m_{adh}	[t]	68
Adhesion factor	μ_{adh}	[ ]	0,24
Traction efficiency	η_{tr}	[ ]	0,88
Permitted speed	v_{max}	[m/s]	22,2
Driving wheel diameter	d_d	[m]	1,60
Cylinder diameter	D_{cyl}	[m]	0,61
Piston stroke	s	[m]	0,70
Piston swept volume/stroke	V_{sw}	[m^3]	0,07
Total displacement = 4 x above	$V_{sw\ tot}$	[m^3]	0,26
Specific enthalpy of steam	h_{sup}	[MJ/kg]	3,15
- " - of feedwater	h_{fw}	[MJ/kg]	0,40
Density of superheated steam	ρ_{sup}	[kg/m^3]	5,73
Addition factor of wall effect to steam consumption	χ	[ ]	1,075
Predicted boiler efficiency	η_B	[ ]	0,67
Coal consumption at idling	c_{idle}	[kg/h]	100,00
Lower heating value (LHV) of coal	LHV_F	[MJ/kg]	28

Table C4: Parameters of locomotive *Tr1*.

Aalto-DD 165/2021

ISBN 978-952-64-0606-0 (printed)
ISBN 978-952-64-0607-7 (pdf)
ISSN 1799-4934 (printed)
ISSN 1799-4942 (pdf)

Aalto University
School of Engineering
Department of Mechanical Engineering
www.aalto.fi

BUSINESS +
ECONOMY

ART +
DESIGN +
ARCHITECTURE

SCIENCE +
TECHNOLOGY

CROSSOVER

**DOCTORAL
DISSERTATIONS**